THE
PHYSICAL REVIEW

A journal of experimental and theoretical physics established by E. L. Nichols in 1893

SECOND SERIES, VOL. 71, No. 12 JUNE 15, 1947

Recoil of Silver Nuclei Due to *K*-Capture in Cadmium

BYRON T. WRIGHT*
Radiation Laboratory, University of California, Berkeley, California
(Received March 7, 1947)

Some evidence has been obtained for the existence of the neutrino by observing recoils following *K*-capture in cadmium. The experiment is inconclusive because the recoiling silver atoms were uncharged, and thus the recoil energy could not be compared with the expected value.

INTRODUCTION

A POSSIBILITY of obtaining considerable evidence for the existence of the neutrino rests in looking for recoils following *K*-capture. The very impressive result of such an attack has been reported in the case of Be by Allen.[1] It is the purpose of this paper to report a somewhat similar experiment for a case of *K*-capture in cadmium.[2,3]

EXPERIMENTAL BACKGROUND

The 6.7 hour cadmium radioactivity has been assigned to isotope 107.[4] This activity has been studied in considerable detail.[5]

The decay scheme is indicated in Fig. 1. The isomeric Ag^{107*} level which is 93.5 kev above ground decays by emitting a γ-ray with a half-life of 44.3 seconds. This γ-ray is converted internally in 99 percent of the cases, giving conversion electrons with a minimum energy of approximately 68 kev.

Now

$$E_R = 540\, E_\nu^2/M \quad (1)$$

$$E_R = 540\, E_x^2/M \quad (2)$$

$$E_R = 540\, E_\beta(E_\beta+1)/M \quad (3)$$

where E_ν, E_x, and E_β equal the energy in Mev of a departing neutrino (zero rest mass), x-ray (or γ-ray), and beta-ray, respectively. E_R is the energy in electron volts of the recoil atom of mass number M.

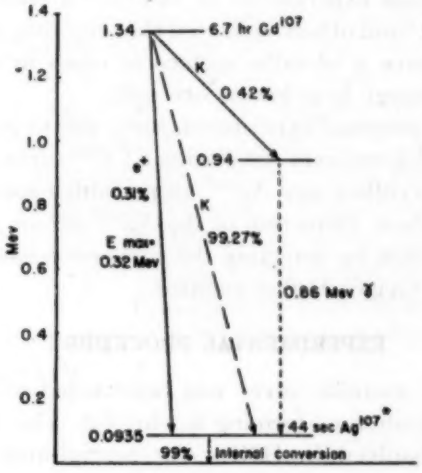

FIG. 1. Energy level diagram for the decay of Cd^{107}. Reproduced from reference 5.

* Now at the University of California at Los Angeles.

[1] James S. Allen, Phys. Rev. **61**, 692 (1942).

[2] Luis W. Alvarez, A. C. Helmholz, and Byron T. Wright, Phys. Rev. **60**, 160 (1941).

[3] Byron T. Wright, Ph.D. thesis, University of California at Berkeley (1941).

[4] A. C. Helmholz, Phys. Rev. **70**, 982 (1946).

[5] H. Bradt, *et al.*, Helv. Phys. Acta **18**, 255–258 (1945), and **19**, 218 (1946).

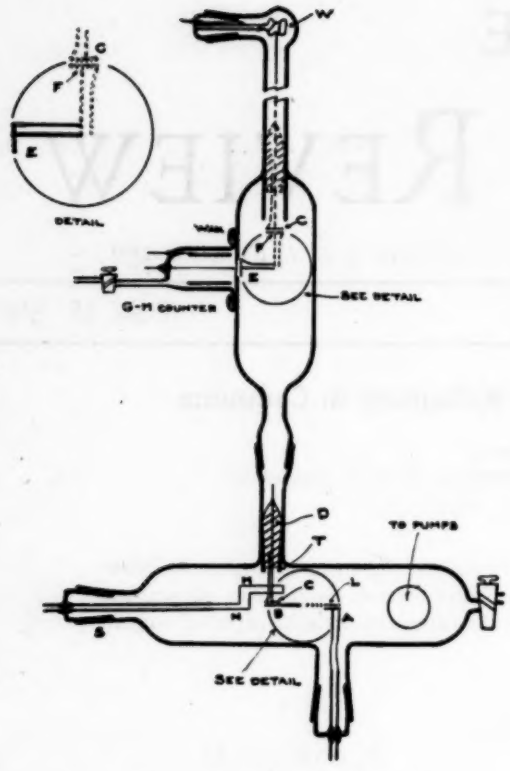

FIG. 2. Apparatus for observing recoils.

In K-capture in Cd^{107}, in 99.27 percent of the cases of radioactivity, $E_\nu = 1.25$ Mev, making the corresponding $E_R = 7.9$ volts.

Equation (1) applies only if the neutrino rest mass is zero. If this is not the case, the recoil energy could be smaller. However, classical beta-recoil experiments of Barton,[6] Donat, and Phillip,[7] and others indicated that recoiling nuclei may leave a metallic surface in cases in which their energy is as low as one volt.

The proposed experiment, then, was to prepare by double vacuum distillation a Cd^{107} surface and then to collect any Ag^{107*} atoms which leave the Cd surface. Detection of the Ag^{107*} atoms would be possible by detecting the conversion electrons with a Geiger-Müller counter.

EXPERIMENTAL PROCEDURE

Pure metallic silver was bombarded with 15-Mev deuterons, forming 6.7-hr. Cd. The target was dissolved in HNO_3, Ag precipitated as a chloride, and then the Cd left in a $2N$ acetic acid solution. Then for an hour the contents of the solution was electroplated on a flat spiral filament A.

After the plating, A was placed in the position shown in Fig. 2, and the system evacuated to 10^{-5} mm Hg. All the filaments were flat spirals made of 12-mil tungsten wire, and all could be cleaned and outgassed by heating. The activity was transferred by distillation in two steps to the filament C, the upper portion of the chamber being isolated during this period by a close fit of the tapered amber turning D into its seat T. This prevented a large background activity from being distilled into the upper portion of the apparatus.

Then the filament C was raised into the upper portion of the chamber, and recoil collection allowed for 20 to 90 seconds with the filaments in the dotted position shown in the detail.

C was then quickly raised, and E turned into the position opposite the counter. This was a bell-jar type of counter which was waxed onto the main glass envelope. A 1-mil Cellophane foil formed the counter wall.

Using the above method, 44-second Ag activity was detected.

EXPERIMENTAL RESULTS

Figure 3 shows the decay of the activity on E, the recoil receiver, for a typical run.

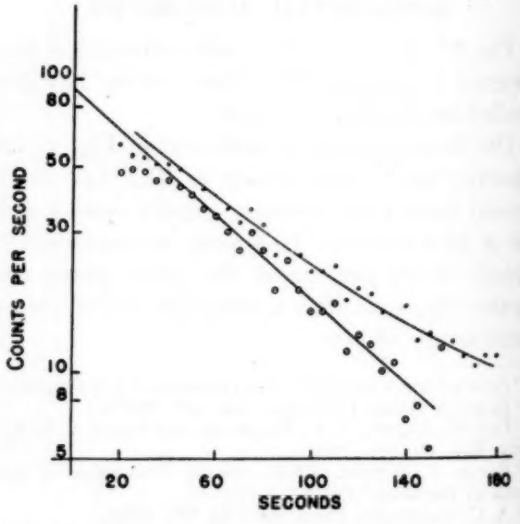

FIG. 3. Decay of the activity on E, the recoil receiver, for a typical run.

[6] Barton, Phil. Mag. 1, 833 (1926).
[7] Donat and Phillip, Zeits. f. Physik 45, 512 (1927).

By comparing the amount of the 6.7-hour Cd activity on the source C with the amount of activity collected on E, a determination of the efficiency of collection could be made. In both cases the radiation being detected is almost entirely the conversion electrons resulting from the decay of the Ag^{107*}.

Such a measurement gave an efficiency greater than 8 percent. That is of all the Ag^{107*} nuclei recoiling into the *hemisphere* available for collection, more than 8 percent were actually collected on the filament E.

The recoil receiver E was made -45 and $+45$ v with respect to a filament C, and no change in the collection efficiency resulted.

CONCLUSIONS

Ag^{107*} recoils result from the K-capture in 6.7-hour Cd^{107}. Because of the collection efficiencies obtained we may say that the observed recoils are not due only to the emitted positrons and/or the 0.846-Mev γ-rays which occur in certain modes of decay.

Some recoil will result from the x-rays and Auger electrons which follow the K-capture. Putting $E_x=0.025$ Mev, the excitation potential for Ag K x-rays, one obtains from (2) $E_R=0.003$ v, or less than $\frac{1}{10}$ of thermal energies, and in (3), putting $E_\beta=0.022$ Mev, the most energetic Auger electron possible from Ag, one obtains $E_R=0.11$ v.

The average energy necessary to remove a Ag atom from the liquid at the normal boiling point is 2.6 electron volts.

It seems very unlikely that the energy necessary to remove a Ag atom from a solid W or Cd surface at room temperature is less than this by a factor of 22. So it appears very unlikely that the observed recoils were *directly* due to the x-rays or Auger electrons.

It has been suggested that the newly born Ag atoms may leave the filament C by a mechanism which does not involve simply the conservation of momentum. Cooper[8] considers in some detail a possible explanation for the dissociation of molecules following an isomeric transition accompanied by an internal conversion. He shows (a) a net charge will build up on the molecule as a result of the greater probability of Auger electron emission as compared with x-ray emission and (b) that the shift in the Frank-Condon curves for the molecule resulting from this charge may be sufficient to lead to dissociation. He believes that a similar calculation for the perturbations of the periodic potential of a metallic surface caused by a similar building up of charge following K-capture will lead to the conclusion that it is possible to account for the departure of the Ag atoms of our experiment without any recoil being essential.

The collection efficiency in our experiment did not depend on a voltage of ± 45 volts between C and F during the period of collection. Therefore, the Ag atoms on leaving the surface were uncharged. It would then appear that in this case, at least, the electronic readjustments in the atom had been completed, including neutralization of the atom as a whole following any Auger electron production, before the atom left the surface on which it originally rested. However, during the time the electronic readjustments were incomplete, the atom could acquire sufficient kinetic energy to leave the surface. Just before leaving the surface it could acquire neutralizing electrons. Further theoretical work is needed to determine whether or not this mechanism is possible.

The case of recoil due to K-capture in cadmium, then, cannot, because of the doubts cast by the possibility of the mechanisms mentioned above, lead to nearly so direct evidence for the neutrino's existence as that provided by Allen;[3] it does corroborate his evidence.

The author wishes to thank Professors Ernest O. Lawrence and J. Robert Oppenheimer for their interest and helpful discussions. Professor Luis W. Alvarez originated the problem in 1940, and he and Dr. A. C. Helmholz did some of the preliminary work on the production of suitable cadmium surfaces.

[8] Eugene P. Cooper, Phys. Rev. **61**, 1 (1942).

The Production of Nucleons by the Cosmic Radiation

S. A. KORFF AND B. HAMERMESH*
New York University, University Heights, New York, New York

(Received March 1, 1947)

The production of protons and neutrons at an elevation of 14,156 feet by the cosmic radiation was studied with the aid of proportional counters. The production of more than one neutron at a time was found to take place. The rate of occurrence of multiple neutron productions was found to be much less frequent than that of single neutrons, even taking the usual distribution into account. The number and rate of production of protons was also determined and was found to be roughly the same as that of the neutrons.

INTRODUCTION

CONTINUING our study[1] of the neutrons and protons associated with the cosmic radiation, a series of tests was carried out during July, 1946, at the Cosmic Ray Laboratory of the University of Denver, located at 14,156 feet (4315 m) elevation on Mt. Evans,[2] Colorado. The experiments were designed to explore two questions: (1) Are neutrons produced singly or in multiples? (2) What can be said about the energy-distribution and number of protons? The affirmative answer to (1) has already been reported by us,[3] and constitutes the first experimental proof that there exist multiple production processes for neutron-production, analogous to multiple production of protons in "stars" in photographic emulsions.

NEUTRON MEASUREMENTS

The neutron experiments were designed to test whether neutrons were produced singly or in groups of more than one at a time. For this purpose, two large neutron counters were arranged to operate in coincidence. The counters were 15 cm in diameter and 150 cm long, and were filled with ordinary BF_3 to a pressure of 30 cm Hg, plus 2 cm argon. They were arranged side by side, in a horizontal plane with their axes parallel and the outsides separated by about 2 cm. The operating potential was between 2000 and 4000 volts. The two counters had been simultaneously filled on a manifold so as to assure identical gas content. The central wires were connected to a conventional Rossi coincidence circuit.

The counters were mounted so that a cadmium shield, 1 mm thick, could be slipped over them or withdrawn. In order to insure that most of the neutrons reaching the counters should be slow, 40 five-gallon cans of water were stacked around so that the counters were effectively inside a large quantity of water. Further, a mass of about 600 pounds of lead was arranged above the counters, in a layer 7 cm thick, to provide some heavy nuclei in which the neutron production might take place.

A reduction in the coincidence counting rate of 0.15 count per minute was found to be produced by the addition of the cadmium shield. Keeping all factors such as voltage and circuit sensitivity as constant as possible, the two counter wires were then connected to a single channel of the same amplifier and recorder, and a single counting rate of the two counters together in parallel was next determined. Thus under comparable conditions, the cadmium shield produced a reduction of 32 counts per minute in the rate of counting single neutrons. The cadmium difference test is necessary, since even in coincidence the arrangement has a definite background; thus for example, giant showers will cause a discharge in both counters. A series of experimental tests for accidentals was made.

DISCUSSION OF NEUTRON MEASUREMENTS

The evidence of the "stars" in photographic emulsions indicates that processes occur in which several ionizing particles are ejected or evaporated out of nuclei. It appears improbable that

* At present National Research Fellow, California Institute of Technology, Pasadena, California.

[1] S. A. Korff and E. T. Clarke, Phys. Rev. **61**, 422 (1942); S. A. Korff and B. Hamermesh, Phys. Rev. **69**, 155 (1946). (See these papers for further bibliography.)

[2] Latitude 39° 35′ North, longitude 105° 38′ West, Geomagnetic latitude 48° 23′ North; elevation from latest Forest Service survey, slightly modifying previously published altitudes.

[3] S. A. Korff and B. Hamermesh, Phys. Rev. **70**, 429L (1946).

several protons or other charged fragments could leave a nucleus without at the same time approximately the same number of neutrons departing. The observation of coincident neutrons, then, is an extension of the "star" observations, in that it indicates that such multiple processes do indeed take place, for neutrons as well as for ionizing particles.

The efficiency of detection may be considered. Since we are concerned with cadmium differences, we are dealing with thermal or nearly thermal neutrons. For such neutrons, a rough estimate of the detection efficiency is possible. The probability G that a neutron shall produce a count is then given by:

$$G = Lpd\sigma, \tag{1}$$

where d is the mean path length of the neutron passing through the counter, p is the pressure of BF_3 in atmospheres, and L is the Loschmidt number, 2.7×10^{19} molecules per cc at S.T.P., and σ is the capture cross section of BF_3 for neutrons. In this case, p being 30/76 atmos., $\sigma = 550\times10^{-24}$ cm^2, if d is assumed 15 cm (one diameter) then G is about 8.8 percent. The coincidence counting efficiency will be the square of the single counting efficiency, or 0.77 percent. This assumes that the two detectors are independent, that neither absorbs a large fraction of the total number of neutrons, and that the mean diffusion distance of the neutrons is long compared to the dimensions of the detector.

It is further evident that if neutrons are produced in events in which 3 or more are set free at once, than the probability of one neutron passing through each of the two counters is increased. The number distribution of protons in stars was determined from the data by Heisenberg and his collaborators,[4] and was found to be of the form

$$R = AN^{-s}, \tag{2}$$

where R is the number of stars having N protons, A is a constant and s is determined experimentally as about 2. Let us assume that a similar distribution applies to the neutrons. Then the total number of neutrons in stars of all sizes per unit area, and per unit time is:

$$\begin{aligned}\Sigma RN &= \Sigma NAN^{-s},\\ &= \Sigma AN^{-1}.\end{aligned} \tag{3}$$

This series is convergent since the unlikely event of a completely disintegrating lead nucleus would only produce 120 neutrons, and the average number of neutrons per star is about 3.

We might therefore expect that the number of neutrons counted in coincidence should be about $\frac{3}{2}\times8.8$ percent of the number counted by a single counter. The actual number observed was considerably less than this figure. Hence we may conclude either that Eq. (2) which is derived from the proton star data for stars of 2 or more particles does not correctly describe the ratio of events in which one and two neutrons are produced, or that the geometry of the experiment was such that at least 90 percent of the doubles were not detected. Further, we may assume that some neutrons are produced in stars and others are left over from originally fast neutrons which were produced elsewhere by some other mechanism.

The absolute number of slow neutrons was not determined in this experiment. The number cannot be computed from the data cited above, because the amplifier sensitivity was kept low, in order to eliminate accidentals, and in consequence some neutrons were missed. The number at Mt. Evans is, however, already known. It will be recalled that, in determining the number of neutrons, a curve of counting-rate as a function of counter-voltage or amplifier sensitivity is desirable, which shall extend into the beta-counting domain, for some neutrons produce pulses of the same order of size as those produced by slow betas. Such curves have been obtained, and the figures are: 0.91 neutron per S.T.P. liter of ordinary BF_3 per minute at sea level (100 m) inside thin (10 cm) paraffin shield,[5] and 0.97 inside thick (50 cm) paraffin,[6] while on Mt. Evans, 10 neutrons per liter per minute were counted inside 50 cm water.[1] The rate of increase with elevation is about 11 in 4 meters of water equivalent, or a factor of 1.8 per meter of water. As has been pointed out before, this rate of increase is about the same as that of the soft component while it is greater than that of the mesotron component near sea level. Assuming all the neutrons to have been produced in the water, a rate of production

[4] W. Heisenberg et al., *Cosmic Radiation* (1943).

[5] C. G. and D. D. Montgomery, Phys. Rev. **56**, 10 (1939).

[6] M. Kupferberg and S. A. Korff, Phys. Rev. **65**, 253A (1944).

of 2×10^{-4} neutron per gram and per second at the 6-meter level on Mt. Evans[1] was found. The rates of production of neutrons determined in balloon flights,[1] are all probably too low because of the low amplifier bias settings necessary to insure that noise is not counted.

PROTON EXPERIMENTS

In order to study the number of protons, a proton counter was employed. This counter was 75 cm long, 15 cm in diameter and filled with methane (CH_4) to a pressure of 48 cm Hg. It was operated in the proportional region, and the number of pulses as a function of voltage was determined. The cylinder was of brass, about 3 mm thick. Hence no protons of less than 15-Mev energy could have entered the counter from outside.

The counting rates obtained with this counter are shown in Fig. 1. In this figure, the curve is the observed counting rate as a function of voltage.

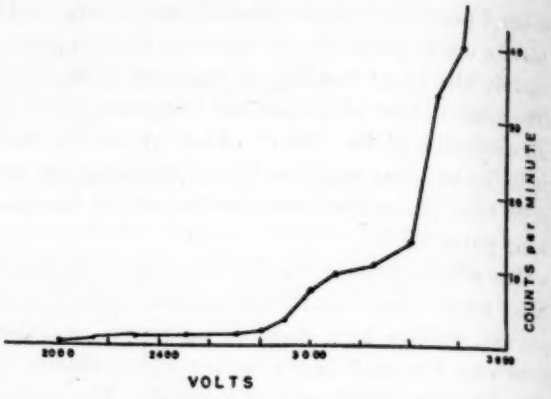

FIG. 1. Curve of counting-rate as a function of voltage for proportional counter filled with methane. Observed at Mt. Evans, altitude 14,156 ft. The pulses at 2000 to 2400 volts are caused by alpha-particle contamination in the counter, those between 3000 and 3600 volts are produced by heavily ionizing events including protons, giant showers, and nuclear disintegrations. This counter started counting beta-particles at about 3600 volts, and the counting rate rises very rapidly at voltages above 3600 due to slow electrons and slow mesotrons.

DISCUSSION OF PROTON EXPERIMENTS

Inspection of Fig. 1, shows a group of pulses extending to low voltages. These are the background contamination-alpha-particles. They were counted at about 1.2 per minute, which for an inside cylinder area of something over 6000 cm², corresponds to about 2×10^{-4} alpha per cm² per minute. The counter used in the 1941 tests had about the same amount of contamination; i.e., a trifle less than half the area and about half the number of alphas per minute.

The main group of protons is seen to be represented by a hump in the differentiated curve suggesting that most of the protons lose about 1 to 2 Mev in traversing the counter. Either the protons had about this energy, or they were higher energy protons which reached the opposite wall having lost 1 to 2 Mev in transit. For example, a 10-Mev proton has a range of about 1 meter in air at S.T.P., and hence in 15 or 20 cm path through methane at 48-cm pressure may lose around 1 to 2 Mev.

The maximum in the curve below the beta-ray threshold is at about 35 to 41, counts per minute. This compares with 10 to 12 in the 1941 experiments. The increase is of the order of a factor of 3.4 as compared to a ratio of cross-sectional areas of 2.3 and a volume ratio of 3.7 between the 1946 and 1941 counters. We have pointed out before that the majority of the protons are produced in the walls and not in the gas of the counter, there being only about 8 grams of gas in our 1946 counter. It had heretofore been assumed that the increase in the number of protons counted, in going to a larger counter with substantially the same gas pressure, would be proportional to the increase in area. The fact that the increase is faster than the increase in area but less than that of volume, suggests that the processes actually occurring are complex and may involve a volume dependent process superposed on one dependent on the area.

The possible entities capable of causing the counter to discharge are (a) contamination alphas, (b) protons, stars and other disintergrations, (c) giant showers, and (d) recoils due to fast neutrons. Slow mesotrons and betas are counted only at the highest voltages. Only process (d) is volume-dependent.

It will be noted that the curve has a definite hump just before the beta-ray counting potential is reached. This same hump was observed in 1941. The definite maximum occurring in pulses of a certain size argues against any monotonically rising distribution such as postulated by Heisenberg and his collaborators.[4] It will be recalled

that they derived, from a study of stars, a distribution described by Eq. (2), in terms of energy per star.

If it is assumed that all the counts are due to protons, then the number of protons may be directly computed from the counting rate and the counter area. If, on the other hand, some of the counts are ascribed to recoil protons produced by fast neutrons, then the efficiency of the counter fast neutrons is given by Eq. (1) modified by taking σ as the recoil cross section. Taking, in this case, $P=48/76$ atmos. $\sigma=10^{-24}$ cm², $d=15$ cm, we find $G=0.0255$ percent.

The number of counts per minute N will be related to the flux i of particle per minute producing the counts through:

$$N=iAG,$$

where A is the cross-sectional area of the counter, in this case 1125 cm². Hence if all 32 counts per minute are ascribed to recoils due to fast neutrons, a fast neutron flux of 11 neutrons per cm² per minute is required. On the other hand, since the efficiency of detection of protons is so nearly unity, a flux of 0.028 proton per cm² per minute will suffice to account for the observed rate. If the number of fast protons and neutrons is equal, then almost all the counts are due to protons, because of the low neutron recoil efficiency.

Consideration of recoils from the wall shows that these are more probable than recoils within the gas by a factor of five or more, depending on what energy is assumed for the neutrons. However, it will still be true that, for an equal flux of neutrons and protrons, most of the counts will be due to protons.

The proton experiments described above do not permit separate evaluation of the numbers of protons or fast neutrons, but only allow limits to be assigned to both possibilities. A set of experiments, designed further to resolve the factors involved and so study the altitude dependence of each, is being undertaken.

A rough evaluation of the rate of production of protons in the walls of the counter may be made if one assumes that the number of protons counted is the number produced in the walls which emerge into the active volume. The photographic plate evidence shows that star particles are produced with spherical symmetry, with no strong dependence on the direction of the producing entity. Consequently, one-half of the protons will be produced with directions away from the sensitive part of the counter. Of the remainder, one-half of those produced within one "range" of the surface will not emerge due to obliquity. If the range R of a proton is taken as 1 gram of matter, and the surface area S of this counter as 1125 cm², then the total counting rate $N=SQR$. Since 0.5 count per second was recorded, the rate of production Q is 5×10^{-4} per gram per second. The true rate of production is four times this, or 2×10^{-3} since not all protons produced were counted; but if an average of 3 protons are produced at once, there are about 7×10^{-4} production events per gram per second. This figure is of the same order of magnitude but somewhat larger than that derived for neutrons. This suggests that, if protons and neutrons are produced at about the same rate, not all the neutrons are detected and hence we may be underestimating the rate of production of neutrons.

The figure of 2×10^{-3} proton per gram per second may be compared to that deducible from Hazen's data.[7] Hazen observed 58 stars and estimates 5800 stars in 8500 photographs. He had about 46 kg of lead in his chamber. If his chamber was sensitive for 0.1 second, then his rate of production would be $(5800/8500)=Q\times(46\times10^3)\times0.1$ whence $Q=1.6\times10^{-4}$ per gram per second, easily in agreement with our figure in view of the crudity of the assumptions.

ACKNOWLEDGMENTS

The authors are indebted to the Research Corporation for financial support of the above investigations. The use of the Mt. Evans Laboratory was made available through the courtesy of the University of Denver. The authors received enthusiastic cooperation and assistance, without which the work could never have been carried out, from Professors Byron Cohn and Mario Iona of the University of Denver. Messrs. L. G. Collyer and A. Krumbein of the New York University staff accompanied the expedition and rendered material assistance, as also did Charles C. Renshaw II and Thomas Baker. To all of these persons, our thanks are hereby expressed.

[7] W. E. Hazen, Phys. Rev. 65, 67 (1944).

Contributions to the Theory of Beta-Phase Alloys*

CLARENCE ZENER
Institute for the Study of Metals, The University of Chicago, Chicago, Illinois
(Received March 6, 1947)

All alloys of the type of β-brass decrease their concentration range in the disordered state as the temperature is lowered. The original theory of Jones is shown to be inadequate, and the observed variation with temperature of the phase boundaries is shown to follow directly from the assumption that the β-phase has a slightly lower characteristic temperature than the neighboring phases.

Beta-brass has an extremely high elastic anisotropy. This property is in part a result of an anomalously low value of $(C_{11}-C_{12})/2$, which is shown to be interpretable in terms of lattice type and inter-ionic interactions. This interpretation also explains the positive value of the temperature coefficient of E_{100}.

1. INTRODUCTION

BETA-PHASE alloys, of which beta-brass is the prototype, are best known to physicists because they exemplify the 3/2 electron-atom rule of Hume-Rothery, and also because they furnish examples of order-disorder phenomena. The purpose of the present paper is to discuss, in a qualitative manner, the origin of certain other characteristics common to these alloys. One characteristic common to all disordered beta-phase alloys is the peculiar shape of their constitution diagram. The concentration range of a disordered beta-phase rapidly narrows as the temperature is lowered, which narrowing causes the phase to disappear unless the critical temperature for ordering is reached in time. Another property which is believed to be common to all beta-phases, but which has as yet been observed only in beta-brass, is the high elastic anisotropy, the ratio of the two shear coefficients C_{44} and $(C_{11}-C_{12})/2$ being 18. Another property which is believed common to all beta-phase alloys, but which has as yet been observed only in beta-brass, is the anomalous temperature coefficient of the elastic constants $E_{[110]}$ and $E_{[100]}$. Below 200°C the temperature coefficients of these constants are positive.

2. CONSTITUTION DIAGRAM

The constitution diagram of a typical beta-phase alloy is reproduced as Fig. 1. The narrowing of the range of the disordered phase could be regarded merely as evidence of certain thermodynamic characteristics of this phase. Thus if this disordered phase has a higher energy per mole at 0°K than the two bordering phases, but a lower effective characteristic temperature, then it must have the general shape given in Fig. 1. The proof of this statement is elementary, but a demonstration is not superfluous, since another theory has been accepted in the current literature.[1,2] In

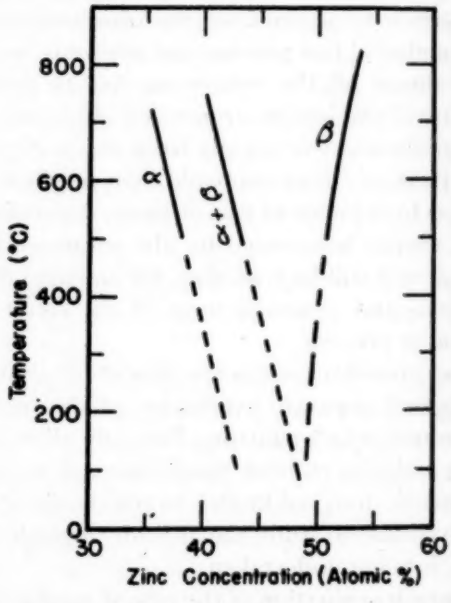

FIG. 1. Boundaries of disordered beta-phase in Cu-Zn system. Solid lines: observed. Dashed lines: extrapolation below critical temperature for ordering.

* This research was supported by ORI (Contract No. N6ori-20-IV).

[1] F. Seitz, *Modern Theory of Solids* (McGraw-Hill Book Company, Inc., New York, 1940), pp. 499–502.
[2] W. Hume-Rothery, *The Structure of Metals and Alloys* (Institute of Metals, London, 1945) p. 83.

this theory, developed by Jones,[3] the shape of the $\alpha|(\alpha+\beta)$ and of the $(\alpha+\beta)|\beta$ boundaries presumably follows from a consideration only of the entropy of mixing and of the variation with concentration of the difference in energies of the two phases at 0°K. In view of the present confusion it appears wise to re-examine in detail the theory of these two boundaries.

An understanding of the manner in which various physical factors influence phase boundaries may best be attained through a study of the customary plot of free energy *vs.* concentration. The ordinate of this plot may be regarded as either the Helmholtz free energy F, or the Gibbs free energy G. These are essentially identical for metallic systems at atmospheric pressure. The abscissa of this plot may be either the atomic concentration X or any linear combination thereof. In order to coordinate this discussion with that of Jones, we follow his lead in expressing free energy in units of electron volts per atom, and concentration in terms of number of valence electrons per atom n. In our present case of a divalent metal dissolved in a monovalent metal, n and X are related by $n=X+1$. A standard F *vs.* n plot does not differentiate sufficiently between the α- and β-phases to be useful for a graphical solution. Sufficient dispersion is obtained, however, by introducing a simple shear parallel to the vertical axis, i.e., by plotting $(F-fn)$ *vs.* n. The coefficient f is to be so chosen that both $(F_\alpha-fn)$ and $(F_\beta-fn)$ have minima in the desired range. Such a homogeneous shear leaves unchanged the essential property of a free energy *vs.* concentration plot, namely that the boundaries of the two phases are given by the points of contact of a common tangent.

A sheared free energy plot is presented in Fig. 2 for 0°K from the theoretical computations given by Jones, in which computations it was implicitly assumed that the β-phase remains disordered throughout the entire temperature range. From this figure it may be seen that the points of contact of a common tangent, and hence the $\alpha|(\alpha+\beta)$ and the $(\alpha+\beta)|\beta$ boundaries, are at n values of 1.41 and 1.45, respectively, values previously obtained by Jones.

In order to find the temperature variation of the phase boundaries, Jones[4] separates the free energy of each phase in the customary manner

$$F_j(X_j, T)=f_j(X_j, T)-TS_m^{(j)}(X_j), \quad j=\alpha, \beta. \quad (1)$$

Here X_j is the atomic concentration in phase j, $S_m^{(j)}$ is the mixing entropy

$$S_m^{(j)}(X_j)=-k\{X_j \ln X_j + (1-X_j)\ln(1-X_j)\}, \quad (2)$$

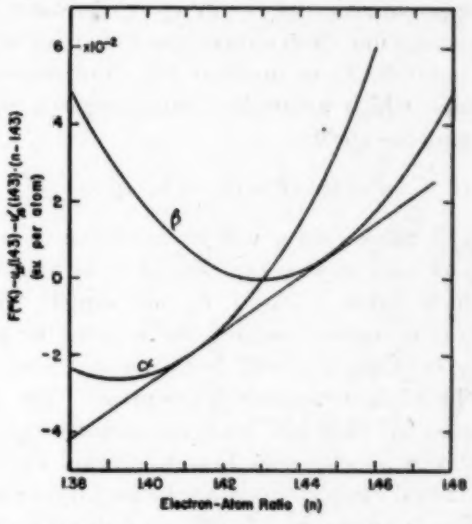

FIG. 2. Sheared free energy-concentration plot for Cu-Zn system.

and

$$f_j(X_j, T)=U_j(X_j)+\int_0^T C_j dT - T\int_0^T T^{-1}C_j dT, \quad (3)$$

U_j being the energy at 0°K. Later in his analysis Jones introduces[5] the simplification

$$f_\alpha(X_\alpha, T)-f_\beta(X_\beta, T)=U_\alpha(X_\alpha)-U_\beta(X_\beta). \quad (4)$$

In the purely analytical method adopted by Jones, where one deals exclusively with the concentrations X_α and X_β at the two boundaries, the seriousness of this approximation is not obvious. In the graphical approach of the present discussion, we have only the one variable X (or n).

[3] H. Jones, Proc. Phys. Soc. London **49**, pp. 243 and 250 (1937).

[4] H. Jones, reference 3, p. 244.

[5] H. Jones, reference 3, p. 256.

Thus Eqs. (1) and (2) become

$$F_j(X, T) = f_j(X, T) + kT\{X \ln X + (1-X)\ln(1-X)\}, \quad (5)$$

and Eq. (4) becomes

$$f_\alpha(X, T) - f_\beta(X, T) = U_\alpha(X) - U_\beta(X). \quad (6)$$

Upon combining these two equations one obtains

$$F_\alpha(X, T) - F_\beta(X, T) = U_\alpha(X) - U_\beta(X).$$

The approximation (4) is therefore equivalent to the assumption that temperature changes alter $F_\alpha(X)$ and $F_\beta(X)$ in precisely the same manner, a change which might be visualized as a non-homogeneous shear

$$F - fn \rightarrow F - fn - TS_m(n)$$

of Fig. 2. Such a shear will always leave the two points of tangency on opposite sides of $n = 1.43$, at which value U_α and U_β are equal. Since $-TS(n)$ is convex towards the n axis, the two points of tangency will both move closer to $n = 1.43$ with increasing temperature. The assumption (4) therefore leads to computed phase boundaries as shown in Fig. 3 by solid curves. The dashed curves, given by Jones, could there fore have been obtained from assumption (4) only through a mathematical error in computation.

In order to obtain the type of variation of phase boundaries actually observed, appropriate account must be taken of the differences in the thermodynamic properties of the two phases. At temperatures above the characteristic temperature of each phase the free energy per atom may be written

$$F_j(X, T) = U_j(X) + kT\{X \ln X + (1-X)\ln(1-X)\} - 3kT \ln(kT/h\nu_j), \quad (7)$$

where ν_j denotes the geometrical mean of the frequencies of all the normal modes of vibration. Equation (6) must therefore be replaced by

$$f_\alpha(X, T) - f_\beta(X, T) = U_\alpha(X) - U_\beta(X) + 3kT \ln(\nu_\alpha/\nu_\beta). \quad (8)$$

The difference in thermodynamic properties of the two phases is thus determined by the ratio ν_α/ν_β.

The equations for the phase boundaries X_α, X_β may be written as

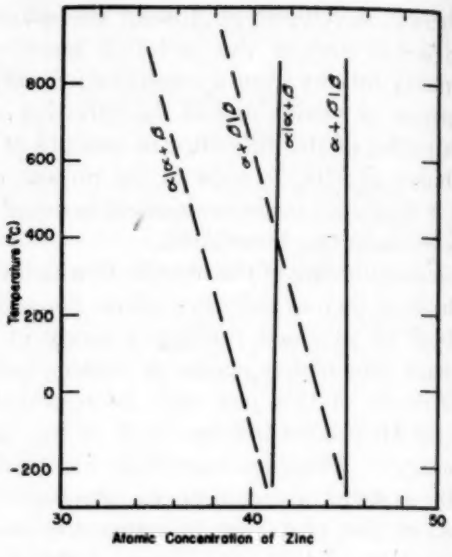

FIG. 3. $\alpha|(\alpha+\beta)$ and $(\alpha+\beta)|\beta$-boundaries in Cu-Zn system according to theory of Jones, as computed by author (———), as computed by Jones (— — — —).

$$F_\alpha'(X_\alpha) = F_\beta'(X_\beta) \quad (9)$$

$$F_\beta(X_\beta) - F_\alpha(X_\alpha) = (X_\beta - X_\alpha) \cdot \{F_\alpha'(X_\alpha) + F_\beta'(X_\beta)\}/2. \quad (10)$$

In order to facilitate the solution of these equations we utilize the experimental observations that the boundaries are confined to a comparatively narrow range of X. We therefore expand F_α and F_β as a power series in $(X - X_0)$, where X_0 is some concentration that lies within the range of interest. In order to reduce the number of physical constants, we shall assume that $U_\alpha''(X) = U_\beta''(X)$, and that ν_α and ν_β are independent of X, which assumptions lead to $F_\alpha''(X) = F_\beta''(X)$. Our expansion therefore becomes

$$\begin{aligned} F_\alpha(X, T) &= A_\alpha + B_\alpha(X - X_0) + \tfrac{1}{2}C(X - X_0)^2 \\ F_\beta(X, T) &= A_\beta + B_\beta(X - X_0) + \tfrac{1}{2}C(X - X_0)^2. \end{aligned} \quad (11)$$

Substitution of these expansions into the equilibrium Eqs. (9) and (10) leads to the solutions

$$X_\beta - X_\alpha = (B_\alpha - B_\beta)/C \quad (12)$$

$$(X_\beta + X_\alpha)/2 = X_0 - (A_\alpha - A_\beta)/(B_\alpha - B_\beta), \quad (13)$$

where

$$A_\alpha - A_\beta = U_\alpha(X_0) - U_\beta(X_0) + 3kT \ln(\nu_\alpha/\nu_\beta) \quad (14)$$

$$B_\alpha - B_\beta = U_\alpha'(X_0) - U_\beta'(X_0) \quad (15)$$

$$C = U_\alpha''(X_0) + kT/X_0(1 - X_0). \quad (16)$$

The solutions given by Eqs. (12) and (13) contain four adjustable constants, namely $U_\alpha(X_0) - U_\beta(X_0)$, $U_\alpha'(X_0) - U_\beta'(X_0)$, $U''(X_0)$, and ν_α/ν_β. On the other hand, since the two boundaries may be represented by two essentially straight lines, the experimental boundaries may likewise be represented by four constants. Agreement with experiment can therefore be forced by appropriate choice of constants. Now Jones has computed the first three constants from considerations based solely upon differences in type of the Brillouin zones of the two phases. It is of interest to see how closely his computed values agree with those chosen to fit the known phase boundaries. Upon choosing X_0 at 0.43, we find agreement is obtained by taking

(a) $U_\alpha(X_0) - U_\beta(X_0) = -0.016$ ev per atom, in contrast to Jones' value of 0,

(b) $U_\alpha'(X_0) - U_\beta'(X_0) = 0.21$ ev per atom, in contrast to Jones' value of 0.14,

(c) $U_\alpha''(X_0) = 3.8$ ev per atom, in complete agreement with Jones' value. The value of the fourth unknown constant required by experiment is

$$\nu_\alpha/\nu_\beta = 1.10.$$

A plot of the phase boundaries according to Eqs. (12) and (13), and according to the above constants, is given in Fig. 1. The constants were chosen to give agreement with experiment above 500°C, which temperature is slightly above the critical temperature for ordering. By extending the $(\alpha+\beta)|\beta$ boundary below 500°C we see that it intersects the $\beta|(\beta+\alpha)$ boundary near 100°C. We conclude that the β-phase of brass would become unstable below 100°C were this phase not to become ordered.

In his early work Hume-Rothery demonstrated the approximate equivalence of the $\alpha|(\alpha+\beta)$ and $(\alpha+\beta)|\beta$ boundaries of different alloys provided the diagrams have as abscissa the electron-atom ratio n rather than atomic concentration X. An identical equivalence would be given by Eqs. (12)–(16) if $U_\alpha(n) - U_\beta(n)$ were the same for all systems, as well as $U_\alpha''(n)$ and ν_α/ν_β. It is expected that small differences in the $T-n$ diagrams will arise as a result of small variations in these quantities. In the derivation of Eqs. (12)–(16) an assumption was introduced which, while apparently justified in the case of β-brass, may lead to appreciable error in other systems. This assumption was that $U_\alpha''(X)$ and $U_\beta''(X)$ were identical, and hence that $U_\alpha'(X) - U_\beta'(X)$ is independent of X over the region of interest. Now Jones has shown that this difference decreases with decreasing X, becoming zero at an electron-atom ratio of 1.25. As may be seen from Eqs. (12)–(13), the effect of this variation will be to decrease the width of the $(\alpha+\beta)$ region as this region moves to the left with increasing temperature, and simultaneously to increase the temperature variation of the center of this region. An indication of such effects may be found in the Cu-Ga and Ag-Zn systems.

TABLE I. Shear elastic coefficients of α- and β-brass (in units of 10^{12} ergs/cm^3).

Metal	C_{44}	$(C_{11}-C_{12})/2$
α-brass (f.c.c.)*	0.72	0.18
β-brass (b.c.c.)**	1.73	0.093

*f.c.c. =face centered cubic.
**b.c.c. =body centered cubic.

3. ELASTIC ANISOTROPY

As was first pointed out by Webb,[6] β-brass has the highest elastic anisotropy of any cubic metal so far examined, the ratio of $E_{[111]}/E_{[100]}$ at room temperature being 8.9. The elastic anisotropy is still greater when expressed in terms of the two shear coefficients C_{44} and $(C_{11}-C_{12})/2$. The first of these coefficients refers to a shear across the (100) plane in an arbitrary direction, the second to a shear across the (110) plane in the $[1\bar{1}0]$ direction. From the measurements of Good[7] one finds that the ratio of these two shear coefficients varies from 18 at room temperature to 19 above the critical temperature for ordering.

A search for the origin of the high elastic anisotropy of β-brass may best start by a comparison of the shear elastic coefficients of α- and of β-brass, given in Table I. It is seen that in passing from the face-centered cubic to the body-centered cubic structure the C_{44} coefficient is more than doubled while the $(C_{11}-C_{12})/2$ coefficient is nearly halved.

The anomalously low value of the $(C_{11}-C_{12})/2$ shear coefficient of β-brass may readily be seen to be a direct consequence of the combination of

[6] W. Webb, Phys. Rev. **55**, 297 (1939).
[7] W. A. Good, Phys. Rev. **60**, 605 (1941).

a body-centered cubic lattice with ions containing only closed shells. Thus a body-centered cubic packing of balls manifests no resistance to a simple (110) $[\bar{1}10]$ shear. This lack of shear resistance is a consequence of the fact that such a shear leaves the distance between closest neighbors unchanged to a first approximation. In metals the resistance to shear arises primarily from two sources:[8–10] (a) the exchange interaction between ions, (b) the electrostatic interaction between conduction electrons and ions. The first type of interaction may be regarded as acting only between closest neighbors, and in a body-centered cubic structure gives a positive contribution to $(C_{11}-C_{12})/2$ when the interaction is one of attraction, a negative contribution when it is repulsive, as is the case when the positive ions contain only closed shells. The second type of contribution, electrostatic interaction, gives a positive contribution which is independent of the ion structure. From the computations of Fuchs[8] on copper, one sees that in a body-centered cubic copper lattice the negative contribution of the exchange interaction will more than compensate for the positive contribution of the electrostatic interaction, and that, therefore, in such a lattice $(C_{11}-C_{12})/2$ would be negative, i.e., the lattice would be mechanically unstable. The low value of this constant in β-brass may therefore be regarded as a manifestation of the tendency of the ion exchange interaction to render the body-centered cubic lattice mechanically unstable with respect to a (110) $[\bar{1}10]$ shear. It is therefore anticipated that all β-type alloys with closed inner shells will have a similarly low value of this shear constant.

The susceptibility of body-centered cubic structures to mechanical instability with respect to a (110) $[\bar{1}10]$ type shear furnishes an interpretation as to the limitations of body-centered cubic lattices to certain places in the periodic table. Aside from the alkali metals where the ions are too small to overlap to an appreciable extent, we would anticipate that no body-centered cubic lattices would be found in metals with completely or nearly completely closed shells. The other non-alkali body-centered cubic metals, V, Cr, Fe, Cb, Mo, Ta, W, Eu, Th, Ba, have as free atoms from three to six electrons in the inner d shell, out of a possible maximum of ten, or (Eu) six f-electrons out of a possible maximum of fourteen, with the two exceptions Tl and Ba.

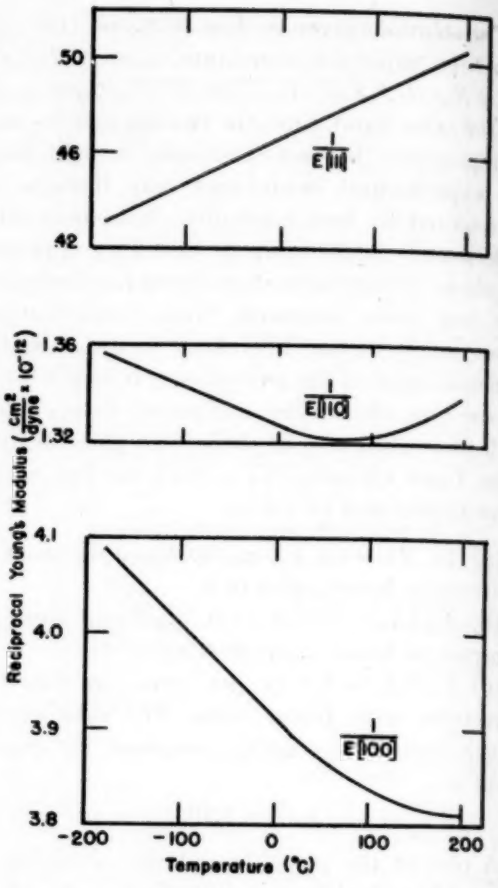

FIG. 4. Reciprocal Young's moduli of beta-brass, after Rinehart.

The high elastic anisotropy of β-brass is in part caused by the anomalously large value of the C_{44} shear constant. No satisfactory interpretation of this anomaly has been found.

4. ANOMALOUS TEMPERATURE COEFFICIENTS OF ELASTIC MODULI

In Fig. 4 are reproduced the observations of Rinehart[11] on the temperature variation of the reciprocal elastic moduli $E^{-1}_{[111]}$, $E^{-1}_{[110]}$, $E^{-1}_{[100]}$ of β-brass. Contrary to the normal behavior of reciprocal moduli, the last two decrease rather

[8] K. Fuchs, Proc. Roy. Soc. [A]151, 585 (1935); 153, 622 (1936); 157, 444 (1936).
[9] N. F. Mott and H. Jones, *The Theory of the Properties of Metals and Alloys* (Oxford Press, 1936), pp. 147–150.
[10] F. Seitz, reference 1, pp. 373–378.
[11] J. S. Rinehart, Phys. Rev. 58, 365 (1940); 59, 308 (1941).

than increase with a rise in temperature, i.e., a rise in temperature increases the elastic resistance of β-brass crystals with respect to tensile stresses along the [110] and [100] axes.

In order that a clue may be obtained as to the anomalous temperature variation shown in Fig. 4, we shall write the reciprocal tensile moduli in terms of the bulk modulus $(C_{11}+2C_{12})/3$ and the two shear coefficients C_{44} and $(C_{11}-C_{12})/2$.

$$E^{-1}_{[111]}=(9K)^{-1}+(3C_{44})^{-1},$$
$$E^{-1}_{[110]}=(9K)^{-1}+(4C_{44})^{-1}+\{12(C_{11}-C_{12})/2\}^{-1},$$
$$E^{-1}_{[100]}=(9K)^{-1}+\{6(C_{11}-C_{12})/2\}^{-1}.$$

From an inspection of these equations we see that the relative importance of the shear modulus $(C_{11}-C_{12})/2$ increases as we pass from $E_{[111]}$ through $E_{[110]}$ to $E_{[100]}$. Since this is the same order in which the temperature coefficient anomaly increases, we are led to suspect that the bulk modulus and the shear coefficient C_{44} have normal temperature coefficients, while only the shear coefficient $(C_{11}-C_{12})/2$ has an abnormal temperature variation.

As was seen in the previous section, in β-brass the shear coefficient $(C_{11}-C_{12})/2$ is the sum of two terms, a positive term arising from the electrostatic interaction of the conduction electrons and the positive ions, and a negative term arising from the repulsive exchange interaction of the positive ions. The positive term varies comparatively slowly with lattice constant a, namely as $1/a^4$. On the other hand, the negative term varies rapidly with the lattice parameter. The effect of thermal expansion *per se* is therefore to decrease the negative term more rapidly than the positive term, leading to a net increase in the shear constant $(C_{11}-C_{12})/2$. Before this interpretation of the anomalous temperature coefficient can be accepted, it is necessary to estimate the order of magnitude of the positive temperature coefficient of $(C_{11}-C_{12})/2$. On using the notation of Mott and Jones,[9] we find the negative contribution to $(C_{11}-C_{12})/2$ to be proportional to $W'(r)$, where W is the exchange energy of two ions at a distance r. The temperature coefficient of this negative term is therefore $(rW''/W')\alpha$, where α is the linear thermal expansion coefficient. On taking the values given by Mott and Jones for r^2W'' and rW' in the case of copper, we obtain the value of -17 for rW''/W'. Using the average value of 15×10^{-6} for copper[12] in the range -200°C to R.T. we obtain 2.5×10^{-4} as the temperature coefficient of the negative term in $(C_{11}-C_{12})/2$. This value is of the same order of magnitude as the temperature coefficient of $E_{[100]}$ in β-brass at low temperatures, which may be obtained from Fig. 4 as 1.7×10^{-4}. The change in sign of the temperature coefficient of $(C_{11}-C_{12})/2$ at about 200°C is caused by the decrease in the coefficient which is associated with disordering, a decrease which is apparent from the work of Good.[7]

The above interpretation of the anomalous temperature coefficients of the elastic moduli leads to an interesting prediction as to the influence of pressure upon the elastic shear coefficient $(C_{11}-C_{12})/2$ of β-brass. If thermal expansion increases $(C_{11}-C_{12})/2$, then we anticipate that contraction caused by pressure will decrease this constant. An elementary computation shows this decrease will be of the magnitude of several percent per 10^3/atmospheres pressure.

The same anomaly in the temperature coefficient of $(C_{11}-C_{12})/2$ is to be expected in all β-phase alloys in which the positive ions have closed shells, as well as in the body-centered cubic element Ba and in the body-centered cubic phase of Tl. On the other hand, in the simple cubic lattices of the NaCl type the repulsive exchange interaction between adjacent ions tends to make the shear coefficient C_{44} negative. The same argument used above for β-brass would lead to the conclusion that in simple cubic lattices the temperature coefficient of C_{44} is positive, or at least only slightly negative. This is indeed the case. From the measurements of Rose,[13] Durand,[14] and Siegel[15] we find that in NaCl and in KCl the temperature coefficient of C_{44} is only one-fifth that of $(C_{11}-C_{12})/2$.

---

[12] F. C. Nix and D. MacNair, Phys. Rev. **60**, 597 (1941).
[13] F. C. Rose, Phys. Rev. **49**, 50 (1935).
[14] M. A. Durand, Phys. Rev. **50**, 449 (1936).
[15] S. Siegel, Phys. Rev. **61**, 84 (1942).

Some Stationary Distributions of Neutrons in an Infinite Medium

M. VERDE AND G. C. WICK*
Istituto Fisico dell'Università, Rome, Italy
(Received March 13, 1947)

Some stationary solutions of the transport equation describing the diffusion and slowing down of neutrons in an infinite homogeneous medium (Sections 1 and 2) are presented for the following cases: constant mean free path, power spectrum in energy and exponential behavior in space (Section 3); constant m.f.p., point source of fast neutrons (Section 4); variable m.f.p. proportional to a power of velocity, point source of fast neutrons (Section 5). For this last case the possibility of actual numerical computation of the neutron distribution is displayed on one example, approximately describing conditions in water or paraffin.

I. INTRODUCTION

THE present paper is concerned with the development of methods for the solution of the transport equation, describing the diffusion and slowing down of neutrons. Attention will be focused especially on the case of a point-source of fast neutrons embedded in an infinite hydrogenous medium.

Usually problems of this kind are attacked by means of a more elementary diffusion equation ("age theory"), which represents a reasonable approximation for most practical purposes. Nevertheless, the greater effort required in solving the more exact equation is not always wholly unrewarding.

The present work was undertaken in 1943 with a view to fill what seemed an unnatural gap in the literature. Since then the writers have become aware that problems of this kind have received a great deal of attention in connection with the development of self-sustaining chain-reactions. Accordingly, this paper has been rewritten, so as to lay the main stress on the methodological aspects of the subject, rather than on the detailed computation of special examples. The numerical results which have been obtained in one case are presented mainly as an illustration of the method. The authors hope in this way that their work will not appear as a wholly useless duplicate of other more concentrated and purposeful efforts, and that some details at least in the method will be found sufficiently new to justify publication.

The main assumptions made throughout are: (a) the medium is homogeneous and infinite, so that a Fourier transform in space can be usefully applied, and: (b) the energy of the neutrons is neither too low (say >1 ev), so that effects due to binding and thermal motion are negligible, nor too high (say <10 Mev), so that the angular distribution after an elastic collision of a neutron with a nucleus is isotropic in the center-of-gravity system.

From the start, the principal aim of this investigation was to develop a method capable of dealing with velocity-dependent mean free paths. The method finally evolved is described in Sec. 5 for a rather special example; some comments on the adaptability of the method to other cases will be found there. The study of the case of a constant mean free path, presented in Secs. 3 and 4, was almost unavoidable as a preliminary to the more complicated case. The authors first believed that if a workable complete solution could not be found for the simpler case, one could not even attempt to study the more difficult case of a variable mean free path. This proved not to be the case; for some types at least of velocity dependence it is perfectly feasible to work out the solution numerically very accurately, although the results for the simpler case are disappointingly inconclusive. One of the writers, however, hopes to show in a forthcoming paper that also the results of Secs. 3 and 4 can be refined in such a way as to yield some information about the asymptotic behavior of the neutron density at large distances from the source.

2. THE TRANSPORT EQUATION

We shall use, among others, the following notations:

* Now at Department of Physics, University of Notre Dame, Notre Dame, Indiana.

$\mathbf{v}$ and $\mathbf{r}$: velocity and position vectors for a neutron;
v_0: velocity of the fast neutrons emitted by the source;
$u=2\ln(v_0/v)$: logarithmic energy variable;
$\boldsymbol{\omega}=\mathbf{v}/v$: unit vector specifying direction of motion;
$d\omega$: element of solid angle for $\boldsymbol{\omega}$;
$l(u)$: total mean free path of a neutron (including all possible processes, as e.g., capture) considered as a function of the logarithmic energy variable;
l_s: scattering mean free path; if several species of nuclei are present in the medium an additional index may be appended to l_s, specifying the nature of the nucleus.

The Boltzmann equation for stationary distributions is too well known as to require any comment. It is written customarily in terms of the distribution function $f(\mathbf{r}, \mathbf{v})$, or the particle-density in phase-space. It is often more convenient, however, to work with the "collision-density" defined by:

$$\psi(\mathbf{r}, u, \boldsymbol{\omega}) = \tfrac{1}{2}v^3(v/l(u))f(\mathbf{r}, \mathbf{v}), \tag{1}$$

the factor $(\frac{1}{2})v^3$ being introduced because we use $d\mathbf{r}dud\omega$ as the phase-space element, and v/l being the collision probability per second.

The Boltzmann equation is then:

$$l(u)\boldsymbol{\omega}\cdot\mathrm{grad}\psi+\psi-a(\psi)=S(\mathbf{r}, u), \tag{2}$$

where S is the function representing the source distribution, and a is an operator representing the effect of collisions. Specifically, $a(\psi)d\mathbf{r}dud\omega$ represents the number of collisions per second taking place within $d\mathbf{r}$ and such that a neutron of arbitrary velocity and direction is thrown into the element $dud\omega$ by the collision. Assuming that a neutron of velocity specified by u' and $\boldsymbol{\omega}'$ suffers a collision (of any kind) let $dud\omega P(u, \boldsymbol{\omega}; u', \boldsymbol{\omega}')$ be the probability for the collision to be such that the neutron is thrown into the element $dud\omega$. Then one finds:

$$a(\psi)=\int_0^u du'\int P(u, \boldsymbol{\omega}; u', \boldsymbol{\omega}')d\boldsymbol{\omega}'\psi(\mathbf{r}, u', \boldsymbol{\omega}'). \tag{3}$$

It may be remarked that if only one nuclear species is present, the above-mentioned probability is the product of $l(u')/l_s(u')$ (representing the probability that the collision be of the scattering type) by a factor depending only on the cosine $\boldsymbol{\omega}\cdot\boldsymbol{\omega}'$ and on the ratio of the velocities (or on the difference $u-u'$). For instance in hydrogen, where $l/l_s=1$, one has

$$P(u, \boldsymbol{\omega}; u', \boldsymbol{\omega}')=(1/2\pi)e^{u'-u}\delta(\boldsymbol{\omega}\cdot\boldsymbol{\omega}'-e^{\frac{1}{2}(u'-u)}). \tag{4}$$

If many nuclear species are present, the probability is a composite of expressions of the above described type. One especially simple case arises when all mean free paths are velocity independent, or more generally if their ratios are velocity independent; then the function P is of the type:

$$P(u, \boldsymbol{\omega}; u', \boldsymbol{\omega}')=p(\boldsymbol{\omega}\cdot\boldsymbol{\omega}', u-u') \tag{5}$$

as is clearly the case for Eq. (4).

3. THE CASE OF CONSTANT MEAN FREE PATH

When all relevant cross sections—or the corresponding m.f. paths—are constant, one is naturally led to apply a Laplace-Mellin transformation with respect to the velocity, i.e., a Laplace transformation with respect to the variable u. The customary inversion formula then yields the distribution function as a superposition of terms of the type:

$$\psi\sim e^{\eta u}=(v_0/v)^{2\eta}, \tag{6}$$

η being the variable of the Laplace transform. Any such term, if taken by itself, represents a power spectrum in velocity. One finds, moreover, as in the cascade theory of showers, that such power spectra are self-sustaining, that is, they are capable of existence even if the source term S on the right-hand side of Eq. (2) is equated to zero, provided the variable u is also allowed to take negative values.[1] More accurately, this means that the source terms are relegated to infinite energies. The properties of the non-homogeneous Eq. (2) are closely related, as usual, to these solutions of the homogeneous equation, which we are now going to investigate.

3.1 Homogeneous Equation. ($S=0$).

The total mean free path being a constant, it can be chosen as a unit of length. It has to be remembered that, in the absence of a source, v_0 means an arbitrary constant velocity. With a power spectrum of type (6), we can write:

$$\psi(\mathbf{r}, u', \boldsymbol{\omega}')=e^{\eta(u'-u)}\psi(\mathbf{r}, u, \boldsymbol{\omega}'); \tag{7}$$

inserting this into (3) and remembering Eq. (5)

[1] In that case the integral in Eq. (3) with respect to u' must also extend from $-\infty$ to u.

and footnote 1, we easily find

$$a(\psi)=\int g(\omega\cdot\omega',\eta)\psi(\tau,u,\omega')d\omega', \quad (8)$$

where

$$g(\omega\cdot\omega',\eta)=\int_0^\infty e^{-\eta u}p(\omega\cdot\omega',u)du. \quad (9)$$

We may also separate the spatial coordinates, setting:

$$\psi=e^{\eta u-kz}\phi(\mu) \quad (10)$$

where μ is the z-component of ω. The choice of the z axis as the direction of exponential decrease entails no loss of generality.

Clearly we may assume ϕ to be symmetric about the z axis as is done in Eq. (10). There are also other solutions in which we are not interested just now. Developing the $\phi(\mu)$ function into a series of Legendre polynomials, we write:

$$\phi=(1/4\pi)\sum_{n=0}^{\infty}(2n+1)\phi_nP_n(\mu). \quad (11)$$

Developing also g in a series of Legendre polynomials:

$$g(\omega\cdot\omega',\eta)=(1/4\pi)\sum_{n=0}^{\infty}(2n+1)\times g_n(\eta)P_n(\omega\cdot\omega'), \quad (11a)$$

and making use of the sum-rule for spherical harmonics:

$$P_n(\omega\cdot\omega')=P_n(\mu)P_n(\mu')+\sum_{m\neq0}Y_n^{(m)}(\omega)\,Y_n^{(m)}(\omega'), \quad (12)$$

we easily find that all terms with $m\neq0$ cancel in Eq. (8), so that:

$$a(\psi)=(1/4\pi)e^{\eta u-kz}\sum_{n=0}^{\infty}(2n+1)g_n(\eta)\phi_nP_n(\mu). \quad (13)$$

Moreover, with ψ given by (10), the first term on the left-hand side of (2) becomes:

$$\omega\cdot\text{grad}\psi=-ke^{+\eta u-kz}(1/4\pi)\textstyle\sum_n\phi_n(2n+1)\mu P_n(\mu)$$
$$=-ke^{+\eta u-kz}(1/4\pi)\textstyle\sum_n\phi_n\times[nP_{n-1}(\mu)+(n+1)P_{n+1}(\mu)], \quad (14)$$

owing to a well-known property of Legendre polynomials. Substituting (10) and (14) into Eq. (2) and rearranging terms, this becomes $\sum x_nP_n(\mu)=0$, where the coefficients x_n, given by the left-hand side of Eq. (15) below, do not depend on μ. This gives the equations $x_n=0$, or:

$$(2n+1)[1-g_n(\eta)]\phi_n-k[n\phi_{n-1}+(n+1)\phi_{n+1}]=0 \quad (15)$$

for $n=0, 1, 2, \cdots$. A further condition is obtained on remarking that for (11) to be meaningful one must have:

$$\lim_{n=\infty}\phi_n=0. \quad (16)$$

Since the solution of (15) contains an arbitrary factor, we may set for instance $\phi_0=1$. Then the first of the equations (15) or:

$$[1-g_0(\eta)]\phi_0-k\phi_1=0 \quad (17)$$

determines ϕ_1, while the remaining equations determine successively $\phi_2, \phi_3 \cdots$. Thus, Eq. (15) is sufficient in itself to determine the solution completely, and Eq. (16) is an additional condition *implying a relation between η and k.*

In order to see this more clearly, we notice that since $\lim_{n=\infty}g_n=0$ the asymptotic form of Eq. (15), for $n\to\infty$, is:

$$2\phi_n-k(\phi_{n-1}+\phi_{n+1})=0, \quad (18)$$

of which two solutions are readily obtained in the form $\phi_n\sim\epsilon^n$ where ϵ is either of the two roots of the characteristic equation:

$$2\epsilon-k(1+\epsilon^2)=0. \quad (19)$$

If k is complex, or if it is real and satisfies the condition $-1<k<1$, the two roots are one larger and one smaller than unity, so that one of the solutions of (18) tends to ∞, the other to 0 when $n\to\infty$. According to a theorem by Poincaré,[2] the same applies to the system (15), Eq. (17) being omitted. The solution selected by Eq. (17) will in general be a linear combination of the two, and will thus tend to infinity. Thus, for every value of η, there will be special values

[2] N. Nörlund, *Differenzenrechnung* (Verlagsbuchhandlung Julius Springer, Berlin, 1924), Chap. 10.

of k, to be called eigenvalues henceforward, for which condition (16) may be satisfied.[3]

3.2 Series Development for Small Values of k.

We now wish to investigate the connection between η and k when k is small ($k \ll 1$), neglecting capture for simplicity. In the limiting case $k=0$, system (15) reduces to:

$$[1-g_n]\phi_n = 0 \quad \text{for} \quad n=0, 1, 2, \cdots$$

showing that either all ϕ's are $=0$, which is trivial, or one at least of the g's must be $=1$.

Equations (9) and (11a) show that $g_0=1$ when $\eta=0$; this merely expresses the normalization condition for probability. One then has:

$$k=0, \quad \eta=0, \quad \phi_1=\phi_2=\cdots=0, \quad \text{or:} \quad \psi=\text{const.} \tag{20}$$

This solution is constant in space ($k=0$) and isotropic and corresponds to the well-known Fermi solution for the energy spectrum of slowed-down neutrons. One may get also other solutions by putting $g_1=1$, or $g_2=1$, $\cdots$ but one immediately suspects that they are less significant from a physical point of view. This is also borne out by the study of the inhomogeneous problem.

We shall therefore limit ourselves to studying the solution which reduces to Eq. (20) for $k=0$. For k small, one is naturally tempted to develop $\phi_0, \phi_1, \cdots$ and η in powers of k. Closer inspection of Eq. (15) then shows immediately that these series must have the form:

$$\phi_n = k^n(\phi_{n0}+k^2\phi_{n1}+k^4\phi_{n2}+\cdots) \tag{21}$$
$$\eta = \eta_1 k^2+\eta_2 k^4+\cdots.$$

We shall not carry out this development in detail. It should be mentioned, that there is a certain arbitrariness in the development for ϕ_0, $\phi_1, \cdots$ (not in that for η!) owing to the fact that the solution can be multiplied by an arbitrary factor, which may be a function of k. One may remove this arbitrariness by setting $\phi_0=1$, for instance.

The coefficients in Eq. (21) are positive and indicate that η is a rapidly increasing function of k. For intermediate values of k it is, however, quite impracticable to try to compute all the coefficients that may be necessary in the development (21). It is much easier to ascertain the connection between η and k by a numerical investigation. One computes $g_0, g_1, \cdots$ for a given value of η, and then solves the system (15) for a tentative value of k, starting for instance with $\phi_0=1$, and determining $\phi_1, \phi_2, \cdots$ by means of the recurrence relation. Unless k is already very near to the eigenvalue, it will very soon become apparent that the solution does not satisfy the boundary condition at infinity. One then starts with a better guess for k, and so on. The work is quite similar to finding an eigenvalue of a Schrödinger equation by means of a step-by-step integration, only it is somewhat simpler.

Until now we have generally assumed that k was real; Eq. (21) shows however that η is real also for purely imaginary values of k, corresponding to a "plane wave" distribution in space. This conclusion holds as long as the series converges. We have carried out a numerical investigation for the case of pure hydrogen, Eq. (4), and the result is given in Fig. 1. When the absolute value of k exceeds a certain limit there is no longer a real value of η corresponding to it; the curve representing η as a function of k joins a lower branch corresponding to an $\eta<0$ for $k=0$, that is one of the branches we have previously neglected (and precisely the one for $g_1=1$ when $k=0$).

4. NON-HOMOGENEOUS EQUATION. CONSTANT MEAN FREE PATHS

We assume now the existence of sources distributed in space and emitting neutrons of velocity v_0. We set therefore in Eq. (2):

$$S(\mathbf{r}, u) = s(\mathbf{r})\delta(u).$$

We choose as before the total mean free path as a unit of length. Moreover we perform a Laplace-transformation with respect to u or a Laplace-Mellin transformation with respect to velocity, setting:

$$\Phi(\mathbf{r}, \eta, \omega) = \int_0^\infty e^{-\eta u}\psi(\mathbf{r}, u, \omega)du, \tag{22}$$

[3] In the forthcoming paper mentioned in Sec. 1, it will be shown that the values of k on the real strips $k<-1$ and $k>+1$, for which the roots of Eq. (19) are complex numbers of modulus "unity," and the solutions of Eq. (18) neither tend to zero nor to infinity, exhibiting an oscillating behavior, may also be considered as eigenvalues. There is thus both a discrete spectrum and a continuum of eigenvalues.

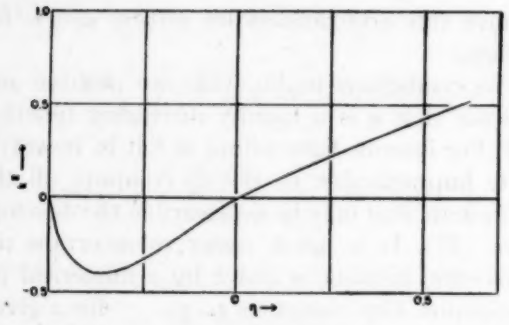

FIG. 1. Dependence of η on eigenvalue k, for real and imaginary values of k (positive and negative k^2). The descending part of the curve on the left corresponds to the lower branch mentioned in the text.

which can be inverted by means of:

$$\psi=(1/2\pi i)\int_{\beta-i\infty}^{\beta+i\infty}\Phi(\mathbf{r},\eta,\omega)e^{\nu u}d\eta, \quad (22a)$$

where β is a constant that can be arbitrarily increased, but not decreased beyond a certain limit. The equation satisfied by Φ is obtained by multiplying Eq. (2) by $e^{-\nu u}$, by making use of Eq. (5), and integrating respect to u. The term containing $a(\psi)$ must be modified as usual by means of the convolution theorem, that is by inverting the order of integrations respect to u and u'. Finally one finds easily:

$$\omega\cdot\text{grad}\Phi+\Phi-\int g(\omega\cdot\omega',\eta)d\omega'\Phi(\mathbf{r},\eta,\omega')=s(\mathbf{r}). \quad (2')$$

We shall now examine two typical source distributions.

4.1 Wave Source

We consider a source of the sinusoidal plane wave type:

$$s(\mathbf{r})=e^{-kz}/4\pi, \quad (23)$$

where k is a pure imaginary, whenever the contrary is not stated explicitly. The choice of the z axis as the wave normal does not of course imply any essential limitation. We look for a solution of the type:

$$\Phi=e^{-kz}\phi(\mu), \quad (23a)$$

suggested by the symmetry of the problem. The equation for ϕ is then:

$$\phi(\mu)-k\mu\phi(\mu)-\int g(\omega\cdot\omega',\eta)d\omega'\phi(\mu')=1/4\pi, \quad (24)$$

which can be again transformed by means of Eqs. (11) and (11a) into the system:

$$(2n+1)[1-g_n(\eta)]\phi_n-k[n\phi_{n-1}+(n+1)\phi_{n+1}]=\delta_{n0}, \quad (24a)$$

differing from (15) only for the Kronecker symbol $\delta_{n0}(=1$ if $n=0$, $=0$ otherwise) on the right-hand side. Various methods can be devised to solve this system of equations. The solution may be given, for instance, in terms of a continued fraction:

$$\phi_0=\cfrac{1}{1-g_0-\cfrac{k^2/3}{1-g_1-\cdots-\cfrac{k^2/(4n^2-1)}{1-g_n-\cdots}}}. \quad (25)$$

This can be formally derived, if one uses the first of Eqs. (24a) to express ϕ_0 in terms of ϕ_1/ϕ_0, then the second to express ϕ_1/ϕ_0 in terms of ϕ_2/ϕ_1, and so on.[4] The fraction (25) defines ϕ_0 in the whole plane of the complex k-variable, except on the real strips:

$$1<k<+\infty; \quad -\infty<k<-1 \quad (26)$$

for reasons which are disclosed by the discussion of the homogeneous system (15) (see the text following Eq. (19)). If the plane is cut along the strips (26), the function ϕ_0 is analytic and one-valued and the only singularities it possesses are poles, at which of course the fraction (25) does not converge.

If our problem were merely to compute ϕ_0 for a few real values of η and ik, the continued fraction would be very suitable, since it converges fairly well for most values of ik. But if we are interested in an integral of the type (22a) we obviously need some expression which is easier to handle than (25). Without entering into too many details, we wish to mention various possible lines of attack.

One possible method consists in developing ϕ_n in powers of k, as in the homogeneous case (see Eq. (21)). The difference is that in the present

[4] For a rigorous justification see: Perron, *Die Lehre von den Kettenbrüchen* (B. G. Teubner, Leipzig), second edition, especially Section 57.

case η is given, and *must* not be developed in powers of k. One finds for instance:

$$\phi_0=(1-g_0)^{-1} + (k^2/3)(1-g_0)^{-2}(1-g_1)^{-1}+\cdots. \quad (27)$$

The convergence radius of this development will be determined by the position of the singular points, two of which (± 1) are fixed, whilst the remaining ones (the poles) are functions of η, see below. Thus the radius will in general be a function of η; when $\eta\to 0$, the convergence radius does the same, so that the series (27) becomes useless in a very important case. Another method, which may help to avoid this disadvantage, consists in using essentially the same type of development, but without taking into account at first the inhomogeneous equation:

$$(1-g_0)\phi_0-k\phi_1=1. \quad (24b)$$

The remaining system is homogeneous, and determines only the ratios between the ϕ's. One may then develop, in powers of k, the ratio ϕ_n/ϕ_N where N is some fixed value. Two values of N are especially interesting, namely $N=0$, and $N=\infty$. In the first case one finds for instance:

$$\phi_1/\phi_0=(1/3)k[1-g_1]^{-1} + (4/45)k^3[1-g_1]^{-2}[1-g_2]^{-1}+\cdots \quad (28)$$

and inserting this into Eq. (24b) one finds ϕ_0 as the reciprocal of a power series in k. The case $N=\infty$ is not so simple because actually $\phi_\infty=0$; it may be proved, however, that, provided the g's tend to zero sufficiently quickly when N tends to infinity, one has:

$$\phi_N\sim CN^{-\frac{1}{2}}\epsilon^N, \quad \text{for large } N\text{'s}; \quad (29)$$

what one can do then, is to develop the ratio ϕ_n/C in powers of k. Finally, taking into account (24b), one finds ϕ_0 as the quotient of two power series. Although this development is somewhat complicated, we think that it is interesting, because the convergence of the power series is only limited by the *fixed* singularities at $k=\pm 1$, as a more detailed consideration shows.

We wish to mention here also another possible method, which consists in developing the solution in powers of ϵ (instead of k). When k is small, one has from Eq. (19):

$$\epsilon=k/2+k^3/8+\cdots \quad (30)$$

so that the two variables k and ϵ are not essentially different; but for large values of k the situation changes considerably. In fact, in the plane of the complex variable ϵ, the interior of the circle:

$$|\epsilon|=1 \quad (31)$$

corresponds to the whole plane of the k-variable, cut along the strips (26); in particular the whole imaginary axis for k is represented on the segment from $\epsilon=-i$ to $\epsilon=+i$. Therefore, *as far as the convergence of the power series under examination is limited by the fixed singularities at:* $k=\pm 1$ (or: $\epsilon=\pm 1$), the power series in ϵ is *much more powerful* than that in k. In fact, the fixed singularities prevent us from reaching any imaginary values of k beyond $k=\pm i$, whilst there is no limitation whatever in the ϵ-development. These advantages will be fully exhibited in the next section.

Let us now turn our attention to the isolated poles of the solution. These arise in the following way. We have seen already that for each value of η there are in general k-values, for which the complete homogeneous system (15) (*including* the equation for $n=0$) admits a solution satisfying Eq. (16). From the preceding discussion it is clear that the inhomogeneous system (24a) does not then have any solution satisfying condition (16). In other words the eigenvalues k give the poles of the solution of the inhomogeneous case. It is possible to investigate the behavior of the function ϕ_0, Eq. (25), when k approaches one of these poles, say $\bar{k}$. In fact, call $\bar{\phi}_n$ the solution of the complete homogeneous system corresponding to $\bar{k}$, and write Eq. (15) for this $\bar{\phi}_n$. Multiplying this equation by ϕ_n and Eq. (24a) by $\bar{\phi}_n$ and subtracting one from the other, and summing with respect to n, one finds:

$$(k-\bar{k})\sum_{n=1}^{\infty} n(\phi_{n-1}\bar{\phi}_n+\phi_n\bar{\phi}_{n-1})=\bar{\phi}_0. \quad (32)$$

Now we must have:

$$\lim_{k=\bar{k}}(\bar{k}-k)\phi_n=N\bar{\phi}_n, \quad (33)$$

where N is a normalization factor. Equation (32) then yields:

$$2N\sum_{n=1}^{\infty} n\bar{\phi}_n\bar{\phi}_{n-1}=\bar{\phi}_0. \quad (34)$$

Equations (33) and (34) describe the behavior of the solution in the neighborhood of $\bar{k}$.

4.2 Point Source

A point source $s(\mathbf{r})=\delta(\mathbf{r})$ and the corresponding solution of Eq. (2′) can be built up from the wave source (23) and the corresponding solution, from the Fourier expansion

$$\delta(\mathbf{r})=(1/2\pi i)^3\int e^{-\mathbf{k}\cdot\mathbf{r}}d\mathbf{k}, \tag{35}$$

where the integrations with respect to the three components of $\mathbf{k}$ run from $-i\infty$ to $+i\infty$. Since we are now considering wave-sources with an arbitrary direction of propagation, it is clear that Eqs. (23a) and (24) still hold, provided we understand by μ the cosine of the angle between the velocity vector (or ω) and the propagation vector $\mathbf{k}$. We then have the solution of Eq. (2′) in the form:

$$\Phi=(1/2\pi i)^3\int e^{-\mathbf{k}\cdot\mathbf{r}}\phi(\omega\cdot\mathbf{k}/k)d\mathbf{k}\quad(k=|\mathbf{k}|). \tag{36}$$

We are mainly interested in the density of slow neutrons of a given velocity, irrespective of the direction of the velocity, which is:

$$\int\Phi d\omega=(1/2\pi i)^3\int e^{-\mathbf{k}\cdot\mathbf{r}}\phi_0(\eta,k)d\mathbf{k}, \tag{37}$$

where ϕ_0 is of course the function given by Eq. (25), but its dependence on both η and k is now explicitly indicated for the sake of clarity. Performing the integrations with respect to the direction of $\mathbf{k}$, one naturally finds that the density (37) only depends on the distance $r=|\mathbf{r}|$ from the point source, and not on the direction of $\mathbf{r}$:

$$\cdots=-(1/2\pi r)(1/2\pi i)\int_0^{+i\infty}(e^{kr}-e^{-kr})\phi_0(\eta,k)kdk,$$

which can be further simplified to:

$$\int\Phi d\omega=-(1/2\pi r)(\partial/\partial r)(1/2\pi i)\times\int_{-i\infty}^{+i\infty}e^{-kr}\phi_0(\eta,k)dk. \tag{38}$$

In order to obtain the density of neutrons of a given energy we must still invert the Laplace-Mellin transform by means of Eq. (22a) so that finally the quantity we are interested in is given by:

$$\int\psi d\omega=-(1/2\pi r)(\partial/\partial r)X(r,u)\text{ with:}$$

$$X(r,u)=(1/2\pi i)^2\int_{\beta-i\infty}^{\beta+i\infty}e^{\eta u}d\eta\int e^{-kr}\phi_0(\eta,k)dk. \tag{39}$$

It is not possible to evaluate these integrals in closed form. It is possible, however, to find approximate expressions for them in the limiting case when u is very large. Strictly speaking the expression obtainable is an asymptotic evaluation for $u\to\infty$ (and r kept fixed or increasing only like the square root of u).

Since we understand that this case has been studied very thoroughly, we shall be content with a few remarks. If u is large it is convenient in Eq. (39) to perform the integration with respect to η first. The integral:

$$\int e^{\eta u}\phi_0(\eta,k)d\eta \tag{40}$$

may be evaluated approximately by pulling the integration path to the left in the η-plane until one meets the first singularity. One may show that this is given by Eq. (21). The integral is thus given by the residue at this singularity, plus the contributions from the remaining singularities. One may show aso that the real part of the second singularity is smaller than that of the first by about $\frac{1}{2}$ (in the hydrogen case) for small k's, so that the contribution deriving from it is of the order of $e^{-u/2}$ with respect to the first residue. The computation of this first residue is quite easy if k is small, and it may be shown later that only small values of k contribute appreciably to the final result in Eq. (39). Namely, if k is small Eq. (21) converges rapidly, so that the solution of the homogeneous system (indicated later with $\bar{\phi}$) is known, and it is possible to express the normalization factor N in Eq. (34) by means of a rapidly convergent series in k. The residue is easily expressed in terms of N and of the derivative $d\eta/dk$, η being the first pole for a given k (comp. Eqs. (33) and (21)). If the residue is indicated by

$R(k)$, being a power series in k, Eq. (39) takes the form:

$$X(r, u) = (1/2\pi i)\int_{-i\infty}^{+i\infty} e^{-kr+u\eta(k)}R(k)dk. \quad (41)$$

Now since k is imaginary, η is negative, and the factor $e^{u\eta(k)}$ decreases very rapidly (large u!) as k increases. One may therefore retain only the first term of the second Eq. (21), or if a better approximation is wanted use an expansion:

$$e^{u\eta(k)} = \exp(u\eta_1 k^2)(1+u\eta_2 k^4+\cdots)$$

so that finally (41) reduces to a Gauss integral, plus terms of higher order, also derivable from the Gauss integral.

5. NON-HOMOGENEOUS EQUATION. VARIABLE MEAN FREE PATH

Quite often, for instance, if the slowing-down medium contains hydrogen, the approximation of constant mean free path is very far from being satisfactory. We want to show now that with suitable assumptions on the velocity dependence of the mean free path, one can still develop an accurate method of solution. The experimental results on this dependence can often be represented quite well by a law:

$$l = a+bv^c \quad (42)$$

with suitable constants a, b, c. A law of this kind may be studied with the methods now to be described. But the problem certainly becomes very involved. If, however, the constant a is neglected, one has a problem that, although more complicated than the case of constant mean free path under some respects, nevertheless presents some features which make it easily amenable to numerical treatment.

Instead of developing the method in general we prefer to examine this case thoroughly, that is, also numerically, for one special example, namely a mixture of hydrogen and of infinitely heavy nuclei, which may be regarded as a sufficiently good model for water or paraffin. We neglect capture, and assume for simplicity that the ratio of the scattering mean free paths l_1 for hydrogen, and l_2 for the heavy nuclei is independent of velocity, so that Eq. (5) is valid. More specifically:

$$p(\omega\cdot\omega', u-u') = (l/2\pi l_1)e^{u'-u}\delta(\omega\cdot\omega' - e^{\frac{1}{2}(u'-u)}) + (l/4\pi l_2)\delta(u-u'),$$

so that, setting $\omega\cdot\omega' = \mu$, one easily finds:

$$g(\mu, \eta) = (l/\pi l_1)\mu^{\eta+\frac{1}{2}} + (l/4\pi l_2) \quad \text{if} \quad \mu>0, \quad (43)$$
$$= l/4\pi l_2 \quad \text{if} \quad \mu<0.$$

Multiplying both sides of Eq. (11a) by $P_n(\mu)$ and integrating with respect to μ from -1 to $+1$, one then finds:

$$g_n = (2l/l_1)\int_0^1 \mu^{2\eta+1}P_n(\mu)d\mu + (l/l_2)\delta_{n0}, \quad (43a)$$

e.g.,

$$g_0 = (l/l_1)(\eta+1)^{-1} + l/l_2$$
$$g_1 = (l/l_1)(\eta+\tfrac{3}{2})^{-1} \quad (43b)$$
$$g_2 = (l/l_1)[\tfrac{3}{2}(\eta+2)^{-1} - \tfrac{1}{2}(\eta+1)^{-1}]; \text{ etc.}$$

Making use of the equation:

$$(n+1)P_{n+1} - \mu P'_{n+1} = -nP_{n-1} - \mu P'_{n-1}$$

one can also easily prove the recurrence relation:

$$g_{n+1} = [(2\eta+2-n)/(2\eta+3+n)]g_{n-1}, \quad \text{for} \quad n>1, \quad (43c)$$

which allows one to compute quickly all g's.

We have found that the law:

$$l = (v/v_0)l(v_0) \quad (42a)$$

represents the data for water or paraffin with very good accuracy down to energies of the order of 100 kev. In other words in Eq. (42) we shall set $a=0$, and $c=1$. But the development would be almost exactly the same if c were $\neq 1$. Of course the assumption that the mean free path tends to zero at zero velocity means that we will grossly underestimate the diffusion of the neutrons in the last stages of slowing down. On the other hand the region between say 6 Mev and 100 kv is already large enough, and the corresponding variation of the mean free path is so strong that it is interesting to investigate what happens in this phase of the slowing down.

We take now $l(v_0)$ as a unit of length. Insert-

ing (42a) into Eq. (2) that is writing:

$$l(u)=e^{-u/2},$$

assuming again that $S(\mathbf{r}, u)=S(\mathbf{r})\delta(u)$, and using the transformation (40) one finds instead of Eq. (2′):

$$\omega\cdot\text{grad}\Phi(\eta+\tfrac{1}{2})+\Phi(\eta)$$
$$-\int g(\omega\cdot\omega', \eta)d\omega'\Phi(\mathbf{r}, \eta, \omega')=s(\mathbf{r}). \quad (44)$$

Again we consider a wave source, Eq. (23); going again through the same steps, Eqs. (23a), (24), and (24a), we find instead of Eq. (24a) the following

$$(2n+1)[1-g_n(\eta)]\phi_n(\eta)-k\{n\phi_{n-1}(\eta+\tfrac{1}{2})$$
$$+(n+1)\phi_{n+1}(\eta+\tfrac{1}{2})\}=\delta_{n0}. \quad (45)$$

Mathematically this is a much more difficult system of equations than (24a); η, instead of appearing simply as a parameter, is a variable within the equation itself. In fact, (45) is a difference equation in *two* independent variables, n and η; very little is known on the mathematical properties of these equations. One may guess, however, what they are, on the simplifying assumption that one may neglect all ϕ_n's with an n larger than some large value N.

This is an approximate way of taking into account condition (16). One has then to do with a finite system of difference equations, and one can apply known theorems.[2] It appears then that in order to define the solution completely, it is necessary to take into account the behavior of $\phi(\eta)$ when η tends to infinity in the complex plane in a direction forming an acute angle with the positive real axis. This behavior can be easily inferred from Eq. (22), because when $\eta\to\infty$ as stated the contribution to the integral arises entirely from the neutrons of highest energy, i.e., the primary neutrons. One then finds the condition:

$$\lim_{\eta\to\infty}\phi_n(\eta)=Q_n(1/k)$$
$$=\tfrac{1}{2}\int_{-1}^{+1}P_n(z)dz/(1-kz). \quad (46)$$

This condition selects among the infinity of possible solutions the so-called "fundamental solution" which is, however, generally defined by means of formulae so involved that they are of little use for computation.

There is, however, the fortunate circumstance that if we try to develop ϕ in powers of k, we find that the development is perfectly definite, and the coefficients of the development satisfy the condition (46) for the fundamental solution. There is little doubt, therefore, although no rigorous proof is available, that for small values of k one gets in this way the correct solution. Actually, instead of the k-development, we shall use, as indicated in Section 4, the more powerful development in powers of ϵ, which allows us to extend the solution analytically to a much wider field, and in fact, can be used for numerical computation up to sufficiently large imaginary values of k, as will be presently shown.

Let us, however, first discuss an obvious, but important, property of the system (45). We know that for large values of $\Re(\eta)$ the solution is a regular analytic function of η, this being a general property of Laplace transforms. Suppose for a moment the solution is known in a strip: $\eta_0\leq\Re(\eta)\leq\eta_0+\frac{1}{2}$, where η_0 is some large positive number; then by means of Eq. (45) we can move in steps $\Delta\eta=-\frac{1}{2}$ towards the left in the complex η-plane, extending the solution to smaller and smaller values of $\Re(\eta)$. No singularity can occur in this process, until some of the factors $(1-g)$ become zero, and in that event we shall find a pole.

In the special case, Eq. (43), the first pole one meets is the root $\eta=0$ of the equation $1-g_0=0$, and this must be true also in many other cases. The next pole is the root $\eta=-\frac{3}{2}+l/l_1$ of the equation $1-g_1=0$, and so on. For higher n-values one finds also complex roots. The essential point in all this is that the poles are entirely determined by the coefficients g, and *do not at all depend on* k. One can easily convince oneself that this behavior which is so different from what we found in the case of constant mean free path, is entirely caused by the fact that here the mean free path is assumed to tend to zero for zero velocity. The general law (42) would not lead to such a simple behavior, and therein lies the great simplification implied in the law (42a). One can say indeed that for purposes of numerical computation the present case is simpler than the case

TABLE I. Computation of $f(k)$.

$ik=0$	0.12	0.18	0.289	0.471	0.615	0.703	0.912	1.12	1.33_5	1.56_5	1.96	2.10
$f(k)=1$	0.98	0.96	0.894	0.756	0.64	0.57	0.43	0.32	0.24	0.18	0.1	0.06

TABLE II.

$r=0$	0.25	0.5	0.75	1	1.25	1.5	1.75	2	2.5	3.26	3.89	4.76	5.18
$I(r)=2.30$	2.07	1.55	1.05	0.68	0.44	0.29	0.18	0.12	0.05	0.025	0.0084	0.0024	0.0013

of constant mean free path, notwithstanding the higher complexity of Eq. (45).

If one is interested in the distribution of neutrons having velocities much smaller than the initial one, it will be enough to know ϕ_0 in the neighborhood of the pole $\eta=0$; this will enable one to compute the residue of the integral (22a) at this pole, while the contribution from poles lying more to the left will be negligible. Now Eq. (45) for $n=0$, shows that, when $\eta\approx 0$:

$$\phi_0(\eta)\approx[1-g_0(\eta)]^{-1}\{1+k\phi_1(\tfrac{1}{2})\} \tag{47}$$

so that it is sufficient to have the development of ϕ_1 for one definite value $\eta=\frac{1}{2}$. This is the simplification which makes a numerical treatment easily possible. In fact, once the variable η is eliminated, it becomes a possible program to compute ϕ_0 numerically for closely spaced values of k, so that one can compute, again numerically, the Fourier integral of Eq. (38), for a sufficient number of values of the distance r. The method becomes inaccurate only at very large values of r, where, however, a different procedure can be adopted (see below).

Here is, very briefly, how the computation can be slightly simplified. First we put:

$$\begin{aligned} U_n&=\{\Gamma(\tfrac{1}{2})\Gamma(1+\tfrac{1}{2}n)/\Gamma(\tfrac{1}{2}+\tfrac{1}{2}n)\}\phi_n \\ E_n(\eta)&=4\{\Gamma(1+\tfrac{1}{2}n)/\Gamma(\tfrac{1}{2}+\tfrac{1}{2}n)\}^2 \\ &\quad\times(2n+1)^{-1}[1-g_n(\eta)]^{-1}, \end{aligned} \tag{48}$$

whereby Eq. (45) becomes:

$$\begin{aligned} 4U_n(\eta)-2kE_n(\eta)\{&U_{n-1}(\eta+\tfrac{1}{2}) \\ &+U_{n+1}(\eta+\tfrac{1}{2})\}=\pi E_0(\eta)\delta_{n0}. \end{aligned} \tag{49}$$

On account of Eq. (19) we then set $k=2\epsilon/(1+\epsilon^2)$ and multiply the whole equation by $(1+\epsilon^2)$. Developing U_n in a series of powers of ϵ which (comp. Eq. (31)) starts with ϵ^n:

$$U_n=\epsilon^n\{U_{n0}+U_{n1}\epsilon^2+U_{n2}\epsilon^4+\cdots\} \tag{50}$$

we find the recurrence relation:

$$\begin{aligned} U_{nm}(\eta)+U_{n,m-1}(\eta)-E_n(\eta)&\\ \times\{U_{n-1,m}(\eta+\tfrac{1}{2})+U_{n+1,m-1}(\eta+\tfrac{1}{2})\}&\\ =(\pi/4)E_0(\eta)\delta_{n0}(\delta_{m0}+\delta_{m1}),& \end{aligned} \tag{51}$$

which yields the various coefficients in the following order: U_{00}, U_{10}, U_{01} and U_{20}, U_{11} and U_{30}, $\cdots$. As indicated in Eq. (47), we need only the coefficients of the development for one value of η, or $\eta=\frac{1}{2}$, but in the course of the computations owing to the peculiar structure of Eq. (49) values $\eta=1$, $\eta=\frac{3}{2}$, $\eta=2$, $\cdots$ occur. In order to compute the residue of ϕ_0 at $\eta=0$ up to the tenth power of ϵ^2, we found it necessary for instance to make use of the values of $E_n(\eta)$ for the following values of the variables:

$$n=0, 1, 2, \cdots, 10 \quad\text{and}\quad \eta=m+\tfrac{1}{2}n,$$
$$\text{with}\quad m=0, 1, \cdots, 10-n.$$

In order to determine the value of the ratio l_1/l_2 to be used in the computation it was necessary to make some compromise between the experimental values at high and at low energies. The value $l_1/l_2=0.27$ was finally adopted. With this value the first ten coefficients in the development of ϕ_0 were computed, finding:

$$\begin{aligned} \phi_0(\eta)=U_0(\eta)\approx(l_1/l)(1/\eta)\{&1+5.586\epsilon^2 \\ &+15.609\epsilon^4+31.143\epsilon^6+52.240\epsilon^8 \\ &+79.420\epsilon^{10}+113.259\epsilon^{12}+154.40\epsilon^{14} \\ &+203.52\epsilon^{16}+261.37\epsilon^{18} \\ &+330.35\epsilon^{20}+\cdots\} \end{aligned} \tag{52}$$

for $\eta\approx 0$. The bracketed series is a function of ϵ

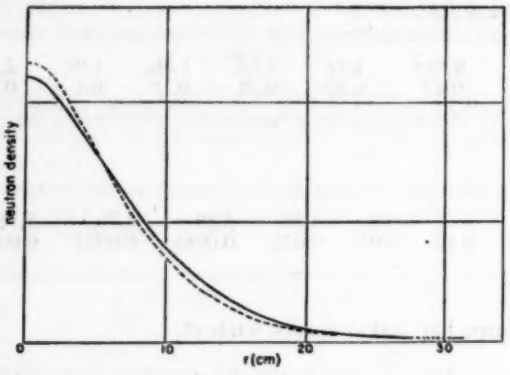

FIG. 2. Dependence of neutron density on the distance for a D+D source. Dotted line theoretical, full line experimental.

and hence of k, which we shall indicate by $f(k)$. The values in Table I were computed by means of Eq. (52). The table indicates that it is quite feasible to compute the function $f(k)$ by means of Eq. (52) up to a point where it is already fairly small. A diagram of the function resembles roughly a gaussian curve, but the tail falls off more slowly than a gaussian, and rather more like an exponential. This also permits one to extrapolate the values of $f(k)$ to values of $ik>2.1$.

Inserting (52) into the integrals (22a), (39), one finds that for large u, or for low velocities, ψ becomes velocity independent. This can be easily understood if one reflects that with a law $l\sim v$, the diffusion of neutrons comes practically to a stop for sufficiently low velocities so that the space distribution tends to a limit for $v\to 0$. The local energy spectrum must then finally coincide with the over-all spectrum which is given by the well-known Fermi law: $dN=l(v)dv/v^2$ which means $\psi=$const.

The space distribution is given by the formula:

$$\int \psi d\omega \sim r^{-1}\int_0^{i\infty} kf(k)\sin(ikr)dk. \qquad (53)$$

By means of Table I, this function has been evaluated numerically for the first ten r-values in Table II. When r becomes very large the evaluation by this method becomes too uncertain; accordingly, the last four values listed were obtained by means of the saddle-point method to be described later. It has to be remembered that r in Table II is really the distance from the source measured in terms of the mean free path of the primary neutrons. Thus on assumption (42a), the limiting distribution in space is given by a universal function; if the initial energy is varied, one has merely to change the unit in which distances are measured. This is of course only approximately true, mainly owing to the fact that the mean free path does not really become zero at zero velocities. Actually formula (53) should hold for neutrons whose final energy is sufficiently small (so that the contribution from the neglected poles is really negligible) and at the same time sufficiently large for formula (42a) to be still valid. It would, however, be perfectly possible to compute the contribution from the next pole to the left of $\eta=0$.

5.1 Comparison With Experiment

If the function on the right-hand side of Eq. (53), which we may indicate by $I(r)$, were correct down to 1 ev it could be directly compared with measurements on Rh or Ag resonance neutrons. The most accurate measurements, however, are made on thermal neutrons, and in order to get the distribution for these neutrons it becomes necessary to apply diffusion theory. One then finds the distribution:

$$I_{th}(r)=(1-A'\Delta)^{-1}I(r)$$
$$=(1/r)\int_0^{\infty} yf(iy)\sin(yr)\times(1+A'y^2)^{-1}dy, \qquad (54)$$

where $A'=D\tau/l^2(v_0)$, D being the diffusion constant and τ the mean lifetime of thermal neutrons.

The integral (54) can be computed just as easily as (53). It is moreover possible in this computation to include also a correction for the defects of formula (42a) below 100 kev. Indeed if we start with neutrons of say 6 Mev, it is clear that by the time their energy is reduced by a factor 60, their distribution in space has flattened and their angular distribution has become isotropic to such an extent that age theory is henceforward quite a good approximation. The distribution of resonance neutrons should then be given by:

$$I_{res}(r)=e^{A\Delta}I(r)=(1/r)\int_0^{\infty} yf(iy)\sin(yr)\times\exp(-Ay^2)dy, \qquad (55)$$

where A is the "age" of 1-ev neutrons starting from 100 kev, or preferably the difference between the ages as computed from Eq. (42a) and the real experimental dependence of the mean free path on velocity. According to Bethe[5] the age in water is given by:

$$\text{Age} = 0.8 \int^{u} l^2(u)du, \tag{56}$$

and in this way an age difference was computed: $A = 7$ cm^2 when formula (42a) was adjusted to fit the experimental value at an energy of 3.5 Mev. Applying corrections (54) and (55) contemporarily one then should take:

$$I_{th} = (1 - A'\Delta)^{-1} e^{A\Delta} I(r) \tag{57}$$

expressing of course A in units $l^2(v_0)$.

A comparison with experiment was made in two cases. First we took the distribution of thermal neutrons from the reaction D+D, as measured by Amaldi, Hafstad, and Tuve[6] with incident deuterons of 0.74 Mev. This source is not quite isotropic, but we assumed for the energy of the primary neutrons the value which may be computed for the neutrons emitted in the direction of observation (at 40° from the direction of the deuteron beam), namely 3.5 Mev. In this case we assumed $l(v_0) = 6.8/1.27 = 5.35$ cm. In Fig. 2 the theoretical curve (dotted) was normalized to coincide with the experimental (full) curve at 5 cm. It should be realized that no adjustment in the unit of length was effected in order to obtain the fairly good agreement of the results. The values for large r were computed with the same saddle-point method, that was used for the computation of $I(r)$.

Another comparison was made with measurements on thermal neutrons from the D+B reaction,[7] with 0.85-Mev deuterons. In this case we did not expect a good agreement, because we assumed the spectrum of the primary neutrons to consist of four lines of energy 14, 9.77, 6.85, and 4.69 Mev respectively, while there are indications that also considerably slower neutrons are emitted. We did not take these into account because we had no reliable data. The relative intensities of the lines were assumed to be in the ratios: 1:2:1:3. The distributions corresponding to the four lines were computed separately with the following data:

$$l(v_0) = 17.7 \quad 12.1 \quad 8.7 \quad 6.45 \text{ cm}$$
$$1/(A'+A) = 15.2 \quad 11.2 \quad 7.1 \quad 4.3$$

(the value of A had to be revised each time so as to take into account the deviation of the experimental law from formula (42a). The computation was greatly simplified by assuming that one could replace

$$(1 - A'\Delta)^{-1} e^{A\Delta} \quad \text{with} \quad (1 - [A'+A]\Delta)^{-1},$$

and moreover that one could interpolate linearly with respect to $(A'+A)$. This should not be very inaccurate since A' and A are small. The result in Fig. 3 shows a deviation in the direction to be expected if the spectrum contains slower neutrons in addition to the four lines taken into account.

5.2 Evaluation of the Integrals (53), (54) for Large r

Let us write for instance:

$$I(r) = (1/2ir) \int_{-i\infty}^{i\infty} kf(k)e^{kr}dk, \tag{58}$$

and deform the integration path in the complex

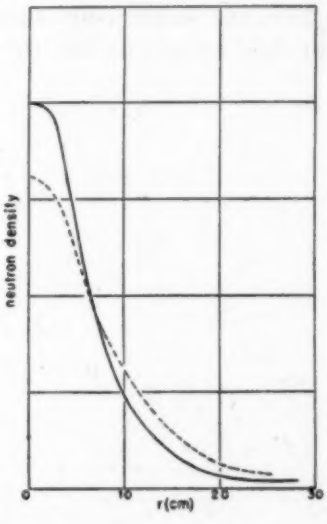

FIG. 3. Neutron density for a D+B source. Full line experimental. Dotted theoretical, not including slow part of primary spectrum.

[5] H. A. Bethe, Rev. Mod. Phys. 9, 69 (1937), esp. p. 129.
[6] E. Amaldi, L. R. Hafstad, and M. A. Tuve, Phys. Rev. 51, 896 (1937).
[7] Amaldi, unpublished.

k-plane to the left, so that it passes through a real point k_0 such that $-1<k_0<0$. If k_0 moves towards the point $k=-1$, $f(k_0)$ tends rapidly to infinity while the exponential factor decreases rapidly (if r is large). As a consequence there is a saddle-point, and we let k_0 coincide with this saddle-point. Moreover we put:

$$f(k)=e^{g(k)} \tag{59}$$

and develop $g(k)$ in powers of $k-k_0$ in the usual way. The known coefficients in Eq. (52) are in sufficient number to allow the computation of $g(k)$ from $k=0$ to about $k=-0.85$ or $\epsilon^2=0.3$. Now it is quite certain, on the basis of formula (61) below, that the conditions for a rigorous application of the saddle-point method are not satisfied even for a very large r. The situation is somewhat similar to that encountered, if one were trying to compute the integral:

$$(1/2\pi i)\int_{\beta-i\infty}^{\beta+i\infty} e^{kr}k^{-\rho}dk=r^{\rho-1}/\Gamma(\epsilon) \tag{60}$$

by a saddle-point method. One would find the value:

$$r^{\rho-1}/\{\rho^{\rho-1}e^{-\rho}(2\pi\rho)^{\frac{1}{2}}\},$$

which according to Stirling's formula coincides with (60) only if ρ is large. In our case we may assume $\rho=1.77$, and therefore the condition is not satisfied. However, the error in Stirling's formula is only about ten percent: we have applied, therefore, the saddle-point formula as an empirical method to extrapolate the results to larger distances. In this way the four last values were computed in Table II, and the same was done in the computations underlying the diagrams 2 and 3.

We may also venture a hypothesis about the asymptotic behavior of such integrals for large r. We could of course derive this behavior rigorously if we knew what type of singularity $f(k)$ possesses at the point $k=-1$, but we have no method for knowing this. We may observe, however, that the coefficients in the development (52) are remarkably close to those of a function:

$$f=C(1-\epsilon^2)^{-2\rho}$$

with $C=2.15$ and $2\rho=3.55$. The first coefficients of course do not coincide, but the agreement becomes quite good after the fourth coefficient. This might indicate that the singularity is well represented by a formula of the above type, which when translated in terms of the variable k would give:

$$f(k)\sim 0.054(1+k)^{-\rho}. \tag{61}$$

Inserting this into formula (53) and remembering Eq. (60) one finds easily (one should really use a Tauberian theorem):

$$I(r)\sim 0.18r^{-0.22}e^{-r},$$

which should hold, however, only for values considerably larger than any in the table. It is unnecessary to stress that this is merely a guess.

Our thanks are due the Nuclear Physics Center of the C.N.R. for support given to this work.

The Theory of Alpha-Radioactivity*

MELVIN A. PRESTON
*Department of Mathematics, University of Toronto,** Toronto, Canada*

(Received October 21, 1946)

A number of authors have developed the theory of α-radioactivity in the case of zero angular momentum of the escaping particle. For $l\neq 0$, formulae have also been given but it is shown that these are inaccurate. In order to discuss the case of non-zero values of l, the one-body theory with a rectangular potential well is treated rigorously. A suitable integral representation of the confluent hypergeometric function is developed by the method of steepest descent into an asymptotic series which represents the solution of the wave equation outside the nucleus for $l=0$. Solutions for $l\neq 0$ are obtained from this by recursion operators. Boundary conditions at the nuclear radius give two equations linking the radius of the nucleus and the depth of its potential hole with the decay constant and the energy of the emitted α-particles. The usefulness and reliability for this problem of the one-body model are examined (Section 6). A re-evaluation of nuclear radii has been performed and the results are tabulated. The possibility that the decay constant, for fixed energy, is not a monotonic function of l but has an initial rise is discussed. A quantitative study is made of the $\lambda-E_\alpha$ relationships in a few α-ray spectra with "fine structure."

1. INTRODUCTION

THE quantum-mechanical theory of spontaneous α-particle radioactivity has been treated by a number of authors,[1–8,11] since the first independent papers of Condon and Gurney[9] and Gamow[10] in 1928. In these papers attention has been centered on the case $l=0$. Gamow[5] has given a formula for $l\neq 0$. In addition to the approximations used in developing the formula for $l=0$, there are two objections which may be raised to Gamow's formula. Firstly, there is no examination of the possibility that the factors which involve the wave function inside the nucleus may depend on l. This point is discussed more fully below. Secondly, ignoring the first objection, Gamow's approximations give incorrect numerical results. For example, his formula (58)[12] gives a correction to the exponent amounting to 0.86σ in the case of Ra decay; accurate numerical integration of the WKB integral gives 0.17σ. (σ is the ratio of "centrifugal" to Coulomb potential at the nuclear radius.) This error in Gamow's theory arises from two sources: (1) Over a significant portion of the range of integration $\sigma r_0/r$ is comparable with $1-Er/2Ze^2$, although it is treated as small. (2) The ratio of nuclear radius to the classical radius of closest approach is about 0.25 which actually is not sufficiently small to permit some of the approximations necessary to obtain Gamow's formula. Also the WKB method is not too reliable itself in that an expression which should be negligible with respect to unity:[12]

$$\frac{\hbar}{(2m)^{\frac{1}{2}}}\left|\frac{d}{dr}\left[\frac{2Ze^2}{r}+\frac{\hbar^2 l(l+1)}{2mr^2}-E\right]^{\frac{1}{2}}\right|,$$

is not particularly small, i.e., it is greater than 0.25 for about one quarter of the range of integration.

A valid formula for $l\neq 0$ could be obtained by more refined considerations along the lines employed by Gamow, but the integrals do not lend themselves to simple treatment and it was therefore decided to make the calculations as rigorous as possible from the beginning. Thus the purpose of this paper is to find formulae for $l\neq 0$; to do so it has been found necessary to re-derive the treatment for $l=0$, although here no significant new results are obtained.

The theory should lead to a relationship be-

* The major part of this work was conducted with the assistance of a National Research Council of Canada Studentship.

** Now at the Department of Mathematical Physics, The University of Birmingham, England.

[1] T. Sexl, Zeits. f. Physik **81**, 163 (1933).
[2] M. Frenkel, Zeits. f. Physik **95**, 599 (1935).
[3] J. Kudar, Zeits. f. Physik **53**, 61, 95, 134; **54**, 297; **57**, 710 (1929).
[4] C. F. von Weizsacker, *Die Atomkerne* (Akad-Verlagsgesellschaft, Leipzig, 1937), p. 95.
[5] G. A. Gamow, *Constitution of Atomic Nuclei and Radioactivity* (Cambridge, 1937).
[6] O. Rice, Phys. Rev. **35**, 1538 (1930).
[7] H. A. Bethe, Rev. Mod. Phys. **9**, 161 (1937).
[8] F. Rasetti, *Elements of Nuclear Physics* (Prentice-Hall, Inc., New York, 1936).
[9] Condon and Gurney, Nature **122**, 439 (1928) and Phys. Rev. **33**, 127 (1929).
[10] G. A. Gamow, Zeits. f. Physik **51**, 204 (1928).
[11] H. A. Bethe, Phys. Rev. **50**, 977 (1936); Kahan, Comptes rendus **206**, 1289 (1938).
[12] See reference 5, p. 103 and p. 91.

tween the decay constant for the process and the energy of emission of the α-particle, reproducing the experimental results expressed in the Geiger-Nuttall law.[13] We shall see that the relationship is contained in an equation involving two undetermined constants, the nuclear *radius* and *potential*; there is a second equation connecting these quantities and the energy of emission. As has been pointed out,[14] in most of the previous work the depth of the potential has been removed by approximate assumptions from the final results, thus obtaining an equation involving the radius of the nucleus as the only undetermined quantity. Sexl[1] and M. Frenkel[2] have improved on these theories, but their work permits of simplification and, in common with all previous theories, is not adapted to the non-zero values of l.

2. FORMULATION OF THE PROBLEM

We represent the action of the nucleus on the α-particle by a force field with a rectangular hole potential V. The accuracy of this model is discussed in Sec. 6. $V=U$, a constant, for $r<r_0$, $V=2Z\epsilon^2/r$, for $r>r_0$, where Z is the charge number of the product nucleus, ϵ is the elementary charge, r is the distance from the center of the product nucleus, r_0 is the "radius of the product nucleus."

All dynamical quantities are modified to refer to the system in which the product nucleus is at rest. Corrections for recoil are made when numerical calculations are performed. α-particles in the sphere $r<r_0$ have a finite probability λ of piercing the potential barrier and emerging with energy E_a. We assume a solution u of the time-dependent Schrödinger equation in the form

$$\begin{aligned} u&=\psi(x,y,z)\exp(-iE_at/\hbar)\exp(-\tfrac{1}{2}\lambda t)\\ &=\psi(x,y,z)\exp(-iEt/\hbar),\end{aligned}$$

introducing the "complex eigenvalue"

$$E=E_a-\tfrac{1}{2}i\hbar\lambda. \tag{2.1}$$

Then uu^* is proportional to $e^{-\lambda t}$, indicating exponential decay. This computational device of complex eigenvalues was first introduced by Gamow[10] and since used and justified by Kudar,[3] Sexl[1] and von Weiszacker.[4]

We require the following of ψ: (a) at $r=0$, ψ is finite, (b) at $r=r_0$, ψ and $d\psi/dr$ are continuous, (c) for $r>r_0$, ψ represents an outgoing wave. Since V is spherically symmetrical,

$$r\psi=\sum_l \mathrm{X}_l(r)P_l(\cos\theta),$$

and

$$\begin{aligned} &d^2\mathrm{X}_l/dr^2+(2m/\hbar^2)\\ &\quad\times[E-V-\hbar^2l(l+1)/2mr^2]\mathrm{X}_l=0, \end{aligned}\tag{2.2}$$

where m is the reduced mass of the α-particle, and P_l are spherical harmonics.

Inside the nucleus, $V=U$ and therefore

$$\mathrm{X}_l^{(i)}=\{2m(E-U)/\hbar^2\}^{\frac{1}{2}}r^{\frac{1}{2}}J_{l+\frac{1}{2}}(\{2m(E-U)/\hbar^2\}^{\frac{1}{2}}r). \tag{2.3}$$

Here J denotes the Bessel function and the superscript (i) refers to the interior of the nucleus. This solution would represent a standing wave, except for the imaginary part of E which permits the "leak" through the potential barrier.

For $r>r_0$, we must write $V=2Z\epsilon^2/r$ in (2.2). In the resulting equation we substitute

$$\begin{aligned} &x=(2mE)^{\frac{1}{2}}r/\hbar=x_R+ix_I,\\ &\kappa=(2mE)^{\frac{1}{2}}(2\epsilon^2Z/\hbar)=\kappa_R+i\kappa_I,\\ &y=\mathrm{X}_l^{(o)},\text{ the "outside" solution,}\end{aligned}\tag{2.4}$$

and we obtain

$$y''+(1-l(l+1)/x^2-\kappa/x)y=0. \tag{2.5}$$

Because of the experimentally known values of the constants of radioactive elements, we see that it is legitimate to write

$$\begin{aligned} x_R+ix_I&\doteq(2mE_a)^{\frac{1}{2}}(r/\hbar)(1-\tfrac{1}{4}i\hbar\lambda/E_a)\\ &\doteq 10-10^{-18}i,\end{aligned}$$

and

$$\begin{aligned} \kappa_R+i\kappa_I&\doteq 4\epsilon^2Z/\hbar v+i\epsilon^2Z\lambda/vE_a\\ &\doteq 50+10^{-18}i,\end{aligned}$$

where we have taken $r_0\doteq 10^{-12}$ cm. The small magnitude of the imaginary parts of x and κ plays an essential role in what follows.

3. THE CASE $l=0$.

For $l=0$, Eq. (2.5) is simply

$$y''+(1-\kappa/x)y=0. \tag{3.1}$$

It is known[15] that $W''+(-\frac{1}{4}+p/z)W=0$, has in-

[13] H. Geiger and J. M. Nuttall, Phil. Mag. 22, 613 (1911).
[14] M. A. Preston, Phys. Rev. 69, 535 (1946).
[15] Whittaker and Watson, *Modern Analysis* (Cambridge, 1927), pp. 339, 343.

dependent solutions

$$e^{-\frac{1}{2}z}\int_0^\infty (1+z/t)^p e^{-t}dt,$$

and

$$e^{\frac{1}{2}z}\int_0^\infty (1-z/t)^{-p} e^{-t}dt,$$

if $R(p)\leqslant\frac{1}{2}$. Therefore, since $-\kappa_I<\frac{1}{2}$, we may write two solutions of (3.1) in the form

$$y^{(1)}(x)=e^{-\frac{1}{2}i\kappa\pi}e^{ix}\int_0^\infty (1-2ix/t)^{-\frac{1}{2}+i\kappa}e^{-t}dt, \quad (3.2)$$

$$y^{(2)}(x)=e^{-\frac{1}{2}i\kappa\pi}e^{-ix}\int_0^\infty (1+2ix/t)^{\frac{1}{2}+i\kappa}e^{-t}dt. \quad (3.3)$$

Under the substitution $t=2ix(\tau+\frac{1}{2})$, $\tau=\xi+i\eta$,

$$y^{(1)}=e^{-\frac{1}{2}i\kappa\pi}2ix\int_C\left(\frac{\tau-\frac{1}{2}}{\tau+\frac{1}{2}}\right)^{-\frac{1}{2}+i\kappa}e^{-2ix\tau}d\tau, \quad (3.4)$$

C is the line $\xi=-\frac{1}{2}+(x_I/x_R)\eta$ in the τ-plane from $\eta=0$ to $\eta=-\infty$. Similarly $y^{(2)}$ is the same integral over the path $\xi=\frac{1}{2}+(x_I/x_R)\eta$.

The factor e^{ix} in (3.2) shows that $y^{(1)}(x)$ represents the outgoing wave for large x (or r). Therefore we now wish to evaluate $y^{(1)}$ as given by (3.4), remembering that $|\kappa|\doteq 50$ and $|x|\doteq 10$.

The "method of steepest descents"[16] is particularly suited to this problem. It serves to evaluate integrals in the complex plane of the form $\int_C e^{-xf(\tau)}d\tau$, where $R\{f(\tau)\}$ approaches infinity (or a "large" value) at both ends of C. This property of $f(\tau)$ implies that appreciable contributions to the value of the integral come from only a certain finite strip of C. To permit this strip to be as small as possible for purposes of approximation, we replace C by a path on which $R\{f(\tau)\}$ increases most rapidly from its minimum value. The path used is called the *curve of steepest descent*, and the point at which $R\{f(\tau)\}$ is a minimum called the *pass point* or *Sattelpunkt*. It is found that, if τ_s represents a pass point, these points are the roots of

$$(df/d\tau)_{\tau=\tau_s}=f'(\tau_s)=0, \quad (3.5)$$

and the curves of steepest descent have the equation

$$I\{f(\tau)\}=I\{f(\tau_s)\}. \quad (3.6)$$

[16] P. Debye, Math. Ann. 67, 535 (1909).

We write

$$y^{(1)}=2ix\int_C e^{-xf(\tau)}d\tau,$$

where

$$f(\tau)=\tfrac{1}{2}i\log(\tau-\tfrac{1}{2})-\tfrac{1}{2}i\log(\tau+\tfrac{1}{2})+2i(x/\kappa)\tau+\tfrac{1}{2}\pi. \quad (3.7)$$

Putting $\tau=\xi+i\eta$, this reduces to

$$f(\tau)=-[\tfrac{1}{2}\arctan\{\eta/(\xi^2-\tfrac{1}{4}+\eta^2)\}+2(x/\kappa)\eta]+i[\tfrac{1}{4}\log\{(\xi-\tfrac{1}{2})^2+\eta^2\}-\tfrac{1}{4}\log\{(\xi+\tfrac{1}{2})^2+\eta^2\}+2(x/\kappa)\xi].$$

Now neglecting 10^{-16} with respect to unity, $x/\kappa=x_R/\kappa_R+i\gamma$, say, where $\gamma>0$. Therefore

$$R\{f(\tau)\}=-[\tfrac{1}{2}\arctan\{\eta/(\xi^2-\tfrac{1}{4}+\eta^2)\}+2(x_R/\kappa_R)\eta+2\gamma\xi], \quad (3.8)$$

and

$$I\{f(\tau)\}=\tfrac{1}{4}\log[\{(\xi-\tfrac{1}{2})^2+\eta^2\}/\{(\xi+\tfrac{1}{2})^2+\eta^2\}]+2(x_R/\kappa_R)\xi-2\gamma\eta. \quad (3.9)$$

Also setting $f'(\tau_s)=0$ and solving for the pass points, we find

$$\tau_s=\pm\tfrac{1}{2}(1-\kappa/x)^{\frac{1}{2}}=\pm\tfrac{1}{2}i\tan\alpha, \quad (3.10)$$

where α is defined by

$$\cos^2\alpha=x/\kappa, \quad (3.11)$$
$$\alpha=\alpha_R+i\alpha_I, \quad \pi/2>\alpha_R>0.$$

Then $x/\kappa=\cos^2(\alpha_R+i\alpha_I)=\cos^2\alpha_R+i\alpha_I\sin 2\alpha_R$, to the order 10^{-16}. Therefore

$$\cos^2\alpha_R=x_R/\kappa_R, \quad \text{and} \quad \alpha_I\doteq\gamma/\sin 2\alpha_R. \quad (3.12)$$

We now study the pass point $\tau_-=-\frac{1}{2}i\tan\alpha$. Substituting in (3.7), we find easily

$$f(\tau_-)=-(\alpha-\cos\alpha\sin\alpha)=-(\alpha_R-\cos\alpha_R\sin\alpha_R)-2i\alpha_I\cos^2\alpha_R. \quad (3.13)$$

Thus from (3.12) the imaginary part of $f(\tau_-)$ is $-\gamma\cot\alpha_R$. From (3.9), the curves of steepest descent through τ_- are

$$\tfrac{1}{4}\log[\{(\xi-\tfrac{1}{2})^2+\eta^2\}/\{(\xi+\tfrac{1}{2})^2+\eta^2\}]+2(x_R/\kappa_R)\xi=\gamma(2\eta-\cot\alpha_R). \quad (3.14)$$

The right side of (3.14) is important only for $\eta>10^{12}$, say, because of the size of γ. In this region the logarithmic term is negligible and the curve is the line

$$\eta-\tfrac{1}{2}\cot\alpha_R=(x_R/\kappa_R)\xi, \quad (3.15)$$

which has a slope of about 10^{15}. For smaller η, (3.14) is approximately

$$\tfrac{1}{4}\log[\{(\xi-\tfrac{1}{2})^2+\eta^2\}/\{(\xi+\tfrac{1}{2})^2+\eta^2\}]+2(x_R/\kappa_R)\xi=0. \tag{3.16}$$

This curve is more conveniently studied in the form

$$\eta^2=\frac{(\xi+\tfrac{1}{2})^2\exp(-4\xi\cos^2\alpha_R)-(\xi-\tfrac{1}{2})^2\exp(4\xi\cos^2\alpha_R)}{\exp(4\xi\cos^2\alpha_R)-\exp(-4\xi\cos^2\alpha_R)}. \tag{3.17}$$

It is easily verified that

1. the curve is centrally symmetric about the origin,
2. the curve meets $\xi=0$ in $\eta=\pm\frac{1}{2}\tan\alpha_R$,
3. the curve intersects $\xi=\pm\frac{1}{2}$ in real points,
4. $\eta^2=0$ only for two specific values $\xi=\pm\xi_0$, and consequently η is real only for $-\xi_0\leqslant\xi\leqslant\xi_0$,
5. $\xi_0>\frac{1}{2}$ by fact 3 above. Actually its value is about 0.8 and it is a root of $(\xi+\frac{1}{2})/(\xi-\frac{1}{2})=\exp(8\xi\cos^2\alpha_R)$.
6. $\xi=0$ is a part of (3.16).

Figure 1 shows the curve (3.14) and the corresponding one through $\tau_+(=\frac{1}{2}i\tan\alpha)$. The imaginary part of α is exaggerated in the figure.

The path of integration for $y^{(1)}(x)$ is the straight line L_1 in Fig. 1. The integrand is without singularities in the region concerned and the integral over L_1+L_4 equals the integral over L_2+L_3. L_3 is the path of steepest descent. We must show that the integrals over L_4 and L_2 are negligible. We have

$$\left|\int_{L_4}\exp\{-\kappa f(\tau)\}d\tau\right|$$
$$=\left|\lim_{\eta\to-\infty}\int_{(x_I/x_R)\eta}^{(\kappa_R/\varkappa_R)\gamma\eta}\exp(2x\eta-2xi\xi)d\xi\right|$$
$$=\lim_{\eta\to-\infty}\frac{1}{2x_R}(e^{2(\varkappa_R-\varkappa_I)\eta}-e^{2(\varkappa_R-\gamma\varkappa_R)\eta})$$
$$=0.$$

On L_2, $\eta=0$ and the integral is

$$\int_{-\frac{1}{2}}^{-\xi_1}\exp\{-i[\tfrac{1}{2}\kappa\log(\xi+\tfrac{1}{2})/(\tfrac{1}{2}-\xi)-2x\xi]\}d\xi,$$

if L_3 cuts $\eta=0$ at $\xi=-\xi_1$. The absolute values of both real and imaginary parts of the integral are less than

$$\int_0^{\frac{1}{2}}\exp[-\tfrac{1}{2}\kappa_I\log(\xi+\tfrac{1}{2})/(\tfrac{1}{2}-\xi)+2x_I\xi]d\xi,$$

which, since $x_I<0$, is less than

$$(\tfrac{1}{2})^{\frac{1}{2}\varkappa_I}\int_0^{\frac{1}{2}}(\xi+\tfrac{1}{2})^{-\frac{1}{2}\varkappa_I}d\xi\doteq 0.5,$$

disregarding terms of order 10^{-16}. This is negligible in comparison with the integral along L_3, which is of the order 10^{13} (see Eq. (3.14)). Therefore L_1 may be replaced by L_3 for the integration.

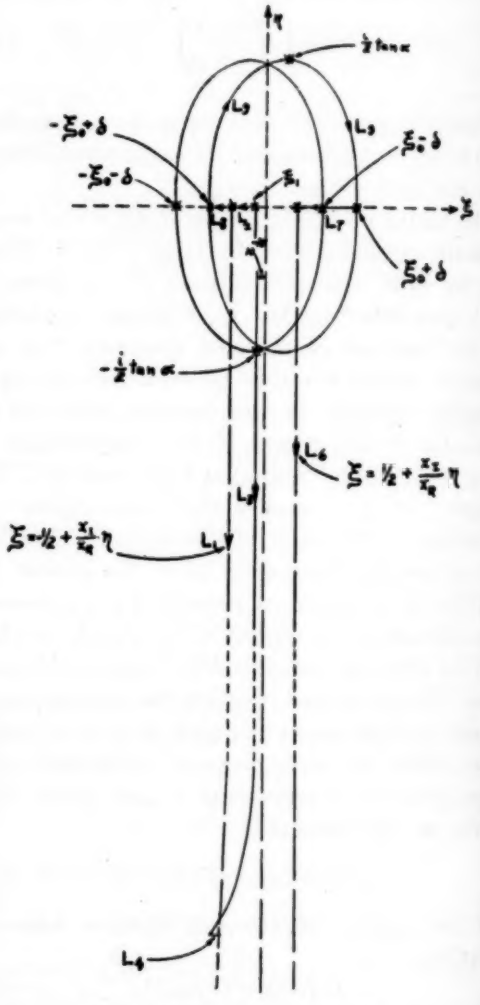

FIG. 1. Lines of steepest descent.

We now proceed to obtain an approximate expression for $y^{(1)}(x)$. The method of the remainder of this section is not mathematically rigorous. Moreover it provides no estimate of the percentage error of its results. To overcome these drawbacks requires a somewhat lengthy argument which is given in Appendix A. In this section we shall obtain the leading terms of the result in a simple manner.

Since L_3 is a path of steepest descent,

$$\int_{L_3} \exp\{-\kappa f(\tau)\}d\tau \doteq \int_{\tau_- - i\beta}^{\tau_- + i\beta} \exp\{-\kappa f(\tau)\}d\tau.$$

Remembering that $f'(\tau_-)=0$, we put

$$\begin{aligned} f(\tau) &\doteq f(\tau_-)+\tfrac{1}{2}f''(\tau_-)(\tau-\tau_-)^2 \\ &= f(\tau_-)-\tfrac{1}{2}f''(\tau_-)\eta^2, \quad \text{on } L_3, \end{aligned}$$

where $\tau=\tau_-+i\eta$. It is found that $f''(\tau_-)=-8\cos^4\alpha\tan\alpha$. Then the integral is

$$\begin{aligned} i\int_{\beta}^{-\beta} &\exp\{-\kappa f(\tau_-)\}\exp\{-4\kappa\cos^4\alpha\tan\alpha\eta^2\}d\eta \\ &= \frac{i\exp\{-\kappa f(\tau_-)\}}{2\cos^2\alpha(\kappa\tan\alpha)^{\frac{1}{2}}}\int_{2\cos^2\alpha(\kappa\tan\alpha)^{\frac{1}{2}}\beta}^{-2\cos^2\alpha(\kappa\tan\alpha)^{\frac{1}{2}}\beta} \\ &\quad\times\exp(-\eta^2)d\eta \\ &\doteq \frac{i\exp\{-\kappa f(\tau_-)\}}{2\cos^2\alpha(\kappa\tan\alpha)^{\frac{1}{2}}}\int_{\infty}^{-\infty} \\ &\quad\times\exp(-\eta^2)d\eta, \text{ for sufficiently large } \kappa, \\ &= -\tfrac{1}{2}i\sec^2\alpha(\pi\cot\alpha/\kappa)^{\frac{1}{2}}\exp\{-\kappa f(\tau_-)\}. \end{aligned}$$

Therefore

$$\begin{aligned} y^{(1)}(x) &\doteq x\sec^2\alpha(\pi\cot\alpha/\kappa)^{\frac{1}{2}}\exp\{-\kappa f(\tau_-)\} \\ &= (\pi\kappa\cot\alpha)^{\frac{1}{2}}e^{\omega}, \end{aligned} \tag{3.18}$$

where

$$\omega=\kappa(\alpha-\cos\alpha\sin\alpha). \tag{3.19}$$

Notice that in this approximation we have ignored the fact that x, κ, α have small imaginary parts. Then (3.18) gives the real part of $y^{(1)}$. The imaginary part of $y^{(1)}$ is much smaller in absolute value and hence does not appear in the expansion about τ_-. However (3.2) and (3.3) show that (if x and κ are real) $y^{(2)}$ is the complex conjugate of $y^{(1)}$. Therefore $I\{y^{(1)}\}$ is $-\frac{1}{2}i(y^{(1)}-y^{(2)})$. This quantity is $x\int\exp\{-\kappa f(\tau)\}d\tau$ integrated over L_1-L_8 or equivalently over $L_8+L_9+L_7$. It is easily seen that the integral over L_8+L_7 is

$$-2\int_{\frac{1}{2}}^{\xi_0}\cos[\tfrac{1}{2}\kappa\log(\xi-\tfrac{1}{2})/(\xi+\tfrac{1}{2})+2x\xi]d\xi. \tag{3.20}$$

When x and κ are real, this integral is zero (see Appendix A). Therefore the integral is taken over L_9 only, which is a path of steepest descent from the pass point $\tau_+=\frac{1}{2}i\tan\alpha$. We have

$$f''(\tau_+)=8\cos^4\alpha\tan\alpha,$$

and

$$\begin{aligned} &\int_{L_9}\exp\{-\kappa f(\tau)\}d\tau \\ &\quad\doteq\int_{-\beta'}^{\beta'}\exp\{-\kappa f(\tau_+)\}\exp\{-4\kappa\cos^4\alpha\tan\alpha\xi^2\}d\xi \\ &\quad=\tfrac{1}{2}\sec^2\alpha(\pi\cot\alpha/\kappa)^{\frac{1}{2}}e^{-\omega}. \end{aligned}$$

Therefore

$$y^{(1)}\doteq(\pi\kappa\cot\alpha)^{\frac{1}{2}}(e^{\omega}+\tfrac{1}{2}ie^{-\omega}). \tag{3.21}$$

The accuracy of this formula is examined in Appendix A.

4. EQUATIONS FOR r_0 AND U FOR $l=0$

If superscripts (i) and (o) refer to properly normalized solutions inside and outside the nucleus, the condition of continuity requires that

$$\left.\begin{aligned} \psi^{(i)}&=\psi^{(o)} \\ d\psi^{(i)}/dr&=d\psi^{(o)}/dr \end{aligned}\right\} \quad \text{at} \quad r=r_0,$$

which is equivalent to the condition

$$\frac{1}{\mathrm{X}_l^{(i)}}\frac{d\mathrm{X}_l^{(i)}}{dr}=\frac{1}{\mathrm{X}_l^{(o)}}\frac{d\mathrm{X}_l^{(o)}}{dr} \quad \text{at} \quad r=r_0. \tag{4.1}$$

When the explicit expressions for X are substituted in (4.1), it becomes a complex equation for E, from which we can deduce two real equations, one for the energy E_α of the α-particle and one for the decay constant λ.

For $l=0$, $\mathrm{X}_0^{(o)}=y^{(1)}$ and $\mathrm{X}_0^{(i)}$ is given by Eq. (2.3). Noting that $d\alpha/dx=-(\kappa\sin2\alpha)^{-1}$, and $dx/dr=mv/\hbar$, straightforward calculation gives, using (3.21),

$$\begin{aligned} \frac{1}{\mathrm{X}_0^{(o)}}\frac{d\mathrm{X}_0^{(o)}}{dr} &= -\frac{mv}{\hbar\sin2\alpha} \\ &\quad\times\left\{2\sin^2\alpha\frac{1-\frac{1}{2}ie^{-2\omega}}{1+\frac{1}{2}ie^{-2\omega}}-\frac{1}{\kappa\sin2\alpha}\right\}. \end{aligned}$$

$(1/\kappa_R)\,\mathrm{cosec}2\alpha_R$ is 1 to 2 percent of $2\sin^2\alpha_R$, which is the value of the first term. (The accurate value of $y^{(1)}$ given by Eq. (A.12) adds other terms, the greatest of which is proportional to $e^{-2\omega}$ which is of the order 10^{-20} to 10^{-30} with $r\doteq 10^{-12}$ cm, and with experimentally known values of E_α.) Therefore we have 2 percent numerical accuracy in writing

$$\frac{1}{X_0^{(o)}}\frac{dX_0^{(o)}}{dr}=-(2mE/\hbar^2)^{\frac{1}{2}}\tan\alpha\left(\frac{1-\frac{1}{2}ie^{-2\omega}}{1+\frac{1}{2}ie^{-2\omega}}\right).$$

Also, from (2.3),

$$\frac{1}{X_0^{(i)}}\frac{dX_0^{(i)}}{dr}$$
$$=\{2m(E-U)/\hbar^2\}^{\frac{1}{2}}\cot[r\{2m(E-U)/\hbar^2\}^{\frac{1}{2}}].$$

These two expressions are to be equated at $r=r_0$ and the substitution $E=E_\alpha-\frac{1}{2}i\hbar\lambda$ is to be made. In the initial factors $E^{\frac{1}{2}}$ and $(E-U)^{\frac{1}{2}}$ we may neglect the imaginary part of E, because it introduces corrections at most 10^{-27} times the real and imaginary parts on each side. Similar arguments apply to the imaginary parts of $\tan\alpha$, and of κ, and α in the exponents.

Introducing

$$\mu=(1-U/E_\alpha)^{\frac{1}{2}},$$
$$k=mv/\hbar,$$
$$\alpha_0=\alpha_R \quad \text{for} \quad r=r_0,$$

and

$$\omega_0=\kappa_R(\alpha_0-\sin\alpha_0\cos\alpha_0),$$

the condition becomes

$$\mu\cot\{\mu kr_0(1-i\hbar\lambda/2E_\alpha\mu^2)\}=-\tan\alpha_0\frac{1-\frac{1}{2}ie^{-2\omega_0}}{1+\frac{1}{2}ie^{-2\omega_0}}. \quad (4.2)$$

Also the cotangent term is

$$\frac{1+(i\hbar\lambda kr_0/4E_\alpha\mu)\tan(\mu kr_0)}{\tan(\mu kr_0)-i\hbar\lambda kr_0/4E_\alpha\mu}.$$

Separating real and imaginary parts of (4.2) we thus obtain

$$\mu=-\tan\alpha_0\tan(\mu kr_0), \quad (4.3)$$

$$\lambda=\frac{2v}{r_0}\frac{\mu^2\tan\alpha_0}{\mu^2+\tan^2\alpha_0}e^{-2\omega_0}. \quad (4.4)$$

TABLE I. Values of r_0 and B for $l=0$.

Nuclei	Radius (10^{-13} cm)	Total decay energy (Mev)	λ (sec.$^{-1}$)	B (Mev)	$R=r_0A^{-\frac{1}{3}}$
UI-UXI	9.37	4.31[a]	4.82×10^{-18}[c]	23.9	1.52
	9.34	4.32[b]		23.9	1.52
UII-Io	9.26	4.89[a]	8.14×10^{-14}[d]	25.6	1.51
	9.21	4.91[b]		25.7	1.51
Io-Ra	9.26	4.80[d]	2.6×10^{-13}[e]	23.1	1.52
*Ra-Rn[f]	9.29	4.879	1.35×10^{-11}	22.3	1.53
Rn-RaA	9.28	5.589	2.097×10^{-6}	21.0	1.54
RaA-RaB	9.14	6.112	3.78×10^{-3}	20.3	1.53
RaF-RaG	8.27	5.410[g]	5.886×10^{-8}[g]	23.8	1.40
Th-MthI	9.92	3.99[h]	1.2×10^{-3}	22.0	1.62
	10.01		1.7×10^{-3}[i]	21.8	1.64
*RdTh-ThX[f]	9.33	5.517	9.7×10^{-7}	22.1	1.54
ThX-Thn	9.29	5.786	2.20×10^{-6}	21.4	1.54
Thn-ThA	9.28	6.400	1.27×10^{-1}	20.2	1.55
ThA-ThB	9.12	6.904	4.95	19.5	1.53
*Pa-Ac[f]	8.68	5.09[k]	5.5×10^{-13}[m]	27.2	1.34
*An-AcA	8.70	6.953	1.22×10^{-1}	21.5	1.45
AcA-AcB	8.99	7.508	3.47×10^{2}	19.3	1.51

The letters in the body of the table refer to the remarks below.
[a] N. Feather, see reference 17.
[b] From the values of range given by Sizoo, Physica 4, 791 (1937); and graphs of range against energy given by M. S. Livingston and H. A. Bethe, Rev. Mod. Phys. 9, 266 (1937). Value then corrected to include recoil energy, since the tabulated figure is total energy.
[c] A. O. Nier, Phys. Rev. 55, 150 (1939).
[d] Obtained as in (b), using range given by Mme. Curie, reference 17.
[e] Hernegger, Akad. Wiss. Wien 143, 367 (1934).
[f] For fuller information see section 5.
[g] W. Y. Chang, Phys. Rev. 69, 60 (1946).
[h] Obtained as in (b), using range given by G. H. Henderson and G. C. Laurence, Phys. Rev. 52, 46 (1937).
[i] The value 1.7×10^{-3} is given by Feather and by Stranathan, reference 17.
[k] Tsien San-Tsiang, M. Bachelet and G. Bouissieres, Phys. Rev. 69, 39, 1946.
[m] Total decay constant 6.7×10^{-13} from Stranathan, reference 17; $l=0$ line is 80 to 85 percent of this according to Tsien San-Tsiang et al, reference (k).

In this we have, summarizing the symbolism for convenience,

$$\left.\begin{aligned}&\mu=(1-U/E_\alpha)^{\frac{1}{2}},\\&\alpha_0=\arccos(mv^2r_0/4\epsilon^2Z)^{\frac{1}{2}},\\&k=mv/\hbar,\\&\kappa_R=4\epsilon^2Z/\hbar v,\\&\omega_0=\kappa_R(\alpha_0-\sin\alpha_0\cos\alpha_0).\end{aligned}\right\} \quad (4.5)$$

Equations (4.3) and (4.4) are to be regarded as two relations between the four variables E_α, λ, r_0, U. This is the form in which the theory expresses the Geiger-Nuttall law. What is more important however is that when E_α and λ are known experimentally, the radius r_0 and the potential U of the nucleus may be calculated.

Table I gives the values of r_0 and the depth B of the potential, calculated from (4.3) and (4.4).

$$B=(2Z\epsilon^2/r_0)-U. \quad (4.6)$$

Only rays for which $l=0$ are listed. Except where indicated by a note in the Table, the values of λ and E_α which we have used are those found generally in reference works.[17] In the case of an

[17] N. Feather, *Nuclear Physics* (Cambridge University Press, 1936); I. Curie, *Radioactivité* (Hermann, Paris,

α-ray spectrum of more than one line, the λ used should refer to the probability of decay with the one energy E_α only. Such cases are indicated by an asterisk in Table I where partial decay constants are used. Birge's[18] values of ϵ, m, h, etc., are used.

The last column in Table I allows a comparison of the results with the empirical law that the nuclear radius is proportional to the cube root of the atomic number.

5. THE CASE $l \neq 0$

When $l \neq 0$, we have, instead of (3.1),

$$\frac{d^2y}{dx^2}+[1-\kappa/x-l(l+1)/x^2]y=0. \quad (5.1)$$

This equation can be studied by means of the factorization method as described by Infeld.[19] The recursion formula is:

$$X_{l+1}^{(\omega)}=G_l\left(\frac{l+1}{x}+\frac{\kappa}{2(l+1)}-\frac{d}{dx}\right)X_l^{(\omega)}, \quad (5.2)$$

where G_l is independent of x. Since our theory requires only the ratio of $X_l^{(\omega)}$ to its derivative (see (4.1)), the form of G_l is immaterial.

It is then apparent that the results for a general l can be expressed in terms of the first $(l+1)$ derivatives of $X_0^{(\omega)}$. The calculations are contained in Appendix B. Here we shall simply state the results. Equations (4.3) and (4.4) for μ and λ are replaced by:

$$\mu=-\tan\alpha_0\frac{S_l(M)\tan D+C_l(M)}{K_l(M)-H_l(M)\tan D}, \quad (5.3)$$

$$\lambda=(2v/r_0)\frac{\mu^2\tan\alpha_0(H_lC_l+K_lS_l)Q_l\epsilon^{-2\omega_0}}{\mu^2(H_l^2+K_l^2)+\tan^2\alpha_0(C_l^2+S_l^2)+2\mu\tan\alpha_0(C_lK_l-S_lH_l)}. \quad (5.4)$$

The notation of these equations is:

$$D=1/M=\mu k r_0, \quad (5.5)$$

Q_l is a rational function of $\tan\alpha_0$ and r_0 (or M), C_l, S_l, H_l, K_l are polynomials in M.

These functions do not have a useful general form for arbitrary l, but are calculated separately for each l. The first five results are:

$l=0$:

$$Q_0=1,\quad S_0=1,\quad C_0=0,\quad H_0=0,\quad K_0=1.$$

$l=1$:

$$Q_1=(\kappa-2\tan\alpha_0)/(\kappa+2\tan\alpha_0);$$

$$S_1=M;\quad C_1=-1;\quad H_1=M^2-1;\quad K_1=M.$$

$l=2$:

$$Q_2=(\kappa+10\mu M-6\tan\alpha_0)/(\kappa+10\mu M+6\tan\alpha_0);$$

$$S_2=3M^2-1;\quad C_2=-3M;$$

$$H_2=3M(2M^2-1);\quad K_2=6M^2-1.$$

$l=3$:

$$Q_3=\frac{\kappa+28\mu M-12\tan\alpha_0+(44/\kappa)\tan^2\alpha_0}{\kappa+28\mu M+12\tan\alpha_0+(44/\kappa)\tan^2\alpha_0};$$

$$S_3=-6M+15M^3;\quad C_3=1-15M^2;$$

$$H_3=1-21M^2+45M^4;\quad K_3=-6M+45M^3.$$

$l=4$:

$$Q_4=\frac{\kappa(\kappa+60\mu M)-20\tan\alpha_0(40\mu M+\kappa)+140}{\kappa(\kappa+60\mu M)+20\tan\alpha_0(40\mu M+\kappa)+140};$$

$$S_4=1-45M^2+105M^4;\quad C_4=10M-105M^3;$$

$$H_4=10M-195M^3+420M^5;$$

$$K_4=1-55M^2+420M^4.$$

In making calculations for r_0 and U in the case of α-ray spectra with fine structure, it is necessary to determine the angular momentum quantum number l. If the spin number of the disintegrating nucleus is s', and that of the relevant level of the product nucleus is s, l is an integer between $|s+s'|$ and $|s-s'|$. Thus if s and s' are known, the possible values of l are easily found. In particular if s' is zero, $l=s$.

1935), Vol. II; J. Hoag, *Electron and Nuclear Physics* (D. Van Nostrand Company, Inc., New York, 1938); J. Stranathan, *The "Particles" of Modern Physics* (The Blakiston Company, Philadelphia, 1942); W. B. Lewis and B. V. Bowden, Proc. Roy. Soc. **A145**, 235 (1934); International Commission, J. de phys. et rad. **2**, 273 (1931).

[18] R. T. Birge, Rev. Mod. Phys. **13**, 233 (1941).

[19] L. Infeld, Phys. Rev. **59**, 743 (1941).

TABLE II. Calculations for line zero, ThC-ThC″. r_0 and l in the first two columns are used to obtain the λ's in the third column. Experimental value is $\lambda=1.83\times10^{-6}$ sec^{-1}.

r_0 (10^{-13} cm)	l	λ (10^{-6} sec^{-1})	r_0 (10^{-13} cm)	l	λ (10^{-6} sec^{-1})
7.57	0	6.93	7.20	2	2.44
	1	10.84		3	2.02
	2	11.29		4	0.48
	3	9.49	7.40	4	1.18
7.20	0	1.52	7.48	4	1.81
	1	2.37	7.49	4	1.89

As an example we take the α-decay ThC→ ThC″. This is a particularly convenient case, as Oppenheimer[20] has assigned spin numbers to the various levels of the ThC″ nucleus; these values were determined by a study of γ-ray data. Where the subscripts refer to the levels of the ThC″ nucleus, Oppenheimer gives

$$s'=1,\quad s_0=3,\quad s_1=1,\quad s_2=3,\quad s_3=3,\quad s_4=0.$$

Thus

$$l_0=2,\ 3\text{ or }4;\quad l_1=0,\ 1\text{ or }2;\quad l_2=2,\ 3\text{ or }4;$$
$$l_3=2,\ 3\text{ or }4;\quad l_4=1.$$

Before considering the calculation in detail, two general remarks will be useful. It is found that, when (5.3) and (5.4) are used to calculate λ for a given r_0 and E_α, the values of λ at first increase with l and then decrease continually. This is caused by the presence of two opposite effects, the increase of μ with l and the decrease of Q. The latter finally becomes of greater importance. Also the value of λ decreases if r_0 is decreased. Table II illustrates these facts.

In calculating r_0 for complex spectra, our procedure is to assume a value for r_0 and for l, and to calculate μ and λ from (5.3) and (5.4), employing experimentally known E_α. The process is repeated until the chosen r_0 and l reproduce the experimental value of λ.

In the case of ThC→ThC″, we examine first line four, for which $l_4=1$. We find $r_0=7.54\times10^{-13}$ cm. We then turn to line one and find that, if $l=0$, $r_0=7.57\times10^{-13}$, if $l=1$, $r_0=7.38\times10^{-13}$, and if $l=2$, r_0 is still smaller. These figures suggest that to obtain agreement with line four we should take for line one $r_0=7.57\times10^{-13}$ and $l=0$. For line zero, the results in Table II are obtained. Since for line zero l must be 2, 3, or 4, it is seen that the greatest possible radius for line zero is 7.48×10^{-13} cm. This agrees reasonably well with the values obtained for lines four and one. Line two gives $r_0=7.40\times10^{-13}$ for $l=3$, and $r_0=7.60\times10^{-13}$ for $l=4$. Line three gives $r_0=7.5\times10^{-13}$ with $l=4$.

Therefore, the most plausible results are those in Table III. Any other combination of l's would yield less consistent (and smaller) radii.

Calculations have been made for certain other complex spectra as in Table IV. For elements in the Ra and Th series, occurring before the C-products in the disintegration series, it is assumed that all ground state transitions have $l=0$; for the lines corresponding to excited states $l=1$ or 2 in virtue of the connection between spin and the emission of γ-rays by the product nucleus in falling to its ground state. If s_0 is the spin of the ground state of the product nucleus, the character of the γ-ray from level j is determined by $|s_j-s_0|$. This quantity must be 0, 1, or 2; dipole radiation occurs when it is 1, otherwise quadrupole; $s_j=s_0$ is forbidden. In particular, if $s'=s_0=0$, $l(=s_j)$ must be either 1 or 2.

It may be mentioned that it is presumably possible that any one line contains particles of various possible l's, present with relative intensities related to the respective λ's. This would seem to require smaller r_0's, but the available data does not in any case permit a test of the hypothesis.

The formulae (5.3) and (5.4) differ considerably from those previously given for $l\neq0$ by Sexl[1] and Gamow.[21] Gamow's formula makes λ a monotonically decreasing function of l for fixed r_0, as opposed to the initial rise possible with our formula. Numerical results with Gamow's formula have been published by Gamow and Rosenblum.[21] Their values of radii are presented by means of a graph of a quantity r_{eff} introduced by these authors. Numerical values of r_{eff} have been

TABLE III. r_0 for ThC-ThC″.

Line	λ (10^{-6} sec^{-1})	Total energy (Mev)	l	r_0 (10^{-13} cm)
0	1.83	6.201	4	7.48
1	4.65	6.161	0	7.57
2	0.12	5.873	4	7.60
3	0.01	5.728	4	7.50±.05
4	0.07	5.709	1	7.54±.02

[20] F. Oppenheimer, Proc. Camb. Phil. Soc. 32, 328 (1936).

[21] G. Gamow and S. Rosenblum, Comptes rendus 197, 1620 (1933).

determined from this graph and converted to r_0 by means of a relation given in their paper, *viz.*

$$r_{eff}=r_0-\frac{\hbar^2}{me^2Z}l(l+1).$$

For this purpose, the l's of Tables III and IV have been used. These r_0's are compared with our results in Table V. The large differences in the radii of corresponding ground states are caused by the employment by Gamow of a more approximate formula for $l=0$. Nevertheless, it will be seen that there is considerable disparity even in the *relative* values of "fine structure radii"; the spread of the r_0's from Gamow's data for ThC→ThC″ is 25 percent of the smallest radius; for our values the corresponding spread is 1.6 percent. In some cases the radius given by Gamow's formula increases when that given by (5.3) and (5.4) decreases. It is clear, therefore, that the earlier approximate formulae, besides giving appreciably lower radii for $l=0$, are unsuited for adaptation to the case $l\neq 0$.

6. EFFECTIVENESS OF ONE-BODY MODEL

It is necessary to examine the objection that possibly too much weight is given to spurious effects resulting solely from the assumption of a rectangular well potential. As Gamow points out, it should not be used to calculate the energy levels of the α-particle in the nucleus. Thus Gamow obtains only one $E_\alpha-\lambda$ relationship not involving U. Now the two equations in this paper do allow a numerical evaluation of U (see Table VI); but this result should be regarded not as a determination of an energy level but rather as a step in the implicit elimination of U to give one equation connecting E_α and λ.

TABLE IV. r_0 for some complex spectra. In Pa-Ac, the separate λ's for lines 1 and 2 are not known: r_0 is chosen to give their sum. The difference between $l=1$ and $l=2$ lies within the limits indicated for r_0.

Nuclei	Line	λ (sec^{-1})	Total energy (Mev)	l	r_0 (10^{-13} cm)
Pa-Ac	0	5.5×10^{13}	5.09	0	8.68
	1	1.2×10^{13}	4.80	1 or 2	9.09
	2		4.77	1 or 2	
RdTh-ThX	0	9.7×10^{9}	5.517	0	9.33
	1	1.9×10^{9}	5.431	1	9.08
				2	9.05
Ra-Rn	0	1.35×10^{11}	4.879	0	9.29
	1	0.03×10^{11}	4.695	1 or 2	8.92±.02

TABLE V. Comparison of r_0's for complex spectra from Gamow's formula and present results.

Nuclei	Line	l	r_0 calculated from r_{eff}	r_0 from Table III or IV
ThC-ThC″	0	4	7.9×10^{-13} cm	7.48×10^{-13} cm
	1	0	6.4	7.57
	2	4	8.1	7.60
	3	4	8.0	7.50
	4	1	6.8	7.54
RdTh-ThX	0	0	7.8_6	9.33
	1	1	7.9_1	9.08
	1	2	8.0_0	9.05
Ra-Rn	0	0	7.9_7	9.29
	1	1	7.9_7	8.92
	1	2	8.0_6	8.92

TABLE VI. Values of U. ThC-ThC″.

l	0	1	4	4	4
Line	1	4	0	2	3
U (Mev)	5.38	4.10	0.74	0.58	0.35
E	6.16	5.71	6.20	5.87	5.73

The decay constant may in a sense be considered as dependent on two factors: the frequency with which the α-particle "strikes the wall" of the potential barrier and the probability of penetration for any one collision. This latter factor is not sensibly dependent on the model of internal forces; it corresponds to the exponential factor $Q_l e^{-2\omega_0}$ in (4.4) and (5.4). The remaining factors in these formulae may be considered to express the "frequency of striking"; they take the form $g_l v/r_0$, where g_l are factors which are dependent on the model of nuclear forces employed. $(v/r_0)Q_l e^{-2\omega_0}$ determines the power of ten in the value of λ; g_l changes the value by a factor of the order of 10 or less for different models.

Now Gamow's results are apparently independent of the model of internal potential. But this is somewhat misleading, since his formulae depend on his Eq. (41) (reference 5, p. 100), which is equivalent to using the potential well and ignoring the dependence of g_l on l.

The assumption here is presumably that the manner in which the change in l affects the internal solution is not highly dependent on the model of internal potential. However, in that case an accurate evaluation should be permissible, and, in fact, a new qualitative effect appears, for with the rectangular well λ increases slightly for small $l(\lesssim 3)$, whereas with Gamow's formula it decreases monotonically.

That g_l increases with l may be seen as follows. Given a fixed radius and internal energy, the introduction of an increased "centrifugal force" raises the value of the potential near the center of the nucleus, implying greater velocity near the surface; the maximum of the internal wave function is also shifted to a greater radius. These effects correspond to a greater frequency of "collision with the barrier" and, with the rectangular well, an over-all increase in λ for the first few l's. More accurate models might well produce the same effect; there is at present insufficient knowledge of the spins of the nuclear levels involved to determine from the experimental results whether or not such an initial rise occurs in the λ *vs.* l curve.

A remark similar to that made in regard to the numerical values of U applies also to r_0, although less strongly. Bethe[11] estimates that a many-body theory would increase the values of nuclear radii by amounts up to about 30 percent of our values in Table I. Thus, although our values are, on the one-body model, usually accurate to the three figures given, it is clear that such a degree of significance cannot be attributed to them if they are considered as actual nuclear dimensions. The quantity r_0 should be regarded as a parameter introduced in the one-body mathematical model, and adjusted to fit experimental data.

It is perhaps surprising that such a complicated problem as the formation and escape of an α-particle from a heavy nucleus can be handled as satisfactorily as it is with a one-body model. The crudest approximation depends only on the penetrability of the barrier, and complete confidence may be felt in this portion of the theory. As we have seen, the behavior of the internal solution is also important, and calculations with the one-body model throw considerable light on its effects, producing new results (for g_l) in agreement with those indicated by general considerations. To obtain further significant progress would require a theory describing the internal forces in detail and, of course, no such technique is at present available.

I wish to express my appreciation of the generous guidance and counsel given by Professor L. Infeld throughout the course of this investigation. I am also indebted to Professor R. Peierls of Birmingham University for helpful criticism, and to Professors A. F. C. Stevenson and W. J. Webber of Toronto for suggestions in connection with particular parts of the work.

APPENDIX A

Accurate Evaluation of $y^{(1)}(x)$

We require the following lemma given by Watson.[12] If $|\kappa|$ is large and $|\arg\kappa| \leqslant \frac{1}{2}\pi-\Delta$, where $\Delta>0$ but otherwise arbitrary, and $n>0$,

$$\int_0^\infty e^{-\kappa\tau}F(\tau)d\tau \sim \sum_{m=1}^{\infty} a_m\Gamma(m/n)\kappa^{-m/n}, \tag{A.1}$$

subject to the following conditions:

1. $F(\tau)$ is analytic for $|\tau| \leqslant a+\delta$, $a>0$, $\delta>0$.

2. $F(\tau)=\sum_{m=1}^{\infty} a_m\tau^{m/n-1}$ for $|\tau| \leqslant a$. (A.2)

3. $|F(\tau)|<Ne^{b\tau}$, $|\tau| \geqslant a$, $N>0$, $b>0$ and independent of τ.
4. $b<\kappa\sin\Delta$.

The symbol $\sim$ is used to denote asymptotic equivalence for large κ. The series is semi-convergent in the sense of Poincaré, i.e., the sum of m terms differs from the function the series represents by less than $K_m\kappa^{-m}$, where K_m is independent of κ.

To use this lemma for the evaluation of $y^{(1)}$ by the method of steepest descents, we let

$$\zeta=f(\tau)-f(\tau_-), \tag{A.3}$$

where τ is on L_2. Then ζ is real and positive. For any real $\zeta<\zeta_0$, where

$$\zeta_0=f(\xi_1)-f(\tau_-)=\alpha-\cos\alpha\sin\alpha+2\gamma\xi_1,$$

there are two values of τ which satisfy (A.3), one above, and one below τ_-. Call these points τ_1 and τ_2, and let τ_1 be below τ_-, τ_2 above τ_-. Then

$$y^{(1)}=2ixe^{-\kappa f(\tau_-)}\left\{\int_{\zeta_0}^{0} e^{-\kappa\zeta}\frac{d\tau_2}{d\zeta}d\zeta+\int_0^\infty e^{-\kappa\zeta}\frac{d\tau_1}{d\zeta}d\zeta\right\}$$

$$=2ixe^{-\kappa f(\tau_-)}\int_0^{\zeta_0} e^{-\kappa\zeta}\frac{d(\tau_1-\tau_2)}{d\zeta}d\zeta. \tag{A.4}$$

It is permissible to neglect the integral from ζ_0 to ∞ because of the smallness of the integrand for $\zeta>\zeta_0$. This is the essence of the Sattelpunkt method. Numerical indications of error appear later.

We wish to see now that $d(\tau_1-\tau_2)/d\zeta$ satisfies the conditions for $F(\tau)$ in the lemma (A.1), and to find the a_m's explicitly.

Since $\zeta=d\zeta/d\tau=0$ for $\tau=\tau_-$, the expansion of ζ in terms of $(\tau-\tau_-)$ begins with the term in $(\tau-\tau_-)^2$. Hence the inverted series are

$$\tau_1-\tau_-=\sum_{m=0}^{\infty}\frac{a_m\zeta^{\frac{1}{2}(m+1)}}{m+1},$$

$$\tau_2-\tau_-=\sum_{m=0}^{\infty}(-1)^{m+1}\frac{a_m\zeta^{\frac{1}{2}(m+1)}}{m+1};$$

---

[12] Watson, *Bessel Functions* (The Macmillan Company, New York, 1944), p. 235ff.

and we find

$$\left.\begin{aligned} d\tau_1/d\zeta &= \sum_0^\infty \tfrac{1}{2}a_m\zeta^{\frac{1}{2}(m-1)} \\ d\tau_2/d\zeta &= \sum_0^\infty (-1)^{m-1}\tfrac{1}{2}a_m\zeta^{\frac{1}{2}(m-1)}. \end{aligned}\right\} \quad (A.5)$$

Therefore,

$$a_m = (2\pi i)^{-1}\int (d\tau_1/d\zeta)\zeta^{-\frac{1}{2}(m+1)}d\zeta,$$

where the path of integration circles the origin of the ζ-plane twice. However if we think of $\zeta^{\frac{1}{2}(m+1)}$ expressed as a function of τ, we can write

$$a_m = (2\pi i)^{-1}\int_{(0+)} \zeta^{-\frac{1}{2}(m+1)}d\tau,$$

where the path circles the origin of the τ-plane once in the positive sense.

Let $T=\tau-\tau_-$. Then

$$\zeta = T^2\sum_{j=0}^\infty B_jT^j,$$

where B_j are certain coefficients, $B_0\neq 0$. We now define coefficients $a_j(m)$ by the following:

$$\zeta^{-\frac{1}{2}(m+1)} = T^{-(m+1)}\left(\sum_0^\infty B_jT^j\right)^{-\frac{1}{2}(m+1)} = T^{-(m+1)}\sum_0^\infty a_j(m)T^j. \quad (A.6)$$

Then

$$\begin{aligned} a_m &= (2\pi i)^{-1}\int_{(0+)}\zeta^{-\frac{1}{2}(m+1)}d\tau, \\ &= \text{coefficient of } T^{-1} \text{ in } \zeta^{-\frac{1}{2}(m+1)}, \\ &= a_m(m). \end{aligned} \quad (A.7)$$

Thus (A.6) and (A.7) indicate how the quantities a_m may be found. These are the coefficients desired for application of (A.1). For, by (A.5),

$$d(\tau_1-\tau_2)/d\zeta = \sum_{m=0}^\infty a_{2m}\zeta^{m-\frac{1}{2}} = \sum_1^\infty b_m\zeta^{\frac{1}{2}m-1},$$

where $b_{2m+1}=a_{2m}$, and $b_{2m}=0$, and thus the last series is in the form quoted in (A.2).

Also

$$|d(\tau_1-\tau_2)/d\zeta| < Ke^{b\zeta}, \quad K>0, \quad b>0$$

for $\zeta>a$. This follows by noting that

$$|(d\zeta/d\tau_i)^{-1}| = |1/(4\tau_i^2-1)+x/\kappa|^{-1}, \quad (i=1,2)$$

is bounded for $\zeta>0$. Since this expression is bounded, b can be taken as small as desired by increasing a.

Also $\arg\kappa = \arctan(\kappa_I/\kappa_R) \doteq 10^{-16}$. In the notation of Watson's lemma, then, Δ can be as great as $\frac{1}{2}\pi-10^{-15}$, say. That is, $\sin\Delta \doteq 1$. Since b can be very small, the condition $b<\kappa\sin\Delta$ is satisfied.

Therefore, all the conditions of the lemma are satisfied by κ and $d(\tau_1-\tau_2)/d\zeta$, and we may write

$$\int_0^\infty e^{-\kappa\zeta}\frac{d(\tau_1-\tau_2)}{d\zeta}d\zeta \sim \sum_1^\infty b_m\Gamma(m/2)\kappa^{-\frac{1}{2}m}. \quad (A.8)$$

The limits of the integral for $y^{(1)}$ in (A.4) are 0 to ζ_0, rather than 0 to ∞. This has the effect of replacing $\Gamma(m/2)\kappa^{-\frac{1}{2}m}$ in (A.8) by

$$\int_0^{\zeta_0} e^{-\kappa\zeta}\zeta^{\frac{1}{2}m-1}d\zeta.$$

However,

$$\zeta_0 \doteq .5, \quad |\kappa| \doteq 50$$

and it can be shown that, if $m<10$,

$$\int_{.5}^\infty e^{-50\zeta}\zeta^{\frac{1}{2}m-1}d\zeta < 10^{-13}.$$

Therefore, we may employ Eq. (A.8) as it stands, or rather in the form

$$\int_0^\infty e^{-\kappa\zeta}\frac{d(\tau_1-\tau_2)}{d\zeta}d\zeta \sim \sum_0^\infty a_{2m}\Gamma(m+\tfrac{1}{2})\kappa^{-(m+\frac{1}{2})}. \quad (A.9)$$

It is now necessary to calculate a_{2m} explicitly. The first step is to find the B_j's. We have

$$\begin{aligned} B_0T^2+B_1T^3+\cdots = \zeta &= f(\tau)-f(\tau_-) \\ &= \tfrac{1}{2}i\log(\tau-\tfrac{1}{2}) - \tfrac{1}{2}i\log(\tau+\tfrac{1}{2}) \\ &\quad +2ix\tau/\kappa - \tfrac{1}{2}\pi+\alpha-\cos\alpha\sin\alpha. \end{aligned}$$

The algebra of writing $\tau = T-\frac{1}{2}i\tan\alpha$ and expanding need hardly be reproduced. In this way B_j is found as a function of α.

Next, from (A.6) we see that a formal expansion of $(\sum_0^\infty B_jT^j)^{-\frac{1}{2}(m+1)}$ gives $a_j(m)$ in terms of B_j and m. Finally. $a_{2m}=a_{2m}(2m)$ gives the coefficients of (A.9) in terms of α, The end results of this tedious computation are:

$$\begin{aligned} a_0 &= -\tfrac{1}{2}i\cos^{-2}\alpha\tan^{-1}\alpha, \\ a_2 &= -\tfrac{1}{8}i\tan^{-1}\alpha\cos^{-2}\alpha(\tfrac{1}{8}+\tfrac{1}{4}\tan^2\alpha+5/36\cot^2\alpha), \\ a_4 &= -\tfrac{1}{128}i\tan^{-5/2}\alpha\cos^{-2}\alpha \\ &\quad \times(-\tfrac{5}{8}\tan^4\alpha-\tfrac{5}{8}\tan^2\alpha+31/12+77/18\cot^2\alpha \\ &\quad +(5.7.11)/(8.27)\cot^4\alpha). \end{aligned}$$

Returning now to (A.4) and remembering that $x=\kappa\cos^2\alpha$, and $f(\tau_-)=\cos\alpha\sin\alpha-\alpha$, we have

$$\begin{aligned} y^{(1)} &\sim 2i\kappa\cos^2\alpha\exp\{\kappa(\alpha-\cos\alpha\sin\alpha)\} \\ &\quad \cdot(a_0\Gamma(\tfrac{1}{2})\kappa^{-\frac{1}{2}}+a_2\Gamma(\tfrac{3}{2})\kappa^{-\frac{3}{2}}+\cdots); \\ y^{(1)} &\doteq (\pi\kappa\cot\alpha)^{\frac{1}{2}}e^{i\alpha}(1+A\kappa^{-1}+B\kappa^{-2}), \end{aligned} \quad (A.10)$$

where

$$A = \tfrac{3}{4}\cot\alpha(\tfrac{1}{6}+\tfrac{1}{4}\tan^2\alpha+5/36\cot^2\alpha);$$

$$B = -(\tfrac{3}{64})\cot^2\alpha\left(\tfrac{5}{8}\tan^4\alpha+\tfrac{5}{8}\tan^2\alpha-31/12 - 77/18\cot^2\alpha-\frac{5.7.11}{8.27}\cot^4\alpha\right).$$

This expression (A.10), in which κ and α have small imaginary parts, is the part of $y^{(1)}$ which is predominantly real. The part of $y^{(1)}$ which is predominantly imaginary is much smaller in absolute value, and hence does not appear in the expansion about τ_-. However, the predominantly imaginary part of $y^{(1)}$ is $x\int e^{-\kappa f(\tau)}d\tau$, integrated over $L_6+L_9+L_7$ (cf. Section 3). The integral over L_6+L_7 is approximately

$$-2\int_{\frac{1}{2}}^{\xi_0-\delta}\cos[\tfrac{1}{2}\kappa\log\{(\xi-\tfrac{1}{2})/(\xi+\tfrac{1}{2})\}+2x\xi]d\xi, \quad (A.11)$$

where δ is the correction to ξ_0 caused by the imaginary part of α. It can be shown that the magnitude of the integral (A.11) is less than 10^{-17}. For (A.11) is

$$-2\int_{\frac{1}{2}}^{\xi_0-\delta}\cos z_1\cosh z_2d\xi+2i\int_{\frac{1}{2}}^{\xi_0-\delta}\sin z_1\sinh z_2d\xi,$$

where

$$z_1=\tfrac{1}{2}\kappa_R\log\{(\xi-\tfrac{1}{2})/(\xi+\tfrac{1}{2})\}+2x_R\xi,$$
$$z_2=\tfrac{1}{2}\kappa_I\log\{(\xi-\tfrac{1}{2})/(\xi+\tfrac{1}{2})\}+2x_I\xi.$$

Take a number θ of the order 10^{-17}. Then, for $\frac{1}{2}\leqslant\xi\leqslant\frac{1}{2}+\theta$

$$-\infty<\tfrac{1}{2}\kappa_I\log(\xi-\tfrac{1}{2})\leqslant\tfrac{1}{2}\kappa_I\log\theta<-8\times10^{-17},$$
$$0<\tfrac{1}{2}\kappa_I\log(\xi+\tfrac{1}{2})<\tfrac{1}{2}\kappa_I\log(1+\theta)<2\times10^{-35},$$
$$0>2x_I\xi>-10^{-18},$$

since over the whole range of natural α-emitters,

$$10^{-18}>-x_I>5\times10^{-40},$$
$$4\times10^{-18}>\kappa_I>2\times10^{-39}.$$

Therefore, for $\frac{1}{2}<\xi\leqslant\frac{1}{2}+\theta$,

$$|\sinh z_2|<\tfrac{1}{2}(\xi-\tfrac{1}{2})^{-\frac{1}{2}\kappa_I},$$
$$|\cosh z_2|<\tfrac{1}{2}(\xi-\tfrac{1}{2})^{-\frac{1}{2}\kappa_I}+\tfrac{1}{2}(\xi-\tfrac{1}{2})^{\frac{1}{2}\kappa_I},$$

and the integrals over the range $\frac{1}{2}$ to $\frac{1}{2}+\theta$ are less than

$$\left[\frac{(\xi-\frac{1}{2})^{1-\frac{1}{2}\kappa_I}}{2-\kappa_I}+\frac{(\xi-\frac{1}{2})^{1+\frac{1}{2}\kappa_I}}{2+\kappa_I}\right]_{\frac{1}{2}}^{\frac{1}{2}+\theta}\doteq\theta.$$

Also for $\frac{1}{2}+\theta\leqslant\xi\leqslant\xi_0-\delta$, the sinh term in the integral may be replaced by z_2, and the cosh term by 1. Then the real part is

$$-2\int_{\frac{1}{2}+\theta}^{\xi_0-\delta}\cos z_1 d\xi.$$

Now choose θ more exactly so that $z_1=n\pi$ for $\xi=\frac{1}{2}+\theta$. n is approximately 200. Note also that $z_1=0$ for $\xi=\xi_0$ and, therefore, for $\xi=\xi_0-\delta$, $z_1=\epsilon=-\delta\{x_R+\kappa_R\xi_0/(\xi_0^2-\frac{1}{4})\}$, which is of the order of 10^{-17}. Then the real part is

$$-2\int_{n\pi}^{\epsilon}\frac{\cos z_1 dz_1}{2x_R+\frac{1}{2}\kappa_R/(\xi^2-\frac{1}{4})}>-2\int_{n\pi}^{\epsilon}\cos z dz\doteq2\epsilon<0.$$

Also the imaginary part is less than

$$2\int_{\frac{1}{2}+\theta}^{\xi_0-\delta}z_2 d\xi.$$

This can be explicitly integrated and, on putting $\xi_0=.8$, the integral is seen to be less than 2×10^{-18}. Therefore, the integral over L_8+L_7 is less than 10^{-17}. We shall see later that the integral over L_9 is of the order of 10^{-14} or more. Hence the path L_8+L_7 may be neglected. (Note that if x_I and κ_I approach zero, (A.11) approaches zero, as stated in section 3.)

L_9 is a path of steepest descent. The expansion of the integral along L_9 about the pass-point $\tau_+(=\frac{1}{2}i\tan\alpha)$ is the same as that about τ_- along L_3, except that 1. α is replaced by $-\alpha$, and 2. the limits of ζ on both branches of the path are finite, *viz.* $R\{f(\xi_0+\delta)\}-R\{f(\tau_+)\}$, and $R\{f(-\xi_0+\delta)\}-R\{f(\tau_+)\}$, but as before these may both be replaced by inifinity. Therefore the imaginary part of $y^{(1)}$ is

$$I\{y^{(1)}\}\sim\tfrac{1}{2}(\pi\kappa\cot\alpha)^{\frac{1}{2}}e^{-\omega}(1-\tfrac{1}{8}a_2/a_0\kappa+\tfrac{3}{4}a_4/a_0\kappa^2+\cdots).$$

Finally, we have

$$y^{(1)}\doteq(\pi\kappa\cot\alpha)^{\frac{1}{2}}\{e^{\omega}(1+A\kappa^{-1}+B\kappa^{-2})+\tfrac{1}{2}ie^{-\omega}(1-A\kappa^{-1}+B\kappa^{-2})\}. \quad (A.12)$$

APPENDIX B

Derivation of Formulae for $l\neq0$

We saw in Section 5, that $X_l^{(\omega)}$ can be expressed in terms of the first $(l+1)$ derivatives of $X_0^{(\omega)}$ by means of the recursion formula

$$X_{l+1}^{(\omega)}=G_l\left(\frac{l+1}{x}+\frac{\kappa}{2(l+1)}-\frac{d}{dx}\right)X_l^{(\omega)}. \quad (B.1)$$

Let us then study these derivatives. We have seen that

$$X_0^{(\omega)}=2ixe^{-\frac{1}{2}\kappa\pi}\int_C(\tau-\tfrac{1}{2})^{-\frac{1}{2}i\kappa}(\tau+\tfrac{1}{2})^{\frac{1}{2}i\kappa}e^{-2ix\tau}d\tau. \quad (B.2)$$

Hence differentiation with respect to x introduces integrals of the form

$$I_n=e^{-\frac{1}{2}\kappa\pi}\int_C\tau^n(\tau-\tfrac{1}{2})^{-\frac{1}{2}i\kappa}(\tau+\tfrac{1}{2})^{\frac{1}{2}i\kappa}e^{-2ix\tau}d\tau,\quad n=1,2,3,\cdots$$

The lth derivative involves integrals from I_0 to I_l linearly. This differentiation assumes that C, the path of integration, is independent of x. Actually C is the line $\xi=-\frac{1}{2}+(x_I/x_R)\eta$, but, as we have seen, the small term dependent on x does not affect the value of any result obtained by the method of steepest descents, which method we shall now apply to I_n.

$$I_n=\int_C\exp\{-\kappa f_n(\tau)\}d\tau,$$

where

$$f_n(\tau)=\tfrac{1}{2}i\log(\tau-\tfrac{1}{2})-\tfrac{1}{2}i\log(\tau+\tfrac{1}{2})+2i(x/\kappa)\tau-(n/\kappa)\log\tau+\tfrac{1}{2}\pi.$$

Possible pass points are the roots of $f_n'(\tau)=0$, that is of

$$1/(2\tau-1)-1/(2\tau+1)+ni/\kappa\tau+2x/\kappa=0.$$

This is a cubic equation for τ. Provided n/κ is not large (and normally it ranges from 0.02 to 0.1), two of the roots will be near the former pass points τ_+ and τ_-. The exact values can be found numerically if x and κ are given. The third root will be found to be near $\tau=0$ for small n. To the first order it is $\frac{1}{2}ni/(\kappa-x)\doteq ni/80$.

Disregarding the imaginary parts of x and κ which we have seen do not modify the form of the paths of steepest descent appreciably, the imaginary part of $f_n(\tau)$ is

$$G(\xi,\eta)=\tfrac{1}{4}\log\frac{(\xi-\frac{1}{2})^2+\eta^2}{(\xi+\frac{1}{2})^2+\eta^2}+2(x/\kappa)\xi-(n/\kappa)\arctan(\eta/\xi).$$

The paths of steepest descent for I_n would be $G(\xi,\eta)=$constant.

The term $(n/\kappa)\arctan(\eta/\xi)$ is a "perturbation" which slightly deforms the curves found for $l=0$. The equation still includes $\xi=0$, the constant term being increased by $n\pi/2\kappa$. Also the real part of $f_n(\tau)$ is

$$-[\tfrac{1}{4}\arctan\{\eta/(\xi^2+\eta^2-\tfrac{1}{4})\}+2(x/\kappa)\eta+(n/\kappa)\log|\tau|].$$

Now $\log|\tau|$ goes to infinity at both ends of the integration path. Hence the method of steepest descents seems applicable, and it can be checked that the conditions for the lemma (A.1) still hold. Therefore, we know that the method of steepest descents can be applied to I_n, and that an asymptotic series in $1/\kappa$ will be obtained.

There is a theorem[23] that, if a function and its derivative both possess expansions in asymptotic series, the term-by-term derivative of an asymptotic series for the function is an asymptotic series for the derivative. Therefore, since I_n possesses an asymptotic series, we may obtain the solutions

[23] E.g., Bromwich, *Theory of Infinite Series* (The Macmillan Company, London, 1926), p. 345.

$X_l^{(\omega)}$ by continued application of Eq. (B.1) in which for $X_0^{(\omega)}$ we substitute its asymptotic expansion.

Explicit general formulae for any l are not obtained, but the method is clear. In this paper, the case $l=2$ will be considered in some detail, and the procedure in the general case will be indicated.

By (B.1), $X_2^{(\omega)}$ is proportional to

$$(2/x+\kappa/4-d/dx)(1/x+\kappa/2-d/dx)X_0^{(\omega)}$$
$$=(3/x^2+5\kappa/4x+\kappa^2/8)X_0^{(\omega)}$$
$$-(3/x+3\kappa/4)\frac{d}{dx}X_0^{(\omega)}+\frac{d^2}{dx^2}X_0^{(\omega)}.$$

Therefore $\frac{d}{dx}X_2^{(\omega)}$ is proportional to

$$-(6/x^3+5\kappa/4x^2)X_0^{(\omega)}+(6/x^2+5\kappa/4x+\kappa^2/8)\frac{d}{dx}X_0^{(\omega)}$$
$$-(3/x+3\kappa/4)\frac{d^2}{dx^2}X_0^{(\omega)}+\frac{d^3}{dx^3}X_0^{(\omega)}.$$

By performing a calculation involving the first three terms of the series for $X_0^{(\omega)}$ and then neglecting terms of the order $1/\kappa$ against unity, committing about a three percent error, we find

$$\frac{d}{dx}X_0^{(\omega)}\Big/X_0^{(\omega)}=-\tan\alpha\cdot(1-\tfrac{1}{2}ie^{-2\omega})/(1+\tfrac{1}{2}ie^{-2\omega}),$$
$$\frac{d^2}{dx^2}X_0^{(\omega)}\Big/X_0^{(\omega)}=\tan^2\alpha,$$
$$\frac{d^3}{dx^3}X_0^{(\omega)}\Big/X_0^{(\omega)}=-\tan^2\alpha\cdot(1-\tfrac{1}{2}ie^{-2\omega})/(1+\tfrac{1}{2}ie^{-2\omega}).$$

Therefore,

$$\frac{d}{dx}X_2^{(\omega)}\Big/X_2^{(\omega)}=-\tan\alpha\cdot\frac{1-\frac{1}{2}ie^{-2\omega}}{1+\frac{1}{2}ie^{-2\omega}}\cdot$$
$$\cdot\frac{1+\dfrac{8\tan^2\alpha}{\kappa(\kappa+10/x)}+\{6\tan\alpha/(\kappa+10/x)\}\dfrac{1+\frac{1}{2}ie^{-2\omega}}{1-\frac{1}{2}ie^{-2\omega}}}{1+\dfrac{8\tan^2\alpha}{\kappa(\kappa+10/x)}+\{6\tan\alpha/(\kappa+10/x)\}\dfrac{1-\frac{1}{2}ie^{-2\omega}}{1+\frac{1}{2}ie^{-2\omega}}}.$$

In the last term $8\tan^2\alpha$ may be neglected in comparison with κ^2, i.e., 32 in comparison with 2500, in both numerator and denominator.

In general, it is found that

$$\frac{d}{dx}X_l^{(\omega)}\Big/X_l^{(\omega)}=-\tan\alpha\cdot\frac{1-\frac{1}{2}ie^{-2\omega}}{1+\frac{1}{2}ie^{-2\omega}}\cdot\frac{1+\sigma_l+\rho_l\dfrac{1+\frac{1}{2}ie^{-2\omega}}{1-\frac{1}{2}ie^{-2\omega}}}{1+\sigma_l+\rho_l\dfrac{1-\frac{1}{2}ie^{-2\omega}}{1+\frac{1}{2}ie^{-2\omega}}}$$
$$=-\tan\alpha\cdot\frac{1-\frac{1}{2}iQ_le^{-2\omega}}{1+\frac{1}{2}iQ_le^{-2\omega}},\qquad(B.3)$$

where ρ_l, σ_l, Q_l are rational functions of $\tan\alpha$ and x, and

$$Q_l=(1-\rho_l+\sigma_l)/(1+\rho_l+\sigma_l).\qquad(B.4)$$

The solution inside the nucleus, given by Eq. (2.3), depends on the properties of

$$(\pi z/2)^{\frac{1}{2}}J_{l+\frac{1}{2}}(z)=\sin(z-l\pi/2)\cdot\sum_{m=0}^{\leq\frac{1}{2}l}\frac{(-1)^m(l+2m)!}{(2m)!(l-2m)!}(2z)^{-2m}$$
$$+\cos(z-l\pi/2)\cdot\sum_{m=0}^{\leq\frac{1}{2}(l-1)}\frac{(-1)^m(l+2m+1)!}{(2m+1)!(l-2m-1)!}(2z)^{-2m-1}$$
$$=S_l(1/z)\sin z+C_l(1/z)\cos z,\qquad(B.5)$$

thus defining S_l and C_l as polynomials in $1/z$. Then

$$\frac{d/dz[z^{\frac{1}{2}}J_{l+\frac{1}{2}}(z)]}{z^{\frac{1}{2}}J_{l+\frac{1}{2}}(z)}=\frac{K_l\cot z-H_l}{C_l\cot z+S_l},$$

where

$$H_l=C_l+(1/z)^2(dS_l/dz^{-1}),\qquad(B.6)$$
$$K_l=S_l-(1/z)^2(dC_l/dz^{-1}).\qquad(B.7)$$

Writing

$$z=\{2m(E-U)/\hbar^2\}^{\frac{1}{2}}r_0$$

and expanding the cotangent to the first order in $\lambda ir_0/v$ as in the case of $l=0$, it follows that

$$\left(\frac{d}{dx}X_l^{(i)}\Big/X_l^{(i)}\right)_{r=r_0}$$
$$=-\frac{H_l(M)\tan D-K_l(M)-(i\lambda r_0/2\mu v)(H_l+K_l\tan D)}{S_l(M)\tan D+C_l(M)-(i\lambda r_0/2\mu v)(S_l-C_l\tan D)},\qquad(B.8)$$

where

$$D=\mu kr_0=1/M.\qquad(B.9)$$

Equating now the right-hand members of Eqs. (B.3) and (B.8) at $r=r_0$, and separating real and imaginary parts, we find the Eqs. (5.3) and (5.4), which are our final results.

In the case $l=2$, we have found

$$\rho_2=6\tan\alpha_0/(\kappa+10/kr_0)\doteq 12/50,$$
$$\sigma_2=8\tan^2\alpha_0/\kappa(\kappa+10/kr_0)\doteq 32/2500\doteq 0.$$

Then

$$Q_2\doteq(1-\rho_2)/(1+\rho_2)$$
$$=(\kappa+10/kr_0-6\tan\alpha_0)/(\kappa+10/kr_0+6\tan\alpha_0).$$

Other Q_l's are found in a similar manner. S_l, C_l, H_l, and K_l are found from (B.5), (B.6), and (B.7). The results for l's as high as 4 are given in section 5.

The Magnetic Moments of the Neutron and the Deuteron*

WAYNE R. ARNOLD AND ARTHUR ROBERTS**
Argonne National Laboratory, Chicago, Illinois

(Received March 6, 1947)

The magnetic moments of the neutron and the deuteron have been measured in terms of the proton moment. The radiofrequency resonance technique of Alvarez and Bloch was used to determine the Larmor frequency of neutron precession in a magnetic field in which the frequency of proton precession had been determined by the method of Purcell, Torrey, and Pound. The ratio of the magnetic moment of the neutron to the magnetic moment of the proton is 0.68479 ± 0.0004. The ratio of the deuteron moment to the proton moment is 0.30702 ± 0.0001, in agreement with the Columbia value. Taking the magnetic moment of the proton as 2.7896 nuclear magnetons, the neutron moment is -1.9103 ± 0.0012 and the deuteron moment 0.85647 ± 0.0003 nuclear magneton. These values lead to a prediction of an admixture of 4.0 percent $^3D_1$ state in the ground state of the deuteron, in agreement with the value 3.9 percent found by Rarita and Schwinger from the magnitude of the electric quadrupole moment of the deuteron. The need for further theoretical investigation of the deuteron magnetic moment is pointed out.

INTRODUCTION

THE discovery of the electric quadrupole moment of the deuteron by Kellogg, Rabi, Ramsey, and Zacharias[1] showed that the ground state of the deuteron cannot be exclusively the $^3S_1$ state it had previously been assumed to be, since S states possess spherically symmetrical charge distributions. It became necessary to assume that Russell-Saunders coupling does not strictly apply, and so spin and orbital angular momentum are not separately conserved. By assuming the existence of a tensor interaction between the neutron and proton, Rarita and Schwinger[2] found it possible to account for the observed magnitude of the quadrupole moment by adjusting the constants of the interaction. In this way they found that the ground state of the deuteron must be $^3S_1$ 96.1 percent of the time, and $^3D_1$ 3.9 percent of the time.

Now, the admixture of $^3D_1$ state means that part of the time the neutron and proton have a relative angular momentum of two units, and accordingly, the magnetic moment of the deuteron should no longer be expected to be the algebraic sum of the proton and neutron moments, even on the assumption that the proton and neutron retain, when combined in the deuteron, the intrinsic moments they possess when free. Rarita and Schwinger calculated the dependence of the deuteron moment on the percentage admixture of $^3D_1$ state. Using the values for the proton and deuteron moments then current, namely, 2.785 and 0.855 nuclear magnetons,[3] they calculated that the magnetic moment of the neutron should be -1.911 nuclear magnetons. This is different from the algebraic difference -1.930 to be expected in the absence of a quadrupole moment. With the latest values for the proton and deuteron moments ($\mu_p=2.7896\pm0.0008$, $\mu_d=0.8565\pm0.0004$[4]), the predicted value becomes -1.9108 and the algebraic difference -1.9331.

The magnetic moment of the neutron has been measured by Alvarez and Bloch,[5] who obtained the value -1.935 ± 0.03 nuclear magnetons. This value is not inconsistent with the value predicted by Rarita and Schwinger; clearly, however, greater precision in the measurement is desirable, in order to see whether the simple mechanism postulated leads to a correct prediction of the neutron moment.

* This report is based on work performed under contract W-31-109-eng-38 with the Manhattan Project at the Argonne National Laboratory. The information presented will appear in Volume IIa, Division IV of the Manhattan Project Technical Series.

** Department of Physics, State University of Iowa, Iowa City, Iowa.

[1] J. M. B. Kellogg, I. I. Rabi, N. F. Ramsey, and J. R. Zacharias, Phys. Rev. **57**, 677 (1940).

[2] W. Rarita and J. Schwinger, Phys. Rev. **59**, 436 (1941).

[3] J. M. B. Kellogg, I. I. Rabi, N. F. Ramsey, and J. R. Zacharias, Phys. Rev. **56**, 728 (1939).

[4] S. Millman and P. Kusch, Phys. Rev. **60**, 91 (1941).

[5] L. W. Alvarez and F. Bloch, Phys. Rev. **57**, 111 (1940); Phys. Rev. **57**, 352 (1940).

Recently, Purcell, Torrey, and Pound,[6] and Bloch, Hansen, and Packard[7] have described two closely related and simple radiofrequency methods for measuring the gyromagnetic ratio, g, of a nucleus. These methods are based on the observation of the resonant frequencies of precession in a magnetic field, which are given by the relation

$$h\nu = gH.$$

The techniques involved are simpler than those used in the molecular beam methods. Radio techniques are employed, and the nuclei are contained in a solid or liquid sample.

Alvarez and Bloch measured the neutron moment by observing the dip in transmission of a polarized beam of neutrons through a ferromagnet, when the neutrons traversed a fixed magnetic field upon which was superposed a radiofrequency magnetic field in resonance with their precession frequency; this method is directly analogous to the molecular beam resonance method of Rabi and his collaborators. We have now remeasured the neutron moment by the same method, using a magnetic field in which the frequency for proton resonance was also observed by the method of Purcell, Torrey, and Pound. Thus we have in effect measured the ratio of the neutron and proton moments. As a partial check on the results, we have also measured the ratio of the deuteron moment to the proton moment. The results, it will be seen, confirm the predictions of Rarita and Schwinger. In neither the experiment by Alvarez and Bloch, nor our experiment, is the sign of the magnetic moment of the neutron determined.

APPARATUS

Neutron Moment

In order to measure the neutron moment three electromagnets were arranged as shown in Fig. 1. The air gap in each magnet was $\frac{3}{4}$ inch; the spacing between the rectangular pole-pieces of successive magnets was adjustable, and was made one-half inch or less. The pole-pieces of the polarizing and analyzing magnets were 3 by 3 inches; the central magnet had 7 by 3 inch pole-pieces. Since all the fields were in the same direction, there were no depolarizing weak field regions for the neutrons to traverse between the polarizing and analyzing iron blocks. Because of the proximity of adjacent magnets, the magnetic field in the central gap depended upon the currents through the exciting coils of the outer magnets. Accordingly, the currents in all three magnets were electronically regulated, and it was possible, by suitable adjustment of the currents in the outer magnets, to reduce considerably the inhomogeneity of the magnetic field in the central gap. This was feasible because the degree of polarization of the neutron beam is not too strongly dependent upon the current when saturation of the magnets is approached. The electronic stabilizers used held the current constant to within 0.01 percent over long periods of time. The magnets were air-cooled.

The polarizing and analyzing blocks were of Armco iron, $1\frac{3}{16}$ inches long in the direction of the beam and $\frac{3}{4}$ by $1\frac{1}{8}$ inches in cross section. They were set near the outer edges of the pole faces. The thermal neutron beam from the Argonne heavy water pile was defined by cadmium slits, and was 1 inch high and $\frac{3}{8}$ inch wide. The detector was a BF_3 proportional counter, heavily shielded. The beam is so well collimated and thermalized that a thin sheet of cadmium placed anywhere along it reduces the counting rate by a factor of well over a thousand. No background corrections were necessary.

The coil used for flipping the neutrons was rectangular in cross section, and large enough to pass the neutron beam. For the first four runs a

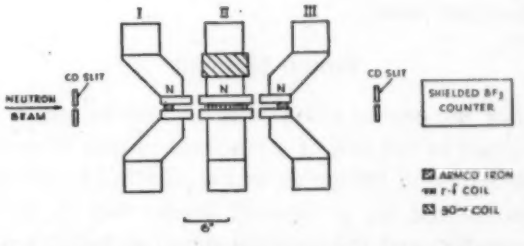

FIG. 1. Arrangement of apparatus for observing neutron resonances. A collimated thermal neutron beam is polarized by passage through a block of saturated iron in the gap of the first magnet. A coil in the center magnet induces transitions which depolarize the beam when the r-f field of the coil oscillates at the Larmor frequency. The depolarization is detected by the change in transmission of the beam through the second block of iron.

[6] E. M. Purcell, H. C. Torrey, and R. V. Pound, Phys. Rev. 69, 37 (1946).

[7] F. Bloch, W. W. Hansen, and M. Packard, Phys. Rev. 69, 127 (1946); *ibid.* 70, 474 (1946); F. Bloch, Phys. Rev. 70, 460 (1946).

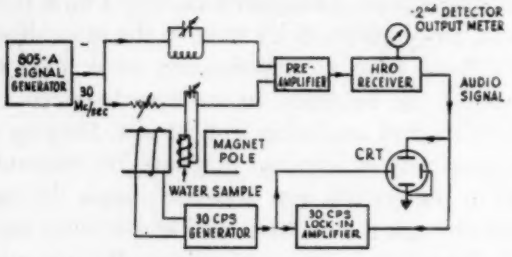

FIG. 2. Apparatus for observing the proton and deuteron moments. Balance in an r-f bridge circuit is detected by means of a receiver. One arm of the bridge contains the water sample in a coil in a magnetic field. At resonance absorption of energy by the induced transitions unbalances the bridge. Unbalance is detected by (a) an increase in the second detector output, (b) a pip on the cathode-ray tube screen each time the magnetic field goes through resonance, and (c) a reading on the output meter of the lock-in amplifier.

coil 4 inches long was used; in the remaining runs a 3-inch coil was used despite the fact that the neutron resonances were slightly widened because of the shorter time spent in the r-f field. In the first four runs different coils were used for the proton and neutron resonances. The shorter coil was used in later runs for both neutron and proton resonances in order to improve the homogeneity of the field in which the flipping took place and to insure its identity for neutrons and protons.

For the neutron resonances, a self-excited oscillator with an output of about six watts was used.

Since there are small fluctuations in the neutron intensity of the heavy water pile, the neutron counting rates were normalized by means of a monitor chamber in the thermal beam. Counting rates in the BF_3 detector were about 30,000 counts per minute, and about 40,000 counts were taken per point.

Proton Moment

For the proton resonances a water sample was inserted in the coil of a resonant circuit forming one arm of a bridge as in Fig. 2.*** The bridge was excited by a General Radio 805-A signal generator, and the residual signal at balance detected by a National HRO receiver with a preamplifier with enough gain to give an observable current from rectified noise in the second detector. Balancing was accomplished by adjusting phase and amplitude in each arm. With care, the residual signal could be made 50 to 60 db below the signal transmitted by each arm. Input signals between 0.01 and 1 volt were used. The signal-to-noise ratio could be improved by narrowing the i-f band width of the receiver with the quartz crystal filter provided in the receiver; the improvement possible is limited by the frequency drift of the signal generator.

Proton resonances were detected in one or more of three ways. At resonance, the protons absorb energy, decreasing the amount of signal passing through one arm of the bridge and thereby unbalancing it; a meter in the output of the second detector in the receiver accordingly shows an increased reading. However, resonances are more easily located, and sensitivity increased if an a.c. field is superposed on the constant magnetic field. For this purpose a small additional coil was added to one arm of the central magnet, and was excited by 30-cycle a.c. from a power amplifier fed by a synchronously driven permanent-magnet generator. If the a.c. field is made 30 to 50 gauss (peak-to-peak), a cathode-ray oscilloscope, whose horizontal sweep is obtained from the 30-cycle generator and whose vertical plates are connected to the receiver output, shows a pip each time the magnetic field sweeps through resonance, twice each cycle. When the resonance has been located, the a.c. field can be gradually reduced and the fixed field adjusted until the resonance is exactly centered, and occupies the entire sweep; the a.c. field is then less than one gauss, and can be turned off without affecting the fixed field.

Finally, a very large factor in sensitivity is gained by using a tuned audio amplifier sensitive only to a narrow band of frequencies centered at 30 cycles. By suitable restriction of the alternating field amplitude, the field can be made to vary over a small portion of the resonance curve, and the tuned "lock-in" amplifier then indicates the amount of 30-cycle component present in the audio output of the receiver. This technique was found unnecessary in the proton measurements because sensitivity was adequate without it; however, it was useful in initially locating the much weaker deuteron resonance.

Radiofrequencies were measured by means of a 1-Mc crystal oscillator provided with frequency

*** We are indebted to Dr. E. M. Purcell for private communication of the improvements in technique here described.

dividers and harmonic generators which gave signals at 10-kc intervals of adequate intensity over the entire frequency range used. A vernier was added to the 500-division dial of the National receiver so that readings could be made to 0.1 division directly. Frequencies were thus read directly to the nearest 10 kc, and the next place obtained by interpolation. In many cases, the band-spread features of the receiver could be used to facilitate frequency measurements.

The deuteron resonances were measured in the same way as the proton resonances. The frequencies were, of course, much lower. Heavy water was used; the resonance of the deuteron in heavy water has an apparent width of the same order of magnitude as that of the proton in ordinary water.

PROCEDURE

The first step in doing the experiment was to determine the strength of the fields in the outer magnets that would give enough polarization of the neutron beam to give a dip in neutron intensity at neutron resonance whose minimum could be accurately determined. It was found that fields of about 8000 gauss in the outer magnets, and 7000 gauss in the center magnet, resulted in the most uniform field in the center magnet (less than 0.05 percent inhomogeneity) and gave neutron resonance dips of 5 to 8 percent. The increase of transmission through either block of iron when it was magnetized and the other block when it was unmagnetized was about 8 percent, indicating that after passing through the first block of iron 69 percent of the neutrons had their moments aligned in one direction, and 31 percent were oppositely aligned. When both blocks of iron were magnetized, the increase of intensity of the neutron beam was 22 to 24 percent. This indicated that some of the neutrons had been depolarized in the iron and that a maximum dip of $23-(2\times 8)$ percent, or about 7 percent could be expected.

The 805-A signal generator was set to a frequency which would give proton resonance at about 7000 gauss, the coil containing water was placed in the center magnet, the bridge was balanced for that frequency, the 30-cycle a.c. component of the field in the center magnet was set at about 30 gauss, and the current to the center magnet was then varied until the pips indicating proton resonance appeared on the oscilloscope. The 30-cycle a.c. field was then decreased in steps, the central field being readjusted each time to center the pips on the oscilloscope screen, until the 30-cycle field was zero. This method of setting the central field was checked by the output meter on the HRO receiver and the lock-in amplifier, and found to give the same result in all cases. The frequency of the signal generator was then measured. In the first four runs the box containing the coil and the water sample was then removed from the center magnet and replaced by a similar box, having a coil 4 inches long and with a cross section large enough to pass the neutron beam. Power from the r-f oscillator was then fed into this second coil and

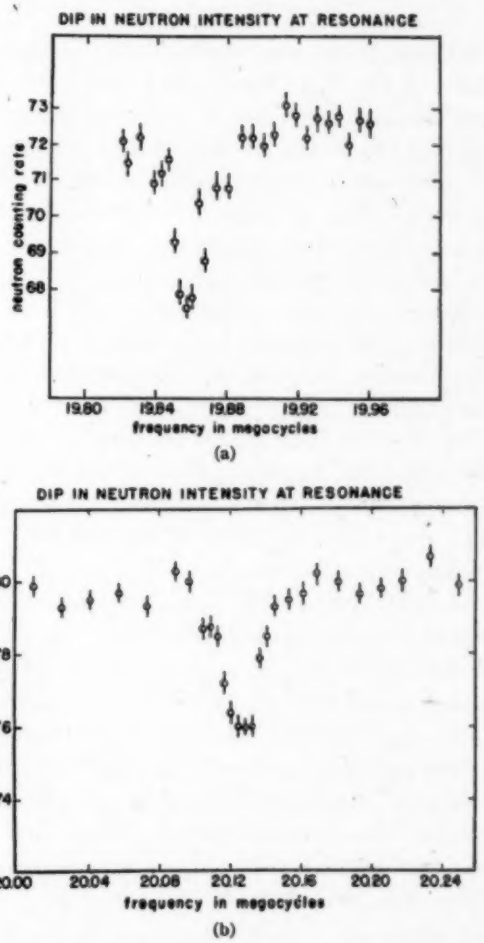

FIG. 3. Typical neutron resonance dips. (a) with 4-in. flipping coil, (b) with 3-in. flipping coil. The dip is wider in (b) than in (a) because of the shorter time spent in the field by the neutrons.

TABLE I. Results of neutron runs.

Run	Neutron frequency f_n Mc/sec.	Proton frequency f_p Mc/sec.	Ratio f_n/f_p	Statistical weight
1	19.820	28.936	0.68496	2
2	19.513	28.491	.68488	1
3	19.507	28.496	.68455	2
4	19.647	28.701	.68454	2
5	19.487	28.452	.68491	4
6	19.520	28.520	.68442	4
7	20.180	29.474	.68468	4
8	20.122	29.402	.68438	4
9	20.125	29.375	.68511	4
10	19.964	29.157	.68470	4
11	19.891	29.038	.68498	4
12	19.174	27.997	.68486	4
13	19.107	27.898	.68489	4
14	19.856	28.997	.68475	8
15	19.858	28.993	.68492	8
16	19.854	28.989	.68488	8
17	19.850	28.987	.68479	8

Weighted average $\mu_n/\mu_p = 0.68479 \pm 0.0002$

a neutron beam sent through the apparatus as shown in Fig. 1. In later runs a new coil 3 inches long was used from which the water sample was removed to permit the neutrons to pass through the same coil that was used to obtain the proton resonance. The frequency of the oscillator was then changed in small steps, and the intensity of the neutron beam coming from the analyser was measured for each frequency until the neutron intensity had increased to its original value again after passing through the dip indicating resonance. The frequency corresponding to the center of the dip was then measured. The signal generator frequency was then changed slightly and the next run made. Figure 3a shows a neutron dip using the 4-inch coil; Fig. 3b shows a similar dip obtained with the 3-inch coil.

Since the r.m.s. deviations in frequency measurements in the first four values were about equal to the uncertainty in reading the HRO dial, a vernier was added to the dial to give greater accuracy, and used in the remaining 13 runs.

Although the currents in the magnets, as measured by a Leeds and Northrup type K potentiometer, remained practically constant over the 30 to 40 minutes between the measurements of the proton and neutron resonance frequencies, and although partial saturation of the iron of the magnets made the change in field with changing current even smaller, an experiment was performed to determine the change in the field of the center magnet with time. This was done by holding the currents to the magnets constant, and observing the change in the proton resonance frequency with time. This showed a continued systematic decrease of frequency of about 3 kc per hour with good air cooling, and up to 10 kc per hour with poor air cooling (at 30 Mc). This change in field is probably caused by the change in dimensions and permeability of the iron in the magnets as they grow warmer.

The last four runs were made to check on the corrections made to the first 13 runs, and were all made without changing the currents to any of the magnets. The values for the proton frequencies shown for the last four runs in Table I are interpolated between the values for proton resonance found before and after each neutron run, and they indicate the drift in the field that occurred during the $3\frac{1}{2}$ hours it took to make the four runs.

Deuteron Moment

The procedure in measuring the ratio of the deuteron magnetic moment to the magnetic moment of the proton was to set the signal generator to a frequency of about 4.3 megacycles, set the 30-cycle a.c. field to about 25 gauss, and, with a coil containing about 20 grams of D_2O in the arm of the bridge that is in the magnetic field, to balance the bridge. The current to the center magnet was then varied until the resonance pips appeared on the oscilloscope screen. The 30-cycle field was then reduced slowly to zero with simultaneous adjustments of the current to the magnet to keep the ever-widening resonance pips centered on the screen. The signal generator frequency was then measured. (In three measurements its frequency was held to zero beat with a harmonic of the crystal oscillator.) The current to the magnet was then held constant while a coil containing ordinary water was substituted for the deuterium coil, and the signal generator set to the necessary frequency, as calculated from the known ratio of the magnetic moments. The 30-cycle field was turned up to 25 gauss, the bridge was balanced, and the pips for proton resonance appeared on the oscilloscope. The 30-cycle field was then reduced to zero in small steps; this time the necessary changes to keep the pips centered were made in the signal generator

frequency. When zero 30-cycle field was reached, the signal generator frequency was measured. Hysteresis from the a.c. cycling of the magnetic field was checked and found not to change the field measurably.

The deuteron resonance was obtained first, since the resonance pips for deuterium were only about 4 times the noise level. The proton pips were about 30 times noise and thus much easier to center, especially when the bridge was some distance off balance.

The values for the proton resonance frequency were adjusted to correct for the small drift in the field, the correction being about three times the r.m.s. deviation between the values obtained in the four runs.

RESULTS

The results of seventeen runs on the neutron moment are summarized in Table I. This table includes every run taken except the very first one. This trial run was discarded because about four hours elapsed between the setting of the magnetic field on the proton resonance and the location of the neutron resonance. The value of the neutron moment obtained in this trial run was lower than the average of the remaining runs by more than three times the standard deviation of the other runs; there were other reasons to suspect that the magnetic field might have changed during that interval.**** After the trial run it was known where to look for the neutron resonance, and the neutron run could be started at 30 to 50 kc off resonance. All runs for which data are given required less than an hour between setting on the proton resonance and passing through the neutron resonance; in most cases the time was about one-half hour.

After the first four runs, the technique of frequency measurement was somewhat improved by the addition of the vernier to the dial of the receiver. The second run was cut short by a power failure before the completion of the neutron resonance dip. Also, in the first four runs different coils were used for the proton and neutron resonances. In runs 1 to 4 considerable heating of the magnet coils occurred; in all later runs better air-cooling reduced the heating of the magnets. After run 13, technique had improved to the point where it was possible to leave the magnetic field fixed after determining the neutron resonance, and to find the proton resonance again by varying the frequency of the signal generator. This is difficult because the bridge must be rebalanced at each frequency—a tedious procedure unless the proton resonance is quite strong. The last four runs were taken without changing the magnetic field at all, and taking proton and neutron resonances alternately. The observed drift in the magnetic field could thus be corrected.

By making repeated observations on the proton resonance frequency as a function of time, it was possible to determine approximately the amount of drift in the magnetic field under the conditions obtaining in runs 1 to 13. The observed proton resonance frequencies have been corrected for this drift. The correction is always in such a direction as to decrease the proton frequency; in runs 1 to 4 it is 5 kc and in runs 5 to 13, 3 kc. Thus the correction is never as great as 0.02 percent. The drift in magnetic field is caused by the heating of the magnets, not by the electronic stabilization, which shows no such drift in the magnet current.

In view of all the above, statistical weights have been arbitrarily assigned to the various runs in accordance with our judgment as to their relative merits. Runs 1–4 are assigned the weight 2, with the exception of the incomplete run No. 2 which is assigned the weight 1. Runs 5–13, taken under improved conditions, are assigned the weight 4, and runs 14–17, in which the magnetic field drift was observed directly, the weight 8. An unweighted average differs from the weighted average by less than the assigned error.

Table II shows the results of four runs on the deuteron-proton moment ratio. Small corrections for the magnetic field drift have been applied in

TABLE II. Results of deuteron runs.

Run	Deuteron frequency f_d Mc/sec.	Proton frequency f_p Mc/sec.	Ratio f_d/f_p
1	4.2900	27.948	0.153499
2	4.3035	28.031	.153526
3	4.4000	28.662	.153513
4	4.4100	28.728	.153509
		Average	0.153512 ± 0.00001
		$\mu_d/\mu_p = I_d f_d / I_p f_p$	$= 0.307023 \pm 0.00002$

**** It is interesting to note that if a correction for drift of the magnetic field is applied, the value obtained becomes concordant with later data.

all cases. Since the deuteron moment has previously been measured with precision as great as our own, no further runs were taken. Our concordant measurement of the deuteron-proton ratio with the same equipment makes it less likely that there are unknown systematic errors in the neutron-proton ratio, and has the further merit of providing all the information necessary to a check on the Rarita and Schwinger calculations. The agreement of the observed deuteron moment with the results of Kellogg *et al.*[3] gives us more confidence in the precision of the neutron value.

The ratio of the neutron resonance frequency to the proton resonance frequency is the ratio of their gyromagnetic ratios. The spin of the proton is one-half, and while there is no direct measurement of the neutron spin, the overwhelming weight of the evidence is that it, too, has a spin of one-half. The ratio of the resonance frequencies is thus the ratio of the magnetic moments. In the case of the deuteron, the ratio of the deuteron resonance frequency to the proton resonance frequency must be doubled to obtain the ratio of the magnetic moments, since the spin of the deuteron is one.

PRECISION OF RESULTS: SOURCES OF ERROR

The standard deviation of the seventeen runs on the neutron-proton ratio is 0.0002. This quantity can be decreased indefinitely by taking more and more observations; the final estimate of the probable error must therefore include other considerations.

Accidental Errors

The accidental errors of the experiment include the following:

1. Errors in Frequency Measurement

We estimate that this error seldom exceeds 2 kc. Better frequency determination is readily possible; however, no suitable equipment was available. This error is as likely to be in one direction as the other.

2. Errors in Determining the Center of the Resonance Peaks

Insofar as the peaks are symmetrical this error is accidental. The proton resonance peaks were visually symmetrical; so were the deuteron peaks. There was no consistent indication of asymmetry in the neutron resonance dips.

3. Statistical Errors in Counting

These amount to 0.3 percent for each neutron point. The dips in intensity at resonance were 5 to 8 percent.

Systematic Errors

Accidental errors are decreased by taking many runs. More important, of course, are systematic errors, both known and unknown.

The known systematic errors are these:

1. Drift in the Magnetic Field

This was measured and corrected for, as described above.

2. Inhomogeneity in the Magnetic Field

This was measured by means of a fluxmeter. It was found possible to reduce the inhomogeneity to less than 0.02 percent over the volume occupied by the r-f coil; the residual inhomogeneity consisted of a slight decrease in the field near the ends of the coil. To a first approximation, such an inhomogeneity tends to broaden the resonances asymmetrically on the low frequency side and could thus shift the peak. The shift is in each case proportional to frequency, however, and thus vanishes to a first approximation in the ratio. In addition, as remarked above, no definite asymmetries were observed.

3. Difference Between the Magnetic Fields for the Neutron and the Proton

In runs 1–4, where different coils were used, this error could be larger than in subsequent runs where the same coil was used. Some of this error might still persist, however, since the water sample occupied the geometric volume of the coil, while neutron flips might be induced outside the ends of the coil. Since the inhomogeneity is slight in any case, and since no systematic difference between the first four and later runs is found, no correction is made.

4. Difference Between the Magnetic Fields Actually Present at the Proton and Neutron Because the Protons are in Water

The diamagnetic susceptibility of water is less than 10^{-6}, and thus of no concern in itself. The

diamagnetic effect of the hydrogen atom[4] is likewise too small to matter (3×10^{-5}). The magnetic field at one proton caused by the magnetic moment of a neighboring proton is of the order of one gauss; the true width of the resonance is due to the average effect of such fields. It is difficult to see how the resonance might be shifted, but such a possibility cannot be excluded. Accordingly, the frequencies of proton resonances in tap water, distilled water, benzene, paraffin, and a 1.5 percent solution of $FeCl_3$ were compared in a fixed magnetic field. They could not be distinguished from one another, and were all within 0.01 percent. The paraffin resonance is considerably wider than the others, which are of about equal width. This width, *ca.* 0.6 gauss, may not yet be the true width, since we could not have detected inhomogeneities in the magnetic field appreciably less than this. Polystyrene shows a resonance even wider than that of paraffin. While this experiment does not exclude the possibility of a systematic shift, it makes it unlikely that it should be large compared to 0.01 percent.

5. *Doppler Shift of Resonance Frequency Caused by Neutron Motion*

The thermal neutrons traverse the r-f coil with a mean speed of about 2.5×10^5 cm/sec. The quantity v/c is thus of the order 10^{-5}. It is clear that any symmetric periodicity or change in the apparent frequency seen by the neutrons in entering and leaving the coil can only change the resonance curve symmetrically. It is difficult to see how there can be an asymmetric change in the frequency seen by the neutrons. The observed widths of the neutron dips are in agreement with values computed from the time they spend in the coil; the dips are narrower with the 4-inch coil than with the 3-inch coil.

Similar arguments apply to the Doppler effect of the thermal agitation of the protons. This is, however, random, and no shift is to be expected.

6. *Systematic Errors in Frequency Determination*

These can be caused by drift of the local oscillator of the receiver, or by backlash in the dial. They can be readily checked by means of the crystal oscillator, and were found to be negligible. The crystal itself was checked against transmissions from WWV; its error was far smaller than the random errors of frequency determination.

7. *Shift of Resonant Frequency by the Radio-frequency Magnetic Field*

Bloch and Siegert[8] have shown that if H_1 is the amplitude of the oscillating field and H_0 the magnitude of the fixed field, a shift in the resonant frequency whose magnitude is given, to the first order, by $H_1^2/16H_0^2$ is to be expected. In our neutron runs, H_1 was about 7 gauss, H_0 7000 gauss; the shift is thus of the order 10^{-7} and thus completely negligible. In the proton runs, the oscillating field is smaller by a factor of 10^2 or more.

Determination of the deuteron-proton ratio is subject to similar errors. While fewer runs were taken, they gave a smaller statistical spread.

It is, of course, impossible to make any reasonable allowance for unknown systematic error.

FINAL RESULTS

In view of the possible sources of error quoted, we think it reasonable to state the **final results** with their probable errors as follows, **on the basis of a proton moment of 2.7896 nuclear magnetons:**

$$\mu_n/\mu_p = 0.68479 \pm 0.0004$$
$$\mu_n = -1.9103 \pm 0.0012 \text{ nuclear magnetons}$$
$$\mu_d/\mu_p = 0.30702 \pm 0.0001$$
$$\mu_d = 0.85647 \pm 0.0003 \text{ nuclear magneton.}$$

Taking into account the probable error 0.0008 in the proton moment, the **absolute values for the neutron and deuteron moments** become

$$\mu_n = -1.9103 \pm 0.0013 \text{ nuclear magnetons}$$
$$\mu_d = 0.85647 \pm 0.0004 \text{ nuclear magneton.}$$

Rabi and his coworkers[3] give for the deuteron-proton ratio 0.30703 ± 0.0001, and for the absolute value of the magnetic moment of the deuteron 0.8565 ± 0.0004.

DISCUSSION OF RESULTS

The value of the magnetic moment of the free neutron which is predicted by the theory of Rarita and Schwinger, using the latest determinations of the proton and deuteron moments of the Columbia investigators, is -1.9108 nuclear

[8] F. Bloch and A. Siegert, Phys. Rev. **57**, 522 (1940).

magnetons. Our observed value is -1.9103 ± 0.0012. The prediction is based upon the value of 3.9 percent admixture of $^3D_1$ state in the ground state of the deuteron, a value obtained from the observed value of the quadrupole moment. Using only the relative values of the neutron, proton, and deuteron moments obtained in this experiment, we find the value 4.0 percent for the $^3D_1$ admixture more directly and with fewer assumptions. The possibility that the deuteron moment is simply the algebraic sum of the proton and neutron moments is far outside the limits of error.

The theory developed by Rarita and Schwinger thus predicts correctly the magnetic moment of the deuteron, provided that the magnetic moments of the proton and neutron and the electric quadrupole moment of the deuteron are given. In order to do this, certain assumptions are made concerning the range of the nuclear forces and the shape of the potential well. However, it appears that the successful prediction cannot be taken as proof of the correctness of the assumed range and potential distribution, since the simple theory used omits certain considerations which must now, because of the high precision of the measurements, be taken into account.

These considerations concern the assumption that the proton and neutron retain, when combined in the deuteron, the magnetic moments they possess when free. This assumption is certainly true to a high degree of approximation, as the numerical values show. It is, however, now necessary to examine it somewhat more critically, before assuming it to be correct to a numerical precision of less than one part in one thousand, which the experimental values have now attained.

There are at least two reasons for doubting the validity of the assumption of unaltered intrinsic moments to this degree of precision. One is that magnetic dipole moments, like other electromagnetic quantities, are subject to relativistic correction. From the point of view of the proton or neutron, the magnetic moment of the other nucleon in the deuteron should appear to be somewhat different from its rest value because of the relative motion of the two particles; the same is true of an observer stationary with respect to the deuteron. In fact, a particle of rest moment μ should appear to possess an electric dipole moment of $\mu p/m_0 c$. Theories of the relativistic correction to the magnetic moment of the deuteron, caused by the relative motion of the neutron and proton, have been proposed by Margenau[9] and by Caldirola.[10] While neither of these theories can be accepted as final, it appears that some such correction is necessary. The corrections proposed by Margenau and Caldirola are of the order of 0.005 nuclear magneton, a value considerably larger than the experimental error.

In addition, a meson theory of nuclear forces of any currently fashionable type will in general imply an alteration of the magnetic moments of two nucleons as close to each other as are the neutron and proton in the deuteron; this is because of the interaction of the meson fields. No detailed calculations of this nature have, so far as we know, yet been made; the subject has, however, been investigated by Pais[11] and by Serpe,[12] who find the usual divergences. In principle, when the relativistic correction to the deuteron moment has been made, it might be possible to use the experimental data to help decide among the various forms of meson theory.

It may be concluded, then, that gratifying as the agreement of the present results with the Rarita-Schwinger theory may be, it is not yet final. The fundamental correctness of the approach seems to be verified. However, the value of 4.0 percent for the $^3D_1$ admixture cannot be taken too literally until further detailed theoretical investigations have been made.

ACKNOWLEDGMENTS

We wish to acknowledge with thanks the cooperation extended by personnel of the Argonne National Laboratory, and especially the encouragement and assistance of the Director, Dr. W. H. Zinn.

[9] H. Margenau, Phys. Rev. **57**, 843 (1940).
[10] P. Caldirola, Phys. Rev. **69**, 608 (1946).
[11] A. Pais, Physica **9**, 407 (1942).
[12] J. Serpe, Thesis, Univ. of Liège, 1943; also in Mémoires de la Soc. Roy. des Sciences de Liège, [1], **1**, No. 2, 251–322.

Thermal Diffusion with Boron Trifluoride*

W. W. WATSON, J. O. BUCHANAN, AND F. K. ELDER, JR.
Sloane Physics Laboratory, Yale University, New Haven, Connecticut

(Received March 10, 1947)

With BF_3 gas at atmospheric pressure in 7 meters of hot wire Clusius and Dickel columns, with $\Delta T = 400°C$, the equilibrium separation factor for $B^{10}F_3/B^{11}F_3$ was 1.32 ± 0.12, reached in slightly over three days. Our best separation factor per meter of column indicates a thermal diffusion constant $\alpha \geqq +5.0 \times 10^{-4}$ and $R_T \geqq 0.06$. Experience in purifying commercial BF_3 gas and with mass spectrometer analyses is discussed.

INTRODUCTION

BORON of mass 10 is of considerable interest in nuclear research because of its large cross section for the $B^{10}(n, \alpha)Li^7$ reaction. To increase the concentration of this isotope in some boron compound, it seemed possible that the thermal diffusion method, which has been so successful in numerous isotope separation experiments,[1] would serve. The only available gaseous compound stable over a sufficiently large temperature range is boron trifluoride. Unfortunately, since the coefficient of viscosity η of BF_3 has not been determined, the thermal diffusion constant could not be predicted, and hence the design of an efficient multi-stage Clusius and Dickel apparatus could not be calculated in advance.

Assuming for purposes of rough calculation, however, that η for BF_3 is about the same as for SO_2, a molecule of about the same molecular weight and size, one can estimate that for maximum separation factor (ratio of the remixing by diffusion to that by convection equal to 2) a Clusius and Dickel hot wire column with the mean temperature 600°K and the gas at atmospheric pressure should have a gap space between hot and cold surfaces of about 3.54 mm. Such a value of η (162 micropoises at 100°C) would mean that R_T, the ratio of α to the hard sphere value for these molecular masses, is close to zero. Experience has shown, however, that one can compensate for this small value of R_T by using a greater length of column in a multi-stage apparatus. Since for most efficient operation of thermal separation columns, the distance $2w$ between hot and cold walls should be somewhat greater than that calculated for maximum separation factor, we have used glass columns of 8 mm I.D. with 20-mil wires along their axes. This makes $2w = 3.75$ mm, a reasonable compromise value even in retrospect. The construction features of our glass columns were similar to those described in other recent research papers from this laboratory.[2-4]

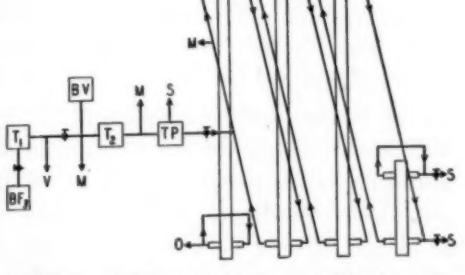

FIG. 1. Schematic diagram of thermal diffusion apparatus for boron trifluoride. Φ, steel valve; T_1, CO_2 trap, T_2, liquid-air trap (gas storage); *BV*, ballast volume; *TP*, Toepler pump; *M*, manometer; *O*, outlet to valve-off system; *S*, outlet to sampling system; *V*, vacuum pump.

SEPARATION APPARATUS AND PROCEDURE

Figure 1 is a schematic diagram of the thermal diffusion apparatus. The three long columns were each 3 meters in length, while the final shorter column was just 1 meter long. The top of each column was connected to the bottom of the succeeding column by a pair of convective coupling pipes, and convective circulation was maintained at the two ends of the apparatus. The first 3-

* This work was done under contract OEMsr-911 with the Office of Scientific Research and Development, and the document will appear in Division III of the Manhattan Project Technical Series.

[1] For a review and bibliography of the subject, cf., W. H. Furry and R. C. Jones, Rev. Mod. Phys. 18, 151 (1946).

[2] E. F. Shrader, Phys. Rev. 69, 439 (1946).
[3] S. B. Welles, Phys. Rev. 69, 586 (1946).
[4] R. Simon, Phys. Rev. 69, 596 (1946).

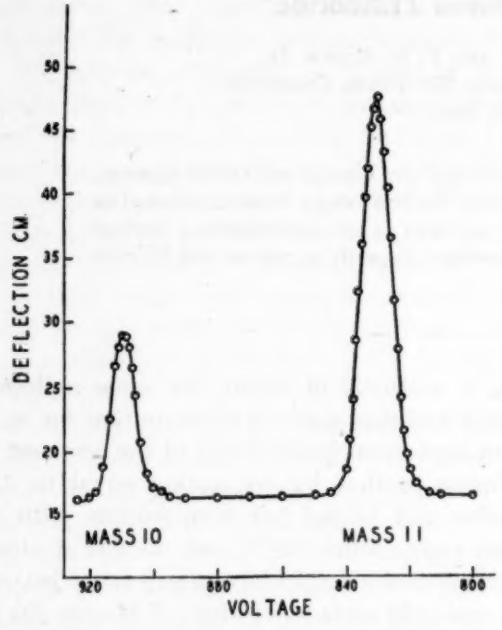

FIG. 2. B^+ mass peaks for BF_3 gas at "light" end of 7 meters of thermal diffusion column after 6 days of operation. B^{11}/B^{10} abundance ratio 2.92 to 1 as compared with 3.88 to 1 for the input "purified" gas.

meter column operated as a scrubber, the identical dimensions of the scrubber and the first separating column being in conformity with the dictates of the theory.[1] Both platinum and steel wires were used for the hot surfaces. Because of the concentration of a heavy, rather corrosive impurity, which was probably SiF_4, at the "heavy" end of the apparatus, we found it desirable to use platinum wire in the scrubber. At the "light" end of the apparatus, though, where this corrosive impurity was not present, we have found that the hot steel is not attacked at 450°C in an atmosphere of BF_3 gas. All valves were of steel.

It is of course essential for isotope separation by thermal diffusion that the working gas be pure. Our mass spectrometer analysis showed that commercial BF_3 gas contains very appreciable amounts of SiF_4, CO_2, N_2, and SO_2, the SiF_4 being the major impurity as judged by a large mass 85 peak assignable to SiF_3^+. To rid the gas as far as possible of these impurities we carried out several vacuum distillations at dry ice and liquid-air temperatures between traps T_1 and T_2 (Fig. 1). The purified gas was then stored at liquid-air temperature in T_2 from which portions were removed periodically to fill a modified Toepler pump. By means of compressed air through a slow leak, the gas was then forced continuously at the average rate of 55 cm^3/hr. from the Toepler pump into one of the convective coupling pipes connecting the scrubber and the first separating column. Samples could be taken in break-seal tubes of our input gas, as well as of the gas continuously exhausted at the bottom of the scrubber, and the gas both at the bottom and top of the final 1-meter column. The wire temperatures were set at 450°C by cathetometer measurement of the elongations produced by the heating current. The power consumption in the hot wires was 8 watts per meter.

This apparatus, with various minor modifications, was operated for different periods of time, the longest of which was 15 days. Even though we had taken great care to purify the BF_3 gas, we found upon shut-down after the 15 days of operation that the wire of the scrubber was coated with a corrosive deposit of solid material, and that a similar deposit, decreasing in amount with distance from the top of the scrubber, existed on the wires of the two 3-meter columns. The wire of the final 1-meter column at the "light" end, however, had no trace of a deposit on it. To explain this deposit we note that it must have come from an impurity heavier than BF_3 since it was being sent to the "heavy" end of the apparatus by the thermal syphoning action. Comparison of our mass spectrometer analyses of gas samples taken from the bottom of the scrubber and from the "light" end of the separating columns indicated, by the presence of a mass 85 peak in the former and its absence in the latter, that SiF_4 was probably the responsible impurity.

It would undoubtedly be possible to purify the BF_3 gas more completely, and then any slight residue of SiF_4 should be practically completely bled-off at the bottom of the scrubber. Our purification process does seem to have effectively removed all the nitrogen. According to our analyses of the gas at the bottom and top of the 1-meter column, quite pure BF_3 was circulating in this part of our system. The best separation factor was produced in this last meter of separating column, and we therefore draw our conclusions almost entirely from its performance.

MASS SPECTROMETER ANALYSES

All of the gas analyses were carried out with a small 60° mass spectrometer modeled after one described by Nier.[5] No trouble was experienced from any corrosive action of BF_3 or SiF_4. In agreement with the findings of Inghram,[6] we observed that BF_2^+ and SiF_3^+ are by far the most abundant positive ions of all those formed by the electron impacts in the ion source of the spectrometer. Because the peaks at mass 10 and mass 11 were better resolved and were uninfluenced by overlapping of other mass peaks, however, we used them exclusively in our determination of the relative abundance of the two boron isotopes in all samples. Figure 2 is representative of the performance of our spectrometer. This particular analysis was of a gas sample withdrawn from the top of the 1-meter column after 6 days of operation, the ratio of the heights of the B^{11} and B^{10} peaks being 2.92 to 1, after the correction for the difference in accelerating voltage is applied, as against 3.88 to 1 for the input "purified" gas.

Since we varied the accelerating voltage in the ion source in order to bring the desired positive-ion masses into the collector of the spectrometer, it is incorrect to compute the abundance ratio directly from the ratio of the observed peak heights. The magnitude of the correction to be applied to give true abundance ratios was determined experimentally by holding the accelerating voltage constant and varying the field of the main deflecting magnet. For small ion masses such as 10 and 11 this voltage correction is very appreciable. Our measured abundance ratio of 3.88/1 for B^{11}/B^{10} in the input BF_3 gas is surprisingly low, since the accepted normal abundance ratio for B^{11}/B^{10} is 4.31/1,[6] and we did get that higher ratio for one lot of specially purified gas which was made available to us. Nevertheless, by taking the ratio of the abundance ratios at the two ends of our columns determined with our mass spectrometer under identical conditions, the correct separation factors for these experiments should result.

EXPERIMENTAL RESULTS

The separation factors for $B^{10}F_3/B^{11}F_3$ determined in this manner during the 15-day run with this apparatus are given in Table I. It is evident that the equilibrium separation factor for the 7 meters of column was about 1.32 ± 0.12, the equilibrium being attained in slightly over three days. That the 7 meters of column should have produced a higher factor than this is shown, for one thing, by the fact that from the samples drawn off at the 6-meters point we determined the factor there to be about 1.21. Now the equilibrium separation factor should vary exponentially with the length of separating column. Taking the ratio of the logs of these factors for $L=7$ meters and 6 meters, we get 0.120/0.080, or 4/3 rather than 7/6. Thus it would seem that the final 1-meter column at the "light" end was functioning satisfactorily, but that the operation of the first 3-meter separating column was being impeded by the presence of a considerable amount of the heavy impurity. We should therefore draw our conclusions from the performance of the "light" end of the apparatus only. Judging from these best results, we can state that with $\Delta T=400$°C between the hot wire and surrounding cold wall of a Clusius and Dickel column using BF_3 gas at atmospheric pressure, and with $2w=3.75$ mm, the separation factor for $B^{10}F_3/B^{11}F_3$ per meter of column is close to 1.1. There was about $\frac{3}{4}$ g of gas in the end volume at the "light" end of the apparatus.

From our observed separation factors we are certain that the thermal diffusion constant α for BF_3 is small but positive. To estimate the value of α, we take 1.1 as the equilibrium separation factor q_e per meter of column, solve for the A constant ($q_e=e^{2AL}$), then assume the viscosity the same as for SO_2 (1.62×10^{-4} poise). This calculation indicates that $\alpha\cong5.0\times10^{-4}$, and therefore R_T, the ratio of α for this molecule to that for a hard sphere molecule of the same mass, is about 0.06. The smallness of this value means that the

TABLE I. Separation factors for $B^{10}F_3/B^{11}F_3$ produced by 6- and 7-meters of hot wire thermal diffusion column for $\Delta T=400$°C, $p=1$ atmos., and $2w=3.75$ mm.

t	$L=6$ meters	$L=7$ meters
3 days	—	1.295 ± 0.117
6	1.205 ± 0.128	1.330 ± 0.126
9½	—	1.303 ± 0.122
12	1.220 ± 0.091	1.290 ± 0.136
15	—	1.343 ± 0.128

[5] A. O. Nier, Rev. Sci. Inst. 11, 212 (1940).
[6] M. G. Inghram, Phys. Rev. 70, 653 (1946).

repulsive force index is but little over the critical value of 5. Undoubtedly the BF_3 molecule becomes "harder" at higher temperatures, as has been noted[7] for NH_3, but one is limited in temperature by the possibilities of increased chemical reactivity and decomposition. We conclude that concentrated B^{10} material may surely be obtained by the thermal diffusion method, but with an over-all efficiency of the plant much too low to make the job attractive.

[7] W. W. Watson and D. Woernley, Phys. Rev. **63**, 181 (1943).

PHYSICAL REVIEW VOLUME 71, NUMBER 12 JUNE 15, 1947

Dielectric and Piezoelectric Properties of Barium Titanate*

SHEPARD ROBERTS**
Laboratory for Insulation Research, Massachusetts Institute of Technology, Cambridge, Massachusetts

(Received March 6, 1947)

The dielectric constant and loss of barium titanate and barium-strontium titanate have been measured at biasing field strengths from 0 to 5 megavolts per meter, at temperatures from −50°C to +135°C and at frequencies from 0.1 to 25 megacycles. The measurements *versus* temperature indicate the expected agreement with the Curie-Weiss law at temperatures above the Curie point. Measurements *versus* field strength indicate that the electric field intensity can be expressed as a simple function of the electric displacement, consisting of a linear and a cubic term. At temperatures below the Curie point the results are more complicated, presumably because there are spontaneously polarized domains which give rise to hysteresis and remanence. At field strengths low enough to avoid hysteresis and remanent polarization, no anomalies in the dielectric characteristics *versus* frequency have been observed. When polarized, however, by a momentary application of a strong d.c. field, a resonance spectrum appears in these ceramics. These resonances are attributed to a piezoelectric effect which exists only in the polarized samples. The piezoelectric voltage developed upon squeezing a specimen of polarized barium titanate has been measured directly with a vacuum tube electrometer. Both the longitudinal effect (electric field parallel to mechanical stress) and the transverse effect (field perpendicular to stress) have been observed.

INTRODUCTION

WHILE surveying the properties of a number of titania ceramics, Wainer and Salomon of the Titanium Alloy Manufacturing Company noticed anomalous polarization effects in barium titanate and in solid solutions of barium-strontium titanate.[1] Further studies in the Laboratory for Insulation Research established that these materials constitute a new class of ferroelectric dielectrics.[2,3] $BaTiO_3$ was shown to have a Curie point at about 116°C, coinciding with a lattice transformation from cubic to a structure of lower symmetry, which Megaw and Rooksby[4] identified as tetragonal. The addition of strontium titanate shifted the Curie point and the lattice transformation to lower temperatures. This shifting of the Curie point was followed by Jackson[5] down to −190°C for a composition containing 80 percent strontium titanate. Two additional singularities resembling Curie points have

* The research reported in this document was made possible through support extended to the Massachusetts Institute of Technology, Laboratory for Insulation Research, jointly by the Navy Department (Office of Naval Research) and the Army Signal Corps under ONR contract N5ori-78, T.O. I. The material forms a portion of a thesis submitted to the Electrical Engineering Department of the Massachusetts Institute of Technology in September, 1946, in partial fulfillment of the requirements for the degree of Doctor of Science. It was presented at the Conference on Electrical Insulation of the National Research Council in Baltimore, November 7, 1946.

** Present address Research Laboratory, General Electric Company, Schenectady, New York.

[1] E. Wainer, and A. N. Salomon; Titanium Alloy Manufacturing Company, Elec. Rep. **8** (1942), **9** and **10** (1943). E. Wainer, Trans. Electrochem. Soc. Preprint 89–3, **89**, 47 (1946).

[2] N.D.R.C. Rep. Div. 14, No. 300, Aug., 1944; N.D.R.C. Rep. Div. 14, No. 540, Oct., 1945.

[3] A. von Hippel, R. G. Breckenridge, F. G. Chesley, and L. Tisza, Ind. Eng. Chem. **38**, 1097 (1946).

[4] H. D. Megaw, Nature, **155**, 484 (1945); **157**, 20 (1946); Proc. Phys. Soc. Lond. **58**, 133 (1946). H. P. Rooksby, Nature **155**, 484 (1945).

[5] W. Jackson, and W. Reddish, Nature **156**, 717 (1945).

been found for barium titanate[2,3] at about +10°C and −70°C, which become especially pronounced at high field strengths.

The same class of ferroelectrics was studied independently in Russia by Wul.[6] A theoretical paper by Ginsburg[7] was available to the author only after his experimental work had been completed. The experimental results are in essential agreement with Ginsburg's theory.

The ferroelectric character of these materials made it obvious that the ceramics might find useful applications as non-linear dielectrics. Consequently the present study was undertaken to investigate in detail the dielectric constant and loss of barium titanate and barium-strontium titanate *versus* biasing voltage. In the course of the investigation it was found that these materials also have interesting piezoelectric properties.

PREPARATION OF SAMPLES AND MEASURING TECHNIQUES

The dielectric samples were prepared in the form of thin sheets by a method originated by G. Howatt and further developed in this Laboratory.[8] The ceramic powder, obtained from the Titanium Alloy Manufacturing Company, was suspended in a toluene "slip" with a resin binder and, after de-airing, was extruded on a flat baseplate previously coated with a thin film of ethyl cellulose. The extruded sheet, when nearly dry, was stripped from the base and cut in the form of disks ¼ inch in diameter, which were fired in a ceramic kiln. The firing temperatures were in the range 1300 to 1500°C for different samples and the time was ½ to 4 hours, the shorter time corresponding to the higher temperature. The thickness of the fired samples ranged between 0.004 and 0.008 inch. Some of the disks were badly warped in firing, but this did not seem to affect their dielectric properties. An electrode of fired-on silver paste about ⅛ inch in diameter was applied on the top surface and the bottom was covered either with silver paste or with a platinum-foil electrode to which the ceramic fused when it was fired.

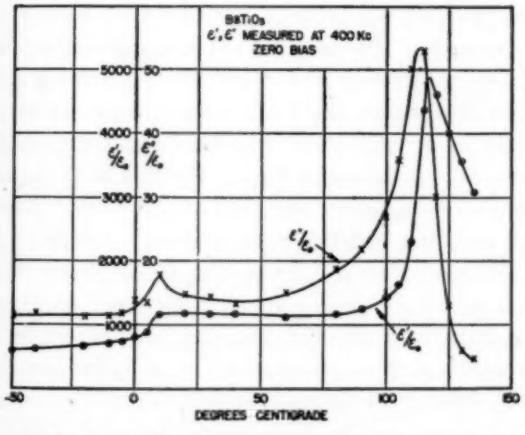

FIG. 1. Dielectric constant and loss factor of $BaTiO_3$ *versus* temperature.

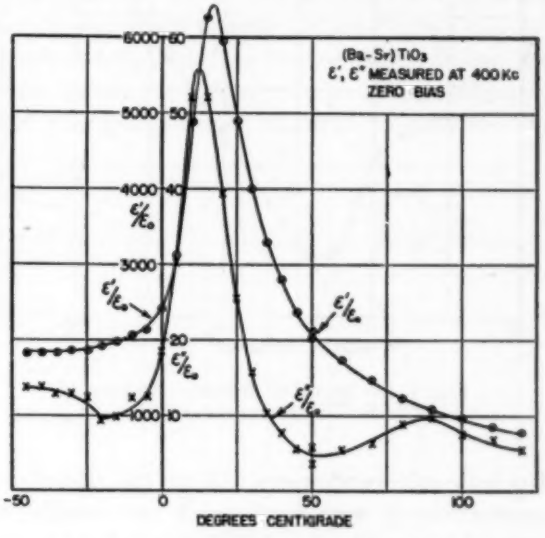

FIG. 2. Dielectric constant and loss factor of $(Ba\text{-}Sr)TiO_3$ *versus* temperature.

The dielectric properties of barium titanate and 75 percent barium/25 percent strontium titanate were derived from impedance measurements of the sample condensers described above. The measurements were made mostly at a frequency of 400 kilocycles per second by means of a radiofrequency bridge, type 916-A (General Radio). In some cases a relatively strong d.c. "biasing" voltage was superimposed on the measuring-frequency voltage in a manner similar to that used by Mueller[9] in measuring nonlinear

[6] B. M. Wul, and I. M. Goldman, Comptes Rendus U.R.S.S. **46**, 139 (1945); **49**, 177 (1945). B. M. Wul, Nature **156**, 480 (1945); Comptes Rendus U.R.S.S. **51**, 21 (1946); J. Phys. U.S.S.R. **10**, 64 (1946); **10**, 95 (1946); Nature, **157**, 808 (1946). B. M. Wul, and L. F. Vereschagin, Comptes Rendus U.R.S.S. **48**, 634 (1945).

[7] V. Ginsburg, J. Phys. U.S.S.R. **10**, 107 (1946).

[8] G. N. Howatt, R. G. Breckenridge, and J. M. Brownlow, J. Am. Ceramic Soc. (to be published).

[9] H. Mueller, Phys. Rev. **47**, 175 (1935).

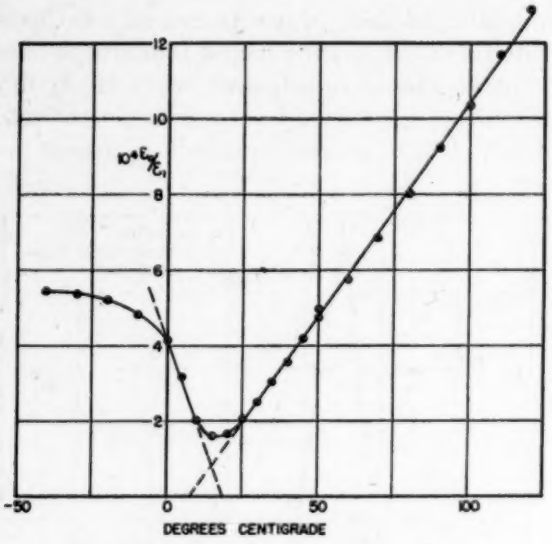

FIG. 3. Reciprocal of dielectric constant of (Ba-Sr)TiO_3 *versus* temperature.

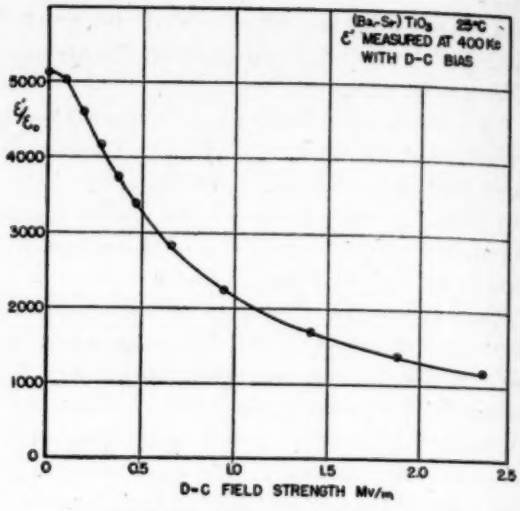

FIG. 4. Dielectric constant of (Ba-Sr)TiO_3 *versus* d.c. field strength.

Rochelle-salt condensers. All of the impedance measurements were made with the sample immersed in an oil bath, which improved the insulation as well as maintaining constant temperature.

EXPERIMENTAL RESULTS

The values of dielectric constant of barium titanate and barium-strontium titanate at low a.c. field strength and in the absence of d.c. bias are shown *versus* temperature in Figs. 1 and 2. In these figures the dielectric constant or permittivity ϵ^* is expressed as a complex quantity in the usual manner in order to account for the dielectric loss.

$$\epsilon^* = \epsilon' - j\epsilon''. \tag{1}$$

The figures show both ϵ' and ϵ'' *versus* temperature.

The temperature at which the dielectric constant of each of these materials has a maximum value has been identified as a Curie point[2, 3, 6, 7, 10] and it has been observed that these materials obey the Curie-Weiss law at temperatures above this point.

$$\epsilon'/\epsilon_0 = \frac{C}{T - T_c}, \tag{2}$$

where:

ϵ_0 = permittivity of free space
C = constant
T = temperature
T_c = Curie temperature (may be a slightly different value from the Curie point mentioned above).

The Curie points indicated by Figs. 1 and 2 are 116°C for barium titanate and 15°C for 75 percent barium/25 percent strontium titanate.

Since Fig. 2 shows ϵ' for barium-strontium titanate in a range of temperature extending considerably above the Curie point, these data can serve as a very good check of the Curie-Weiss law. This is shown in Fig. 3, where $1/\epsilon'$ is plotted *versus* temperature and the experimental points fall on a straight line in accordance with Eq. (2).

At temperatures above the Curie point there is a relatively simple relation between dielectric constant and the d.c. biasing field strength. A typical result is shown in Fig. 4, with the d.c. field strength expressed in megavolts per meter. This curve can be interpreted by postulating a simple equation between the electric field intensity E and the electric displacement D.

$$E = \alpha D + \beta D^3, \tag{3}$$

where α and β are parameters which depend only on temperature. It is noted that Eq. (3) takes no account of losses, which, experiment indicates, are relatively small (<1 percent).

[10] D. F. Rushman and M. A. Strivens, Trans. Faraday Soc. (to be published).

The permittivity is by definition the slope of the curve of D *vs.* E.

$$\epsilon' = dD/dE. \tag{4}$$

At very small field strengths (zero d.c. bias) the permittivity (initial) is

$$\epsilon_1 = \frac{1}{\alpha} = \frac{\epsilon_0 C}{T - T_c}. \tag{5}$$

By differentiating Eq. (3) and solving the result for D in terms of α, β, and ϵ', and substituting this value of D back in Eq. (3) one obtains

$$\frac{E}{E_0} = \tfrac{1}{4}\left(\frac{\epsilon_1}{\epsilon'} - 1\right)^{\frac{1}{2}}\left(\frac{\epsilon_1}{\epsilon'} + 2\right), \tag{6}$$

where

$$E_0 = 4\left(\frac{\alpha}{3}\right)^{\frac{1}{2}}\beta^{-\frac{1}{2}}. \tag{7}$$

According to Eq. (6), E_0 is simply the field strength required to reduce ϵ' to half its initial value.

The experimental results shown in Fig. 4 agree accurately with Eq. (6) if one puts $E_0 = 0.75$ Mv/m, and $\epsilon_1/\epsilon_0 = 5130$.

E_0 is shown *versus* temperature in Fig. 5 for barium-strontium titanate. Even though Eq. (6) is not strictly valid at temperatures below the Curie point, Fig. 5 neverthelss shows values of field strength actually required to reduce ϵ' to half its initial value in this temperature range. Figure 6 gives the corresponding curve for barium titanate. This figure clearly shows the anomalous dielectric response near 10°C at high field strengths previously mentioned.

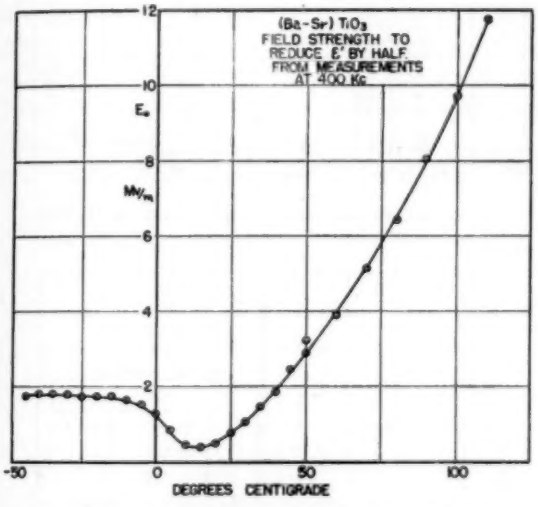

FIG. 5. Critical field strength E_0 of (Ba-Sr)TiO_3 *versus* temperature.

TABLE I. Values of $\epsilon_0^3\beta$ in meters^3 volts^{-2} calculated from experimental values of E_0 and ϵ_1 by means of Eq. (8).

Temp. °C	$\epsilon_0^3\beta$	Temp. °C	$\epsilon_0^3\beta$
10	26×10^{-24}	50	7.6×10^{-24}
15	16	60	7.5
20	11	70	7.2
25	9.0	80	7.5
30	8.4	90	7.2
35	7.8	100	7.0
40	7.8	110	6.9
45	7.4		

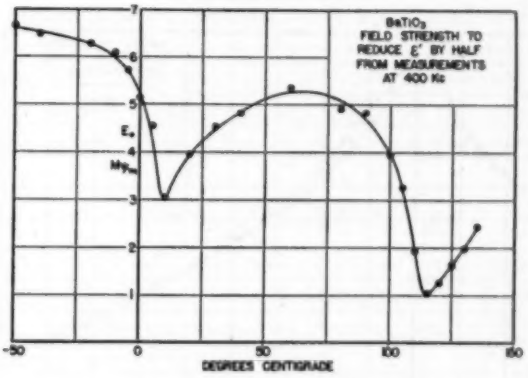

FIG. 6. Critical field strength E_0 of $BaTiO_3$ *versus* temperature.

ϵ_1 and E_0 can be determined experimentally, therefore Eq. (7) can be solved for β.

$$\beta = \frac{16}{27}\frac{\alpha^3}{E_0^3} = \frac{16}{27}\epsilon_1^{-3}E_0^{-2}. \tag{8}$$

Values of $\epsilon_0^3\beta$ have been calculated by means of Eq. (8) and are tabulated for different temperatures in Table I. These results indicate that β is practically constant at temperatures above the Curie point.

The extrapolation of Eq. (3) to temperatures below the Curie point leads as in the ferromagnetic case to the phenomena of hysteresis and spontaneously polarized domains. The curve showing D *vs.* E obtained by extrapolating this equation is given in Fig. 7. Part of this curve is shown with a broken line because it has a negative slope and is therefore unstable. A negative

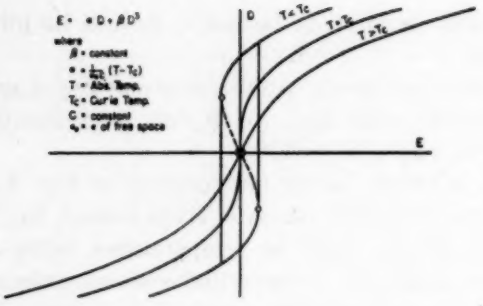

FIG. 7. Theoretical curves for electric displacement *versus* field strength.

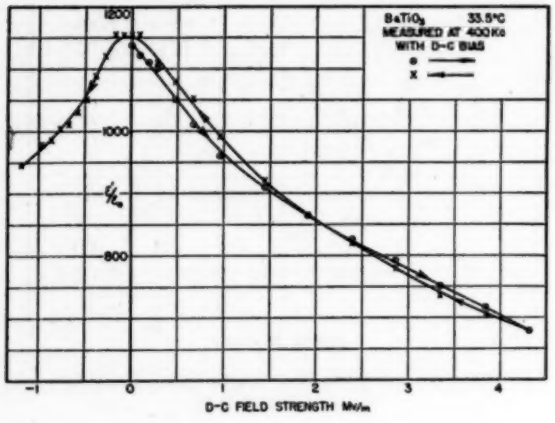

FIG. 8. Dielectric constant of $BaTiO_3$ *versus* d.c. field strength.

slope would correspond to a negative value of static capacitance, which could give rise to exponentially increasing transients. Therefore, as the electric field is shifted, the polarization may be expected to jump suddenly from one branch of the curve to the other along the vertical lines indicated. At zero field strength the electrical displacement cannot be zero but must assume either a positive or negative value determined by the intersections of the curves on the vertical axis.

Although the above interpretation of Fig. 7 is qualitatively correct in that it predicts hysteresis at temperatures below the Curie point, it is inconsistent with the experimental results for two reasons. Firstly, the experimental hysteresis curves do not have the exact shape of Fig. 7, and secondly, the polarization can be zero when the external field is zero. These discrepancies may be resolved by the assumption that the ceramic dielectrics, like other ferroelectric and ferromagnetic materials, are made up of domains, each of which is spontaneously polarized in a direction independent of the others. Figure 7 would then describe the polarization of a single domain.

Hysteresis and remanent polarization have a pronounced effect on the dielectric properties, especially the loss, at temperatures below the Curie point. However, the variation of permittivity *versus* field strength is not always very different from that observed at temperatures above the Curie point. An example is shown in Fig. 8. A detailed description of the non-linear dielectric properties in the range of temperature below the Curie point will be omitted here for the sake of brevity.

In measuring the impedance of the ceramic condensers *versus* frequency, a series of reso-

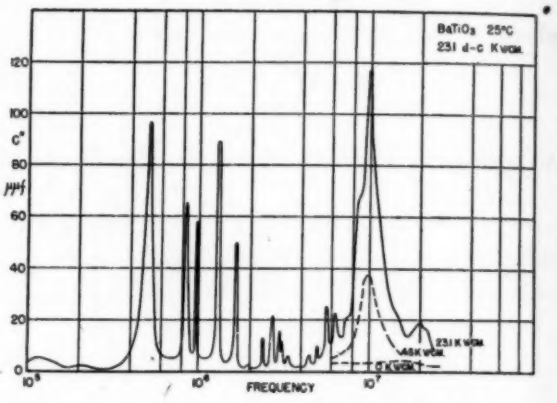

FIG. 9. Loss component of capacitance of $BaTiO_3$ condenser *versus* frequency.

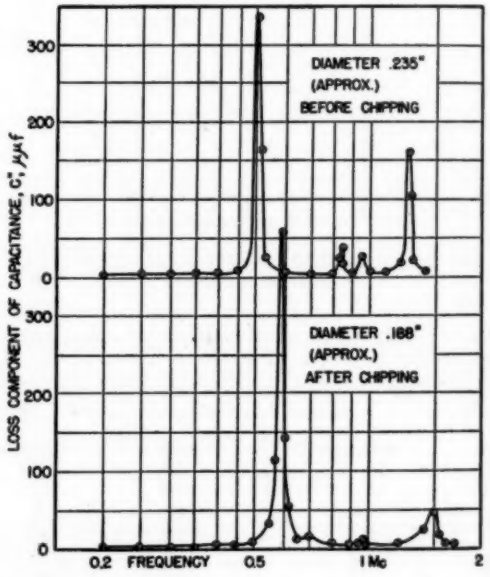

FIG. 10. Loss component of capacitance before and after chipping edge.

nances was found. The impedance is expressed in the form of a complex capacitance.

$$\frac{1}{Z}=j\omega C^*=\omega C''+j\omega C'. \qquad (9)$$

The loss component of capacitance, C'', is shown *versus* frequency in Fig. 9 for a typical sample of barium titanate. The solid line gives C'' when a relatively strong d.c. field is superimposed on the measuring voltage. The lower broken line shows C'' for the unpolarized material, indicating that the resonant losses do not appear in this case. If the ceramic is polarized by applying a strong d.c. field and the field is then turned off, the material retains an appreciable amount of polarization, which is indicated by resonant losses similar to the solid curve in Fig. 9. Resonances of the type shown in this figure tend to disappear at temperatures above the Curie point even when a strong field is maintained.

If the resonances shown in Fig. 9 are to be attributed to a piezoelectric effect, the resonance frequencies must depend on the mechanical dimensions of the ceramic. That this is so was shown by a simple experiment. The resonance frequencies were determined for a disk sample, then pieces of ceramic were broken away from the edge, thereby reducing the effective diameter of the disk. The resonances were shifted to higher frequencies by a constant ratio as a consequence of the reduction in sample diameter. These results are shown in Fig. 10.

A further confirmation of the piezoelectric effect in polarized barium titanate was obtained by squeezing a sample of about $\frac{1}{2}$ inch in diameter and $\frac{1}{8}$ inch in thickness, polarized by momentary application of a d.c. potential of 6000 v. The piezoelectric voltage was measured by means of a vacuum tube electrometer and was found to be several volts for a force of several (not measured) kilograms. Both the longitudinal effect (electric field parallel to mechanical stress) and the transverse effect (field perpendicular to stress) were observed.

ACKNOWLEDGMENT

This work was carried out in the Laboratory for Insulation Research at Massachusetts Institute of Technology under the direction of Professor A. von Hippel.

The author is especially indebted to Professor von Hippel for encouragement and advice during the course of the work. He also wishes to thank J. M. Brownlow for help in preparation of samples.

Note on a Variation with Frequency of the Torsional Modulus of German Silver Wire and its Relation to Gyromagnetic Measurements

S. J. Barnett and D. S. Webber
The University of California, Los Angeles and The California Institute of Technology, Pasadena, California

(Received March 12, 1947)

A quite unmistakeable deficit of the mean gyromagnetic ratio for certain ferromagnetic substances as reported some years ago by W. Sucksmith and L. F. Bates from the mean ratio obtained for the same substances in much more elaborate investigations in the laboratories of one of us, might be explained by such a variation alone if the torsional modulus of German silver wire in rapid oscillation (dynamic modulus, M_d) were smaller by four or five percent than the modulus for steady twist (static modulus, M_s)—a result, however, which we should not expect to find. The calibrating operations of the authors referred to were carried out partly with rapid oscillations, partly with steady deflections; and they assumed (implicitly) that the two moduli were equal. We have not worked with the true static modulus, but have determined the ratio of M_d for frequencies ranging approximately from 17 to 50 per second, comparable with those used in the work mentioned, to M_d for periods ranging approximately from 4 sec. to 28 sec.—times doubtless quite comparable with or greater than the times required to produce steady twists in this work. We have detected no certain change of modulus in the high frequency range, or in the range of periods between 4 sec. and 28 sec. However, the modulus has been found to diminish by 1 percent in passing from oscillations with the period 5 sec. to those in the high frequency range. This unexpected diminution reduces somewhat the discrepancy that initiated the experiments described in this note, and it seems important to us for other reasons also. But much the greater part of the discrepancy must be accounted for in other ways.

I. INTRODUCTION AND THEORY

In three extensive investigations on the gyromagnetic ratios of many ferromagnetic substances it has been found that this ratio, ρ, ranges from about $1.00\times m/e$ for Heusler alloy to about 1.08 or $1.09\times m/e$ for cobalt.[1] The value of ρ for iron is about $1.03\times m/e$; that for nickel, Hipernick, and Permalloy about $1.05\times m/e$. There is no disagreement, within the limits of the experimental errors, between these results and the few obtained by others in recent years and sufficiently precise to be at all comparable with them; but the work done some years ago by Sucksmith and Bates[2] gave about $1.00\times m/e$ for both iron and nickel, with an experimental error which they claimed to be not over 1 or 2 percent. Indeed, they considered $1.00\times m/e$ correct for all the substances they tried.

In earlier papers[1] attention has been called to several sources of error which the authors mentioned had not considered. The effects of some of these errors, but not all, tend to disappear in the means from a sufficiently large number of independent observations, which may not have been made. In searching a number of years ago for possible constant sources of systematic error making all values too small, it appeared that an error of this kind might be involved in the work referred to because the authors in one of the calibrating operations used German silver wire in rapid torsional vibration, whereas in another they used a steady twist of the same wire. If the static modulus of torsion were greater than the dynamic modulus, the low values might be at least in part accounted for by this fact.

The matter will become clear from the following brief discussion: In the paper of Sucksmith and Bates the quantity ρ should be calculated from the equation

$$\rho = CA_s,$$

where C is a quantity which does not enter into the present discussion and A_s is the static torsional constant of the wire. Instead of using A_s in calculating ρ, however, they used A_d, the dynamic constant, which they determined from high frequency oscillations. Thus they obtained an *apparent* value, which may be designated by ρ_{app}, from the equation

$$\rho_{app} = CA_d,$$

whereas the true value is

$$\rho = \rho_{app}(A_s/A_d).$$

[1] See especially S. J. Barnett, Proc. Am. Acad. **73**, 401–455 (1940); **75**, 109–129 (1944); and *Le Magnétisme* (Proceedings of the Strasbourg *Réunion sur le Magnétisme*) **2**, 203–244 (1940).

[2] W. Sucksmith and L. F. Bates, Proc. Roy. Soc. **A104**, 499 (1923); **A108**, 638 (1925).

With the object of investigating this question, we have recently made some experiments on wires of German silver. It has not been convenient for us to make any experiments of a truly static character, but we have made low frequency observations, in some of which the period was greater than 28 seconds, an interval doubtless much greater than the time required for reaching the steady deflections in the work of Sucksmith and Bates, as well as observations with frequencies up to more than 1000 times as great.

We have used the classical method of torsional oscillations in such ways as to give the ratio of the torsional constant at one frequency to that at another frequency. The higher frequency oscillations were produced magnetically at the natural frequencies determined by resonance. The lower frequency oscillations were produced and their periods determined in the usual way.

We may proceed conveniently by either of two processes: (1) the length of the wire may be kept constant and the moment of inertia changed, or (2) the moment of inertia may be kept constant and the length of the wire changed. It was evidently advantageous to use the first method in the part of the work in which most of the frequencies were relatively high; both methods have been used in the part in which all the frequencies were low. Possible lack of uniformity of the wire is a disadvantage in the second case.

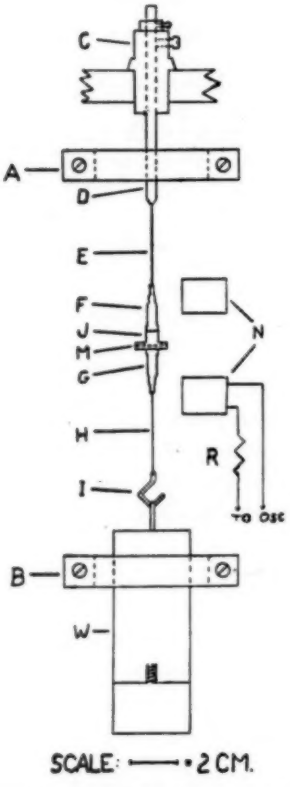

FIG. 1. Apparatus arranged for vibration of the system S alone. Approximate mass of weight $W = 567$ grams. In use the axis of the magnet M is normal to that of the coil N, instead of parallel as shown in the figure.

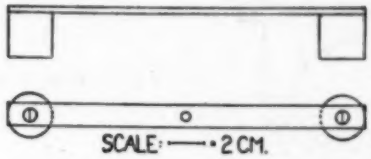

FIG. 2. The system S_2. Approximate masses in grams: bar 69.0; each cylinder 108.4; each screw, 0.5.

Because the result of the experiments seems to us quite different from what would be expected, we give the procedure in some detail, as only in this way can it be shown that the possible errors have been eliminated.

II. WORK AT HIGHER FREQUENCIES

The method used in the part of the work at higher frequencies will be clear from what follows. The essential parts of the inertia apparatus were made as nearly symmetrical about a central vertical line as practicable. The dimensions of most of the apparatus are indicated in Figs. 1–4. The wire under test is divided into two nearly equal parts E and H, about 35 mm long. The upper part E is soldered at the upper end into a brass rod D passing through a torsion head C, and at the lower end into a lug F threaded at the lower end. The lower wire H is soldered at the upper end into a lug G similar to F, except as indicated below, and at the lower end into a brass hook I, on which a stretching weight W can be hung. The hooks have rectangular cross sections and thus form a rigid joint. Between the two lugs and screwed to them is a brass piece J with two cylindrical surfaces. The diameter of the upper cylinder is about 0.476 cm and the height is about the same. The lower cylinder has a diameter of 10 mm and a height of 2 mm. A hard magnetized steel rod, 10 mm long and 0.5 mm in diameter, passes symmetrically through a horizontal hole in the lower cylinder. Details of the system F, J, M, G are given in Fig. 5.

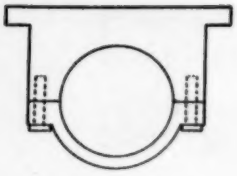

FIG. 3. Ring A or Ring B.

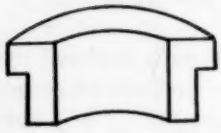

FIG. 4. One of the wooden half-rings.

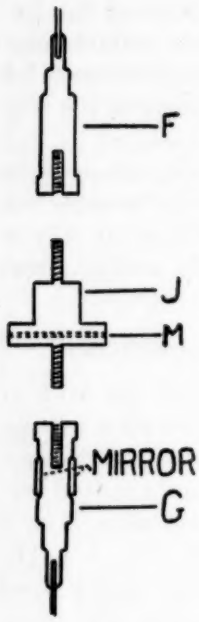

FIG. 5. Details of the system S.

The weight W is divided into two parts, screwed together so that the lower part can readily be removed or attached. Parts of two sides of the lug G are milled flat, parallel, and normal to the axis of the magnet. They carry two similar small plane mirrors (Fig. 5) which make it possible to study the angular motion of the system with lamp, lens, and scale.

The torsion head is so adjusted that the axis of the magnet points approximately east and west. The earth's magnetic field did not alter the frequency appreciably; but if it had done so the effect would have been eliminated in the calculation of the result sought.

To change the moment of inertia and frequency of the system small toroidal rings, not illustrated in the figures, or a weighted bar (Figs. 2 and 6) can be slipped over the upper cylinder of J.[3] The axis of the system passes through two fixed horizontal rings A and B, Figs. 1 and 3. The upper ring, together with a small bar laid across it, was used to hold one of the inertia rings when not in use; the other, or one half of it, to clamp the weight W in position, by means of cotton wads, two half-cylinders of wood, or one half-cylinder and soft wax. One of the half-cylinders of wood is illustrated in Fig. 4.

There are three processes involved in each series of measurements: (1) With the complete weight W in place, the system S, as illustrated in the figure, is set into torsional oscillations, and the frequency, ν_1, determined. Let K_1 denote the moment of inertia of this (unloaded) system, A_1 the torsional constant. Then

$$A_1=\nu_1^2 4\pi^2 K_1. \tag{1}$$

(2) The system is loaded with one or more small rings, with moment of inertia K, the total moment of inertia being now $K_2=K+K_1$, and the frequency ν_2 is determined. If the torsional constant is now A_2, we have

$$A_2=\nu_2^2 4\pi^2 K_2. \tag{2}$$

Assume (consistently with experiment) $A_2=A_1=A_{12}$. Then

$$K_1=\frac{(K)\nu_2^2}{\nu_1^2-\nu_2^2};\quad K_2=\frac{(K)\nu_1^2}{\nu_1^2-\nu_2^2}, \tag{3}$$

and

$$A_{12}=\frac{4\pi^2(K)\nu_1^2\cdot\nu_2^2}{\nu_1^2-\nu_2^2}. \tag{4}$$

(3) The ring is replaced by a system S_3 with a much larger moment of inertia K', such that the total moment of inertia is now $K_3=K_1+K'$. At the same time the detachable part of the weight

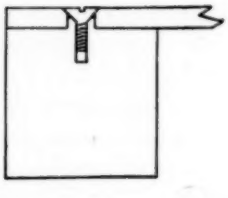

FIG. 6. Details of one end of S_3.

[3] To insure that relative motion between the rings and the ring holder should always be impossible we have used, in some cases, very small quantities of wax, which did not affect the moments of inertia appreciably.

W is removed. The frequency ν_3, very much lower than either ν_1 or ν_2, is determined. The torsional content A_3 is now computed from the relation

$$A_3=\nu_3^2\cdot 4\pi^2\cdot K_3=\nu_3^2 4\pi^2(K'+K_1). \qquad (5)$$

Let T_u denote the tension of the upper wire and T_L that of the lower wire in (1); and T_u' and T_L' the tensions in (3). Let W_1 and W_3 be the weights of the systems S_1 and S_3, and let B_1 and B_3 denote the stretching weights in (1) and (3). Then we have

$$T_u=T_L+W_1=B_1+W_1,$$
$$T_u'=T_L'+W_3=B_3+W_3.$$

Then

$$T_u'-T_u=T_L'-T_L+(W_3-W_1).$$

If now $T_L-T_L'\equiv B_1-B_3$ is made equal to $\frac{1}{2}\cdot(W_3-W_1)$, as was done in this work, we get

$$T_u'-T_u=-(T_L'-T_L)=\tfrac{1}{2}\cdot(W_3-W_1).$$

Thus in changing from (1) to (3), the tension of the upper wire is increased and that of the lower wire decreased by the same amount. Hence if there is any dependence of the torsional constant of the material on tension and stretch, there is nevertheless no change on that account in the constant or the double wire systems used in this part of the work.

As a matter of fact experiment shows that if no other change is made the removal or addition of the lower part of W has not more than a minute effect on the frequency.

The ratio $R\equiv A_{12}/A_3$ is the quantity sought.

Temperature changes were so small as to be of no consequence in this work; and even if this were not so it is easy to prove that their effects would be almost completely eliminated in taking the ratio R.

All the higher frequencies in this work were measured with reference to the frequency of the power line from Hoover Dam, which is now ordinarily constant to at least a tenth or twelfth percent at 60 cycles per second. We have continually checked this frequency with a standard Weston meter permanently connected to the line. The low frequencies have been determined in the usual way, with negligible error, by means of a synchronous clock driven by the 60 cycle per second supply, or by means of a reliable watch.

The vibrations at higher frequencies, with one exception, have been obtained in the following way. A coil N is mounted with its axis A normal the length of the small magnet M, Fig. 1 (instead of parallel, as indicated in the figure). A sine wave oscillator OSC is connected to the coil N through a high resistance R and has its frequency varied while the amplitude of the torsional oscillation is measured, and the frequency of resonance thus determined. The e.m.f. supplied by the oscillator and the current in the coil N were independent of the frequency for ranges far beyond those of any resonance curve. The oscillator was provided with a special circle graduated in degrees, which were read to .°1, and was very steady after being operated for two hours. It was calibrated in the usual way with the help of an oscilloscope; and the calibration curve was checked, and corrected when necessary, for every frequency determination. Ordinarily, for each such determination, three closely concordant resonance curves were obtained.

The lowest of the higher frequencies was below the range of the oscillator and was therefore obtained from an electrically driven tuning fork. The wave form in this case was by no means sinusoidal, but this was of no consequence since the resonance was exceedingly sharp.

The inertia system S_3, used to obtain the low frequency, was made of brass. Its various parts had the approximate dimensions indicated in Fig. 2. One end is illustrated in more detail in Fig. 6. Its moment of inertia is 19.65×10^3 g cm^2 with negligible error. The brass bar alone has the moment of inertia 23.41×10^2 g cm^2, also with negligible error.

Two double suspensions were used, almost exactly alike. Only the wires and mirrors differed in the two. Both were made with No. 28 German silver wire, probably from the same stock. The wire of the first system was cut from wire actually used in experiments made here on the Einstein-deHaas effect; those of the second system were cut from the ends of the 60-cm wire of the long suspension referred to below.

The period of oscillation of the first double suspension vibrator with S_3 in place was 4.81$_5$

TABLE I. Data with regard to inertia systems and frequencies with first double suspension.

1 System	2 Approx. thickness	3 Approx. outer diameter	4 Approx. mass	5 Approx. moment of inertia	6 Observed frequency and mean error	7 Approx. calc. max. error in frequency	8 $100\times\frac{\delta A_{12}}{A_{12}}$ $\left(\frac{\delta\nu_1}{\delta\nu_2}>0\right)$	9 $100\times\frac{\delta A_{12}}{A_{12}}$ $\left(\frac{\delta\nu_1}{\delta\nu_2}<0\right)$
Ring holder				0.33 g cm²	50.02±0.03	0.08		
Ring 1	0.16 cm	2.0 cm	0.75 g	0.25	37.92±0.08	0.06	0.27	1.14
Ring 2	0.10	2.0	2.42	1.28	22.78±0.03	0.02	0.17	0.34
Rings 1+2				1.52	21.2	0.02	0.14	0.28
Ring 3	1.6	2.0	1.29	0.68+	28.79±0.04	0.03	0.2	0.5
Ring 4	1.6	2.0	1.29	0.68+				
Rings 3+4				1.37−	22.16±0.01	0.02	0.16	0.31
Ring 5	3.2	2.0	2.59	1.37	22.12			
Ring 6	3.2	2.0	2.59+	1.37				
Rings 5+6				2.74	16.58	0.02	0.3	0.4

seconds; that of the second, and very similar, suspension, 4.82_2 seconds.

For use with the higher frequencies six small inertia rings were constructed and used, each in the form of a precise toroid with rectangular cross section. Their *approximate* thicknesses, outer diameters, masses, and moments of inertia are given in Table I. All were cut from rolled aluminum sheet except No. 2, which was turned from a brass cylinder. All had the same internal diameter, *viz.*, 0.476 cm. Table I includes also data with regard to the ring holder, and other (frequency) data referred to below.

All the moments of inertia except that of the ring holder were calculated from the standard formulae, which it is unnecessary to quote here. In making the calculations the precise dimensions and masses were of course used, not the approximate values given above. All the linear measurements and masses were measured with such precision that possible errors due to them were negligible. For the precise determination of all the masses we are much indebted to Professor Yost and Mr. Whittaker of the Gates and Crellin Laboratories.

The aluminum rings 3 and 4 were cut from adjoining parts of the same aluminum sheet, one just after the other in the direction of rolling. Each was marked to indicate this direction appropriately. When mounted together (3+4) the marks were ordinarily placed in opposition to compensate for possible variation of density and thickness. But tests in which the marks were placed in the same direction gave the same frequency, showing that no error from this source occurred when a single ring was used.

Numbers 5 and 6 were cut in the same manner from another aluminum sheet and were marked like Nos. 3 and 4. When both rings were used the marks were opposed.

Accurate measurements of the thicknesses showed that no appreciable errors could be produced by their departure from uniformity.

Error from imperfect knowledge of the frequencies is more difficult to eliminate. If we assume that for each frequency a maximum error of 0.1 degree on the oscillator circle is possible, we obtain from the calibration curve the values of $\delta\nu_1$ and $\delta\nu_2$ given in column 7 of Table I. The actual mean errors in the frequencies are given in column 6 of the same table for the first double suspension.

To show how A_{12} depends on the errors in frequency we differentiate Eq. (4) and thus obtain

$$\frac{\delta A_{12}}{A_{12}}=2\left(\frac{\delta\nu_1}{\nu_1}+\frac{\delta\nu_2}{\nu_2}-\frac{\nu_1\delta\nu_1-\nu_2\delta\nu_2}{\nu_1^2-\nu_2^2}\right). \quad (6)$$

The maximum calculated value of $\delta A_{12}/A_{12}$ is calculated for each case by inserting in Eq. (6) the tabular maximum magnitudes of $\delta\nu_1$ and $\delta\nu_2$ and giving them opposite signs; the minimum, by giving them the same sign. These values are given in percent in columns 8 and 9 of Table I. The maxima are of course much greater than the mean experimental errors to be expected. All these values assume the constancy of the frequency of the mains.

The observations with the second double suspension were still more precise and the frequency errors less.

The resulting values of the ratio $R\equiv A_{12}/A_3$

obtained with both double suspensions are given in Table II.

From each series of observations the difference between unity and the mean value of the ratio $R \equiv A_{12}/A_3$ is much greater than would be expected, even from column 9 of Table I, on the hypothesis of no real effect of frequency on A. The change in A with frequency is in the right direction to account for the discrepancy which initiated this work, but its magnitude is much too small—about 1 percent instead of some 4 or 5 percent.

The precision is not sufficient to detect any differences in A for the different values of the higher frequency ν_2.

III. WORK AT LOWER FREQUENCIES

To investigate the possible variation of the torsion modulus when the period of vibration ranged from about 4 seconds to about 28 seconds, three additional suspensions, designated as Nos. 1, 2, and 3, were prepared and the period of each determined when vibrated (A) with the bar only on the ring holder and (B) with the cylindrical weights added. They were all cut from a continuous length of No. 28 German silver wire from the same stock from which the wires of the second double suspension were cut, and probably also those of the first double suspension. Suspension No. 3, about 60 cm long, was cut from the central part of the wire; No. 1 and No. 2, each about 10 cm long, from the ends.

The periods for these slow oscillations, except in preliminary work, were determined with precision by means of a reliable watch, the frequency of the mains happening to be less than usually stable while these observations were in progress.

TABLE II. Results obtained with double suspensions I and II. (Periods from about 1/50 second to about 5 seconds.)

Suspension	Group	Rings Used	$R = A_{12}/A_3$	Mean A_{12}/A_3
I	1	1, 2, 1+2, 3+4, 5+6	0.987 ±0.002	
	2	1, 2, 3, 3+4, 5+6, 5	0.987 ±0.003	
	3	3	1.004 ±0.001	0.992 ±0.007
	4	3	0.998 ±0.000	
	5	3+4	0.985 ±0.001	
II	1	3+4 (opposed)	0.990	
	2	3	0.990	
	3	3+4 (together)	0.987	0.989 ±0.002
	4	3+4 (opposed)	0.987	
	5	3	0.991	

TABLE III. Data for low frequency vibrators.

	A. Inertia bar without cylinders			B. Inertia bar with cylinders		
Suspensions	l_A	T_A	$R_A = \frac{l_A}{T_A^2}$	l_B	T_B	$R_B = \frac{l_B}{T_B^2}$
No. 1	9.98 cm	3.990	0.6270	9.98 cm	11.57$_8$	0.0745$_2$
No. 2	9.95	3.976	0.6294	9.95	11.52$_4$	0.0749$_0$
No. 3	59.95	9.769	0.6282	59.97	28.28	0.0749$_3$

For this work the small magnet was removed from the holder.

On the assumption that the material of the wire, the radius and the tension are the same in two sets (1) and (2) of vibrations we have the relation

$$\frac{M_1}{M_2} = \frac{(l_1/T_1^2)}{(l_2/T_2^2)} \frac{K_1}{K_2}$$

for the ratio of the moduli. Table III gives the length l, the period T, and the quantity $R \equiv l/T^2$ for each of the wires for the cases designated above as A and B.

We shall proceed first by method (2) of p. 897. Here $K_1 = K_2$. For case A the ratio R_1 for No. 1 to R_3 for No. 3 is 0.998. The ratio R_2 for No. 2 to R_3 for No. 3 is 1.002. Neither gives correctly the ratio of the modulus for the period 4 sec. to that for the period 10 sec., as the radii of Nos. 1 and 2 and their materials cannot be exactly the same. But the mean, *viz.* 1.000, must give this ratio with close approximation.

For case B, the corresponding ratios are 0.994 and 0.999, with the mean of 0.9965, which, if there were no errors, would be the value of the ratio of the modulus at period about 11.5 sec. to that at about 28.3 sec. In view of the ratio unity obtained in case A, we should expect to obtain the same ratio for the slower vibrations of case B. It is important to notice that, as would be expected if the observations are correct, $(R_3 - R_1)_A = 0.004$ is practically equal to $(R_3 - R_1)_B = 0.005$.

If now we proceed by method (1), and assume that the frequency is not appreciably affected by the change in the tension from case A to case B, we apply the complete formula, with $K_2/K_1 (\equiv K_B/K_A) = 8.395$. This process gives for suspensions Nos. 1 and 2 the ratios 1.002 and 1.001 for the change of period from 4 sec. to 11.5 sec. approximately; and for No. 3, the ratio 0.998 for the change from 10 sec. to 28 sec.

In view of the approximations made in the assumptions and the (slight) observational errors both methods agree in showing no certain variation of the modulus for periods between 4 sec. and 28 sec.

IV. CHECK ON CALCULATIONS OF MOMENTS OF INERTIA

If we assume that this result is established by method (2) we may of course reverse method (1) to give a valuable check on the correctness of the calculations of the moments of inertia of the inertia system S_3 and the bar which forms a part of it. Thus, for each suspension, if in the experiments there is no appreciable change of modulus with frequency or tension, we should have

$$K_B/K_A=(l_A/l_B)(T_B/T_A)^2,$$

where K_B and K_A are the moments of inertia in cases B and A, *viz.*, 19.65×10^3 g cm^2 and 2.341×10^3 g cm^2. (The [negligible] moment of inertia, *ca.* 0.33, g cm^2, of the holder is included.) The ratio $K_B/K_A=8.395$; while the ratios $l_A/l_B(T_B/T_A)^2$ for the three suspensions are 8.413, 8.395, and 8.377, with the mean 8.395, exactly equal to K_B/K_A.

This work has been done in the Norman Bridge Laboratory of the California Institute with facilities provided by the University of California, the Institute, the Carnegie Institution of Washington, and the National Research Council.

We have desired to make further observations on German silver, with wires of different diameters and in the frequency range between our higher and lower values, as well as precise observations on other substances; but the pressure of other work has hitherto prevented this.

PHYSICAL REVIEW VOLUME 71, NUMBER 12 JUNE 15, 1947

A Note on Weinstein's Variational Method

W. KOHN
Department of Physics, Harvard University, Cambridge, Massachusetts
(Received February 27, 1947)

Weinstein's modification of the Ritz principle is used to derive (1) a lower bound for the n-th energy-level of a quantum mechanical system if a lower bound for the $(n+1)$-st level is known; and (2) an upper bound for the n-th level if an upper bound for the $(n-1)$-st level is known.

1. INTRODUCTION

BY applying the Ritz variational principle to the equation

$$(H-\lambda)^2\psi=W\psi \qquad (1)$$

Weinstein[1] was able to obtain both lower and upper bounds for the energy levels of the Schroedinger equation

$$H\psi=E\psi. \qquad (2)$$

The chief theoretical weakness of this method is that it gives no hint as to which one of the energy levels the bounds obtained refer to.

Stevenson and Crawford[2,3] have made use of Weinstein's method in an improved form to establish a theoretical lower bound for the ground-level of the helium atom. In their calculations both the lower and upper bounds obtained lie well below the experimental value of the second energy level and therefore, of necessity, refer to the ground state.

In section 2 of the present note the method of Stevenson and Crawford is generalized to give a lower bound for E_n if a lower bound of E_{n+1} is known. Since no general theoretical method is available for determining the latter, its value may

[1] D. H. Weinstein, Proc. Nat. Acad. of Sci. **20**, 529 (1934).

[2] A. F. Stevenson, Phys. Rev. **53**, 199 (1938).

[3] A. F. Stevenson and M. F. Crawford, Phys. Rev. **54**, 374 (1938).

have to be taken from experimental data. The process can be repeated and lower bounds for $E_{n-1}, E_{n-2}, \cdots E_1$ obtained in succession.

In section 3 an analogous procedure leads to an upper bound for E_n (and by iteration for $E_{n+1}, E_{n+2}, \cdots$) if an upper bound of E_{n-1} is known.

2. LOWER BOUND

If we use the notation

$$A_{kl} \equiv \int \psi_k^* A \psi_l dx,$$

where the integral is extended over the whole configuration space, we can express Weinstein's basic result by the statement that some energy level, E, will be found in any one of the intervals

$$\lambda - [(H^2)_{kk} - 2\lambda (H)_{kk} + \lambda^2]^{\frac{1}{2}} \leqslant E \leqslant \lambda + [(H^2)_{kk} - 2\lambda H_{kk} + \lambda^2]^{\frac{1}{2}}, \quad (3)$$

where λ can be given an arbitrary real value and H_{kk}, $(H^2)_{kk}$ are formed with an arbitrary, normalized ψ_k.

Suppose that $E_{n+1}{}^l$ is a lower bound of E_{n+1}. Then, if we choose λ so that

$$\lambda + [(H^2)_{kk} - 2\lambda H_{kk} + \lambda^2]^{\frac{1}{2}} = E_{n+1}{}^l \quad (4)$$

it is clear from (3) that

$$E_n \geqslant \lambda - [(H^2)_{kk} - 2\lambda H_{kk} + \lambda^2]^{\frac{1}{2}} \quad (5)$$

since otherwise no level would fall into the range (3).[4] Evaluating λ from (4) and substituting into (5) we find

$$E_n \geqslant H_{kk} - \frac{(H^2)_{kk} - (H_{kk})^2}{E_{n+1}{}^l - H_{kk}},$$

or

$$E_n{}^l = H_{kk} - \frac{(H^2)_{kk} - (H_{kk})^2}{E_{n+1}{}^l - H_{kk}}. \quad (6)$$

We can now use $E_n{}^l$ as a lower bound for E_n and repeat the procedure to obtain an $E_{n-1}{}^l$, etc.

Two remarks must be made here. It is easily verified that for fixed H_{kk}, $(H^2)_{kk}$ the left-hand side of (4) is an increasing function of λ. Therefore its minimum value is reached when $\lambda = -\infty$ and equals H_{kk}. Its maximum value is $+\infty$. It follows that a real solution, λ, of (4) exists if and only if $H_{kk} \leqslant E_{n+1}{}^l$. (This has been tacitly assumed in deriving (6).) The trial-function ψ_k, which we use in the computation of H_{kk} and $(H^2)_{kk}$ in (6), is therefore not entirely arbitrary, but subject to the condition

$$H_{kk} \leqslant E_{n+1}{}^l. \quad (7)$$

This inequality will be satisfied whenever $E_{n+1}{}^l$ is a fair approximation to E_{n+1}, and ψ_k is a reasonable trial-function for the n-th (or indeed any lower) state.

Secondly, we might have taken λ to satisfy

$$\lambda + [(H^2)_{kk} - 2\lambda H_{kk} + \lambda^2]^{\frac{1}{2}} = A < E_{n+1}{}^l \quad (8)$$

instead of (4) and, by an analogous argument, would have found that

$$E_n \geqslant H_{kk} - \frac{(H^2)_{kk} - (H_{kk})^2}{A - H_{kk}}, \quad (9)$$

provided that

$$H_{kk} \leqslant A. \quad (10)$$

But we observe that (6) is a better estimate for E_n than (9) and that (7) is less restrictive on ψ_k than (10). Therefore (6) represents the best result obtainable by this method.

3. UPPER BOUND

In a precisely similar manner we can show that if $E_{n-1}{}^u$ is an upper bound of E_{n-1}, then

$$E_n \leqslant H_{kk} + \frac{(H^2)_{kk} - (H_{kk})^2}{H_{kk} - E_{n-1}{}^u}, \quad (11)$$

as long as ψ_k is normalized and satisfies the condition

$$H_{kk} \geqslant E_{n-1}{}^u. \quad (12)$$

It is clear that if only $E_{n-1}{}^u < 0$, we can always satisfy (12) by taking a ψ_k of sufficiently oscillatory nature.

The inequality (11) allows of two types of application:

(1) If by any method one has obtained an upper bound of E_{n-1} he can, by the use of a single trial-function, determine an upper bound of E_n. This process may be continued.

[4] Strictly speaking, if $E_{n+1}{}^l = E_{n+1}$, then a level, namely, E_{n+1}, would fall into the interval (4), even if (5) were not satisfied. However, by a simple limiting process, one can easily verify that (5) must hold even in this case.

(2) One can determine an upper bound for E_1 by the usual Ritz method and then construct successively upper bounds of $E_2, E_3, \cdots, E_k, \cdots$. At each stage a single trial-function, ψ_k, is used, and three integrals, $N=\int\psi_k^*\psi_k dx$, $H_{kk}=\int\psi_k^* H\psi_k dx$, $(H^2)_{kk}=\int\psi_k^* H^2\psi_k dx$ must be evaluated. It is important that successive ψ's need not be orthogonal. For energy levels of high order this procedure would seem to be a simplification over the conventional method, due to Hylleraas and Undheim,[5] and an alternative method suggested by the author.[6] For these methods require that the successive ψ's must be normal and orthogonal and that at each stage the integrals $\int\psi_i^* H\psi_k dx$ $(i=1, 2, \cdots k)$ be evaluated. This means that at the k-th stage a total of $2k$ integrals must be found. Furthermore, in the procedure of Hylleraas and Undheim, a determinantal equation of order k must finally be solved. One must keep in mind, however, that the integrals for $(H^2)_{kk}$ which occur in our method, are in general quite difficult to evaluate.

[5] E. A. Hylleraas and R. Undheim, Zeits. f. Physik, p. 759 (1930).
[6] W. Kohn, Phys. Rev. **71**, 635 (1947).

For convenience we combine the inequalities (6) and (11) and the conditions (7) and (12) for the case when both E_{n+1}^l and E_{n-1}^u are known:

$$H_{kk}-\frac{(H^2)_{kk}-(H_{kk})^2}{E_{n+1}^l-H_{kk}}\leqslant E_n\leqslant H_{kk}+\frac{(H^2)_{kk}-(H_{kk})^2}{H_{kk}-E_{n-1}^u} \quad (13)$$

for any normalized trial-function ψ satisfying

$$E_{n-1}^u\leqslant\int\psi^* H\psi dx\leqslant E_{n+1}^l. \quad (14)$$

Let us note that all the results derived above retain their validity in the case of degeneracy (non-degeneracy was nowhere assumed) as long as the levels are ordered according to non-decreasing magnitude.

The author wishes to express his sincere thanks to Professor J. Schwinger for helpful discussions, and to Harvard University for the award of the Arthur Lehman Fellowship.

Letters to the Editor

PUBLICATION of brief reports of important discoveries in physics may be secured by addressing them to this department. The closing date for this department is, for the issue of the 1st of the month, the 8th of the preceding month and for the issue of the 15th, the 23rd of the preceding month. No proof will be sent to the authors. The Board of Editors does not hold itself responsible for the opinions expressed by the correspondents. Communications should not exceed 600 words in length.

Width of 985-Kev Al (p, γ) Resonance

R. S. BENDER, F. C. SHOEMAKER, AND J. L. POWELL
University of Wisconsin, Madison, Wisconsin
May 21, 1947

A CYLINDRICAL electrostatic analyzer[1] has been constructed for use with the Wisconsin pressure generator. With this instrument, which has a radius of curvature of forty inches, and ninety degree deflection, one can obtain a steady proton beam with an energy spread as small as 0.02 percent of the proton energy. Only protons which pass through the analyzer strike the target, so that the openings of the slit system determine the energy spread of the beam. The electric field between the analyzer plates is obtained from a stack of dry batteries which can be set to any desired voltage up to plus and minus 10,000 volts, and has negligible drift. Work up to the present has been limited to examination of the width of a narrow proton-gamma resonance, the 985-kev level of aluminum.[2]

The targets were prepared by evaporating aluminum onto sheets of tantalum. It was necessary to heat the target to over 200 degrees centigrade and to use a liquid air trap to avoid deterioration of the target. The beam, about 1/20 of a microampere of protons, was integrated by measuring, by means of an electrometer, the voltage produced across a condenser. The total voltage swing of the target was less than ten volts. The thickness of the target was determined by two methods. First, one can calculate the mass per cm² of the film from the weight of aluminum evaporated, assuming an isotropic distribution and the inverse square law. The data of Parkinson *et al*,[3] give then the energy absorption of the target. Second, the area under the thin-target yield curve, divided by the step in the thick-target yield, gives the energy absorption thickness directly in electron volts.

The number of coincidence counts from two thin-wall glass counters placed close to the target, divided by the integrated proton beam, was plotted against the energy of the bombarding protons. Assuming a Breit-Wigner formula for the resonance and the values determined for the target thickness and energy spread of the proton beam, we computed the resonance half-width both from the peak amplitude and from the half-width of the experimental yield curve. Effects of target non-uniformity and of straggling were not taken into account. The resonance half-width, Γ, is the energy spread at half-maximum for an infinitely thin target and a monoenergetic proton beam. Results from two targets, prepared at the same time so that their relative thicknesses should be accurate, are shown in Table I. The proton energy distribution is assumed to be triangular in shape with the energy spread quoted corresponding to width at half-maximum. The same target was used for the first two sets of data.

TABLE I. Determination of the half-width (all quantities in electron volts).

Target absorption thickness by weight	Target absorption thickness by area under curve	Energy spread of proton beam	Resonance half-width by half-width of curve	Resonance half-width by peak amplitude
200	215	400	372	284
200	192	200	313	288
100	85	200	276	255

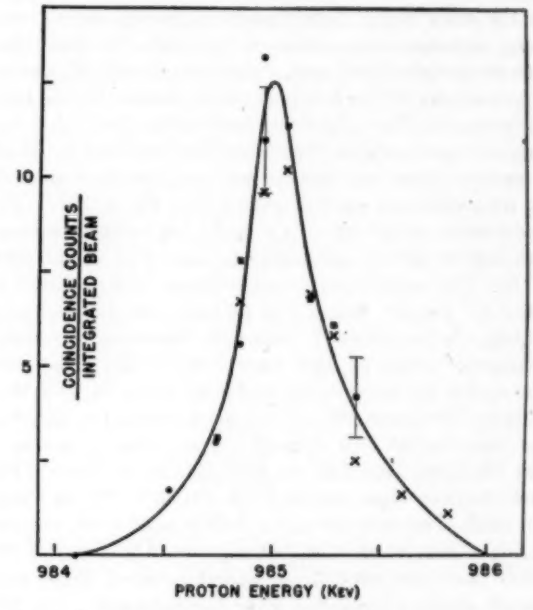

FIG. 1. Al (p, γ) yield curve covering 985-kev resonances. Three independent runs are shown by circles, crosses, and squares, respectively. Absolute voltage position taken from data of reference 1.

From these data, the value for Γ is 300 ± 50 electron volts. While there is little doubt about this value for the upper limit, great weight should not be attached to our value for the lower limit unless it is checked by further experiments which are now in progress. A typical curve (Fig. 1) showing gamma-ray yield *versus* proton energy shows the reproducibility of data obtained in three separate runs.

The writers wish to thank Professor R. G. Herb for suggesting this work and for his continued interest and guidance, and R. V. Smith for his generous assistance. The work was supported by the Wisconsin Alumni Research Foundation.

[1] Description to appear soon in Rev. Sci. Inst.
[2] G. J. Plain *et al.*, Phys. Rev. **57**, 187 (1940).
[3] D. B. Parkinson *et al.*, Phys. Rev. **52**, 75 (1937).

On the Alleged Gamma-Ray of N^{13}

L. M. LANGER, C. S. COOK, AND M. B. SAMPSON
Indiana University, Bloomington, Indiana
May 17, 1947

THE interpretations of the data on the disintegration of N^{13} have resulted in many contradictions.

Evidence for a complex beta-spectrum has been reported by Lyman,[1] Kikuchi *et al.*,[2] and Oppenheimer and Tomlinson.[3] On the other hand, evidence for a simple spectrum has been found by Townsend.[4]

The existence of a gamma-ray of about 0.280 Mev has been reported to accompany from 20 to 40 percent of the positron emission.[5] It has been further suggested by Watase and Itoh, and by Oppenheimer and Tomlinson, that there might be more than one gamma-ray of about that energy. On the other hand, Valley[6] finds no gamma-ray of such energy accompanying as many as 5 percent of the positrons.

In the present experiment, a search was made for gamma-radiation from N^{13} by means of an instrument having high resolution and low scattering and background. A large magnetic spectrometer, which will be described in detail in another paper, was used to measure the momentum of the photoelectrons ejected from a thin Pb radiator. The spectrometer makes use of a radially inhomogeneous magnetic field in order to accomplish focusing to a second order in 180°. The radius of curvature is 40 cm. The resolution is about 0.5 percent. Because of its large size and strategic baffling, the instrument is essentially free from scattering.

Graphite strips of high purity, 0.015 in. thick, were bombarded by an external cyclotron beam of 11.5-Mev deuterons for about 100 microampere hours. The graphite was then loaded into a small copper cassette having a wall thickness sufficient to stop all the positrons. The photoelectrons were ejected from a strip of Pb 26.3 mg/cm² thick. The detector was a double bead G.M. counter having a mica window of 2.68 mg/cm². The decay of the source was monitored by a second counter. Runs were started about 12 minutes after bombardment. The observed decay was found to be simple with a half-life of 9.8 minutes. The data plotted in Fig. 1 represent several overlapping runs. The points are corrected for decay, and each run is adjusted for intensity at one point.

Figure 1 shows the lines due to the photoelectrons ejected from the *K*, *L*, and *M* levels of Pb by the 0.51 Mev-radiation from the annihilation of the N^{13} positrons. Compton electrons from the annihilation radiation are also evident. However, no indication of a nuclear gamma-ray in the region of 0.280 Mev is observed.

From the intensity of the photoelectrons from the annihilation gamma-rays, and taking into account the increased efficiency of the photoelectric process at the lower energy, we can say that there are not as many as 0.002 gamma-rays per disintegration with energy in the neighborhood of 0.280 Mev. In addition, one can say that no evidence is found for a gamma-ray of energy between 0.135 Mev and 0.700 Mev with a probability of as much as 0.002 per disintegration at the low energy end to 0.06 per disintegration at the high end. From the fact that there are no Compton electrons of measurable intensity beyond the *M* line, one can also conclude that there is no gamma-ray of appreciable intensity at even higher energy.

Theoretically, the ground state and the first excited state of C^{13} and also N^{13} are expected to be members of a doublet (^2P).[7] From the measured spin of C^{13} one would assign $^2P_{\frac{1}{2}}$ to the ground state[8] and thus $^2P_{\frac{1}{2}}$ to the excited state. Then, whether N^{13} is $^2P_{\frac{1}{2}}$ or $^2P_{\frac{3}{2}}$, Gamow-Teller selection rules would allow forming both of the C^{13} levels after positron emission from N^{13}. From the calculated intensities

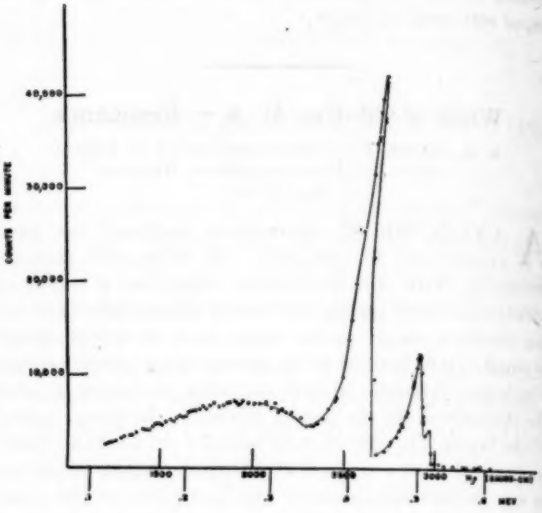

FIG. 1. Momentum distribution of photo and Compton electrons ejected from a Pb radiator by the radiation from N^{13}.

one would expect to find both these transitions in the energy region covered by this investigation. Fermi rules would permit only the $^2P_{\frac{1}{2}}$ to $^2P_{\frac{1}{2}}$ transition.

From the fact that no gamma-ray is found in the region 0.135 to 0.700 Mev, one must conclude that either Fermi rules apply, or that the excited state of C^{13} is less than 0.135 Mev or more than 0.700 Mev above the ground level.[9]

We are grateful to Professor Konopinski for many helpful discussions.

This work is supported by a grant from the Frederick Gardner Cottrell Fund of the Research Corporation and by the U. S. Navy.

[1] E. M. Lyman, Phys. Rev. **55**, 234 (1939).
[2] Kikuchi, Watase, Itoh, Takeda, and Yamagachi, Proc. Phys. Math. Soc. Japan **21**, 52 (1939).
[3] F. Oppenheimer and E. P. Tomlinson, Phys. Rev. **56**, 858 (1939).
[4] Townsend, Proc. Roy. Soc. **A177**, 357 (1941).
[5] J. R. Richardson, Phys. Rev. **53**, 619 (1938); **55**, 609 (1939). E. M. Lyman, Phys. Rev. **55**, 1123 (1939). Watase and Itoh, Proc. Phys. Math. Soc. Japan **21**, 389 (1939).
[6] G. E. Valley, Phys. Rev. **56**, 838 (1939).
[7] E. J. Konopinski, Rev. Mod. Phys. **15**, 233 (1943).
[8] F. A. Jenkins, Bull. Am. Phys. Soc. **22**, 24 (1947).
[9] Note added May 20, 1947. Since submitting this letter for publication, a paper by Siegbahn and Slätis, Ark. f. Mat., Astr. o Fysik **32A**, No. 9 (1945) has come to our attention. Their results are in general agreement with ours. Because of their geometrical arrangement, the ratio of photoelectrons to Compton's is much less favorable than in our experiment. Our measurements would have detected a 0.280-Mev gamma-ray of less than 1/10 the intensity that could have been distinguished by Siegbahn and Slätis.

The Critical Ionization Potentials of Uranium Hexafluoride and Hydrogen Fluoride

J. R. WHITE AND A. E. CAMERON
Tennessee Eastman Corporation, Oak Ridge, Tennessee
May 19, 1947

THE critical ionization potentials of uranium hexofluoride and of hydrogen fluoride were determined by using a VG1A ion gauge. The filament emission was held constant at such a value that the grid current was in a plateau region. The grid-to-filament potential was then varied and the onset of ionization determined by plotting the ion current as a function of the applied voltage. The ions were collected on the plate by application of a small fixed potential. The effects of secondary emission and space charge were evaluated by measuring the ionization potential of mercury. The correction was determined, using the value of 10.4[1] volts for the first ionization potential of mercury, and was subtracted from the potential observed for uranium hexafluoride. Measurements were made with hydrogen fluoride to eliminate the possibility that the potential observed with uranium hexafluoride was due to hydrolysis products. The measurements upon uranium hexafluoride were repeated in a 60° mass spectrometer of the Nier type so that ions other than the UF_5^+ could be identified and measured. The ionizing case and the electron trap were operated at the same potential so that the voltage drop from the filament to these elements was a measure of the ionization potential. The effect of space charge, thermal excitation, and secondary emission in the ionizing region were evaluated by using mercury as reference gas. The filament emission was held constant at 1.4 ma and no potentials except that between filament and ionizing case were varied after measurements upon mercury. The potentials were measured with a voltmeter which had been calibrated carefully against a laboratory potentiometer. The critical potential was determined by the intersection of the plots of ion current against voltage before and after reaching the critical potential. The mean value for several determinations upon the mercury standard was 15.1 volts. A correction of −4.7 volts was accordingly applied to the observed critical ionization potentials for the individual uranium fluoride ions. The critical ionization potentials are shown in Table I. These data

TABLE I. Critical ionization potentials of U, UF, and HF.

Ion	Critical ionization potential (ev) Spectrometer	Triode
UF_5^+	15.5	15.9
UF_4^+	20.1	—
UF_3^+	23.5	—
UF_2^+	29.9	—
UF_1^+	37.9	—
U^+	50.3	—
HF	—	5.4

may be regarded as giving a correct representation of the order of magnitude, but a probable error range of from 5 percent for the UF_5^+ ion to 15 percent for the U^+ appears likely because of the wide departure of the potentials from that of the reference gas.

This paper is based on the results of research performed under Contract W-704-eng-23, with the Manhattan Project, Oak Ridge, Tennessee.

[1] W. Bleakney, Phys. Rev. 35, 139 (1930).

A Note on the Spectrum of Th III

R. J. LANG
University of Alberta, Edmonton, Alberta, Canada
May 12, 1947

THE second spark spectrum of thorium has been photographed on the three-meter vacuum spectrograph from 2000A to 350A, using a vacuum spark source between metallic electrodes which is known to excite the III and IV spectra most intensely. As a further aid in distinguishing the lines of Th III, the same electrodes were used in an atmosphere of nitrogen at a lowered potential. The strong lines of Th IV are easily spotted for the most part, but the measurement of their wave-lengths leaves something to be desired in the way of accuracy.

The lines of Th III, which are the subject of this note, are very numerous especially in the region between 600A and 350A. These short lines in higher orders occur throughout

TABLE I.

First system Even terms	Second system Even terms	Second system Odd terms
201361 ($j=3$ or 4)	221728 ($j=2$)	105474.8 ($7p7s$) $^1P_2$
69708.7 ($j=3$)	224520 ($j=2$)	107722.6 ($j=2$ or 3)
64713.6 ($j=3$)	265075 ($j=1$)	107875.9 ($j=2$)
	69419.5 ($j=5$)	108841.0 ($j=1$ or 2)
		118756.1 ($j=2$) (uncertain)
		116475.4 ($j=2$)
		120168.4 ($j=2$ or 3)

the spectrum up to the fifth and even the sixth order. An attempt has been made to employ them to tie the whoel spectrum together, so as to obtain consistent accuracy below 2000A.

The spectrum of Th III has been partially analyzed into two systems of terms[1] without any intercombinations between them. The author has sought these intercombination lines in the vacuum region without any certain success. A factor which gives a promising number of possible intercombination lines has the value 12328 cm^{-1} to be added to the term values of the second system, so that based upon $5f6d\ ^3H_4$ as zero, the value of $6d7s\ ^1D_2$ would be 69328. I am informed privately by Dr. Klinkenberg that there are theoretical objections to a factor of such numerical size in the general structure of the III spectrum and its relation to the II spectrum.

In the work so far, a number of terms have been found which constitute an extension of Th III into the Schumann region. These, together with their j values, are shown in Table I.

[1] T. L. De Bruin, P. F. A. Klinkenberg, and P. Shuurmans, Zeits. f. Physik 118, 58 (1941).

Decay of K^{40}

H. A. MEYER, G. SCHWACHHEIM, AND M. D. DE SOUZA SANTOS
Departamento de Physica, Universidade de São Paulo, Brasil
May 20, 1947

THE energy of the γ-rays emitted by natural radioactive K^{40} was measured by the absorption method, with copper and lead used as absorbers. We found an energy of 1.5 Mev in accord with the value 1.54 Mev obtained by Wäffler and Hirzel.[1] This energy, however, is a little higher than the upper limit 1.35 Mev of the continuous β-spectrum[2] and so it seemed difficult to associate this γ-ray with the β-transitions. On the other hand, positron emission or K-capture could take place to account for the great abundance of A^{40}. Evidence for a K-capture process was given[3] recently, and no positron activity has been detected. We undertook β–γ coincidences to show that the γ-rays should be associated with the K-capture process. Measurements were taken with a precision of 1 percent, and no coincidences were obtained. These experiments show that no γ-rays can be associated with the β-transitions and that, therefore, the nucleus of Ca^{40} is not left in an excited state, showing that the disintegration scheme proposed by Wäffler and Hirzel is a correct one.

[1] H. Wäffler and O. Hirzel, Helv. Phys. Acta **XIX**, 216 (1946).
[2] Dzelepow, Vorobjov, and Kopjova, Comptes rendus (U.R.S.S.) **52**, 121 (1946).
[3] E. Bleuler and M. Gabriel, Helv. Phys. Acta **XX**, 67 (1947).

The Collision of Neutrons with Deuterons and the Reality of Exchange Forces

JOHN H. WILLIAMS
University of Minnesota, Minneapolis, Minnesota
May 13, 1947

IN a recent letter under the above title, Massey and Buckingham[1] have presented some experimental evidence for the reality of exchange forces between a neutron and proton. It is the purpose of this note to point out that experimental evidence exists which does not confirm their argument.

In Fig. 2 of Massey and Buckingham's letter (which unfortunately was misplaced to page 563 of the April 15 issue of the Physical Review), a comparison is made between the theoretical predictions for the total elastic cross section for the scattering of fast neutrons by deuterons as a function of neutron energy and the experimental observations of Ageno, Amaldi, Bocciarelli, and Trabacchi.[2] This comparison is repeated in Fig. 1 of this letter. In addition, the experimental results of Nuckolls, Bailey, Bennett, Bergstralh, Richards, and Williams[3] are shown.

The complete agreement between the results of Ageno *et al.*, and Nukolls *et al.*, for neutrons of 4 Mev is evident. Since the experimental techniques used by the two groups were so greatly different, there is reason to feel confident about the reality of the experimental results in the energy region up to 6 Mev. It is in just this region that agreement between experiment and Massey and Buckingham's theory might be expected. As these authors point out, their theory would be expected to give lower values for the cross section than the measured values for 12- and 14-Mev neutrons,

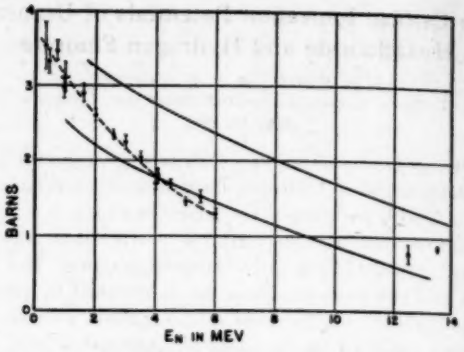

FIG. 1. Comparison of the observed and calculated total cross sections for the collision of neutrons with deuterons. The upper and lower full curves are calculated by Massey and Buckingham[1] on the respective assumptions of ordinary and exchange forces. The crosses are the experimental results of Ageno *et al.*[2] The circles are the results of Nuckolls *et al.*[3] The vertical dashes are the observational errors given by the experimenters.

since the additional contributions to the cross section for higher states of angular momentum have been neglected.

The probable conclusion that one can draw from the comparison in the lower energy region is that the interaction potential chosen by Massey and Buckingham does not represent the existing experimental facts. Consequently, the total cross section for neutron-deuteron scattering cannot be interpreted on the basis of their theory as strong evidence for the reality of exchange forces.

[1] H. S. W. Massey and R. A. Buckingham, Phys. Rev. **71**, 558 (1947).
[2] M. Ageno, E. Amaldi, D. Bocciarelli, and G. C. Trabacchi, Nuovo Cimento **1**, 253 (1943); Phys. Rev. **71**, 20 (1947).
[3] R. G. Nuckolls, C. L. Bailey, W. E. Bennett, T. Bergstralh, H. T. Richards, and J. H. Williams, Phys. Rev. **70**, 805 (1946).

Interaction between Meson and Nucleon

CHARLES L. CRITCHFIELD
University of Minnesota, Minneapolis, Minnesota
May 21, 1947

IT is known[1,2] that the Proca equations for a charged meson, (spin $\hbar$), moving in a coulomb field do not have a complete set of acceptable solutions. This has been shown[1,3] to be due to the appearance of an inverse cube, (r^{-3}), attractive potential in the second-order wave equations. The results of reference 2 indicate that this potential produces spin-orbit coupling.

Since the theory applies to a point charge, the central force may be thought of as arising on an "elementary nucleon," i.e., an electron of nucleonic mass. If we assume this hypothetical nucleon to have spin $\frac{1}{2}\hbar$, and consider the meson-nucleon states of total angular momentum $\frac{1}{2}\hbar$, the disastrous potential appears for those meson waves, $(\mathbf{U}, U_0)$, in which the space components, $\mathbf{U}$, contain both S and D waves. These waves are coupled in such a way that as $r \to 0$, the eigenvalues of the operator d^2/dr^2 obey the condition

$$d^2/dr^2 \to \pm\sqrt{2}e^2/\mu c^2 r^3 \text{ as } r \to 0, \qquad (1)$$

where μ is the mass of the meson. The essence of this formulation of the difficulty is presented in reference 3.

As shown by Landau,[4] the Proca equations are prob-

ably not adequate to describe the motion of a charged meson in orbits of radius comparable to $r_0=e^2/\mu c^2$, because the reaction of the meson to its own field becomes important at such distances. Apart from this possibility, however, there is a formal method of saving the solutions for the meson wave. Suppose the elementary nucleon to have a mass, M, and a magnetic moment in the direction of its spin of ν characteristic magnetons, ($\nu eh/2Mc$). If we put the vector potential due to this moment in the Proca equations, we may analyze the solutions by methods and approximations previously used on Dirac's equations.[5] This has been done for the $S+D$ meson wave alluded to above, with the result that Eq. (1) is replaced by one for the *lower* eigenvalue:

$$d^2/dr^2 \rightarrow \tfrac{1}{4}(\nu e^2/Mc^2)^2/r^4 \text{ as } r\rightarrow 0 \qquad (2)$$

for all states of finite energy. Thus the mesons face a *repulsive* potential at very small values of r, and a complete set of acceptable solutions should exist.

Depending upon the value of ν and M and the more exact evaluation of the radiation reaction on the meson, the magnetic forces may be of importance in determining the nature of the bound meson-nucleon states. In particular, such forces often lead to r^{-3} attractive potentials at intermediate radii and, in the case of Dirac's equations in the field of an uncharged magnetic dipole, one bound state has been found due to them, under the approximations made (reference 5). It appears possible, therefore, to make an explicit model for bound meson-nucleons systems that would lead to the type of nuclear forces proposed by Landau and Tamm,[3] i.e., those of purely electromagnetic type, without first evaluating the radiation reaction. Owing to attractive magnetic forces, the elementary nucleon may possibly bind more than one meson, so that the proton could be a composite system as well as the neutron.

[1] I. Tamm, Phys. Rev. 58, 952 (1940).
[2] H. C. Corben and J. Schwinger, Phys. Rev. 58, 953 (1940).
[3] L. Landau and I. Tamm, Phys. Rev. 58, 1006(L) (1940).
[4] L. Landau, Phys. Rev. 58, 1006(L) (1940).
[5] C. L. Critchfield, Phys. Rev. 71, 258 (1947).

Erratum: Transition from Classical to Quantum Statistics in Germanium Semiconductors at Low Temperature

[Phys. Rev. 71, 374 (1947)]

VIVIAN JOHNSON AND K. LARK-HOROVITZ
Purdue University, Lafayette, Indiana

THE following corrections should be made in our Letter to the Editor of the above title:

(1) The sentence at the end of the first paragraph should read ". . . between impurity centers, while the constant D is to be determined from the experiments."

(2) The last equation should read

$$\rho_I = 6270n^{-1} \text{ ohm-cm.}$$

(3) The sentence reading "Thus the transition from classical to quantum statistics leads to a constant residual resistance due to impurity scattering in degenerate samples, in agreement with experiment," which appears below Table I, should have been the last sentence of the text.

Electrostatic Field Strengths in Molecules and Nuclear Quadrupole Moments

C. H. TOWNES
Bell Telephone Laboratories, Murray Hill, New Jersey

May 21, 1947

THE magnitude of coupling between nuclear quadrupole moments and electric fields in certain molecules, as determined from microwave spectroscopy, has been given.[1-3] Since the quadrupole coupling involves the product of the nuclear quadrupole moment and the second derivative of the electric potential at the nucleus, excluding the effect of charge in a small sphere around the nucleus, $[eQ(\partial^2V/\partial z^2)]$, a knowledge of $\partial^2V/\partial z^2$ is necessary in order to determine the quadrupole moment, Q. Nordsieck[4] has calculated this quantity for the hydrogen molecule, but a similar calculation for other molecules appears very tedious. It is here proposed that $\partial^2V/\partial z^2$ may be determined in many cases from atomic data. In determining this quantity, the distortion of the spherical atomic electron distribution around each nucleus due to its proximity to other nuclei must be considered for molecules such as H_2 and the alkali halides. However, in case a heavy nucleus is covalently bonded in a molecule by use of one or two p electrons, the effect of the resulting non-spherical distribution of charge inside of the valence shell is very large, and contributions to $\partial^2V/\partial z^2$, because of distortion of the atomic electron distribution, are negligible by comparison. In such cases $\partial^2V/\partial z^2$ is large and is easily calculable by the same method as is used for determination of quadrupole moments from atomic spectra.[5] If, on the other hand, the atomic state which is approximated by an atom in a molecule has a spherical distribution of electrons, then $\partial^2V/\partial z^2$ is small and much more difficult to calculate.

Assuming, then, a heavy nucleus bonded in a molecule with a simple covalent p bond, the value of $\partial^2V/\partial z^2$ is fairly accurately given by $(8e\Delta\nu/15Z_1Ra^2a_0^3)$ e.s.u., where standard spectroscopic notation is used, and $\Delta\nu$ is the fine structure separation for an isolated atom in the same state. Actual values of $\partial^2V/\partial z^2$, of quadrupole couplings,[1] and of quadrupole moments for Cl and Br nuclei, are collected in Table I. The sign of $\partial^2V/\partial z^2$ corresponds to an excess positive charge located on the molecular axis. The Br quardupole moments obtained here are consistent with a rough estimate which can be made from atomic spectra.[6] In further justification of the procedure used, it should be observed that effects caused by distortion of the atomic wave functions and proximity of other nuclei will be of the order of magnitude of the contribution of one electron

TABLE I. Quadrupole coupling and moment for Br and Cl nuclei.

Molecule	Nucleus	$\partial^2V/\partial z^2$ (e.s.u.)	Quadrupole coupling $[eQ(\partial^2V/\partial z^2)$ in mc]	Quadrupole moment (Q in cm^2)
BrCN	Br^{79}	48×10^{15}	720	0.21×10^{-24}
	Br^{81}	48×10^{15}	556	0.16×10^{-24}
ClCN	Cl^{35}	17×10^{15}	84	-0.067×10^{-24}
	Cl^{37}	17×10^{15}	64	-0.051×10^{-24}

charge place 1A from the nucleus, or 1×10^{15}, which is much smaller than the p electron contribution for heavy atoms as may be seen from the table. For H_2, these effects produce a contribution[4] of 1.13×10^{15}.

It may happen, of course, that the atom in question is not bonded by a pure p bond, but its bonding electron is in a state represented by a combination of p and s wave functions. In most cases, the contribution to $\partial^2V/\partial z^2$ of the p wave function would still predominate. If the nuclear quadrupole moment is known, the value of $\partial^2V/\partial z^2$ determined from the quadrupole coupling would then give a measure of the importance of the p state in the complete wave function for the molecule. For example, a large quadrupole coupling for halide nuclei in alkali halide molecules would indicate the occurrence of resonance between ionic and covalent bonding.

Both BrCN and ClCN resonate between a state represented by a single p bond and one represented by two p bonds to the halide,[7] the double-bond character of the bond being 30 percent or less. Both of these states produce the same deviation from a spherical p shell, hence the presence of this resonance should not invalidate the calculation of $\partial^2V/\partial z^2$ given here.

The nitrogen quadrupole coupling in NH_3 and ClCN does not allow such a simple interpretation, since it is not clear whether or not the p shell is spherically filled around the N in these molecules, and also because the contribution of a p electron would not completely predominate for this light nucleus. A single p electron would contribute a value of approximately 4×10^{13} to $\partial^2V/\partial z^2$. If the N atom is surrounded by four tetrahedral bonds[8] of which one is unoccupied, the resulting contribution would be 3×10^{13}. If it is bonded by three pure p bonds, then the p shell is spherically filled, and the contribution to $\partial^2V/\partial z^2$ by the undistorted atomic electron distribution is zero. With this information about $\partial^2V/\partial z^2$, it can only be said that the magnitude of the N^{14} quadrupole moment is probably between 0.1×10^{-24} and 0.01×10^{-24} cm².

[1] C. H. Townes, A. N. Holden, J. Bardeen, and F. R. Merritt, Phys. Rev. 71, 644 (1947).
[2] B. P. Dailey, R. L. Kyhl, M. W. P. Strandberg, J. H. Van Vleck, and E. B. Wilson, Jr., Phys. Rev. 70, 984 (1946).
[3] D. E. Coles and W. E. Good, Phys. Rev. 70, 979 (1946).
[4] A. Nordsieck, Phys. Rev. 58, 310 (1940).
[5] H. A. Bethe and R. F. Bacher, Rev. Mod. Phys. 8, 226 (1936).
[6] S. Tolansky, Proc. Roy. Soc. 136, 585 (1936).
[7] J. Beach and A. Turkevich, J. Am. Chem. Soc. 61, 299 (1939).
[8] L. Pauling, *Nature of the Chemical Bond* (Cornell University Press, Ithaca, New York, 1945), p. 86.

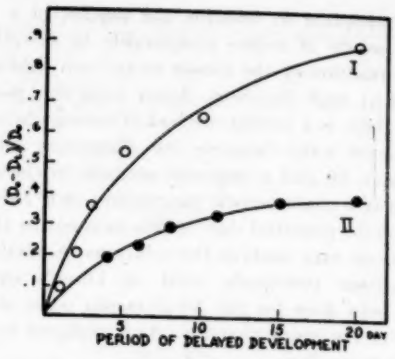

FIG. 1. Relationship between fractional loss of photographic density $(D_0-D_t)/D_0$ and time of delayed development for alpha-particles of radium in equilibrium.
I. Low silver halide emulsion.
II. High silver halide emulsion.

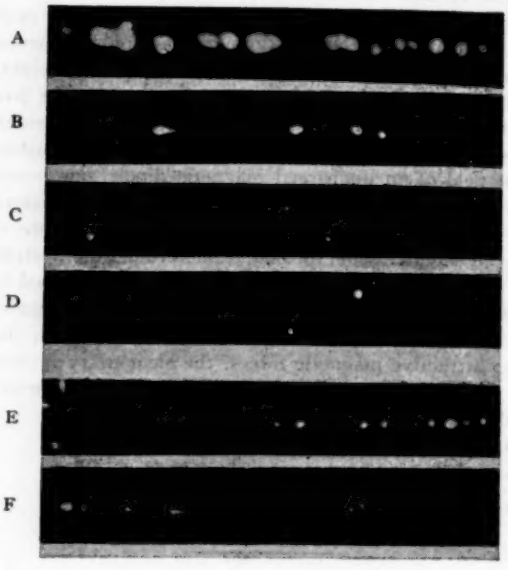

FIG. 2. Dark field photo-micrographs at 2000 × magnification, showing progressive deterioration of track structures on delayed development.
I. Low silver halide emulsion
A. Undelayed development
B. After 5 days delay
C. After 10 days delay
D. After 20 days delay
II. High silver halide emulsion
E. Undelayed development
F. After 20 days delay

Fading of Latent Alpha-Ray Image in Emulsions

HERMAN YAGODA AND NATHAN KAPLAN
National Institute of Health, Industrial Hygiene Research Laboratory, Bethesda, Maryland
May 10, 1947

STUDIES on the properties of fine grained silver bromide emulsions as recording media for localized alpha-radiation[1] revealed a 90 percent loss in photographic density after a 20-day delay in the development of the latent image. Marked fading effects have also been observed in plates of diverse European manufacture by Blau,[2] Lauda,[3] and more recently by Occhialini.[4] In view of the importance of this factor in experiments of long duration, such as cosmic-ray studies, and in the measurement of low levels of alpha-ray activity, comparative data between the old and new types of Eastman alpha-particle emulsions are of interest.

The emulsions characterized in Table I were exposed to a flux of 5000 alpha-particles per sec. per cm² for 2 hours, and development was delayed for measured periods of time. The source of radiation was a thin film of equilibrated barium-radium sulfates separated by 1 mm of air from the

TABLE I. Emulsion characteristics.

Designation	Old type*	New type**
Emulsion thickness	40 μ	24 μ
Emulsion weight	5.4 mg/cm²	7.2 mg/cm²
Percentage gelatin	56	27
Percentage silver halide	44	73

* Characteristic of Eastman Emulsion No. 276,296.
** Characteristic of Eastman Emulsion No. 329,489.

emulsion. The photographic density of the images produced by delayed development, D_t, and of the control developed immediately after the exposure, D_0, were measured on a recording densitometer. The fractional loss of photographic density as a function of the period of delayed development is exhibited in Fig. 1. The data shows that fading takes place in both emulsions, but is less pronounced in the newer type of high silver halide content.

Since the density is an integration of the blackening produced by the individual alpha-particles, variations in either the length, grain size, or grain spacing of the individual tracks can be anticipated after prolonged delay in their development. Photo-micrographs of the tracks (Fig. 2) show that alterations of this character are produced, the deterioration depending on the emulsion type and the extent of delayed development. It is noteworthy that the tracks are completely obliterated in the emulsions of low silver content if development of the latent image is delayed beyond 5 days, whereas in the improved plates the track is still recognizable after a delay period of 20 days.

These studies indicate that the abundance of stars in emulsions exposed at high elevations may have been underestimated as a result of the fading of the latent image of the multiple tracks in disintegrations produced during the initial stages of the cosmic-ray exposure. In the new type emulsion the exposure can probably be prolonged for 20 days without appreciable loss in the total track count. Further experiments are in progress on the rate of fading as a function of the energy and the relative flux of the alpha-particles.

[1] H. Yagoda, Am. Mineralogist 31, 87 (1946).
[2] M. Blau, Sitz. Akad. Wien, Math.-Naturw. Klasse, Abt. 2A 140, 623 (1931).
[3] J. Lauda, *ibid.*, Abt. 2A 145, 707 (1936).
[4] G. P. S. Occhialini and C. F. Powell, Nature 159, 186 (1947).

Hyperfine Structure and the Nuclear Spin of U^{235}*

O. E. ANDERSON AND H. E. WHITE
University of California, Berkeley, California
May 22, 1947

THE hyperfine structure and isotope shift in the arc lines of uranium have been studied using Fabry-Perot etalons with a resolving power of 500,000. The source was a liquid-air cooled hollow cathode tube into which was placed a 50-mg piece of metallic uranium with the isotope 235 considerably enriched. While many of the arc lines in the visible region show isotope shift, only λ5915 and λ6926, throughout the range of 4000 to 8500A, show resolvable and measurable hyperfine structure. λ5027

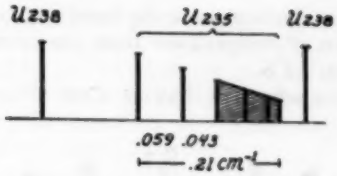

FIG. 1. Flag pattern in the hyperfine structure of U^{235}.

shows a very large isotope shift of 0.426 cm^{-1} or 0.108A. Since this line showed no hyperfine splitting of any kind, it was used to check the relative intensities of the two components due to the two isotopes 235 and 238 of the enriched sample.

Using 6-mm etalon spacers, the two components of λ5027 are so sharp and well separated that this line lends itself quite well to relative abundance measurements by either photographic or direct reading photo-voltmeter methods. The photographic method was used in this experiment to compare relative intensities with relative abundance. Agreement to within one percent of the values known from other reliable data is well within the accuracy expected by the photographic method.

Using J-values supplied to us from other sources,[1] as 6 and 7 for λ5915, the relative intensities of the components were studied. The flag pattern in the photographs shows three clearly resolved components as indicated in Fig. 1. Knowing the relative abundance of the two isotopes, and hence the relative energies falling into the two isotope patterns, a reasonably good determination of the nuclear spin I can be made by comparing the 238 sharp component with the first component of the flag pattern. This turned out to be more reliable than a comparison of the relative intensities of the lines within the hyperfine structure pattern or a comparison of their relative intervals.

Assuming the J-values of 6 and 7, intensity measurements indicate $I=5/2$, or $7/2$. The over-all width and the relative intensity of the tail of the pattern favor the lower value of $I=5/2$.

* This report is based on work performed under Contract No. W-7405-eng-36 with the Manhattan Project at the Los Alamos Scientific Laboratory of the University of California.
[1] C. C. Kiess, C. J. Humphreys, and D. D. Laun, J. Opt. Soc. Am. 36, 357 (1946).

The Concentration of He^3 in the Liquid and Vapor Phases of He^4*

HENRY A. FAIRBANK AND C. T. LANE
Sloane Physics Laboratory, Yale University, New Haven, Connecticut
AND
L. T. ALDRICH AND ALFRED O. NIER
Department of Physics, University of Minnesota, Minneapolis, Minnesota
May 21, 1947

IT is known[1] that helium contains a stable isotope of mass 3 and that this isotope has an abundance ratio of approximately 1.3×10^{-6} in atmospheric helium and 1.6×10^{-7} in helium derived from natural gas.[2] In order to obtain information on the possibility of separating this isotope with the use of liquid helium, we have studied the

distribution of the isotopes in the liquid and vapor phases as a function of temperature from the normal boiling point down to 2.2°K.

Figure 1 is a schematic drawing of the helium cryostat.

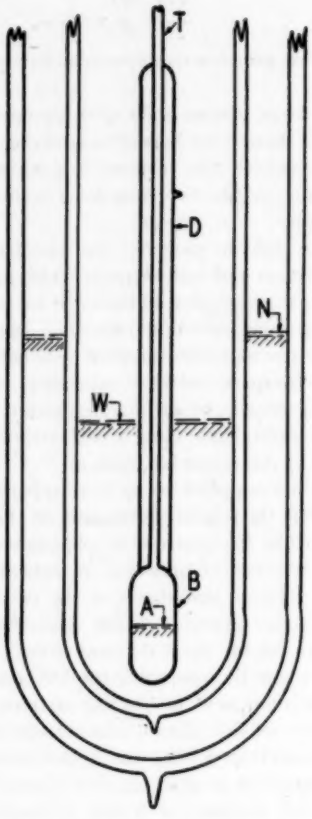

FIG. 1. Schematic drawing of the helium cryostat.

Approximately 2 liters of Air Reduction Company atmospheric helium were condensed into the small Pyrex bulb, B, of volume 6 cm³. The gas is introduced through a glass capillary, T, approximately 1.5 mm in diameter. Surrounding T is a vacuum jacket, D, serving as an insulating Dewar to prevent solidification of impurities which might block the capillary. A mercury Toepler pump is employed to displace the helium into bulb B from the storage flask. Surrounding bulb B is a bath of liquefied well helium, W, the temperature of which may be controlled by reducing its vapor pressure by means of a vacuum pump. A second bath of liquid nitrogen, N serves as a radiation shield. By means of slits in the Dewars the bulb B is visible at all times. Approximately 3 cm³ of liquid atmospheric helium was condensed in the bulb, and a differential manometer was employed to assure that the temperatures inside and outside the bulb were equal. Samples of the helium vapor from B were collected in break-seal tubes at each temperature listed in Table I. The liquid and vapor in B were kept at a constant temperature for 30 minutes before each sample was withdrawn. Sample 0 was taken from the original supply of atmospheric helium and sample 9 from the helium gas recovered at the end of the experiment when the liquid helium in bulb B had completely evaporated.

The isotope analyses were made with the same instrument mentioned in reference 2. Sample 10 was from another batch of atmospheric helium also supplied by the Air Reduction Company and happens to be one used as a comparison standard for current work on the mass spectrometer. All analyses except that of sample 0 were done the same day. One would expect samples 0 and 10 to be identical, whereas sample 9 should show a slightly smaller He³ concentration because of preferential depletion of He³ caused by successive sampling. While samples 0 and 10 agree within the error to be expected in measurements of this sort, it seems preferable to use sample 9 in our computations. In Table I are listed also the He³/He⁴ concentrations in the vapor (C_v) and in the liquid (C_L). C_L is computed from C_v and the mass and composition balance equations making use of the Leiden data for vapor and liquid densities.[3] Correction has been applied for the successive depletion in He³ because of the withdrawal of the samples. The average sample was roughly 10 cm³ (STP).

Figure 2 is a plot of the relative concentrations in the vapor and liquid as a function of temperature. Since 5.2°K is the critical temperature of helium, this ratio must be unity at this temperature.

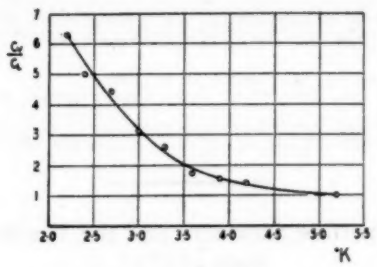

FIG. 2. The relative He³/He⁴ concentration in the vapor to that in the liquid as a function of temperature.

TABLE I. Concentration of He³ relative to He⁴.

Sample	He³/He⁴ in reference samples	He³/He⁴ in vapor (C_v)	He³/He⁴ in liquid (C_L)	$\frac{C_v}{C_L}$	T (°K)
0	1.2×10^{-6}				297
1		1.9×10^{-6}	1.33×10^{-6}	1.4	4.21
2		2.1	1.33	1.6	3.90
3		2.3	1.33	1.7	3.60
4		3.3	1.28	2.6	3.30
5		4.0	1.27	3.1	3.00
6		5.6	1.28	4.4	2.69
7		6.5	1.29	5.0	2.40
8		8.0	1.27	6.3	2.20
9	1.3				297
10	1.3				297

No attempt has been made to interpret these data theoretically, but it is clear that if pure He³ exists as a liquid it must have a lower boiling point than He⁴. Inasmuch as the liquid contains a sizable proportion of the He³ isotope, it appears possible to check whether this isotope participates in the superflow properties of He⁴ by

allowing the liquid to leak out of a closed container through a superleak and measuring the concentration of the residual gas.

* The work at Yale University was assisted by the Office of Naval Research under Contract N6ori-44 and that at the University of Minnesota by grants from the Research Corporation and the Graduate School.
[1] L. W. Alvarez and R. Cornog, Phys. Rev. **56**, 613 (1939); **56**, 379 (1939).
[2] L. T. Aldrich and A. O. Nier, Phys. Rev. **70**, 983 (1946). At the time this work was done we did not feel that the accuracy of the measurements justified a correction for the difference in pumping speeds of He^3 and He^4 in the mass spectrometer pump lead. We now feel that the accuracy justifies this correction. Hence He^3 abundances previously given should be multiplied by (4/3).
[3] E. Mathias, C. A. Crommelin, H. K. Onnes, and J. C. Swallow, Leiden Comm. 172b (1925).

Conductivity Pulses Induced in Diamond by Alpha-Particles

D. E. Wooldridge,* A. J. Ahearn, and J. A. Burton
Bell Telephone Laboratories, Murray Hill, New Jersey
May 21, 1947

THE modern theory of the solid state predicts that when alpha-particles bombard an insulator, the electrons freed by ionization will be raised to the conduction band. Under the influence of an applied electric field, these electrons, and the positive holes in the normally filled band, should move just as in the case of photo-conductivity. With a sufficiently high electric field across an insulator crystal which is relatively free of electron traps, it should be possible under favorable conditions to detect the movement of these charges and thus observe conductivity pulses.

With an amplifier and cathode-ray oscilloscope we have observed such pulses, produced by individual alpha-particles from radium, in diamond crystals at room temperature. The number of ions produced in diamond is of the same order as the number of ions produced by alpha-particles in an air ionization chamber. These conductivity pulses have been observed with two markedly different electrode arrangements on the diamond. One system consists of a pair of metal electrodes deposited by evaporation on the surface of the diamond, these electrodes being separated by a gap of 0.003 cm. Here the conductivity pulses consist of charges which travel across the top surface layers of the gap on the diamond. Good pulses were obtained with 5 volts applied across this gap. The second arrangement consists of evaporated electrodes on opposite sides of a diamond chip of about 0.5-mm thickness. Here the conductivity pulses consist of charges which travel from one surface toward the other surface of the diamond. Good pulses were obtained with 100 volts across such a diamond. In general, applied fields as low as 2000 volts per cm may be sufficient to approach saturation.

With each of the above electrode systems, pulses of comparable size are obtained with either direction of the applied field. When the applied field is reduced to zero, pulses are observed but for a short time only. These "space-charge" pulses are opposite in direction to those that occur when the voltage is applied, i.e., the diamond becomes polarized.

Our diamond specimens consist chiefly of "saw cuts," i.e., small chips sawed from a natural diamond in eliminating flaws, etc. Most of the diamonds which we have tested show this alpha-particle bombardment-induced conductivity. However, no conductivity pulses were observed in some diamonds even though saturation in photo-conductivity is approached at the applied fields used in the alpha-particle bombardment tests.

The electrodes apparently need to be in intimate contact with the diamond surface. Electrodes of gold, aluminum, or platinum formed by evaporation are satisfactory.

Van Heerden[1] has observed conductivity pulses induced by alpha-particle bombardment of silver chloride crystals at liquid nitrogen temperature, but he found none in the single diamond that he tried.

This phenomenon of bombardment-induced conductivity in diamond immediately suggests its use as a solid counter for nuclear physics experiments, particularly since it operates at room temperature. Its small size, high density, low operating voltage, and the possibility of rapid counting rate may give the diamond solid counter certain advantages over the conventional gas type counter.

* Now at Hughes Aircraft Company, Culver City, California.
[1] P. J. Van Heerden, Thesis (Utrecht, 1945).

Structure of the Quadrielectron*

Aadne Ore
Sloane Physics Laboratory, Yale University, New Haven, Connecticut
May 15, 1947

A PREVIOUS calculation led to the approximate value 0.11 ev for the binding energy of a system of two electrons and two positrons against dissociation into two free bielectrons.[1] The variational function leading to this result is the generalized "atomic" function

$$\psi_\beta = \tfrac{1}{2}\{\exp -\tfrac{1}{2}[(1+\beta)(r_{1a}+r_{2b})+(1-\beta)(r_{1b}+r_{2a})] + \exp -\tfrac{1}{2}[(1-\beta)(r_{1a}+r_{2b})+(1+\beta)(r_{1b}+r_{2a})]\}$$

where 1 and 2 refer to the electrons and a and b to the positrons.

This numberical result represented a considerable improvement as compared with the energy values resulting from earlier calculations, but it gave little information regarding the true value of the energy. For this reason an attempt has been made to determine the energy of the quadrielectron with greater accuracy.

The function, ψ_β, is related to the function used by S. C. Wang in the problem of the energy of the normal hydrogen molecule. A calculation has now been performed which is similar rather to Weinbaum's treatment of the hydrogen molecule by means of a linear combination of "atomic" and "ionic" functions,[2] which led to a considerable improvement in the energy value as compared to Wang's result.

For this purpose the following function has been used: $\Psi = \psi_\beta + c\psi_\alpha$, where the "ionic" function, ψ_α, is defined by

$$\begin{aligned}2\psi_\alpha = &\exp -\tfrac{1}{2}[(1+\alpha)(r_{1a}+r_{2a})+(1-\alpha)(r_{1b}+r_{2b})] \\ &+\exp -\tfrac{1}{2}[(1-\alpha)(r_{1a}+r_{2a})+(1+\alpha)(r_{1b}+r_{2b})] \\ &+\exp -\tfrac{1}{2}[(1+\alpha)(r_{1a}+r_{1b})+(1-\alpha)(r_{2a}+r_{2b})] \\ &+\exp -\tfrac{1}{2}[(1-\alpha)(r_{1a}+r_{1b})+(1+\alpha)(r_{2a}+r_{2b})].\end{aligned}$$

Since Ψ does not contain the distances between particles

of the same kind, the method of calculating matrix elements developed in reference 1 is applicable. The calculations are tedious, however, and the resulting expression for the energy in terms of α, β, and c is rather complicated. Minimization of the energy leads to an optimum value for the binding energy of roughly 0.135 ev, when $\alpha=\beta=(0.5)^{\frac{1}{2}}$ and $c=0.052$, approximately.

In previous calculations considerable improvement could be obtained by a slight improvement in the function. The fact that this is no longer true suggests that we might be near the convergence limit.

If we let ψ_β approximate the quadrielectron wave function, the mean distance between the various particles constituting this cluster is found to be roughly $\bar{r}_{12}=\bar{r}_{ab}=4.5\times10^{-8}$ cm and $\bar{r}_{1a}=\bar{r}_{2b}=\bar{r}_{1b}=\bar{r}_{2a}=3.0\times10^{-8}$ cm, that is, ψ_β gives reasonable relative values of the "repulsive" and the "attractive" distances. Furthermore, using the same function we find the value 1.16 for the ratio of the root mean square value of r_{12} to the mean value of this quantity. For the bielectron in the ground state, on the other hand, the corresponding ratio for the separation of the two particles has the value 1.15.

The values of the various mean distances reveal that the quadrielectron has a considerable size and, consequently, a large breakup probability when passing through matter even of small density.[3]

* The work here reported forms part of a dissertation presented for the degree of Doctor of Philosophy in Yale University.

[1] E. A. Hylleraas and A. Ore, Phys. Rev. 71, 493 (1947).

[2] S. Weinbaum, J. Chem. Phys. 1, 593 (1933).

[3] For more details regarding the probability of breakup vs. annihilation of light polyelectrons see: J. A. Wheeler, Ann. New York Acad. Sci. 48, 219 (1946).

The Hyperfine Structure of Atomic Hydrogen and Deuterium†

J. E. Nafe, E. B. Nelson, and I. I. Rabi
Columbia University, New York, New York
May 19, 1947

THE hyperfine structure separation, ν_H and ν_D, of atomic hydrogen and deuterium were measured directly by means of the atomic beam magnetic resonance method.[1-3] For each atom two resonance lines were measured, each at the same value of the magnetic field, and the ν_H and ν_D were evaluated entirely from differences in the frequencies. Neither the value of the magnetic field nor the g values of the atomic and nuclear systems enter into the final result.

In H, where the value of the nuclear spin $I=1/2$ and the atomic $J=1/2$, the π-transitions $(1,1)\leftrightarrow(0,0)$ and $(1,0)\leftrightarrow(1,-1)$ were measured at the same value of the magnet current. The difference between these two frequencies gives ν_H directly (see Eqs. 9–12 of reference 3). For D, where $I=1$ and $J=1/2$, the line $(3/2,1/2)\leftrightarrow(1/2,-1/2)$, $(3/2,-1/2)\leftrightarrow(1/2,1/2)$, an unresolved doublet, and the line $(3/2,3/2)\leftrightarrow(1/2,1/2)$ were measured in quite weak fields of the order of one gauss. The first line gives ν_D almost directly, and the difference in frequency of the two lines gives a small correction of less than 0.01 percent.

The measured values of ν_H and ν_D, in megacycles per second, are

$$\nu_H=1421.3\ \pm0.2$$
$$\nu_D=\ 327.37\pm0.03.$$

The method is inherently capable of greater precision with the improvement of our frequency meter.

Since the theory of the H and D atoms is considered to be complete and exact, these values can be compared directly with calculations. The formula for the hyperfine structure separation of S states was given by Fermi[4] and is

$$\nu=\frac{8\pi}{3h}\left(\frac{2I+1}{I}\right)\mu_N\mu_0\psi^2(0). \tag{1}$$

The nuclear spin is denoted by I, μ_N is the magnetic moment of the nucleus in question, μ_0 is the Bohr magneton, and $\psi(0)$ is the value of the Schroedinger wave function evaluated at $r=0$. $\psi^2(0)$ is proportional to $(1/a)^3$, the cube of the reciprocal of the radius of the first Bohr orbit. Since a is inversely proportional to the reduced mass, the appropriate value of the reduced mass, m_r, has to be inserted. If the values of the quantities in Eq. (1) are expressed in terms of the fundamental constants, Eq. (1) becomes

$$\nu=\frac{4}{3}\left(\frac{2I+1}{I}\right)\frac{\mu_N}{1836.6}\left(\frac{m_r}{m_0}\right)^3\alpha^2CR_\infty. \tag{2}$$

R_∞ is the Rydberg constant for infinite mass, α is the fine structure constant, and μ_N is the nuclear moment in terms of the nuclear magneton, $\mu_0/1836.6$. For μ_P and μ_D we have the accurate values of Millman and Kusch[5]

$$\mu_P=2.7896\ \pm0.0008$$
$$\mu_D=0.85648\pm0.00037,$$

for α^2, R_∞, and C we have the values given by Birge[6]

$$\alpha^2=(5.3256\pm0.0013)\times10^{-5}$$
$$R_\infty=109737.303\pm0.017\ \text{cm}^{-1}$$
$$C=(2.99776\pm0.00004)\times10^{10}\ \text{cm sec.}^{-1}$$

With these values and the value of the ratio μ_P/μ_D given by Kellogg, Rabi, Ramsey, and Zacharias[2] and by Arnold and Roberts[7] as 3.2571 ± 0.001, we obtain the results given in Table I.

Table I. The hyperfine structure separation of H and D.

	Measured	Computed from Eq. (2)
ν_H	1421.3±0.2 Mc	1416.90±0.54 Mc
ν_D	327.37±0.03 Mc	326.53±0.16 Mc
ν_H/ν_D	4.3416±0.0007	4.3393±0.0014

There is clearly an important difference between the measured and calculated values of ν_H and ν_D of about 0.26 percent compared with the probable error of the calculated value of 0.05 percent. The difference is five times greater than the claimed probable error in the natural constants. Whether the failure of theory and experiment to agree is because of some unknown factor in the theory of the hydrogen atom or simply an error in the estimate of

one of the natural constants, such as α^2, only further experiment can decide.

The comparison of the experimental ratio to the calculated ratio is particularly important, since most of the natural constants cancel out. The agreement is much better than for the absolute value but still not exact. The experimental value is about 0.06 percent greater than the calculated value. The error of the calculated ratio arises chiefly from the measured ratio of μ_P/μ_D which is claimed to be accurate to about 0.03 percent. Clearly this interesting deviation is worthy of further study.

† Publication assisted by the Ernest Kempton Adams Fund for Physical Research of Columbia University.

[1] J. M. B. Kellogg, I. I. Rabi, and J. R. Zacharias, Phys. Rev. **50**, 472 (1936).
[2] J. M. B. Kellogg, I. I. Rabi, N. F. Ramsey, Jr., and J. R. Zacharias, Phys. Rev. **56**, 728 (1939).
[3] P. Kusch, S. Millman, and I. I. Rabi, Phys. Rev. **57**, 765 (1940).
[4] E. Fermi, Zeits. f. Physik **60**, 320 (1930).
[5] S. Millman and P. Kusch, Phys. Rev. **60**, 91 (1941).
[6] R. T. Birge, Rev. Mod. Phys. **13**, 233 (1941).
[7] W. R. Arnold and A. Roberts, Phys. Rev. **70**, 320 (1946).

Phase of Scattering of Thermal Neutrons by Aluminum and Strontium*

E. FERMI AND L. MARSHALL
Argonne National Laboratory and University of Chicago, Chicago, Illinois
May 15, 1947

IN a previous paper[1] we have described a method for determining whether neutrons scattered by an atom have the same phase as the primary neutron wave or opposite phase. The method has now been applied to two more elements, Al and Sr. The crystals investigated were Al_2O_3 (corundum) and $SrSO_4$ (celestite). The measured intensities of various orders of Bragg reflections of monochromatic neutrons are given in the following table, which is arranged like Table I of reference 1.

TABLE I. Intensities of reflection of thermal neutrons by Al_2O_3 and $SrSO_4$.

Crystal	Plane	Order	Form factor	Intensity
Al_2O_3	$1\bar{1}0$	1	2Al − 1.44 O	480
		2	2Al − 1.34 O	700
		3	2Al + 2.09 O	5940
$SrSO_4$	001	1	0.44 Sr + 0.77 S + 0.12 O	4351
		2	0.62 Sr − 0.19 S + 0.67 O	3576
		3	0.98 Sr + 0.48 S + 1.01 O	2182
		4	0.24 Sr + 0.93 S − 1.81 O	1682
	210	1	0.78 Sr + 0.66 S − 0.01 O	6021
		2	0.21 Sr − 0.14 S + 0.36 O	413
		3	0.44 Sr + 0.84 S + 1.09 O	1493
	101	1	0.46 Sr − 0.65 S − 0.54 O	702
		2	0.55 Sr − 1.16 S − 2.54 O	3182
		3	1.94 Sr + 0.83 S + 0.50 O	5759

Attempts to fit these data with actual values of the scattering length for aluminum and strontium have not been satisfactory. It seems unambiguous, however, that the sign of the scattering of aluminum is the same as that of oxygen, namely, positive according to our convention. This is proven by the low intensity of first and second order compared with that of the third order.

A similar behavior of the reflection from the (101) plane of celestite indicates that the scattering length of strontium is also positive. From the scattering cross sections of these two elements, 1.4×10^{-24} cm² for Al and 9.5×10^{-24} for Sr, one can calculate the scattering lengths 0.35×10^{-12} cm for Al and 0.88×10^{-12} cm for Sr.

* This document is based on work performed under Manhattan Project sponsorship at the Argonne National Laboratory.
[1] E. Fermi and L. Marshall, Phys. Rev. **71**, 666 (1947).

Pressure and Temperature of the Atmosphere to 120 km

N. BEST, R. HAVENS, AND H. LAGOW
Naval Research Laboratory, Washington, D. C.
May 9, 1947

PRESSURES and temperatures of the atmosphere up to 120 km were determined from data taken on the V-2 rocket fired at White Sands, New Mexico on March 7, 1947. The methods used in obtaining these data were similar to those used in a previous flight.[1] The pressure measurements were made with bellows gauges for pressures between 1000 mm Hg and 10 mm Hg. For pressures between 2 mm Hg and 10^{-2} mm Hg, tungsten and platinum wire Pirani gauges were used. A Philips gauge was used for pressures between 10^{-3} and 10^{-5} mm Hg.

Ambient pressures (Fig. 1) were measured up to about

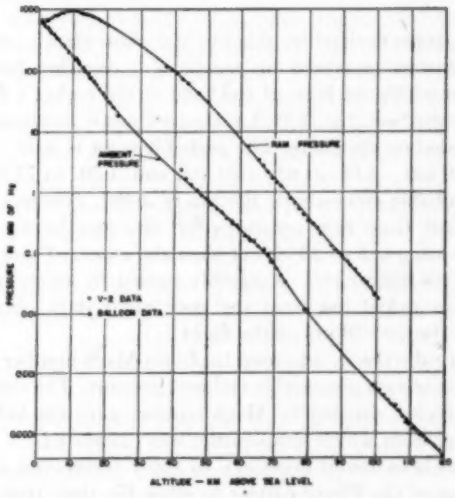

FIG. 1. Ambient and ram pressures as a function of altitude.

80 km with gauges mounted on the side of the V-2, just forward of the tail section. Pirani gauges, mounted in similar positions on opposite sides of the rocket, gave readings which agree within experimental errors, indicating that no appreciable error was introduced by yaw of the missle up to this altitude. A single Philips gauge was mounted on the 15° cone of the warhead. The readings of this gauge were reduced to ambient pressures by use of theories of Taylor and Maccoll.[2] Photographs of the earth made from the missile and gyroscope data indicated a yaw of about 15° at 110 km and a roll period of 40 seconds.

From the above data it has been calculated that at 110 km the aspect of the rocket was such that the Taylor and Maccoll corrections used were valid (Fig. 1). However, at 100 km the pressure shown is probably too high, while at 120 km it is too low, in each case by a factor of less than two.

The temperature of the atmosphere was calculated from the slope of the pressure *vs.* altitude curve and from the ratio of ram to ambient pressures. Figure 2 is a plot of the

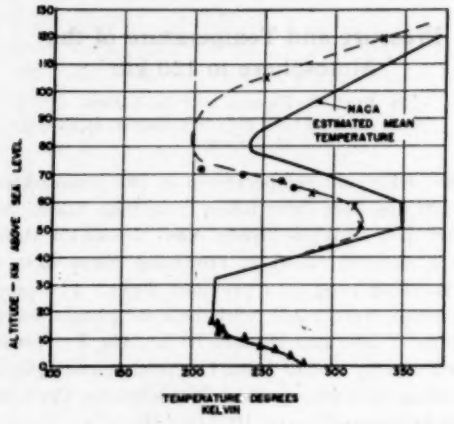

FIG. 2. Temperature as a function of altitude. The crosses indicate data calculated from slope of pressure curve; the black circles, data calculated from ram pressure; the triangles represent balloon data.

temperatures derived by this method. Also shown are the temperatures measured by means of a weather balloon released within an hour of the time of the rocket's flight. For comparison, the NACA estimated mean temperature[3] is included on the curve. The probable error is ±25° from 50 to 60 km., ±15° at 65 to 70 km, and ±20° at 72.5 km. The probable error above 100 km is ±40°. Temperatures calculated from ram pressures for altitudes between 10 and 20 km are 5 to 20° lower than the expected temperature. This discrepancy is possibly caused by errors in the velocities calculated from the poor radar data obtained during the first 20 km of the flight.

Pitot tube theory was used to obtain Mach number from the ratio of ram pressure to ambient pressure. The velocity of the rocket divided by Mach number gave the velocity of sound from which temperature was calculated.

It has been found necessary to apply corrections in the readings of the Pirani gauges to allow for their time constants. This effect resulted in a 1.5-second lag in the gauge used in October, corresponding to 2 km at altitudes between 60 and 80 km. When the October data were recalculated to allow for the lag, they were found to agree with the March data at 60 km, but to be higher than the March data at 80 km. This difference may be a seasonal effect and not experimental error. To establish the seasonal effect definitely, accurate data are needed between 75 and 100 km.

Two platinum resistance temperature gauges were installed to measure temperature of sections of the 15° nose cone. The temperature rise on the 0.1-inch thick aluminum forward section of the nose was 120°±5°C. On the 0.1-inch steel section immediately behind the aluminum, the temperature rise was 85°±5°C.

[1] Best, Durand, Gale, and Havens, Phys. Rev. **70**, 985 (1946).
[2] G. I. Taylor and J. W. Maccoll, Proc. Roy. Soc. **139**, 278 (1922).
[3] National Advisory Committee for Aeronautics, TN 1200 "Tentative Tables for the Properties of the Upper Atmosphere" (1947).

The λ-Point of NH_4Cl and Thermodynamic Equilibria of the Second Order

E. O. HALL
Victoria University College, Wellington, New Zealand
May 16, 1947

IN a recent article, E. F. Lype[1] undertook a discussion of thermodynamic equilibria of higher orders. Using Lype's equations, an interesting correlation has been found between the observed and the calculated slope of the equilibrium curve for NH_4Cl at its λ-point.

We substitute in Lype's formula (18a) which gives for second-order equilibria,

$$dp/dT=\tfrac{1}{2}(c_p''-c_p')/T(\partial v''/\partial T-\partial v'/\partial T),$$

where the dashes refer to the two phases. From the data of Simon, v. Simson, and Ruhemann,[2] we have the maximum specific heat given as $c_p=177.4$ cal./mole-deg., with the specific heat immediately after transition as 18 cal./mole-deg. Hence,

$$c_p''-c_p'=159.4 \text{ cal./mole-deg.}$$
$$=\frac{159.4\times4.2\times10^7}{53.5\times981}\text{cm/deg.}$$

The transition temperature is $T_0=242.8°$K.

There are, unfortunately, no data giving in absolute measure the variation of v, (the specific volume) with T. Smits and McGillavry[3] express their results in terms of arbitrary dilatometer readings. The writer was therefore forced to modify the equation as follows:

$$\frac{dp}{dT}=\frac{c_p''-c_p'}{2Tv(\partial v''/v\partial T-\partial v'/v\partial T)},$$

and assuming $v''=v'=v$ (which is only approximately the case), this may be written as

$$dp/dT=(c_p''-c_p')/2Tv(\alpha''-\alpha'),$$

where α'' and α' are the coefficients of cubical expansion in the two phases. These were determined from the graph given by Adenstedt,[4] and it was found from linear extrapolation of the highest values given on either side of T_λ that

$$\alpha''\doteqdot19.0\times10^{-3}\text{/deg., and } \alpha'\doteqdot13.0\times10^{-3}\text{/deg.}$$

The density of NH_4Cl is given by Wulf and Cameron[5] as 1.527 g/cc.

Substituting in the formula, we now obtain

$$\frac{dp}{dT}=\frac{159.4\times4.2\times10^7\times1.527\times10^3}{2\times53.5\times981\times6\times242.8}=6.68\times10^4\text{ g/cm}^2\text{-deg.}$$
$$=66.8\text{ kg/cm}^2\text{-deg.}$$

Variation of the λ-point with pressure has been studied by Bridgman,[6] who found that under pressures of 3370

kg/cm² and 9390 kg/cm², T_λ was 0°C and +30°C. These points, together with T_λ at atmospheric pressure, enabled the equilibrium curve to be drawn. The slope at −30°C could thus be found, and was, in fact, 68.2 kg/cm²-deg., differing from the calculated value by 2 percent.

While the agreement is to a certain extent fortuitous, in view of the assumptions involved, the fact that the results will be of the same order can only mean further support for the thermodynamical interpretation of the λ-point phenomena.

[1] E. F. Lype, Phys. Rev. 69, 652 (1946).
[2] Simon, v. Simson, and Ruhemann, Zeits. f. physik. Chemie A129, 339 (1927).
[3] Smits and McGillavry, Zeits. f. physik. Chemie A166, 143 (1932).
[4] H. Adenstedt, Ann. d. Physik 26, 69 (1936).
[5] Wulf and Cameron, Zeits. f. physik. Chemie B10, 347 (1930).
[6] P. W. Bridgman, Phys. Rev. 38, 182 (1931).

Microwave Spectra: Methyl Iodide*

WALTER GORDY, A. G. SMITH, AND JAMES W. SIMMONS
Department of Physics, Duke University, Durham, North Carolina
May 22, 1947

THE $J=1$ to $J=2$ rotational transition of the symmetrical top molecule, CH_3I, has been examined in the region of 30,000 megacycles with the method previously described.[1] Figure 1 shows the relative positions and estimated intensities of the eleven lines which were observed. Since no isotopes exist in sufficient amounts to cause detectable lines, the hyperfine structure observed appears to be caused by the interaction of the quadrupole moment of the iodine nucleus with the molecular field. About ten percent of the molecules would be in an excited vibrational state at the temperature of observation, and it is possible that some of the lines on the low frequency side originate from these excited molecules. We will test this by repeating the observations at lower temperatures.

The exact value of the moment of inertia, I_B, depends upon a quantitative interpretation of the hyperfine structure. The I_B determined from the strongest line, which is near the center of gravity of the group, is 111×10^{-40} g cm². Assuming the bond angles and CH distances to be the same as those in methane, the C—I bond length is determined as 2.13A. This value is probably accurate to one percent. The deviation from the configuration assumed for the CH_3 is not likely to influence the C—I distance more than one percent, and the uncertainty caused by the hyperfine frequency spread is of this order. Widely conflicting values for the C—I bond length in this molecule have been obtained from infra-red vibrational spectra[2] (2.00A) and from electron diffraction (2.28A). The value obtained in the present work is close to the electron diffraction value[3] for the C—I distance in CI_4 (2.12A).

A more complete analysis of the spectra of this molecule is being made.

We wish to thank Dr. Walter M. Nielsen for his constant interest in this project.

* The research described in this report was supported by Contract No. W-28-099-ac-125 with the Army Air Forces, Watson Laboratories, Air Materiel Command.
[1] W. Gordy and M. Kessler, Phys. Rev. 71, 640 (1947).
[2] G. Herzberg, *Infrared and Raman Spectra of Polyatomic Molecules* (D. Van Nostrand Company, Inc., New York, 1945), p. 439.
[3] L. R. Maxwell, J. Opt. Soc. Am. 30, 374 (1940).

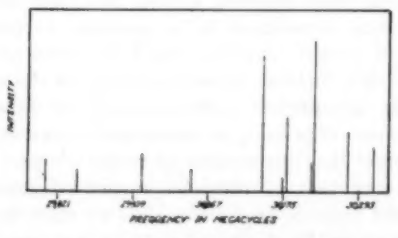

FIG. 1. Chart showing frequencies and estimated intensities of $J=1$ to $J=2$ transition in methyl iodide.

Protons from the Deuteron Bombardment of Separated Neon Isotopes

F. K. ELDER, JR.,* H. T. MOTZ, AND P. W. DAVISON
*Sloane Physics Laboratory, Yale University,***
New Haven, Connecticut
May 16, 1947

ENRICHED neon samples obtained by thermal diffusion have been bombarded with 3.2-Mev deuterons from the cyclotron. Samples of 99.5 percent Ne^{20}, of 0.5 percent Ne^{22}, and of 55 percent Ne^{20} with 45 percent Ne^{22}, have provided sufficient change in concentration of the heavy isotope to allow definite assignment of several proton groups to each of the two reactions $Ne^{20}(d, p)Ne^{21}$ and $Ne^{22}(d, p)Ne^{23}$.

The gas was bombarded within a bombardment chamber[1] at a pressure of approximately 15 cm of mercury. This pressure provided a sufficiently high yield of protons for fast counting, and sufficiently low absorption for the gas to be treated as a thin target (about 0.4 cm of air equivalent). The 3.7-Mev deuteron beam passed through an aluminum foil (1.86-cm air) into the gas bombardment chamber. Protons were counted at right angles to the incident beam by the use of double coincidence proportional counters.[2,3]

Composite curves of typical runs are shown in Fig. 1. The curve for the 99.5 percent Ne^{20} sample shows the proton groups from the $Ne^{20}(d, p)Ne^{21}$ reaction alone. Comparison with the curve for the sample enriched in the heavy isotope shows clearly the additional groups due to the $Ne^{22}(d, p)Ne^{23}$ reaction. Subtraction of curves of the two types (after correcting for the proportion of Ne^{20} present) allows a more accurate determination of the groups due to the heavy isotope. Table I lists the Q values

TABLE I. Reaction energies and energy levels of the neon isotopes.

Proton range (cm)	Q (Mev)	Energy level (Mev)
$Ne^{20}(d, p)Ne^{21}$		
20.7 ±0.6	0.90 ±0.11	3.58
28.1 ±0.5	1.65 ±0.10	2.83
40.3 ±0.5	2.73 ±0.09	1.75
59.4 ±0.7	4.17 ±0.09	0.31
63.6 ±0.8	4.48 ±0.10	0.00
$Ne^{22}(d, p)Ne^{23}$		
24.4 ±1.0	1.23 ±0.15	1.66
31.1 ±1.0	1.90 ±0.15	0.99
42.9 ±0.9	2.89 ±0.11	0.00

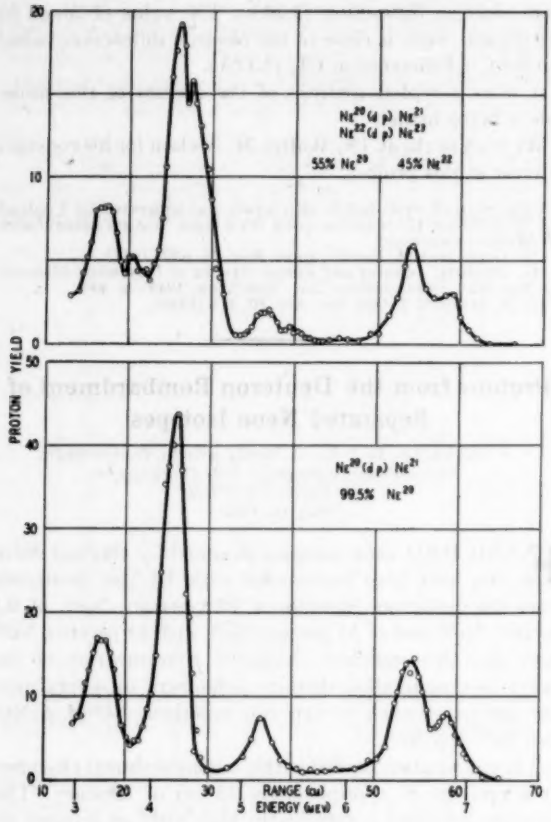

FIG. 1. Proton groups from deuteron bombardment of neon.

calculated from the extrapolated ranges and maximum beam energy, and also the corresponding energy levels.

The levels obtained for Ne^{21} are in essential agreement with previous work by Pollard and Watson[4] and Schultz and Watson.[5] The doubling of the ground state found by the latter is here confirmed. The levels for Ne^{23} are new values. The ground-state Q value agrees with the value suggested by Pollard and Watson,[4] although in their work the concentration of the heavy isotope was not sufficiently high for detailed measurement.

Mass values obtained from these reactions are summarized in Table II and compared with other values. The mass value (II) obtained for Ne^{21} exceeds the mass spectrograph value (III) by more than the estimated error. There is no mass spectrograph value for comparison with the value (V) for Ne^{23}. A cross check on the values obtained for Ne^{21} and Ne^{23} can be derived, however, from an independent calculation of the mass of Na^{23} from each of the two neon masses. The value (VI) in the table is obtained from the data given by Murrell and Smith[6] on the reaction $Na^{23}(d, \alpha)Ne^{21}$, using our value (II) for Ne^{21}. Using Pollard and Watson's[4] value for the maximum beta-ray energy from the disintegration of Ne^{23} into Na^{23}, the independent value (VII) is obtained. These two values are in excellent agreement with each other, and also with the value of Pollard and Brasefield[7] (VIII) as corrected by Pollard and Watson[4] (and recalculated using Mattauch's Ne^{20} value (I) instead of the earlier one of Jordan and Bainbridge[9]).

TABLE II. Mass determinations of the neon isotopes.

	Isotope	Mass	Source	Reference
I	Ne^{20}	19.99896±0.00007	Mass spectrograph	8
II	Ne^{21}	21.00074±0.00019	$Ne^{20}(d, p)Ne^{21}$ with (I)	
III	Ne^{21}	20.99983±0.00027	$Ne^{20}H^{+}-Ne^{21+}$ doublet with (I)	9
IV	Ne^{22}	21.99864±0.00036	Mass spectrograph	9, 10
V	Ne^{23}	23.00213±0.00048	$Ne^{22}(d, p)Ne^{23}$ with (IV)	
VI	Na^{23}	22.99714±0.00038	$Na^{23}(d, \alpha)Ne^{21}$ with (II)	6
VII	Na^{23}	22.99717±0.00009	$Ne^{23}\rightarrow Na^{23}+\beta$ with (V)	4
VIII	Na^{23}	22.99715±0.00020	$Ne^{20}(\alpha, p)Na^{23}$ with (I)	4, 7

A check on the consistency of these masses could be obtained by observing the $Ne^{21}(d, p)Ne^{22}$ end group. So far the enrichment of Ne^{21} has not been adequate to enable this to be done.

The authors are very grateful to Professor E. C. Pollard and Professor W. W. Watson, who have shared the guidance of this research, for their encouragement and aid.

* Part of a dissertation submitted by FKE in partial fulfillment of the requirements for the degree of Doctor of Philosophy at Yale University.

** Assisted by the Office of Naval Research under contract N6ori44.

[1] P. W. Davison and E. C. Pollard, Bull. Am. Phys. Soc. 22, 16 (1947).
[2] H. L. Schultz, Bull. Am. Phys. Soc. 21, 20 (1946).
[3] A. B. Martin, Phys. Rev. 71, 127 (1947).
[4] E. C. Pollard and W. W. Watson, Phys. Rev. 57, 567 (1940).
[5] H. L. Schultz and W. W. Watson, Phys. Rev. 58, 1047 (1940).
[6] E. B. M. Murrell and C. L. Smith, Proc. Roy. Soc. 173, 410 (1939).
[7] E. C. Pollard and C. J. Brasefield, Phys. Rev. 51, 8 (1937).
[8] F. Mattauch, Physik. Zeits. 39, 892 (1938).
[9] E. B. Jordan and K. T. Bainbridge, Phys. Rev. 51, 385 (1937).
[10] M. S. Livingston and H. A. Bethe, Rev. Mod. Phys. 9, 370 (1937).

Further Cosmic-Ray Experiments above the Atmosphere

S. E. GOLIAN AND E. H. KRAUSE
Naval Research Laboratory, Washington, D. C.
May 9, 1947

ANOTHER in the series of experiments to determine the nature and reaction of the primary cosmic radiation above the atmosphere was performed in a V-2 fired on March 7, 1947 from the White Sands Proving Ground, New Mexico, to an altitude of 102 miles. A counter-tube telescope was arranged so that the percentage of particles penetrating 2 cm, 6 cm, and 12 cm of lead could be determined. The number of threefold showers under these same thicknesses was also measured.

The telescope was mounted vertically in a specially designed warhead so that it looked directly through the warhead nose as shown in Fig. 1.

The heavy load shielding aroung the lower half of the telescope was introduced in an attempt to reduce the number of rocket showers found in previous experiments.[1,2] This shielding in conjunction with the absorbing lead plates was sufficient to eliminate most of the registered rocket showers of primary or non-primary electronic origin. It was found that the number of rocket showers actually doubled over that of previous unshielded experiments. This would indicate that these showers must be of non-electronic origin. By the use of eight anticounters 2, 4, and 5 used in groups of 2, 4, 6, and 8 (quantity, not counter

numbers) it was established that the policing efficiency was very good.

The information obtained included the following coincidences and anticoincidences: [1, 3, 6]; [1, 3, 6, −5]; [1, 3, 6, −2]; [1, 3, 6, −(2+4+5)]; [1, 3, 6, 7+8+9]; [1, 3, 6, 10+11+12]; [1, 3, 6, 13+14+15]; [1, 3, 6, 13 +14+15, −(2+4+5)]; [1, 3, 6, 7, 8, 9, −(2+4+5)]; [1, 3, 6, 10, 11, 12, −(2+4+5)]; [1, 3, 6, 13, 14, 15, −(2+4 +5)]. The negative sign in front of a symbol signifies anticoincidence. The data reported here were all obtained above the atmosphere (pressure less than 2 mm Hg). A total of 887 events were recorded of which 275 were events not involving rocket showers. Of the 275, it was found that above the atmosphere 25 percent were absorbed in 6 cm of lead. Although this is somewhat less than that reported by Perlow and Shipman[2] it is assumed to be the same type of non-primary electron component discussed by them. The different percentages in the two experiments are attributed to the variation of this component with zenith angle. A total of 59 percent of the particles penetrated 12 cm of lead. Of these, the most frequent single event penetrated without producing showers under the lead plates. About half the particles penetrating the 12 cm produced showers in one or more of the counter trays. The remaining 14 percent was absorbed in 12 cm. Here again the larger portion did not produce showers under the lead. Thus, primary electrons would be ruled out, since these would produce large showers under 2 and 4 cm. As a matter of fact, it is difficult to understand how any of this component could be due to primary particles, since the large energies associated with the primaries should produce some type of reaction below 12 cm of lead unless, of course, neutral particles are involved. Although it does not seem very probable, it is possible that this affect could be produced by neutral particles coming up from below due to nuclear explosions produced by the primaries in the lower part of the rocket.

If we assume that all of the radiation except that absorbed in 6 cm is primary, then we find that the electron component determined on the basis of shower production could not be more than a maximum of 14 percent of the primary; the non-electronic component absorbed in 12 cm is 18 percent of the primary, and the non-electronic component penetrating 12 cm is 68 percent of the primary.

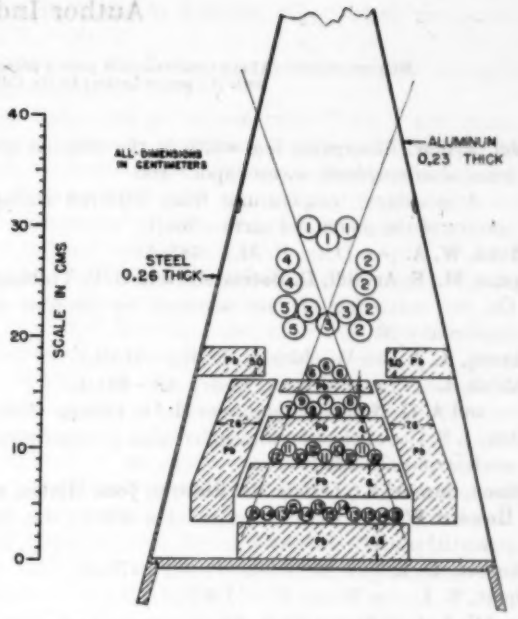

FIG. 1. Counter-tube telescope arrangement.

The ratio of the total radiation, determined by the events [1, 3, 6, −(2+4+5)], in free space to that at sea level was 11.5. The ratio of the hard component, determined by the events [1, 3, 6, 13+14+15, −(2+4+5)], in free space to that at sea level was 9.0.

We wish to acknowledge the very helpful discussions and suggestions of J. A. Wheeler, N. Arley, and their associates at Princeton.

[1] S. E. Golian, E. H. Krause, and G. J. Perlow, Phys. Rev. 70, 776 (1946).
[2] G. J. Perlow and J. D. Shipman, Jr., Phys. Rev. 71, 325 (1947).

Author Index to Volume 71

References with (A) are to abstracts of papers presented at meetings of the American Physical Society. References with (L) are to Letters to the Editor, and those with (T) designate title only.

Adel, Arthur. Absorption line width in the rotation spectrum of atmospheric water vapor—806

—— Atmospheric temperatures from infra-red emission spectra of the moon and earth—564(L)

Affens, W. A. (see Doty, P. M.)—485(A)

Ageno, M., E. Amaldi, D. Bocciarelli, and G. C. Trabacchi. On the scattering of fast neutrons by protons and deuterons—20

Ahearn, A. J. (see Wooldridge, D. E.)—913(L)

Aldrich, L. T. (see Fairbank, Henry A.)—911(L)

—— **and A. O. Nier.** Abundance of He^3 in helium—143(A)

Allen, J. S. Use of electron multiplier tubes in experimental nuclear physics—462(T)

Allison, Samuel K., Leticia Del Rosario, Joan Hinton, and Howard Wilcox. Reconstruction of a 400-kv d.c. high potential source—139(A)

Allmand, D. E. (see Metzelaar, P. N.)—475(A)

Alpert, N. L. (see Bitter, F.)—738(L)

Amaldi, E. (see Ageno, M.)—20

—— **and B. N. Cacciapuoti.** On the dependence of nuclear radius on the mass number—739(L)

Anderson, E. E. (see Sutton, R. B.)—272(L)

Anderson, H. L. and A. Novick. Magnetic moment of the triton—372(L)

Anderson, O. E. and H. E. White. Hyperfine structure and the nuclear spin of U^{235}—911(L)

Andrews, C. L. Diffraction pattern of a circular aperture at short distances—777

Andrews, R. D. (see Mochulsky, M.)—487(A)

Apker, L., E. Taft, and J. Dickey. Total-energy distributions of photoelectrons from poly-crystalline tungsten—473(A)

Arley, Niels. Remarks on Dr. Bhabha's note "On the expansibility of solutions in powers of the interaction constants"—272(L)

Armistead, Fontaine C. (see Ney, Edward P.)—14, 138(A)

Arnold, George P. (see Sturm, William J.)—556(L)

Arnold, Wayne R. and Arthur Roberts. Magnetic moments of the neutron and the deuteron—878

Arrøe, O. H. (see Bøggild, J. K.)—281

Ashkin, J. and R. E. Marshak. Neutron-proton and proton-proton scattering at 200 Mev—467(A)

Aten, A. H. W., Jr. High energy ions in crystal lattices—641(L)

Baez, A. V. (see Kirkpatrick, Paul)—470(A), 521

Bailey, Carl L. (see Nuckolls, Richard G.)—140(A)

Baker, E. B. (see Boyer, R. F.)—488(A)

Baldwin, G. C. (see Klaiber, G. S.)—649

—— (see Luebke, E. A.)—657

—— **and G. S. Klaiber.** Analysis of high energy x-ray spectra—554(L)

—— **and G. S. Klaiber.** Photo-fission in heavy elements—3

Bale, W. F. Biological effects of nuclear radiation—744(T)

Balseiro, A. José. Angular momentum of photons—79

Band, William (see Meyer, Lothar)—828(L)

Baños, Alfredo, Jr. and M. L. Perusquía. Cosmic ray directional counter for the determination of the azimuthal variation of primary cosmic radiation at fixed zenith angles—276(A)

Barbre, N. H. and M. Goldhaber. Resonance scattering of neutrons by Mn—141(A)

Bardeen, John. Surface states and rectification at a metal semi-conductor contact—717

—— (see Townes, C. H.)—644(L), 829(L)

Bargmann, V. On nearly glancing reflection of shocks—473(A)

Barker, Edgar C. Total disintegration energy of Na^{24}—453(L)

Barnes, S. W. The 130 cyclotron at Rochester—744(T)

Barnett, S. J. and D. S. Webber. Note on a discrepancy in gyromagnetic measurements and the question of a possible variation of the torsional modulus of German silver with frequency—143(A)

—— **and D. S. Webber.** Note on a variation with frequency of the torsional modulus of German silver wire—895

Barr, E. Scott. Voltaic effects in waterglass—832(A)

Barton, Vola P. and George A. Lindsay. The K x-ray absorption edge of silicon—406; Erratum—736(L)

Beams, J. W. and James L. Young, III. Centrifugal fields—131(L)

—— **and James L. Young, III.** Production of constant high rotational speeds—835(A)

Beck, Paul A., Joseph C. Kremer, and L. Demer. Grain growth in high purity aluminum—555(L)

Becker, Robert A., A. O. Hanson, and B. C. Diven. Thresholds for the photo-disintegration of Li^7, Mg^{24}, Al^{27}, Si^{28}, S^{32}, and Ca^{40}—466(A)

Bell, P. R. (see Jordan, W. H.)—482(A)

Bender, R. S., F. C. Shoemaker, and J. L. Powell. Width of 985 kev Al (p, γ) resonance—905(L)

Benedikt, Elliot T. and Herta R. Leng. On the existence of single magnetic poles—454(L), 480(A)

Bennett, G. S. Gyroscopic effects in a vibratory system—481(A)

Bennett, W. E. and H. T. Richards. Neutrons from $C^{13}+D$—565

——, **T. W. Bonner, H. T. Richards, and B. E. Watt.** Disintegration of Li^7 by deuterons—11

Bennett, William E. (see Nuckolls, Richard G.)—140(A)

Benson, B. B. (see Pollard, E. C.)—134(A)

Benzer, S. Ge—Ge contacts—141(A)

Berenda, Carlton W. Notes on the Wheeler-Feynman theory—550(L)

Bergman, Stefan. On an operator method in the theory of two-dimensional flows of a compressible fluid—474(A)

Bergmann, Peter G. Scattering from statistically distributed scatterers—469(A)

Bergstrahl, Thor (see Nuckolls, Richard G.)—140(A)

Beringer, R. Experiments in gaseous absorption at microwave frequencies—133(T)
Bernstein, S., W. M. Preston, G. Wolfe, and R. E. Slattery. High energy gamma-rays from U(235) fission—463(A)
——, **W. M. Preston, G. Wolfe, and R. E. Slattery.** Yields of photo-neutrons from U^{235} fission products in heavy water—140(A), 573
Best, N., R. Havens, and H. LaGow. Pressure and temperature of the atmosphere to 120 km—915(L)
Bethe, H. A. (see Von der Lage, Fred C.)—612
Bhagavantam, S. and D. Suryanarayan. Elastic constants of sodium chlorate—553(L)
Billmeyer, Fred W. Measurements of the refractive index of films—489(A)
Biondi, Manfred A. and Sanborn C. Brown. High frequency probe measurements of electron attachment and ambipolar diffusion—481(A)
Birch, A. J. (see MacDonald, D. K. C.)—563(L); Erratum—829(L)
Birch, Francis. Finite elastic strain of cubic crystals—809
Birkhoff, Garrett and Thomas E. Caywood. Fluid flow patterns—470(A)
Bitter, F., N. L. Alpert, H. L. Poss, C. G. Lehr, and S. T. Lin. Nuclear magnetic resonances at low temperature—738(L)
Blackburn, Wayne E. Temperature coefficient of electrical resistivity for crystalline selenium containing various percentages of bromine—277(A)
Blatt, John M. On the Heitler theory of radiation damping—468(A)
Bleakney, Walker (see Mariner, Thomas)—139(A)
Bloch, F., A. C. Graves, M. Packard, and R. W. Spence. Relative moments of H_1 and H_3—551(L)
——, **A. C. Graves, M. Packard, and R. W. Spence.** Spin and magnetic moment of tritium—373(L)
Bloembergen, N., R. V. Pound, and E. M. Purcell. Width of the nuclear magnetic resonance absorption line in gases, liquids, and solids—466(A)
Bocciarelli, D. (see Ageno, M.)—20
Bøggild, J. K., O. H. Arrøe, and T. Sigurgeirsson. Cloud-chamber studies of electronic and nuclear stopping of fission fragments in different gases—281
Bohm, D. and C. Richman. On the neutron-proton scattering cross section—567
Bonner, N. A., G. Freidlander, L. P. Pepkowitz, and M. L. Perlman. Search for the transmutation products of gamma-meson reactions induced by 100-Mev x-rays—511
Bonner, T. W. (see Bennett, W. E.)—11
Boothby, O. L. and R. M. Bozorth. New material of high permeability—472(A)
Bottom, Virgil E. Effect of x-rays on the elastic constants of quartz—476(A)
Boyd, G. E. (see Motta, E. E.)—210(L)
Boyer, R. F., E. B. Baker, and P. C. Woodland. Some dielectric properties of butadiene-containing polymers and copolymers—488(A)
Bozorth, R. M. (see Boothby, O. L.)—472(A)
Bradner, Hugh. Photoelectric emission from a rough surface—269(L)
Bradt, H. L. and P. Scherrer. Ninety-three kev-γ-line of UX_1—141(A)
Brattain, R. R. Recent progress in applied absorption spectroscopy—274(T)
Bray, Ralph and K. Lark-Horovitz. Photo- and thermo-effects in *p*-type germanium rectifiers—141(A)
Breit, G. Relativistic corrections to magnetic moments of nuclear particles—400
—— Scattering of slow neutrons by bound protons I. Methods of calculation—215
—— **and B. T. Darling.** Calculation of angular distributions in resonance reactions—141(A)
—— **and B. T. Darling.** Note on the calculation of angular distributions in resonance reactions—402
—— **and P. R. Zilsel.** Scattering of slow neutrons by bound protons. II. Harmonic binding—neutrons of zero energy—232
Brentano, J. C. M. and L. van Clief Spencer. Determination of the lattice spacing of silver bromide for varying x-ray exposures—142(A)
Bridge, Herbert and Bruno Rossi. Cosmic-ray bursts in an unshielded chamber and under one inch of lead at different altitudes—379(L)
Brillouin, L. Wave guides for slow waves—483(A)
Brinkley, Stuart R., Jr. and John G. Kirkwood. Theory of the propagation of shock waves—606
Brobeck, W. M., E. O. Lawrence, K. R. MacKenzie, E. M. McMillan, R. Serber, D. C. Sewell, K. M. Simpson, and R. L. Thornton. Initial performance of the 184-inch cyclotron of the University of California—449
Brody, S. B. (see Nierenberg, W. A.)—466(A)
Brosi, A. R. (see Motta, E. E.)—210(L)
Broström, K. J., T. Huus, and R. Tangen. Gamma-ray yield curve of aluminum bombarded with protons—661
Brown, F. C. Transmission of energy from radiation on silicon crystals—472(A)
Brown, Leon J. (see Mitchell, Allan C. G.)—140(A)
—— (see Ogle, Wm.)—378(L)
Brown, S. C. Microwave studies of electrical discharges in gases—133(T)
—— (see Biondi, Manfred A.)—481(A)
—— (see Kerr, Donald E.)—480(A)
Browne, S. H. and T. Dantzig. On the theory of slowing down neutrons in substances with periodic absorption lines—463(A)
Buchanan, J. O. (see Watson, W. W.)—887
Buckingham, R. A. (see Massey, H. S. W.)—558(L); Erratum—829(L)
Buechner, W. W., E. A. Burrill, A. Sperduto, R. J. Van de Graaff, and H. Feshbach. Further experiments on the elastic single scattering of electrons by nuclei—142(A)
——, **R. J. Van de Graaff, E. A. Burrill, and A. Sperduto.** Investigation of thick targets x-ray production in the range from 1250 to 2350 kv—470(A)
Burrill, E. A. (see Buechner, W. W.)—142(A), 470(A)
Burton, J. A. (see Wooldridge, D. E.)—913(L)

Cacciapuoti, B. N. (see Amaldi, E.)—739(L)
Callen, H. B. (see von Hippel, A.)—488(A)
Cameron, A. E. (see White, J. R.)—907(L)

Cary, Howard and K. P. George. Sensitive high speed radiation thermocouple—276(A)
Caywood, Thomas E. (see Birkhoff, Garrett)—470(A)
Chako, N. Motion of charged particles in inhomogeneous anisotropic media—469(A)
—— Piezoelectric vibrations of Rochelle salt plates—485(A)
Chamberlain, O., J. W. Gofman, E. Segrè, and A. C. Wahl. Range measurements of alpha-particles from 94^{239} and 94^{238}—529
Chao, S. C. (see Wu, C. K.)—118
Chastel, R. (see Tsien, San-Tsiang)—382(L)
Cheka, J. S. Preliminary evaluation of "special fine grain particle film" for use in neutron monitoring—836(A)
Christian, S. M. Integrating $\sin^2 x/x$—836(A)
Christy, Robert F. Design of a small nuclear reactor—274(T)
—— (see Mills, M. M.)—275(A)
—— **and S. Rubin.** Angular distribution of α-particles from Li^7+p—275(A)
Clarke, E. T. Nuclear excitation functions. II. Al^{27} $(d; p, \alpha)$ Na^{24}—187
Clauser, Francis. Notes on the thermodynamic propulsion of wind tunnels—465(A)
Cobine, J. D. (see Gallagher, C. J.)—481(A)
Coggeshall, Norman D. Fringing flux corrections for magnetic focusing devices—482(A)
Cole, R. H. and J. S. Coles. Propagation of spherical shock waves in water—128(L)
Coles, D. K. (see Dakin, T. W.)—640(L)
—— (see Good, W. E.)—383(L)
Coles, J. S. (see Cole, R. H.)—128(L)
Collins, G. B. Plans of the Brookhaven National Laboratory—744(T)
Conklin, Richard (see Ogle, Wm.)—378(L)
Conversi, M., E. Pancini, and O. Piccioni. On the disintegration of negative mesons—209(L); Erratum—557(L)
Cook, C. S. (see Langer, L. M.)—906(L)
Cork, J. M. Escape probability of protons and neutrons from bombarded bismuth—144(A)
—— (see Tatel, H. E.)—159
Cork, James M. and Franklin B. Shull. Internally converted gamma-radiation from tantalum (182)—467(A)
Corson, E. M. Invariant form of quantum equations and the Schroedinger-Heisenberg parallelism—200
—— **and I. Kaplan.** Oscillator concept in the theory of solids—130(L)
Corvalen, M. I. Concentration of plutonium in pitchblende—132(L)
Crane, H. R. (see Levinstein, H.)—476(A)
Crawford, G. W. and F. T. Rogers, Jr. Two non-linear springs—833(A)
Creutz, Edward C. (see Wilson, Robert R.)—339
Critchfield, Charles L. Electron waves in the magnetic dipole fields of a neutron—258
——. Interaction between meson and nucleon—908(L)
Cross, Paul C. (see King, Gilbert W.)—433

Dakin, T. W., W. E. Good, and D. K. Coles. Bond distances in OCS from microwave absorption lines—640(L)
Daly, J. F. (see Langer, R. M.)—464(A)
Daniel, J. H. (see Hanson, E. E.)—487(A)
Dantzig, T. (see Browne, S. H.)—463(A)
Darling, B. T. (see Breit, G.)—141(A), 402
Dauphinee, T. McC. (see Smith, H. D.)—487(A)
Davison, B. Remark on the variational method—694
—— **and W. H. Watson.** On the distribution of electric charge in nuclei—742(L)
Davison, P. W. (see Elder, F. K., Jr.)—917(L)
De Benedetti, S. and E. H. Kerner. Gamma-rays of Po^{210}—122(L)
—— **and F. K. McGowan.** Metastable state of half-life about 10^{-6} second in Re^{187}—380(L)
Debye, P. Relation between intrinsic viscosity and molecular weight in polymer solutions—486(A)
Del Rosario, Leticia (see Allison, Samuel K.)—139(A)
Demer, L. (see Beck, Paul A.)—555(L)
Demers, Pierre. Pairs of fission fragments—483(A)
Dempster, A. J. Abnormal isotope abundances produced by neutron absorption in cadmium—144(A)
——, Isotopic changes in cadium by neutron absorption—829(L)
—— (see Lapp, R. E.)—745
Dennison, David M. (see Shull, Franklin B.)—681
de Oyarzábal, J. (see Vallarta, M. S.)—393
D'Eustachio, D. Some new results on the recrystallization of quartz—476(A)
Deutsch, M. (see Osborne, R. K.)—467(A)
—— (see Siegbahn, Kai)—483(A)
Dibeler, Vernon H., C. Edward Wise, Jr., and Fred L. Mohler. Metastable ion transitions in the mass spectra of the monochloropropenes—381(L)
Dicke, R. H. Čerenkov radiation counter—737(L)
Dickey, J. (see Apker, L.)—473(A)
Diven, B. C. (see Becker, Robert A.)—466(A)
Doermann, A. H. (see Underwood, N.)—834(A)
Doty, P. M., W. A. Affens, and B. H. Zimm. Determination of macromolecular configurations in dilute solution by light scattering—485(A)
Dresden, M. Hydrodynamical equations in quantum mechanics—143(A)
Dubs, Charles and F. T. Rogers, Jr. Alternative basic theories for the carbon-pile type of voltage-regulator—834(A)
Duckworth, Henry E. and Benjamin G. Hogg. Relative abundance of the copper isotopes and the suitability of the photometric method for detecting small variations in isotopic abundance—212(L)
Duffin, R. J. Lower bounds for eigenvalues—827(L)
Dunlap, W. Crawford, Jr. Hall effect and magneto-resistance in germanium—471(A)
Dunning, J. R. (see Rainwater, L. J.)—65
Durand, E., J. J. Oberly, and R. Tousey. Solar absorption lines between 2950 and 2200 Angstroms—827(L)

Eastmond, E. J. Spectrophotometric study of reflectance color changes in foods—274(A)
Eckart, Carl. Viscous and thermal absorption of sound as relaxation phenomena—277(A)
Edwards, R. R. (see Glendenin, L. E.)—742(L)

Eggler, C. (see Hughes, D. J.)—269(L)
Ehrenhaft, Felix. Electrophotophoresis and electric charges smaller than the electronic charge—143(A)
—— General movement of matter possessing six degrees of freedom in fields is helical—480(A)
—— Single magnetic poles and cosmic radiation—138(A)
Einstein, H. A. On the hydraulic analogy between surface waves on a liquid and pressure waves in a compressible fluid—473(A)
Eisenstein, A. Study of the barium silicate interface of oxide coated cathodes—473(A)
Eisner, Melvin and Nathan Rosen. Neutron-proton scattering—835(A)
—— **and Joseph W. Straley.** Conductivity of sodium-ammonia solutions—832(A)
Elder, F. K., Jr. (see Watson, W. W.)—887
——, **H. T. Motz and P. W. Davison.** Protons from the deuteron bombardment of separated neon isotopes—917(L)
Elder, F. R. (see Pollock, H. C.)—462(T)
——, **A. M. Gurewitsch, R. V. Langmuir, and H. C. Pollock.** Radiation from electrons in a synchrotron—829(L)
Eliezer, C. Jayaratnam. The hydrogen atom in a generalized classical electrodynamics—49
Engelkemeir, Don (see Seren, Leo)—409
English, W. N. Corona from fine positive points—638(L)
Ergen, William Krasny. Bridge type electrical computers—138(A)
Estermann, I., A. Foner, and J. A. Randall. Resistivity of germanium at low temperatures and the effect of additions—484(A)
——, **S. N. Foner, and O. Stern.** Mean free paths of cesium atoms in helium, nitrogen, and cesium vapor—250
——, **O. C. Simpson, and O. Stern.** Free fall of atoms and the measurement of the velocity distribution in a molecular beam of cesium atoms—238
Eyestone, S. F. (see Gilvarry, John J.)—482(A)

Fairbank, Henry (see Lane, C. T.)—477(A)
——, **William Fairbank, and C. T. Lane.** Temperature dependence of "second sound" velocity—477(A)
——, **C. T. Lane, L. T. Aldrich, and Alfred O. Nier.** Concentration of He^3 in the liquid and vapor phases of He^4—911(L)
Fairbank, William (see Fairbank, Henry)—477(A)
—— (see Lane, C. T.)—477(A), 600
Fano, U. Fluctuations of ionization yield—480(A)
Farwell, G., E. Segrè, and C. Wiegand. Long range alpha-particles emitted in connection with fission. Preliminary report—327
Feenberg, Eugene. Nuclear energy surface—468(A)
Feld, Bernard T., R. Scalettar, and L. Szilard. Use of threshold detectors for fast neutron studies—464(A)
Fermi, E. and L. Marshall. Interference phenomena of slow neutrons—666
—— **and L. Marshall.** Phase of scattering of thermal neutrons by aluminum and strontium—915(L)
——, **W. J. Sturm, and R. G. Sachs.** Transmission of slow neutrons through microcrystalline materials—589
——, **E. Teller, and V. Weisskopf.** Decay of negative mesotrons in matter—314
Feshbach, H. (see Buechner, W. W.)—142(A)
——, **D. C. Peaslee, and V. F. Weisskopf.** On the scattering and absorption of particles by atomic nuclei—145; Erratum—564(L)
Fields, R., B. Russell, D. Sachs, and A. Wattenberg. Total cross sections measured with photo-neutrons—508
Finkelstein, R. Normal reflection of shock waves—42
Fitzgerald, J. W. (see Weissler, Alfred)—488(A)
Foldy, Leslie L. On the meson theory of nuclear forces—276(A)
Foley, H. M. Note on the nuclear electric quadrupole spectrum of a homonuclear diatomic molecule in a magnetic field—747
Foner, A. (see Estermann, I.)—484(A)
Foner, S. N. (see Estermann, I.)—250
Forrester, A. Theodore (see Gerjuoy, Edward)—276(A), 375(L)
Forstat, H. (see Jesse, W. P.)—478(A)
Fowler, W. A. (see Lauritsen, C. C.)—279(A)
—— (see Lauritsen, T.)—275(A)
—— (see Rubin, Sylvan)—212(L)
Frei, H. and M. Schiffer. Separation by diffusion in fields of ultrasonic waves—555(L)
Freidlander, G. (see Bonner, N. A.)—511
Fretter, William B. Meson showers under lead at sea-level—462(A)
Friedland, S. S. Mass spectroscopic analysis of the polyatomic gases in a fast counter—377(L)
Friedlander, H. N. (see Seren, Leo)—409, 454, 463(A)
Frisch, David H. Distribution in energy of fission fragments near the fast fission threshold—478(A)
Frosch, C. J. (see Teal, G. K.)—462(T)
Froslie, H. M. (see Winans, J. G.)—137(A)
Furry, W. H. Remark on the correspondence treatment of radiation—468(A)
—— Two notes on phase-integral methods—360

Gallagher, C. J. and J. D. Cobine. Retrograde motion of an arc cathode spot in a magnetic field—481(A)
Gamow, G. Erratum: Expanding universe and the origin of elements—273(L)
—— Probability of nuclear meson-absorption—550(L)
George, K. P. (see Cary, Howard)—276(A)
Gerjuoy, Edward and A. Theodore Forrester. Possible use of thermal noise for low temperature thermometry—276(A), 375(L)
Getting, I. A. Proposed detector for high energy electrons and mesons—123(L)
Gideon, Donald (see Fu-Chun Yu)—382(L)
—— **and J. D. Kurbatov.** Correction of G.M. counter data for high counting rates. III—140(A)
Giese, John H. Compressible flows with degenerate hodographs—474(A)
Gigli, Alberto (see Giulotto, Luigi)—211(L)
Gill, Piara Singh. Azimuthal variations of cosmic radiation at Lahore—398, 462(A)

—— Production of mesotrons up to 30,000 feet at a magnetic latitude of 22° north—82
Gilvarry, John J. and S. F. Eyestone. Static method of simulating accelerations above one g—482(A)
Giulotto, Luigi. Fine structure of H_α—562(L)
—— **and Alberto Gigli.** Electrical conductivity of Na-ammonia solutions at low temperatures—211(L)
Glendenin, L. E. and R. R. Edwards. Note on the long-lived radio iodine—742(L)
Gofman, J. W. (see Chamberlain, O.)—529
—— (see Seaborg, G. T.)—378(L)
Goldberger, M. L. and Frederick Seitz. Theory of the refraction and the diffraction of neutrons by crystals—294
Goldhaber, M. (see Barbre, N. H.)—141(A)
——, **C. O. Muehlhause, and S. H. Turkel.** *L*-converted isomeric transitions—372(L), 467(A)
Golian, S. E. and E. H. Krause. Further cosmic-ray experiments above the atmosphere—918(L)
Good, W. E. (see Dakin, T. W.)—640(L)
—— **and D. K. Coles.** Microwave absorption frequencies of $N^{14}H_3$ and $N^{15}H_3$—383(L)
Goodman, B., A. W. Lawson, and L. I. Schiff. Thermal ionization of impurity levels in semi-conductors—191
Goodman, Leon J. and M. L. Pool. Radioactive isotopes of Re, Os, and Ir—288
Gordy, Walter. Microwave spectra—831(T)
—— **and Myer Kessler.** Microwave spectra: the hyperfine structure of ammonia—640(L)
——, **A. G. Smith, and James W. Simmons.** Microwave spectra: methyl iodide—917(L)
Gottschalk, Winston M. Line strengths in the FeI spectrum in intermediate coupling, with application to the solar curve of growth—133(A)
Goudsmit, S. A. Why Germany had no atomic bomb—137(T)
—— **and H. S. Snyder.** Statistics of single and plural scattering—478(A)
Graves, A. C. (see Bloch, F. A.)—373(L), 551(L)
—— **and R. L. Walker.** A method for measuring half-lives—1
Gregg, E. C. Alternating current probe for the measurement of magnetic fields—482(A)
Gross, B. On creep and relaxation—144(A)
Gross, Eugene, Shuichi Kusaka, and George Snow. Production of cosmic ray stars—463(A)
Gunn, Ross. Electrical charge on precipitation at various altitudes and its relation to thunderstorms—139(A), 181
Gurewitsch, A. M. (see Elder, F. R.)—829(L)
Guth, Eugene (see Holroyd, L. V.)—488(A)
—— (see Thompson, W. B.)—486(A)

Hagstrum, H. D. Molecular ionization and dissociation induced by electron impact—137(T)
—— On the dissociation energy of CO—376(L)
Hainer, R. M. (see King, Gilbert W.)—135(A), 433
Hall, E. O. λ-point of NH_4Cl and thermodynamic equilibria of the second order—916(L)
Hall, Leonard. Origin of excess ultrasonic absorption in water—318(L)
Halpern, Otto. Proposed experiment on the ponderomotive forces exerted by microwaves on dielectric media—277(A)
Halsey, George. Six rules for analyzing stress-strain curves—487(A)
Hamermesh, B. (see Korff, S. A.)—842
Hamermesh, Morton and Julian Schwinger. Neutron scattering in ortho- and parahydrogen—678
Hamilton, Donald R. Electron-neutrino angular correlation in beta-decay—456(L)
Hamilton, J. G. Behavior of fission products and of very heavy elements in biological phenomena—462(T)
Hannum, L. A. (see Jesse, W. P.)—478(A)
Hansen, J. M. and H. W. Webb. Specular reflection from mercury vapor—483(A)
Hanson, A. O. (see Becker, Robert A.)—466(A)
Hanson, E. E. and J. H. Daniel. Instrument for measuring particle diameters and constructing histograms from electron micrographs—487(A)
Harish-Chandra. On the relativistic wave equations—793
Harris, W. T. Proposed focusing cosmic-ray telescope—135(A), 310
Hart, A. L. (see Jesse, W. P.)—478(A)
Hartman, Lawton M. Thermal analog of the high frequency electron distribution—469(A)
——, **and Henry Margenau.** Harmonic components in a.c. discharges—481(A)
Harvey, E. Newton (see McMillen, J. Howard)—475(A)
Harworth, Keith (see Pockman, Leonard T.)—330, 470(A)
Havens, R. (see Best, N.)—915 (L)
Havens, W. W., Jr. (see Rainwater, L. J.)—65
—— (see Wu, C. S.)—174
——, **C. S. Wu, L. J. Rainwater, and C. L. Meaker.** Slow neutron velocity spectrometer studies II. Au, In, Ta, W, Pt, Zr—165
Hayden, Richard J. (see Inghram, Mark G.)—130(L), 144(A), 270(L), 561(L), 643(L), 743(L)
Haynes, S. K. Evaporation of gallium—832(A)
Henderson, W. J. Upper energy limit of the K^{40} beta-ray spectrum—323(L)
Herschberger, W. D. Absorption of microwaves by gases—133(T)
—— **and John Turkevich.** Absorption of methyl alcohol and methylamine for 1.25-cm waves—554(L)
Hess, David C., Jr. (see Inghram, Mark G.)—270(L), 561(L), 643(L), 743(L)
Hicks, Bruce L. On the characterization of fields of diabatic flow—476(A)
Hildebrand, J. H. Entropy of liquids and solutions—462(T)
Hill, E. L. Note on rotational motion in relativity theory—318(L)
—— Relativistic clock paradox—143(A)
Hillger, R. E. (see Strandberg, M. W. P.)—326(L), 639(L)
Hilton, W. F. Variation of aerodynamic lift in the transonic speed range—465(A)
Hinton, Joan (see Allison, Samuel K.)—139(A)
von Hippel, A., H. B. Callen, and W. B. Westphal. Frequency response characteristics of dielectric materials and their interpretation—488(A)

Hipple, J. A. Peak contour and half-life of metastable ions appearing in mass spectra—139(A), 594
Ho, Zah-Wei (see Tsien, San Tsiang)—382(L)
Hogg, Benjamin G. (see Duckworth, Henry E.)—212(L)
Holden, A. N. (see Townes, C. H.)—64(L), 479(A), 644(L), 829(L)
Holroyd, L. V., B. A. Mrowca, and Eugene Guth. Dielectric properties of rubber—particularly of loaded stock—488(A)
Holt, R. B. and O. Oldenberg. Spectroscopic study of the role of hydrogen peroxide in the thermal combination of hydrogen and oxygen—479(A)
Howland, J. J., D. H. Templeton, and I. Perlman. Artificial radioactive isotopes of polonium, bismuth, and lead—552(L)
Huddleston, C. M. (see Hughes, D. J.)—269(L)
Hughes, D. J., C. Eggler, and C. M. Huddleston. Half-life of Be^{10}—269(L)
Hughes, Donald J. Mass of the mesotron as determined by cosmic-ray measurements—387
Hughes, Richard H. and E. Bright Wilson, Jr. Microwave spectrograph—562(L)
Hulubei, Horia. Search for element 87—740(L)
Huntington, H. B. Pulsed ultrasonic measurements on some single crystals—472(A)
Huus, T. (see Broström, K. J.)—661
Hylleraas, Egil A. Electron affinity of positronium—491
—— **and Aadne Ore.** Binding energy of the positronium molecule—493
—— **and Aadne Ore.** Stability of polyelectrons—468(A)

Inghram, Mark G. and R. J. Hayden. Artificial activities produced in europium and holmium by slow neutron bombardment—130(L)
—— **and R. J. Hayden.** Some neutron induced activities in the rare earths—144(A)
——, **Richard J. Hayden, and David C. Hess, Jr.** Activities induced by pile neutron bombardment of samarium—643(L)
——, **Richard J. Hayden, and David C. Hess, Jr.** Neutron induced activities in lutecium, ytterbium, and dysprosium—270(L)
——, **David C. Hess, Jr., and Richard J. Hayden.** Neutron cross section for mercury isotopes—561(L)
——, **David C. Hess, Jr., Richard J. Hayden, and George W. Parker.** Fifty-five-hour element 61 formed in fission—743(L)
Ivey, D. G. (see Smith, H. D.)—487(A)

Jacobs, Harold and Armand P. LaRocque. Minimum sparking potentials of barium, magnesium, and aluminum in argon—138(A)
James, Hubert M. Decay of phosphorescence in Cu-activated ZnS—137(A)
Jehle, Herbert. Irreversible processes in stellar dynamics—469(A)
Jelatis, Demetrius G. High performance photo-galvanometer feedback amplifier—483(A)
Jesse, W. P., L. A. Hannum, H. Forstat, and A. L. Hart. Ionization chamber techniques in measurement of C^{14}—478(A)
Johnson, G. W. Ionization currents in cylindrical electrode systems—278(A)
Johnson, M. H. (see Rado, G. T.)—472(A)
——, **G. T. Rado, and M. Maloof.** Ferromagnetism at very high frequencies. I—Magnetic iron at 200 Mc—322(L)
——, **G. T. Rado, and M. Maloof.** Method to measure complex permeabilities of metals at UHF—472(A)
Johnson, V. A. and K. Lark-Horovitz. Low temperature resistivity of germanium semi-conductors—483(A)
—— **and K. Lark-Horovitz.** Transition from classical to quantum statistics in germanium semi-conductors at low temperatures—374(L); Erratum—909(L)
Jones, W. M. (see Stout, J. W.)—582
Jordan, Walter. New developments in instruments for counting and detecting nuclear particles—831(T)
Jordan, W. H. and P. R. Bell. Linear amplifier for general laboratory use—482(A)
Jurney, Ed. T. (see Mitchell, Allan C. G.)—324(L), 825(L)

Kane, Brother Gabriel. Magnetic ions and magnetic currents—458(L)
Kantrowitz, Arthur. Formation and stability of normal shock waves in channel flows—465(A)
Kaplan, I. (see Corson, E. M.)—130(L)
Kaplan, Joseph. Atmospheric bands of oxygen—274(A)
Kaplan, Nathan (see Yagoda, Herman)—910(L)
von Karman, Theodore (see Von Neumann, John)—462(T)
Kastler, A. and A. Rousset. Origin of low frequency Raman lines in organic crystals—455(L)
Katcoff, Seymour. Preliminary determination of the neutron absorption cross section of long-lived I^{129}—826(L)
Kê, T'ing-Sui. Boltzmann's superposition principle and the viscous behavior of grain boundaries in metals—142(A)
—— Experimental evidence of the viscous behavior of grain boundaries in metals—533
Kern, Walter P. (see Kerr, Donald E.)—480(A)
Kerner, E. H. (see De Benedetti, S.)—122(L)
Kerr, Donald E., Sanborn C. Brown, and Walter P. Kern. Microwave studies of dielectric properties of arcs—480(A)
Kerst, D. W. Design of the large Illinois betatron—137(T)
Kessler, Myer (see Gordy, Walter)—640(L)
King, Allen L. Arterial pulse wave velocities—482(A)
King, Gilbert W. and R. M. Hainer. Interpretation of the microwave absorption of HDO at 1.3 centimeters—135(A)
——, **R. M. Hainer, and Paul C. Cross.** Expected microwave absorption coefficients of water and related molecules—433
King, Ronold W. P. Physical interpretation of electromagnetic radiation from an antenna—134(A)
Kirkpatrick, Paul (see Pockman, Leonard T.)—330, 470(A)
—— **and A. V. Baez.** Absolute energy of $K\alpha$-radiation from thick silver targets—470(A), 521

Kirkwood, John G. (see Brinkley, Stuart R., Jr.)—606
Kittel, Charles. Interpretation of anomalous Larmor frequencies in ferromagnetic resonance experiment—270(L)
Klaiber, G. S. (see Baldwin, G. C.)—3, 554(L)
—— (see Luebke, E. A.)—657
——, **E. A. Luebke, and G. C. Baldwin.** Range-momentum measurements of particles emitted in nuclear disintegrations induced by 100-Mev x-rays—649
Kofoed-Hansen, O. Maximum β-energies and the mass of the neutrino—451
Kohn, W. Note on Weinstein's variational method—902
—— Two applications of the variational method to quantum mechanics—635
Kopal, Zdeněk. Some remarks on the limitations of linearized theory of supersonic flow around cones—474(A)
Korff, S. A. and B. Hamermesh. Production of nucleons by the cosmic radiation—842
Krause, E. H. (see Golian, S. E.)—918(L)
Kremer, Joseph C. (see Beck, Paul A.)—555(L)
Kruger, P. G. (see Laughlin, J. S.)—484(A), 736(L)
Kundu, D. N. and M. L. Pool, d-H^3 reaction in Cb and Ag—140(A)
—— **and M. L. Pool.** Results of H^3 bombardments of Ag and Rh—467(A)
Kuo, Y. H. On the initial motion of a strong spherical shock—476(A)
Kurbatov, J. D. (see Gideon, Donald N.)—140(A)
—— (see Kurbatov, M. H.)—466(A)
—— (see Yu, Fu-Chun)—382(L)
Kurbatov, M. H. and J. D. Kurbatov. Determination of stable species $_{39}Y^{89}$, $_{40}Zr^{90}$, and $_{56}Ba^{134}$ produced by nuclear transmutations—466(A)
Kusaka, Shuichi (see Gross, Eugene)—463(A)
Kyhl, R. (see Strandberg, M. W. P.)—326(L), 639(L)

Ladenburg, Rudolf. Interferometry of faster-than-sound phenomena—464(A)
LaGow, H. (see Best, N.)—915(L)
Lamer, V. K. and David Sinclair. Higher-order Tyndall spectra in monodisperse colloids—462(T)
Lane, C. T. (see Fairbank, Henry)—477(A); 911(L)
——, **Henry A. Fairbank, and William M. Fairbank.** Second sound in liquid helium II—600
——, **William Fairbank, and Henry Fairbank.** Pressure and temperature waves in liquid helium—477(A)
Lang, R. J. Note on the spectrum of Th III—907(L)
Langer, Lawrence M. (see Mitchell, Allan C. G.)—140(A)
——, **C. S. Cook, and M. B. Sampson.** On the alleged gamma-ray of N^{13}—906(L)
Langer, R. M. and J. F. Daly. Scattering of thermal neutrons in polycrystalline materials—464(A)
Langmuir, Irving, V. J. Schaefer, and Bernard Vonnegut. Production of ice crystals in artificial and in natural clouds—462(T)
Langmuir, R. V. (see Pollock, H. C.)—462(T)
—— see Elder, F. R.—829(L)
Lapp, R. E., J. R. Van Horn, and A. J. Dempster—Neutron absorbing isotopes in gadolinium and samarium—745
Lark-Horovitz, K. (see Bray, Ralph)—141(A)
—— (see Johnson, V. A.)—374(L), 483(A), 909(L)
LaRocque, Armand, P. (see Jacobs, Harold)—138(A)
Laslett, L. Jackson. Nomogram to facilitate the determination of the resolving time of counter equipment—144(A)
Laughlin, J. S. and P. G. Kruger. Neutron spectra of Li, Al, and Be bombarded with 10-Mev deuterons—484(A)
—— **and P. Gerald Kruger.** Scattering of neutrons of energy between 12 Mev and 13 Mev by protons—736(L)
Lauritsen, C. C. (see Lauritsen, T.)—275(A)
—— (see Rubin, Sylvan)—212(L)
——, **T. Lauritsen, and W. A. Fowler.** Gamma-radiation from Be^9+H^1—279(A)
Lauritsen, T. (see Lauritsen, C. C.)—279(A)
——, **W. A. Fowler, and C. C. Lauritsen.** Device for introducing short-lived radioactive samples into a cloud chamber—275(A)
Lavatelli, L. S. (see Sutton, R. B.)—272(L)
Lawrence, E. O. (see Brobeck, W. M.)—449
Lawson, A. W. (see Goodman, B.)—191
Lehr, C. G. (see Bitter, F.)—738(L)
Leng, Herta R. (see Benedikt, Elliot T.)—454(L), 480(A)
Levinger, J. and E. Meiners. Radioactivity of Be^{10}—586
Levinstein, H. and H. R. Crane. Structure of evaporated antimony films—476(A)
Liepmann, H. W. On the interaction between boundary layer and shock waves—465(A)
Lin, C. C. Some recent investigations in hydrodynamic stability—471(A)
Lin, S. T. (see Bitter, F.)—738(L)
Linder, E. G. Nuclear electrostatic generator—129(L)
Lindsay, George A. (see Barton, Vola P.)—406, 736(L)
Livens, G. H. Note on magnetic energy—58
Loeb, Leonard B. Mechanism of negative point corona at atmospheric pressure in relation to the first Townsend coefficient—712
Lofgren, Edward J. (see Wilson, Robert R.)—560(L)
Longini, R. L. Note concerning the motion of arc cathode spots in magnetic fields—642(L)
Ludeke, Carl A. Experimental investigation of forced vibrations in a mechanical system having a non-linear restoring force—481(A)
Luebke, E. A. (see Klaiber, G. S.)—649
——, **G. S. Klaiber, and G. C. Baldwin.** Cloud-chamber study of multiple scattering of protons in air—657

Ma, S. T. Equivalence of the Riesz method and the λ-limiting process for the classical electromagnetic field of a point source—787
—— Further remarks on the redundant zeros in Heisenberg's theory of characteristic matrix—210(L)
—— On a general condition of Heisenberg for the S matrix—195
MacDonald, D. K. C., K. Mendelssohn, and A. J. Birch. Conductivity of sodium-ammonia solutions—563(L), Erratum—829(L)
MacKenzie, K. R. (see Brobeck, W. M.)—449
Malmlöw, Goethe and Frederick Seitz. On the theory of dielectric breakdown in the alkali halides—125(L)

Maloof, M. (see Johnson, M. H.)—322(L), 472(A)
—— (see Rado, G. T.)—472(A)
Mann, A. K. (see Ney, E. P.)—835(A)
Marcus, Jules A. deHaas-van Alphen effect in a single crystal of zinc—559(L)
—— Temperature dependence of the diamagnetic susceptibility of gamma-brasses—471(A)
Margenau, Henry (see Hartman, Lawton M.)—481(A)
Mariner, Thomas and Walker Bleakney. Ionization and dissociation of formic acid monomer by electron impact —139(A)
Mark, H. (see Singer, S.)—487(A)
Markham, Jordan J. Infra-red vibrations in NaCl—473(A)
Marshak, R. E. Note on the spherical harmonic method as applied to the Milne problem for a sphere—443
—— Variational method for asymptotic neutron densities —688
—— (see Ashkin, J.)—467(A)
Marshall, L. (see Fermi, E.)—666, 915(L)
Martin, A. B. Energy levels in the nucleus Mn^{56}—127(L), 466(A)
Martin, Emmett. Diffraction of visible radiation by cellulose acetate yarn—488(A)
Marvin, H. H. Mutual magnetic interactions of electrons —102
Masriera, Miguel. On the number of elements—458(L)
Massey, H. S. W. and R. A. Buckingham. Collision of neutrons with deuterons and the reality of exchange forces—558(L), Erratum, 829(L)
May, Albert and Jean C. Woodhull. Drag coefficient of steel spheres entering water—475(A)
Mayer, J. G. Theories of helium II—462(T)
McDaniel, B. D. (see Sutton, R. B.)—272(L)
McGowan, F. K. (see De Benedetti, S.)—380(L)
McMillan, E. M. (see Brobeck, W. M.)—449
McMillan, J. Howard and E. Newton Harvey. Drag and cavity of fast spheres shot into water—475(A)
Meaker, C. L. (see Havens, W. W. Jr.)—165
Meiners, E. (see Levinger, J.)—586
Mendelssohn, K. (see MacDonald, D. K. C.)—563(L), Erratum—829(L)
Merritt, F. R. (see Townes, C. H.)—64(L), 479(A), 644(L), 829(L)
Metzelaar, P. N. and D. E. Allmand. Impact pressure produced by flat plate striking water surface—475(A)
Meyer, H. A., G. Schwachheim, and M. D. de Souza Santos. Decay of K^{40}—908(L)
Meyer, Lothar and William Band. On a connection between the fountain effect, second sound, and thermal conductivity in liquid helium II—828(L)
Meyerhof, Walter E. Contact potential difference in silicon crystal rectifiers—727
Meyerott, Roland. Metastable state $\alpha^1\pi g$ of N_2 as a factor in active nitrogen—133(A)
—— Validity of the Franck-Condon principle in collisions of the second kind—553(L)
—— (see Setlow, R. B.)—133(A)
Miller, V. V. (see Skobeltzyn, D. V.)—315
Millikan, Robert A. Interpretation of the east-west effect —275(A)
Mills, M. M. (see Seifert, H. S.)—279(A)
—— **and R. F. Christy.** Auger showers—275(A)
Mitchell, Allan C. G., Ed. T. Jurney, and Margaret Ramsey. Coincidence experiments on Ga^{72}—324(L)
——, **Lawrence M. Langer, and Leon J. Brown.** Radiations from radioactive lanthanum (140)—140(A)
——, **Ed. T. Jurney, and Margaret Ramsey.** Radiations from As^{72}—825(L)
Mochulsky, M., R. D. Andrews, and A. V. Tobolsky. Relaxation of stress in plastic materials—487(A)
Mohler, Fred L. (see Dibeler, Vernon H.)—381(L)
Mohr, E. I. Positive corona in freon air mixture at n.t.p. —278(A)
Montgomery, C. G. Microwave circuits—133(T)
Morgan, Karl. Educational program in atomic energy for the southeast—831(T)
Morgan, Karl Z. Tolerance concentrations of radio-active substances—835(A)
Morris, Peter A. (see Swann, W. F. G.)—462(A)
Morrison, H. L. and F. T. Rogers, Jr. Preliminary experiment on convection currents in a porous medium—834(A)
—— Statistical significance of some measurements on the permeabilities of unconsolidated sands—837(A)
Moseley, H. M. and Nathan Rosen. Neutron-proton interaction—835(A)
Motta, E. E., G. E. Boyd, and A. R. Brosi. Production and isotopic assignment of a 90-day activity in element 43—210(L)
Motz, H. T. (see Elder, F. K., Jr.)—917(L)
Mrowca, B. A. (see Holroyd, L. V.)—488(A)
—— (see Thompson, W. B.)—486(A)
Muehlhause, C. O. (see Goldhaber, M.)—372(L), 467(A)
Myers, Vernon. Quantum corrections for the second virial coefficient of water—478(A)

Nafe, J. E., E. B. Nelson, and I. I. Rabi. Hyperfine structure of atomic hydrogen and deuterium—914(L)
Nelson, E. B. (see Nafe, J. E.)—914(L)
Newman, Brownie and Nathan Rosen. Problem of homogeneous incompressible fluid sphere in general relativity —833(A)
Ney, Edward P. and Fontaine C. Armistead. Measurement of the self-diffusion coefficient of uranium hexafluoride —138(A), 14
—— **and Fontaine C. Armistead.** Self-diffusion coefficient of uranium hexafluoride—14
—— **and A. K. Mann.** Mass measurement with a single field mass spectrometer—835(A)
Nielsen, Alvin H. Automatically recording grating spectrograph for the infra-red—831(A)
——, **and Y. T. Yao.** Erratum: Analysis of the vibration-rotation band ω_3 for $C^{12}O^{16}_2$ and $C^{13}O^{16}_2$—825(L)
Nielsen, Harald H. (see Noble, Robert H.)—484(A)
—— (see Yates, Kenneth P.)—349
Nier, A. O. (see Aldrich, L. T.)—143(A)
—— (see Fairbank, Henry A.)—911(L)
Nierenberg, W. A., N. F. Ramsey, and S. B. Brody. Measurements of nuclear quadrupole interactions—466(A)

Noble, Robert H. and Harald H. Nielsen. Infra-red absorption spectrum of H_2S—484(A)
Novick, A. (see Anderson, H. L.)—372(L)
Nuckolls, Richard G., Carl L. Bailey, William E. Bennett, Thor Bergstrahl, Hugh T. Richards, and John H. Williams. Total scattering cross sections of deuterium and oxygen for fast neutrons—140(A)

Oberly, J. J. (see Durand, E.)—827(L)
O'Bryan, H. M. Perot-Fabry interferometers as filters—134(A)
Ogg, A., Jr. (see Sienko, M. J.)—319(L)
Ogle, Wm., Leon Brown, and Richard Conklin. Evidence for a γ–p reaction in Be^9—378(L)
Oldenberg, O. (see Holt, R. B.)—479(A)
Oppenheimer, J. R. Creation and destruction of mesons—462(T)
Ore, Aadne. Structure of the quadrielectron—913(L)
—— (see Hylleraas, Egil A.)—468(A), 493
Osborne, R. K. and M. Deutsch. Disintegration scheme of the 21-minute isomer of Mn^{52}—467(A)

Packard, M. (see Bloch, F. A.)—373(L), 551(L)
Pancini, E. (see Conversi, M.)—209(L), 557(L)
Parker, George W. (see Inghram, Mark G.)—743(L)
Pearson, G. L. and W. Shockley. Measurements of Hall effect and resistivity of germanium and silicon from 10° to 600°K—142(A)
Peaslee, D. C. (see Feshbach, H.)—145, 564(L)
Peck, R. A., Jr. Photographic neutron detection—464(A)
Pekeris, C. L. Note on the scattering of radiation in an inhomogeneous medium—268(L); Erratum—457(L)
Pellam, J. R. and C. F. Squire. Ultrasonic absorption and velocity measurements in liquid helium—477(A)
Pepkowitz, L. P. (see Bonner, N. A.)—511
Perlman, I. (see Howland, J. J.)—552(L)
Perlman, M. L. (see Bonner, N. A.)—511
Perlow, G. J. and J. D. Shipman, Jr. Non-primary cosmic-ray electrons above the earth's atmosphere—325(L)
Perusquía, M. L. (see Baños, Alfredo, Jr.)—276(A)
—— (see Vallarta, M. S.)—393
Piccioni, O. (see Conversi, M.)—209(L), 557(L)
Pierce, J. A. Ionization by meteoric bombardment—88
—— True height of an ionospheric layer—698
Pockman, L. T., D. L. Webster, P. Kirkpatrick, and K. Harworth. Probability of K-ionization of nickel by electrons—330, 470(A)
Pollard, E. C. and B. B. Benson. Large angle scattering of gamma-radiation—134(A)
Pollard, Ernest. Yields of protons in transmutations—467(A)
Pollard, W. G. Report on the Oak Ridge Institute of Nuclear Studies—831(T)
Pollock, H. C., R. V. Langmuir, and F. R. Elder. Operation of a 70-Mev synchroton—462(T)
Pool, M. L. (see Goodman, Leon J.)—288
—— (see Elder, F. R.)—829(L)
—— (see Kundu, D. N.)—140(A), 467(A)
—— (see Schwarz, W. M.)—122(L)
Poss, H. L. (see Bitter, F.)—738(L)
Pound, R. V. (see Bloembergen, N.)—466(A)
Powell, J. L. (see Bender, R. S.)—905(L)
Present, R. D. On the division of nuclear charge in fission—831(T)
Preston, Melvin A. Theory of alpha-radioactivity—865
Preston, W. M. (see Bernstein, S.)—140(A), 463(A), 573
Prizibram, K. Remarks on C. Frondel's letter: "Elastic deficiency and color of natural smoky quartz"—319(L)
Purbrick, R. L. An experimental relation between ω_e and reduced mass for diatomic molecules—137(A)
Purcell, E. M. (see Bloembergen, N.)—466(A)

Rabi, I. I. (see Nafe, J. E.)—914(L)
Rado, G. T. (see Johnson, M. H.)—322(L), 472(A)
——, **M. H. Johnson, and M. Maloof.** Complex permeability of magnetic iron at 200 Mc as a function of polarizing field—472(A)
Rainwater, L. J. (see Havens, W. W., Jr.)—165
—— (see Wu, C. S.)—174
——, **W. W. Havens, Jr., C. S. Wu, and J. R. Dunning.** Slow neutron velocity spectrometer studies I. Cd, Ag, Sb, Ir, Mn—65
Rall, Waldo and Roger G. Wilkinson. Gamma- and beta-ray energies of some radioactive isotopes as measured by a thin magnetic lens beta-ray spectrometer—321(L)
Ramsay, B. P. and F. L. Yost. Magnetic facilities provided by the Kensington Magnetic Laboratory—834(A)
Ramsey, Margaret (see Mitchell, Allan C. G.)—324(L), 825(L)
Ramsey, N. F. (see Nierenberg, W. A.)—466(A)
Randall, J. A. (see Estermann, I.)—484(A)
Raub, H. L. (see Sack, H. S.)—486(A)
Reinhardt, Paul W. Portable instrument for the detection of fast neutrons in the presence of gamma radiation—836(A)
Rense, Wm. A. Diffuse reflection from dielectrics—832(A)
Resnick, Irving (see Weissler, Alfred)—488(A)
Richards, H. T. (see Bennett, W. E.)—11, 565
—— (see Nuckolls, Richard G.)—140(A)
—— **and Lyda Speck.** Range distribution of U^{235} fission fragments in photographic emulsion—141(A)
Richardson, J. Reginald (see Wilson, Robert R.)—560(L)
Richman, C. (see Bohm, D.)—567
Rigterink, M. D. (see Teal, G. K.)—462(T)
Rivlin, R. S. Torsion of a rubber cylinder—487(A)
Roberts, Arthur (see Arnold, Wayne R.)—878
Roberts, Shepard. Dielectric and piezoelectric properties of barium titanate—890
Rogers, F. T., Jr. Effect of scattering on experimental determinations of XR for high-energy particles—833(A)
—— On the reduction of data which are values of a definite integral—837(A)
—— Rational design of the computor for a certain class of mechanical system containing feedback-control—836(A)
—— (see Crawford, G. W.)—833(A)
—— (see Dubs, Charles)—834(A)
—— (see Morrison, H. L.)—834(A); —837(A)
—— **and Marguerite M. Rogers.** Differential equation for the over-all behavior of a servo-operated recording potentiometer—836(A)

Rogers, Marguerite M. Redetermination of the nuclear magnetic moment of sodium by the polarization of resonance radiation—833(A)
—— (see Rogers, F. T., Jr.)—836(A)
Rojansky, V. Auger showers and the comets—552(L)
Romberg, Werner. Calculation of the coordinate matrix elements for helium—706
Rosen, Nathan. Notes on rotation of rigid bodies in relativity theory—54
—— Quantum mechanics of vibrating string—833(A)
—— (see Eisner, Melvin)—835(A)
—— (see Moseley, H. M.)—835(A)
—— (see Newman, Brownie)—833(A)
Rossi, Bruno (see Bridge, Herbert)—379(L)
Rousset, A. (see Kastler, A.)—455(L)
Rubin, S. (see Christy, R. F.)—275(A)
Rubin, Sylvan. Angular distribution of long-range alpha-particles from excited Ne^{20}—275(A)
——, **W. A. Fowler, and C. C. Lauritsen.** Angular distribution of the $Li^7(p,\alpha)\alpha$ reaction—212(L)
Russell, B. (see Fields, R.)—508
Russell, B. R. (see Wahlin, H. B.)—139(A)

Sachs, D. (see Fields, R.)—508
Sachs, R. G. On the magnetic moment of the triton—457(L)
—— (see Fermi, E.)—589
Sack, H. S. and H. L. Raub. Elastic losses of natural and synthetic rubber as a function of frequency and temperature—486(A)
Sampson, M. B. (see Langer, L. M.)—906(L)
Scalettar, R. (see Feld, Bernard T.)—464(A)
Schaefer, V. J. (see Langmuir, Irving)—462(T)
Scherrer, P. (see Bradt, H. L.)—141(A)
Schiff, L. I. (see Goodman, B.)—191
Schiffer, M. (see Frei, H.)—555(L)
Schmidt, J. M. Atomization of liquids—278(A)
Schockley, W. (see Pearson, G. L.)—142(A)
Schubauer, G. B. (see Skramstad, H. K.)—475(A)
Schultz, H. L. The determination of small time intervals between related nuclear events—134(A)
Schwachheim, G. (see Meyer, H. A.)—908(L)
Schwarz, W. M. and M. L. Pool. Gamma-rays from tungsten and molybdenum—122(L)
Schwinger, Julian (see Hamermesh, Morton)—678
Seaborg, G. T., J. W. Gofman, and R. W. Stoughton. Nuclear properties of U^{233}: A new fissionable isotope of uranium—378(L)
Seaton, S. L. Temperature of the upper atmosphere—557(L)
Segrè, E. Possibility of altering the decay rate of a radioactive substance—274(A)
—— (see Chamberlain, O.)—529
—— (see Farwell, G.)—327
Seifert, H. S. and M. M. Mills. Problems in the application of nuclear energy to rocket propulsion—279(A)
Seitz, Fredrick. Some aspects of the theory of neutron diffraction by crystals—831(T)
—— (see Goldberger, M. L.)—294
—— (see Malmlöw, Goethe)—125(L)
—— Training school program at Clinton Laboratories—831(T)
Serber, R. (see Brobeck, W. M.)—449
Seren, Leo, Don Engelkemeir, William Sturm, H. N. Friedlander, and S. Turkel. Forty-three day $_{48}Cd^{115}$—409
——, **Herbert N. Friedlander, and Solomon Turkel.** Reaction $_{38}Sr^{86}(n,\gamma)_{38}Sr^{87}$ produced by thermal neutrons—454(L)
——, **Herbert N. Friedlander, and Solomon H. Turkel.** Thermal neutron activation cross sections—463(A)
Setlow, R. B., Roland Meyerott, and W. W. Watson. Ultraviolet bands of nitrogen—133(A)
Sewell, D. C. (see Brobeck, W. M.)—449
Shankland, Robert S. (see Wilson, Robert R.)—560(L)
Shaw, A. E. Intense positive ion source for solids—277(A)
Shearin, Paul E. Mechanism for ductile failure in a notched steel bar—832(A)
Sherwin, Chalmers W. Delays in firing time of Geiger-Müller counters—479(A)
Shipman, J. D., Jr. (see Perlow, G. J.)—325(L)
Shoemaker, F. C. (see Bender R. S.)—905(L)
Shull, Franklin B. (see Cork, James M.)—467(A)
—— **and David M. Dennison.** Double focusing beta-ray spectrometer—681
Siegbahn, Kai and Martin Deutsch. Decay scheme of Cs^{134}—483(A)
Siegert, A. J. F. Note on the recurrence time problem for the two-dimensional Markoffian random function—469(A)
—— On the first passage time problem for the stationary Markoffian random function—485(A)
Sienko, M. J. and R. A. Ogg, Jr. Magnetic quenching of superconductivity—319(L)
Sigurgeirsson, T. (see Bøggild, J. K.)—281
—— **and A. Yamakawa.** Decay of mesons stopped in light materials—319(L)
Simmons, James W. (see Gordy, Walter)—917(L)
Simpson, K. M. (see Brobeck, W. M.)—449
Simpson, O. C. (see Estermann, I.)—238
Sinclair, David (see Lamer, V. K.)—462(T)
Singer, S. and H. Mark. Studies of cellulose acetate with the ultracentrifuge—487(A)
Singer, Willard E. Infra-red absorption in formaldehyde beyond 10μ—531
Skobeltzyn, D. V., G. T. Zatsepin, and V. V. Miller. Lateral extension of Auger showers—315
Skramstad, H. K. and G. B. Schubauer. Laminar boundary-layer oscillations and stability of laminar flow—475(A)
Slattery, R. E. (see Bernstein, S.)—140(A), 463(A), 573
Smith, A. E. Determination of particle size by the low angle scattering of x-rays—277(A)
Smith, A. G. (see Gordy, Walter)—917(L)
Smith, Charles G. Free ring discharge in a metallic torus—135(A)
Smith, H. D., T. McC. Dauphinee, and D. G. Ivey. Heat conductivity of natural and synthetic rubbers under stretch and at low temperatures—487(A)
Smith, J. H. Theoretical range-energy values for protons in air and aluminum—32

Smith, W. V. Determination of nuclear spin from the Stark effect of microwave rotational spectra—126(L)
Snow, George (see Gross, Eugene)—463(A)
Snyder, H. S. Quantized space-time—38
——. Theory of multiple scattering—478(A)
—— (see Goudsmit, S. A.)—478(A)
de Souza Santos, M. C. (see Meyer, H. A.)—908(L)
Speck, Lyda (see Richards, H. T.)—141(A)
Spence, R. W. (see Bloch, F.)—373(L), 551(L)
Spencer, L. van Clief (see Brentano, J. C. M.)—142(A)
Spencer, Roy C. Optical theory of the corner reflector—134(A)
Sperduto, A. (see Buechner, W. W.)—142(A), 470(A)
Squire, C. F. (see Pellam, J. R.)—477(A)
Stabler, H. P. Reversible binary counter and shaft position indicator—135(A)
Stephenson, S. T. X-ray absorption structure of $GeCl_4$ and $AsCl_3$—84
Stern, O. (see Estermann, I.)—238, 250
Stevenson, D. P. Recent progress in applied mass spectrometry—274(T)
Stewart, D. W. Separation of stable tracer isotopes—744(T)
Stoughton, R. W. (see Seaborg, G. T.)—378(L)
Stout, J. W. Magnetic quenching of superconductivity—741(L)
—— **and W. M. Jones.** Calorimetric determination of the energy produced by plutonium(239)—582
Straley, Joseph W. (see Eisner, Melvin)—832(A)
Strandberg, M. W. P., R. Kyhl, T. Wentink, Jr., and R. E. Hillger. Inversion spectrum of ammonia—326(L), 639(L)
Stuhlman, Otto, Jr. Limits of visibility and the maximum brightness of continuous spectra at various color temperatures—834(A)
Sturm, William J. Measurement of neutron cross sections with a crystal spectrometer—757
—— (see Fermi, E.)—589
—— (see Seren, Leo)—409
——, **and George P. Arnold.** Total neutron cross section of dysprosium and neodymium—556(L)
Summerfield, Martin. Escape from the earth by multiple-step rockets—279(A)
Suryan, B. Bounded linear harmonic oscillator and phase transitions of second order—741(L)
Suryanarayan, D. (see Bhagavantum, S.)—553(L)
Sutton, R. B., B. D. McDaniel, E. E. Anderson, and L. S. Lavatelli. Capture cross section of boron for neutrons of energies from 0.01 ev to 1000 ev—272(L)
Swann, W. F. G. Possible effect of the sun upon cosmic radiation—485(A)
—— **and Peter A. Morris.** Variation with altitude and latitude of the vertical component of the cosmic radiation passing through 15 cm of lead—462(A)
Szilard, L. (see Feld, Bernard T.)—464(A)

Taft, E. (see Apker, L.)—473(A)
Tangen, R. (see Broström, K. J.)—661
Tatel, H. E. and J. M. Cork. Formation of radium E and polonium by deuteron bombardment of bismuth—159
Taub, A. H. Refraction of shocks in ideal gases—465(A)
Teal, Gordon K. Photoelectron emission from liquid ammonia solutions of the alkali metals—138(A)
——, **M. D. Rigterink and C. J. Frosch.** Attenuator materials, attenuators, and terminators for microwaves—462(T)
Teller, E. (see Fermi, E.)—314
Temple, G. F. J. (see Von Neumann, John)—462(T)
Templeton, D. H. (see Howland, J. J.)—552(L)
Thomas, R. N. Comments on the motion of a solid body at high velocity through a compressible medium—474(A)
Thompson, W. B., B. A. Mrowca, and Eugene Guth. Velocity and attenuation of sound in rubber—486(A)
Thorndike, A. M. (see Wilson, E. Bright, Jr.)—479(A)
Thornton, R. L. (see Brobeck, W. M.)—449
Ticho, Harold K. New determination of the mean life of mesotrons at an altitude of 11,500 feet—463(A)
Tisza, L. On the theory of "second sound" in helium II—477(A)
Tobolsky, A. V. (see Mochulsky, M.)—487(A)
Tousey, R. (see Durand, E.)—827(L)
Townes, C. H. Electrostatic field strengths in molecules and nuclear quadrupole moments—909(L)
——. Molecular line spectra in the microwave region—133(T)
——, **A. N. Holden, J. Bardeen, and F. R. Merritt.** Quadrupole moments and spins of Br, Cl, and N nuclei—644(L), Erratum: 829(L)
——, **A. N. Holden, and F. R. Merritt.** Rotational spectra of some linear molecules near 1-cm wave-length—64(L)
——, **A. N. Holden, and F. R. Merritt.** Rotational spectra of some linear molecules near 1-cm wave-length and nuclear quadrupole moments of Br and Cl—479(A)
Trabacchi, G. C. (see Ageno, M.)—20
Tsien, San-Tsiang, Ho Zah-Wei, R. Chastel, and L. Vigneron. On the new fission process of uranium nuclei—382(L)
Tukey, J. W. Linearization of solutions in supersonic flow—471(T)
Turkel, S. H. (see Goldhaber, M.)—372(L), 467(A)
—— (see Seren, Leo)—409, 454(L), 463(A)
Turkevich, John (see Hershberger, W. D.)—554(L)
Turner, Alfrey, Jr. Time-dependent strain birefringence in visco-elastic materials—486(A)

Underwood, N. and A. H. Doermann. Photoelectric nephelometer—834(A)

Valatin, J. G. On molecular coupling effects—458(L)
Vallarta, M. S., M. L. Perusquía, and J. de Oyarzábal. Determination of the sign and the energy spectrum of primary cosmic radiation—393
Van de Graaff, R. J. (see Buechner, W. W.)—142(A), 470(A)
Van Horn, J. R. (see Lapp, R. E.)—745
Van Vleck, J. H. Absorption of microwaves by uncondensed water vapor—425
—— Absorption of microwaves by oxygen—413
—— Formula for the coupling of nuclear quadrupole moments in symmetrical polyatomic molecules—468(A)

Van Voorhis, S. N. Nuclear physics and machines—744(T)
Varela, Arthur A. Effect of direct-current potential on initiation of radiofrequency discharge—124(L)
Varsonyi, A. New derivation of the method of characteristics for axially symmetrical supersonic flow—278(A)
Verde, M. and G. C. Wick. Some stationary distributions of neutrons in an infinite medium— 852
Vigneron, L. (see Tsien, San-Tsiang)—382(L)
Von der Lage, Fred C. and H. A. Bethe. Method for obtaining electronic eigenfunctions and eigenvalues in solids with an application to sodium—612
Vonnegut, Bernard (see Langmuir, Irving)—462(T)
Von Neumann, John, G. F. J. Temple, and Theodore von Karman. Recent developments in compressible flow—462(T)
Vought, R. H. Molecular dissociation by electron bombardment: a study of $SiCl_4$—93

Wack, Paul E. Electrical resistivity of conducting rubber —489(A)
Wahl, A. C. (see Chamberlain, O.)—529
Wahlin, H. B. and B. R. Russell. Biological effects of low frequency vibrations—139(A)
Walker, R. L. (see Graves, A. C.)—1
Wallace, P. R. Band theory of graphite—476(A), 622
Waltner, Arthur. Measurement of the ionization potential of gases in photoelectric cells—834(A)
Wang, K. C. Proposed methods of detecting the neutrino —645(L)
Wantuch, Ernest. Velocity of propagation of the discharges in Geiger-Müller counters—646(L)
Wataghin, Gleb. Showers of penetrating particles at altitude of 26,000 feet—453(L)
Watson, W. H. (see Davison, B.)—742(L)
Watson, W. W. (see Setlow, R. B.)—133(A)
——, **J. O. Buchanan, and F. K. Elder, Jr.** Thermal diffusion with boron trifluoride—887
Watt, B. E. (see Bennett, W. E.)—11
Wattenberg, A. Photo-neutron sources and the energy of the photoneutrons—497
—— (see Fields, R.)—508
Watts, Richard J. and Dudley Williams. Nuclear quadrupole moment effects in the microwave spectrum of ammonia—639(L)
Wayland, Harold. Scale factors in water entry—470(A)
Webb, H. W. (see Hansen, J. M.)—483(A)
Webb, J. H. Photographic plates for use in nuclear physics —744(T)
Webber, D. S. (see Barnett, S. J.)—143(A), 895
Webber, Robert T. Magnetic transition curves in superconducting tantalum—471(A)
Webster, David L. (see Pockman, Leonard T.)—330, 470(A)
Weisskopf, V. (see Fermi, E.)—314
—— (see Feshbach, H.)—145, 564(L)
Weissler, Alfred, J. W. Fitzgerald, and Irving Resnick. Sound velocity method for determination of molecular weight of liquid polymers—488(A)
Weissler, G. L. Negative corona in freon-air mixtures at n.t.p.—278(A)
Wentink, T., Jr. (see Strandberg, M. W. P.)—326(L), 639(L)
Westendorf, W. F. Biased betatron in operation—271(L)
Westphal, W. B. (see von Hippel, A.)—488(A)
Wheeler, John A. Mechanism of absorption of negative mesons—462(A)
—— Mechanism of capture of slow mesons—320(L)
Whiffen, D. H. Absorption of microwaves by liquids—133(T)
Whipple, Fred L. Supersonic problems in astronomy—474(A)
White, H. E. (see Anderson, O. E.)—911(L)
White, J. R. and A. E. Cameron. Critical ionization potentials of uranium hexafluoride and hydrogen fluoride—907(L)
Wick, G. C. (see Verde, M.)—852
Wideröe, Rolf. On bringing the beam out of a betatron—376(L)
Wiegand, C. (see Farwell, G.)—327
Wightman, A. S. Pais' *f*-field theory and the mirror nuclei —447
Wilcox, Howard (see Allison, Samuel K.)—139(A)
Wilkinson, Roger G. (see Rall, Waldo)—321(L)
Williams, Dudley (see Watts, Richard J.)—639(L)
Williams, Ferd E. Mechanism of luminescence of infra-red-sensitive phosphors—831(A)
Williams, John H. Collision of neutrons with deuterons and the reality of exchange forces—908(L)
—— (see Nuckolls, Richard G.)—140(A)
Williams, H. J. Direction of domain magnetization in powder patterns—646(L)
Williams, W. E. Interferometry—274(T)
Wilson, E. Bright, Jr. (see Hughes, Richard H.)—562(L)
—— **and A. M. Thorndike.** Absolute intensities of molecular vibrational absorption bands—479(A)
Wilson, Robert R. Delayed neutrons from Pu^{239}—560(L)
—— Proton-proton scattering at 10 Mev—384(L)
—— Range, straggling, and multiple scattering of fast protons—385(L)
—— **and Edward C. Creutz.** Proton-proton scattering at 8 Mev—339
——, **Edward J. Lofgren, J. Reginald Richardson, Byron T. Wright, and Robert S. Shankland.** Proton-proton scattering at 14.5 Mev—560(L)
Winans, J. G. Classical model for the nucleus—379(L)
—— **and H. M. Foslie.** Rotational structure of InCl bands at 2670A—137(A)
Wintner, Aurel. On the momentum operator in wave mechanics—547
—— Unboundedness of quantum-mechanical matrices—738(L)
Wise, C. Edward, Jr. (see Dibeler, Vernon H.)—381(L)
Witmer, Enos E. Analysis of molecular spectra and the calculation of thermodynamic quantities—137(A)
—— Integral and rational numbers in the nuclear domain and their significance—126(L)
Wolfe, G. (see Bernstein, S.)—140(A), 463(A), 573
Wood, George W. Positive grid characteristics of a triode —832(A)

Wood, R. W. Interaction of shock-waves, the spectra of cavity charge explosions, and the production of artifical meteors—471(A)
Woodhull, Jean C. (see May, Albert)—475(A)
Woodland, P. C. (see Boyer, R. F.)—488(A)
Wooldridge, D. E., A. J. Ahearn, and J. A. Burton. Conductivity pulses induced in diamond by alpha-particles—913(L)
Wright, Byron T. Recoil of silver nuclei due to *K*-capture in cadmium—839
—— (see Wilson, Robert R.)—560(L)
Wu, C. K. and S. C. Chao. Relation between the force constant and the interatomic distance of a diatomic linkage. II. A modified Huggins relation—118
Wu, C. S. (see Havens, W. W., Jr.)—165
—— (see Rainwater, L. J.)—65
——, **L. J. Rainwater, and W. W. Havens, Jr.** Slow neutron velocity spectrometer studies, III. I, Os, Co, Tl, Cb, Ge—174
Wu, Ta-You. Excitation of molecular vibrations by electrons—111

Yagoda, Herman and Nathan Kaplan. Fading of latent alpha-ray image in emulsions—910(L)
Yamakawa, A. (see Sigurgeirsson, T.)—319(L)
Yao, Y. T. (see Nielsen, Alvin H.)—825(L)
Yates, Kenneth P. and Harald H. Nielsen. Infra-red spectrum of methyl fluoride—349
Yost, F. L. (see Ramsay, B. P.)—834(A)
Young, James L., III. (see Beams, J. W.)—131(L),835(A)
Yu, Fu-Chun, Donald Gideon, and J. D. Kurbatov. Disintegration by consecutive orbital electron captures $_{56}Ba^{131} \rightarrow _{55}Cs^{131} \rightarrow _{54}Xe^{131}$—382(L)

Zachariasen, W. H. Direct determination of stacking disorder in layer structures—715
Zartman, I. F. Precision ultrasonic interferometer—479(A)
Zatsepin, G. T. (see Skobeltzyn, D. V.)—315
Zener, Clarence. A defense of the Cauchy relations—323(L)
—— Contributions to the theory of beta-phase alloys—846
—— Stress induced preferential orientation of pairs of solute atoms in metallic solid solution—34
Zilsel, P. R. (see Breit, G.)—232
Zimm, B. H. (see Doty, P. M.)—485(A)
Zinn, W. H. Diffraction of neutrons by a single crystal—752

Analytic Subject Index to Volume 71

References with (A) are to abstracts of papers presented at meetings of the American Physical Society. References with (L) are to Letters to the Editor.

Absorption of neutrons
Absorbing isotopes in Gd and Sm, R. E. Lapp, J. R. Van Horn, and A. J. Dempster—745
Capture cross section of boron for neutrons of energies from 0.01 ev to 1000 ev, B. R. B. Sutton, B. D. McDaniel, E. E. Anderson, and L. S. Lavatelli—272(L)
Cross sections with a crystal spectrometer, William J. Sturm—757
By iodine, Seymour Katcoff—826(L)

Absorption of radiation
Nuclear magnetic resonance, N. Bloembergen, R. V. Pound, and E. M. Purcell—466(A)

Acoustics
Absorption of sound as relaxation phenomena, Carl Eckart—277(A)
Pressure and temperature waves in He, C. T. Lane, William Fairbank, and Henry Fairbank—477(A)
Scattering in an inhomogeneous medium, C. L. Pekeris—268(L), Erratum—457(L)
Second sound in liquid helium II, C. T. Lane, Henry A. Fairbank and William M. Fairbank—600
Second sound in He II, Lothar Meyer and William Band—828(L)
Separation by ultrasonic waves, H. Frei and M. Schiffer—555(L)
Temperature dependence of "second sound" velocity in He, Henry Fairbank, William Fairbank, and C. T. Lane—477(A)
Theory of "second sound" in helium, L. Tisza—477(A)
Ultrasonic absorption and velocity measurements in He, J. R. Pellam, and C. F. Squire—477(A)
Ultrasonic absorption in water, Leonard Hall—318(L)
Velocity and attenuation of sound in rubber, W. B. Thompson, B. A. Mrowca, and Eugene Guth—486(A)

Aerodynamics (see also **Hydrodynamics**)
Variation of lift at transonic speed, W. F. Hilton—465(A)

Astrophysics
Erratum: Expanding universe and the origin of elements, G. Gamow—273(L)
Irreversible processes in stellar dynamics, Herbert Jehle—469(A)
Motion at high velocity through compressible medium, R. N. Thomas—474(A)
Production of artificial meteors, R. W. Wood—471(A)
Solar curve of growth, Winston M. Gottschalk—133(A)
Supersonic problems in astronomy, Fred L. Whipple—474(A)

Atmosphere (see also **Meteorology**)
Ionization by meteoric bombardment, J. A. Pierce—88
Pressure and temperature of the atmosphere to 120 km, N. Best, R. Havens, and H. LaGow—915(L)
Temperature of upper atmosphere, S. L. Seaton—557(L)

Atomic and molecular beams
Free paths of Cs atoms in He, N, and Cs vapor, I. Estermann, S. N. Foner, and O. Stern—250
Velocity distribution in a beam of Cs atoms, I. Estermann, O. C. Simpson, and O. Stern—238

Atomic structure (see also **Spectra, atomic**)
Hydrogen atom and generalized classical electrodynamics, C. Jayaratnam Eliezer—49
Magnetic interactions of electrons, H. H. Marvin—102
Of the quadrielectron, Aadne Ore—913(L)

Biophysics
Arterial pulse wave velocities, Allen L. King—482(A)
Biological effects of low frequency vibrations, H. B. Wahlin and B. R. Russell—139(A)
Neutron monitoring, J. S. Cheka—836(A)
Photoelectric nephelometer, N. Underwood and A. H. Doermann—834(A)
Tolerance concentrations of radioactive substances, Karl Z. Morgan—835(A)
Visibility at various color temperatures, Otto Stuhlman, Jr.—834(A)

Collisions of second kind
Validity of Franck-Condon principle, Roland E. Meyerott—553(L)

Contact potentials
Silicon rectifiers, Walter E. Meyerhof—727

Cosmic radiation
Auger showers, M. M. Mills and R. F. Christy—275(A)
Auger showers and comets, V. Rojansky—552(L)
Azimuthal variation, Alfredo Baños, Jr. and M. L. Perusquía—276(A), Piara Singh Gill—398, 462(A)
Bursts in unshielded chamber, Herbert Bridge and Bruno Rossi—379(L)
Disintegration of negative mesons, M. Conversi, E. Pancini, and O. Piccioni—209(L)
East-west effect, Robert A. Millikan—275(A)
Effect of sun, W. F. G. Swann—485(A)
Electrons above the earth's atmosphere, G. J. Perlow and J. D. Shipman, Jr.—325(L)
Focusing telescope, W. T. Harris—135(A), 310
Further cosmic-ray experiments above the atmosphere, S. E. Golian and E. H. Krause—918(L)
Lateral extension of Auger showers, D. V. Skobeltzyn, G. T. Zatsepin, and V. V. Miller—315
Mass of mesotron, Donald J. Hughes—387
Mean life of mesotrons at 11,500 feet, Harold K. Ticho—463(A)
Meson showers under lead, William B. Fretter—462(A)
Production of mesotrons at 30,000 feet, P. S. Gill—82
Production of nucleons, S. A. Korff and B. Hamermesh—842

Cosmic Radiation (continued)
Production of stars, Eugene Gross, Shuichi Kusaka, and George Snow—463(A)
Showers of penetrating particles at 26,000 feet, Gleb Wataghin—453(L)
Sign and energy spectrum of primary radiation, M. S. Vallarta, M. L. Perusquía, and J. de Oyarzábal—393
Variation of vertical component, W. F. G. Swann and Peter A. Morris—462(A)
Cross section, measurements, theory
Of B for neutrons from 0.01 ev to 1000 ev, R. B. Sutton, B. D. McDaniel, E. E. Anderson, and L. S. Lavatelli—272(L)
Of deuterium and oxygen for fast neutrons, Richard G. Nuckolls, Carl L. Bailey, William E. Bennett, Thor Bergstrahl, Hugh T. Richards, and John H. Williams—140(A)
Of Au, In, Ta, W, Pt, Zr for neutrons, W. W. Havens, Jr., C. S. Wu, L. J. Rainwater, and C. L. Meaker—165
Of I, Os, Co, Tl, Cb, Ge for neutrons, C. S. Wu, L. J. Rainwater, and W. W. Havens, Jr.—174
Neutron cross section—Cd, Ag, Sb, Ir, Mn, L. J. Rainwater, W. W. Havens, Jr., C. S. Wu, and J. R. Dunning—65
Neutron cross section for Hg isotopes, Mark G. Inghram, David C. Hess, Jr., and Richard J. Hayden—561(L)
Neutron-proton scattering, theory, D. Bohm and C. Richman—567
Total neutron cross section of Dy and Nd, William J. Sturm and George P. Arnold—556(L)
Transmission through microcrystalline materials, E. Fermi, W. J. Sturm, and R. G. Sachs—589
Of twenty-three elements for photo-neutrons, R. Fields, B. Russell, D. Sachs, and A. Wattenberg—508
Crystal structure
Lattice spacing of AgBr, J. C. M. Brentano and L. van Clief Spencer—142(A)
Stacking disorder in layer structures, W. H. Zachariasen—715
Crystalline state
Band theory of graphite, P. R. Wallace—476(A), 622
Barium silicate interface of oxide coated cathodes, A. Eisenstein—473(A)
Beta-phase alloys, Clarence Zener—846
Color of natural smoky quartz, K. Przibram—319(L)
deHaas-van Alphen effect in zinc, Jules A. Marcus—559(L)
Diamagnetic susceptibility of gamma-brasses, Jules A. Marcus—471(A)
Dielectric breakdown in the alkali halides, Goethe Malmlöw and Frederick Seitz—125(L)
Effect of x-rays on elastic constants of quartz, Virgil E. Bottom—476(A)
Grain boundaries in metals, T'ing-Sui Kê—142(A)
Grain growth in aluminum, Paul A. Beck, Joseph C. Kremer, and L. Demer—555(L)
Hall effect and magnetoresistance in Ge, W. Crawford Dunlap, Jr.—471(A)
High energy ions in lattices, A. H. W. Aten, Jr.—641(L)
Infra-red vibrations in NaCl, Jordan J. Markham—473(A)
Material of high magnetic permeability, O. L. Boothby and R. M. Bozorth—472(A)
Orientation of atoms in metallic solid solution, Clarence Zener—34
Oscillator concept, theory of solids, E. M. Corson and I. Kaplan—130(L)
Radiation on Si crystals; effects of, F. C. Brown—472(A)
Recrystallization of quartz, D. D'Eustachio—476(A)
Rectification at a metal semi-conductor contact, John Bardeen—717
Stress induced preferential orientation of atoms in metallic solid solution, Clarence Zener—34
Structure of evaporated Sb films, H. Levinstein and H. R. Crane—476(A)
Ultrasonic measurements on single crystals, H. B. Huntington—472(A)
Viscous behavior of grain boundaries, T'ing-Sui Kê—533
Dielectrics and dielectric properties
Of barium titanate, Shephard Roberts—890
Breakdown in the alkali halides, Goethe Malmlöw and Frederick Seitz—125(L)
Properties of butadiene-containing polymers and co-polymers, R. F. Boyer, E. B. Baker, and P. C. Woodland—488(A)
Of rubber, L. V. Holroyd, B. A. Mrowca, and Eugene Guth—488(A)
Diffraction of atoms and neutrons
Theory of refraction and diffraction of neutrons, M. L. Goldberger and Frederick Seitz—294
Diffraction of radiation
Pattern of a circular aperture, C. L. Andrews—777
Diffusion
Of BF_3 gas, thermal, W. W. Watson, J. O. Buchanan, and F. K. Elder, Jr.—887
By fields of ultrasonic waves, H. Frei and M. Schiffer—555(L)
Self-diffusion of UF_6, Edward P. Ney and Fontaine C. Armistead—14, 138(A)
Discharge of electricity in gases
Constant field and initiation of radiofrequency discharge, Arthur A. Varela—124(L)
Corona from positive points, W. N. English—638(L)
Electron attachment and ambipolar diffusion, Manfred A. Biondi and Sanborn C. Brown—481(A)
Harmonic components in a.c. discharges, Lawton M. Hartman and Henry Margenau—481(A)
High frequency electron distribution, Lawton M. Hartman—469(A)
Ionization currents in cylindrical systems, G. W. Johnson—278(A)
Mechanism of negative point corona, Leonard B. Loeb—712
Microwave studies of dielectric properties of arcs, Donald E. Kerr, Sanborn C. Brown, and Walter P. Kern—480(A)
Motion of cathode spots in fields, R. L. Longini—642 (L)
Negative corona in freon air, G. L. Weissler—278(A)
Positive corona in freon air, E. I. Mohr—278(A)

Propagation of discharges in counters, Ernest Wantuch —646(L)
Retrograde motion of arc cathode spot, C. J. Gallagher and J. D. Cobine—481(A)
Ring discharge in metallic torus, Charles G. Smith—135(A)
Sparking potentials of Ba, Mg, and Al in A, Harold Jacobs and Armand P. LaRocque—138(A)
Discharge of electricity in high vacuum (see **High voltage tubes and machines**)
Disintegration and excitation of nucleus (see also **Radioactivity**)
Alpha-particles from excited Ne^{20}, angular distribution, Sylvan Rubin—275(A)
Angular distributions in resonance reactions, calculation, G. Breit and B. T. Darling—402
Angular distribution of α-particles from $Li^7(p,\alpha)\alpha$, Sylvan Rubin, W. A. Fowler, and C. C. Lauritsen—212(L), R. F. Christy and S. Rubin—275(A)
Of As^{72}, Allan C. G. Mitchell, Ed. T. Jurney, and Margaret Ramsey—825(L)
Consecutive orbital electron captures, Fu-Chun Yu, Donald Gideon, and J. D. Kurbatov—382(L)
$d-H^3$ reaction in Cb and Ag, D. N. Kundu and M. L. Pool—140(A)
Deuteron bombardment of neon isotopes, F. K. Elder, Jr., H. T. Motz, and P. W. Davison—917(L)
Disintegration energy of Na^{24}, Edgar C. Barker—453(L)
Escape of protons and neutrons from bombarded Bi, J. M. Cork—144(A)
Formation of RaE and Po by deuteron bombardment of Bi, H. E. Tatel and J. M. Cork—159
Gamma-meson reactions induced by 100-Mev x-rays, search for, N. A. Bonner, G. Freidlander, L. P. Pepkowitz, and M. L. Perlman—511
Gamma-radiation from Be^9+H^1, C. C. Lauritsen, T. Lauritsen, and W. A. Fowler—279(A)
Gamma-rays from Al bombarded with protons, K. J. Broström, T. Huus, and R. Tangen—661
Gamma$-p$ reactions in Be^9, Wm. Ogle, Leon Brown, and Richard Conklin—378(L)
Internally converted gamma-radiation from Ta, James M. Cork and Franklin B. Shull—182, 467(A)
H^3 bombardment of Ag and Rh, D. N. Kundu and M. L. Pool—467(A)
L-converted isomeric transition, M. Goldhaber, C. O. Muehlhause, and S. H. Turkel—372(L), 467(A)
Of Li^7 by deuterons, W. E. Bennett, T. W. Bonner, H. T. Richards, and B. E. Watt—11
Neutron spectra of Li, Al, and Be bombarded with deuterons, J. S. Laughlin and P. G. Kruger—484(A)
Performance of the 184-inch cyclotron, W. M. Brobeck, E. O. Lawrence, K. R. MacKenzie, E. M. McMillan, R. Serber, D. C. Sewell, K. M. Simpson, and R. L. Thornton—449
Photo-disintegration of Li^7, Mg^{24}, Al^{27}, Si^{28}, S^{32}, and Ca^{40}, thresholds, Robert A. Becker, A. O. Hanson, and B. C. Diven—466(A)
Photo-fission in heavy elements, G. C. Baldwin and G. S. Klaiber—3
Range-momentum of particles emitted in disintegrations induced by 100-Mev x-rays, G. S. Klaiber, E. A. Luebke, and G. C. Baldwin—649
Reaction Al^{27} $(d; p, \alpha)$ Na^{24}, E. T. Clarke—187
$_{38}Sr^{88}(n,\gamma)_{38}Sr^{87}$ reaction produced by thermal neutrons, Leo Seren, Herbert N. Friedlander, and Solomon Turkel—454(L)
Of twenty-one minute isomer of Mn^{52}, R. K. Osborne and M. Deutsch—467(A)
Width of 985 kev Al (p, γ) resonance, R. S. Bender, F. C. Shoemaker, and J. L. Powell—905(L)
Yields of protons in transmutations, Ernest Pollard—467(A)
Dissociation
By electron bombardment of $SiCl_4$, R. H. Vought—93
Energy of CO, H. D. Hagstrum—376(L)
Of formic acid monomer by electron impact, Thomas Mariner and Walker Bleakney—139(A)
Dynamics
Escape from earth by multiple-step rockets, Martin Summerfield—279(A)
Forced vibrations, non-linear restoring force, Carl A. Ludeke—481(A)
Gyroscopic effects in a vibratory system, G. S. Bennett —481(A)
Nuclear energy and rocket propulsion, H. S. Seifert and M. M. Mills—279(A)
Shock-waves, R. W. Wood—471(A)
Efficiency of ionization
Probability of *K*-ionization of Ni by electrons, L. T. Pockman, D. L. Webster, P. Kirkpatrick, and K. Harworth—330, 470(A)
Elasticity
Of beta-phase alloys, Clarence Zener—846
Cauchy relations, Clarence Zener—323(L)
Creep and relaxation, B. Gross—144(A)
Effect of x-rays on elastic constants of quartz, Virgil E. Bottom—476(A)
Elastic losses in rubber, H. S. Sack and H. L. Raub—486(A)
Finite elastic strain of cubic crystals, Francis Birch—809
Grain boundaries in metals, T'ing-Sui Kê—142(A)
Mechanism for ductile failure, Paul E. Shearin—832(A)
Non-linear springs, G. W. Crawford and F. T. Rogers, Jr.—833(A)
Refraction of shocks in gases, A. H. Taub—465(A)
Relaxation in plastic materials, M. Mochulsky, R. D. Andrews, and A. V. Tobolsky—487(A)
Of sodium chlorate, S. Bhagavantam and D. Suryanarayan—553(L)
Stress-strain curves, analysis, George Halsey—487(A)
Torsion of a rubber cylinder, R. S. Rivlin—487(A)
Variation of torsional modulus with frequency, S. J. Barnett and D. S. Webber—143(A), 895
Viscous behavior of grain boundaries, T'ing-Sui Kê—533
Electrical conductivity and resistance
Of conducting rubber, Paul E. Wack—489(A)
Conductivity pulses induced in diamond by alpha-particles, D. E. Wooldridge, A. J. Ahearn, and J. A. Burton—913(L)

Electrical conductivity and resistance (continued)
Of Ge and Si from 10° to 600°K, G. L. Pearson and W. Shockley—142(A)
Ge-Ge contacts, S. Benzer—141(A)
Of graphite, theory, P. R. Wallace—622
Ionization of impurity levels in semi-conductors, B. Goodman, A. W. Lawson, and L. I. Schiff—191
Low temperature resistivity of Ge semi-conductors, V. A. Johnson and K. Lark-Horovitz—483(A)
Magnetic transition curves in superconducting Ta, Robert T. Webber—471(A)
Photo- and thermo-effects in Ge rectifiers, Ralph Bray and K. Lark-Horovitz—141(A)
Quenching of superconductivity, M. J. Sienko, and R. A. Ogg, Jr.—319(L)
Rectification at a metal semi-conductor contact, John Bardeen—717
Resistivity of Ge, effect of additions, I. Estermann, A. Foner, and J. A. Randall—484(A)
Silicon rectifiers, contact potential difference, Walter E. Meyerhof—727
Of sodium-ammonia solutions, Luigi Giulotto and Alberto Gigli—211(L), D. K. MacDonald, K. Mendelssohn, and A. J. Birch—563(L), Erratum—829(L), Melvin Eisner and Joseph W. Straley—832(A)
Temperature coefficient for crystalline Se, Wayne E. Blackburn—277(A)
Transition from classical to quantum statistics in semi-conductors, Vivian A. Johnson and K. Lark-Horovitz—374(L), Erratum—909(L)

Electromagnetic theory
Angular momentum of photons, José A. Balseiro—79
Čerenkov radiation, R. H. Dicke—737(L)
Diffraction pattern of a circular aperture, C. L. Andrews—777
Field of a point source, Riesz method and λ-limiting process, S. T. Ma—787
Hydrogen atom and generalized classical electrodynamics, C. Jayaratnam Eliezer—49
Magnetic energy, G. H. Livens—58
Radiation from accelerated electrons, F. R. Elder, A. M. Gurewitsch, R. V. Langmuir, and H. C. Pollock—829(L)
Radiation from an antenna, Ronold W. P. King—134(A)
Theory of corner reflector, Roy C. Spencer—134(A)

Electron optics
Motion of charged particles in inhomogeneous anisotropic media, N. Chako—469(A)

Electronic tubes (see also **Methods and instruments**)
Positive grid characteristics of a triode, George W. Wood—832(A)

Electrons (see also **Positrons**)
Electron affinity of positronium, Egil A. Hylleraas—491

Electrophoresis
And electric charges, Felix Ehrenhaft—143(A)

Elements
Number of elements, Miguel Masriera—458(L)
Search for element 87, Horia Hulubei—740

Errata
Analysis of the vibration-rotation band ω_3 for $C^{13}O^{16}_2$ and $C^{13}O^{18}_2$, Alvin H. Nielsen and Y. T. Yao—825(L)
Collision of neutrons with deuterons and the reality of exchange forces, H. S. W. Massey and R. A. Buckingham—829(L)
Conductivity of sodium-ammonia solutions, D. K. C. MacDonald, K. Mendelssohn and A. J. Birch—829(L)
Expanding universe and the origin of elements, G. Gamow—273(L)
K x-ray absorption edge of silicon, Vola P. Barton and George A. Lindsay—736(L)
Note on the scattering of radiation in an inhomogeneous medium, C. L. Pekeris—457(L)
On the disintegration of negative mesons, M. Conversi, E. Pancini, and O. Piccioni—557(L)
On the scattering and absorption of particles by atomic nuclei, H. Feshbach, D. C. Peaslee, and V. F. Weisskopf—564(L)
Quadrupole moments and spins of Br, Cl, and N nuclei, C. H. Townes, A. N. Holden, J. Bardeen, and F. R. Merritt—829(L)
Transition from classical to quantum statistics in germanium semiconductors at low temperature, Vivian A. Johnson and K. Lark-Horovitz—909(L)

Excitation of atoms and molecules
Molecular vibrations excited by electrons, Ta-You Wu—111

Excitation of nuclei (see also **Disintegration and excitation of nucleus; Nuclear structure**)
Nuclear excitation functions. II. Al^{27} $(d; p, \alpha)$ Na^{24}, E. T. Clarke—187

Field theory
Pais' *f*-field theory and mirror nuclei, A. S. Wightman—447
Quantized space-time, Hartland S. Snyder—38

Films, properties of
Structure of evaporated Sb films, H. Levinstein and H. R. Crane—476(A)

Fission of nucleus
Alpha-particles emitted, G. Farwell, E. Segrè, and C. Wiegand—327
Distribution of fission fragments, David H. Frisch—478(A)
Fifty-five-hour element 61, Mark G. Inghram, David C. Hess, Jr., Richard J. Hayden, and George W. Parker—743(L)
Fission fragments, Pierre Demers—483(A)
Gamma-rays from U(235) fission, S. Bernstein, W. M. Preston, G. Wolfe, and R. Slattery—463(A)
Nuclear properties of U^{233}, G. T. Seaborg, J. W. Gofman, and R. W. Stoughton—378(L)
Photo-neutrons from fission products in heavy water, S. Bernstein, W. M. Preston, G. Wolfe, and R. E. Slattery—140(A)
Range of fission fragments in photographic emulsion, H. T. Richards and Lyda Speck—141(A), J. K. Bøggild, O. H. Arrøe, and T. Sigurgeirsson—281
Ternary and quaternary fission, San-Tsiang Tsien, Ho Zah-Wei, R. Chastel, and L. Vigneron—382(L)

Fluid dynamics (see also **Hydrodynamics**)
Atomization, J. M. Schmidt—278(A)
Axially symmetrical supersonic flow, A. Vazsonyi—278(A)
Hydrodynamic stability, C. C. Lin—471(A)
Interferometry of faster-than-sound phenomena, Rudolf Ladenburg—464(A)
Scale factors in entry of projectiles into water, Harold Wayland—470(A)

Gamma-rays (see also **Disintegration and excitation of nucleus; Radioactivity**)
Gamma-ray yield curve of aluminum bombarded with protons, K. Broström, T. Huus, and R. Tangen—661
Gases
Refraction of shocks in gases, A. H. Taub—465(A)
Gyromagnetization (see also **Magnetic properties**)
Discrepancy in gyromagnetic measurements, S. J. Barnett and D. S. Webber—143(A)

Hall effect
In Ge, W. Crawford Dunlap, Jr.—471(A)
Of Ge and Si from 10° to 600°K, G. L. Pearson and W. Shockley—142(A)
High voltage tubes and machines (see also **Methods and instruments**)
Beam from a betatron, Rolf Wideröe—376(L)
Biased betatron, W. F. Westendorf—271(L)
400-kv source, Samuel K. Allison, Leticia Del Rosario, Joan Hinton, and Howard Wilcox—139(A)
Nuclear electrostatic generator, E. G. Linder—129(L)
Performance of the 184-inch cyclotron, W. M. Brobeck, E. O. Lawrence, K. R. MacKenzie, E. M. McMillan, R. Serber, D. C. Sewell, K. M. Simpson, and R. L. Thornton—449
Hydrodynamics
Axially symmetrical supersonic flow, A. Vazsonyi—278(A)
Characterization of fields of diabatic flow, Bruce L. Hicks—476(A)
Compressible flows with degenerate hodographs, John H. Giese—474(A)
Drag coefficient of spheres entering water, Albert May and Jean C. Woodhull—475(A)
Drag forces and cavity formation, J. Howard McMillen and E. Newton Harvey—475(A)
Interaction between boundary layer and shock waves, H. W. Liepmann—465(A)
Interferometry of faster-than-sound phenomena, Rudolf Ladenburg—464(A)
Limitations of linearized theory of supersonic flow around cones, Zdenek Kopal—474(A)
Motion at high velocity through compressible medium, R. N. Thomas—474(A)
Oscillations and stability of laminar flow, H. K. Skramstad and G. B. Schubauer—475(A)
Pressure produced by flat plate striking water, P. N. Metzelaar and D. E. Allmand—475(A)
Stability of shock waves in channel flows, Arthur Kantrowitz—465(A)
Supersonic problems in astronomy, Fred L. Whipple—474(A)
Two-dimensional flows of a compressible fluid, operator method, Stefan Bergman—474(A)
Hyperfine structure (see also **Nuclear moments and spin**)
Of atomic hydrogen and deuterium, J. E. Nafe, E. B. Nelson, and I. I. Rabi—914(L)
Of NH_3, Walter Gordy and Myer Kessler—640(L)

Ionization by collision (see also **Ionization potentials**)
Critical ionization potentials of uranium hexafluoride and hydrogen fluoride, J. R. White and A. E. Cameron—907(L)
Ionization potentials
By use of photoelectric cells, Arthur Waltner—834(A)
Critical ionization potentials of uranium hexafluoride and hydrogen fluoride, J. R. White and A. E. Cameron—907(L)
Of formic acid monomer, Thomas Mariner and Walker Bleakney—139(A)
Of $SiCl_4$ and $SiCl_2$, R. H. Vought—93
Ionization by radiation (see also **Photo-ionization**)
Thermal ionization of impurity levels in semi-conductors, B. Goodman, A. W. Lawson, and L. I. Schiff—191
Ionosphere
Ionization by meteoric bombardment, J. A. Pierce—88
True height of layer, J. A. Pierce—698
Ions
Half-life of metastable ions, J. A. Hipple—594
Isotopes
Abnormal abundance produced by neutron absorption in Cd, A. J. Dempster—144(A)
Abundance of copper isotopes, Henry E. Duckworth and Benjamin G. Hogg—212(L)
Abundance of He^3, L. T. Aldrich and A. O. Nier—143(A)
Changes in Cd by neutron absorption, A. J. Dempster—829(L)
Concentration of He^3 in liquid and vapor He^4, Henry A. Fairbank, C. T. Lane, L. T. Aldrich, and Alfred O. Nier—911(L)
Single field mass spectrometer, E. P. Ney and A. K. Mann—835(A)

Liquids (see also **Hydrodynamics**)
Atomization, J. M. Schmidt—278(A)
Convection currents in a porous medium, H. L. Morrison and F. T. Rogers, Jr.—834(A)
Permeabilities of unconsolidated sands, H. L. Morrison—837(A)
Pressure and temperature waves in He, C. T. Lane, William Fairbank, and Henry Fairbank—477(A)
Second sound in liquid helium II, C. T. Lane, Henry A. Fairbank, and William M. Fairbank—600
Second sound in He II, Lothar Meyer and William Band—828(L)
Second virial coefficient of water, Vernon Myers—478(A
Temperature dependence of "second sound" velocity i\ He, Henry Fairbank, William Fairbank, and C. .. Lane—477(A)

Liquids (continued)
Theory of "second sound" in He, L. Tisza—477(A)
Ultrasonic absorption and velocity measurements in He, J. R. Pellam, and C. F. Squire—477(A)

Magnetic fields
Facilities of Kensington Magnetic Laboratory, B. P. Ramsay and F. L. Yost—834(A)
Magnetic properties (see also **Nuclear moments and spin**)
Anomalous Larmor frequencies, Charles Kittel—270(L)
Complex permeability of iron at 200 Mc, G. T. Rado, M. H. Johnson, and M. Maloof—472(A); M. H. Johnson, G. T. Rado, and M. Maloof—322(L)
Complex permeabilities of metals at UHF, M. H. Johnson, G. T. Rado, and M. Maloof—472(A)
Diamagnetic susceptibility of gamma-brasses, temperature dependence, Jules A. Marcus—471(A)
Direction of domain magnetization, H. J. Williams—646(L)
Discrepancy in gyromagnetic measurements, S. J. Barnett and D. S. Webber—143(A)
deHaas-van Alphen effect in zinc, Jules A. Marcus—559(L)
Of graphite, theory, P. R. Wallace—476(A), 622
Gyromagnetic ratio, S. J. Barnett and D. S. Webber—895
Magnetic ions and currents, Brother Gabriel Kane—458(L)
Magnetic moment of triton, R. G. Sachs—457(L)
Material of high permeability, O. L. Boothby and R. M. Bozorth—472(A)
Quenching of superconductivity, M. J. Sienko and R. A. Ogg, Jr.—319(L)
Single magnetic poles, existence of, Elliot T. Benedikt and Herta R. Leng—454(L), 480(A); Felix Ehrenhaft—138(A), 480(A); Brother Gabriel Kane—458(L)
Mechanics, quantum—atomic structure and spectra
Matrix elements for He, Werner Romberg—706
Weinstein's variational method, W. Kohn—902
Mechanics, quantum—general
Applications of variational method, Walter Kohn—635, Remarks, B. Davison—694
Correspondence treatment of radiation, W. H. Furry—468(A)
Expansibility of solutions, Niels Arley—272(L)
General condition of Heisenberg for the *S* matrix, S. T. Ma—195
Heitler theory of radiation damping, John M. Blatt—468(A)
Hydrodynamical equations, M. Dresden—143(A)
Invariant form of quantum equations, E. M. Corson—200
Lower bounds for eigenvalues, R. J. Duffin—827(L)
Momentum operator in wave mechanics. Quadratic integrability, Aurel Wintner—547
Quantized space-time, Hartland S. Snyder—38
Redundant zeros in Heisenberg's theory, S. T. Ma—210(L)
Relativistic wave equations, Harish-Chandra—793
Stability of polyelectrons, Egil A. Hylleraas and Aadne Ore—468(A)
Theory of alpha-radioactivity, Melvin A. Preston—865
Unboundedness of quantum-mechanical matrices, Aurel Wintner—738(L)
Of vibrating string, Nathan Rosen—833(A)
Mechanics, quantum—of solid bodies
Eigenfunctions and eigenvalues in solids, application to Na, Fred C. Von der Lage and H. A. Bethe—612
Mesotrons (see also **Cosmic radiation**)
Decay in matter, M. Conversi, E. Pancini, and O. Piccioni—209(L), 557(L); E. Fermi, E. Teller, and V. Weisskopf—314; T. Sigurgeirsson and A. Yamakawa—319(L)
Mass, Donald J. Hughes—387
Mean life at 11,500 feet, Harold K. Ticho—463(A)
Mechanism of absorption, John A. Wheeler—320(L), 462(A)
Probability of absorption, George Gamow—550(L)
Production at 30,000 feet, P. S. Gill—82
Showers under lead, William B. Fretter—462(A)
Metastable atoms and molecules
Half-life of metastable ions, J. A. Hipple—139(A), 594
Metastable ion transitions, Vernon H. Dibeler, C. Edward Wise, Jr., and Fred L. Mohler—381(L)
Meteorology
Electrical charge on precipitation, Ross Gunn—139(A), 181
Height of ionospheric layer, J. A. Pierce—698
Pressure and temperature up to 120 km, N. Best, R. Havens, and H. LaGow—915(L)
Temperature of ozone layer, Arthur Adel—564
Temperature of upper atmosphere, S. L. Seaton—557(L)
Upper air ionization by meteoric bombardment, J. A. Pierce—88
Methods and instruments
Absorption of HDO at 1.3 cm, Gilbert W. King and R. M. Hainer—135(A)
Alpha-ray image in emulsions, Herman Yagoda and Nathan Kaplan—910(L)
Angular distributions in resonance reactions, calculation, G. Breit and B. T. Darling—402
Applications of variational method, Walter Kohn—635
Automatically recording spectrograph for infra-red, Alvin H. Nielsen—831(A)
Beam from a betatron, Rolf Widerŏe—376(L)
Biased betatron, W. F. Westendorf—271(L)
Binary counter and shaft position indicator, H. P. Stabler—135(A)
Bridge type electrical computers, William Krasny Ergen—138(A)
Carbon-pile voltage-regulator, theories for, Charles Dubs and F. T. Rogers, Jr.—834(A)
Centrifugal fields, 4×10^8 g, J. W. Beams and James L. Young, III—131(L)
Čerenkov radiation, R. H. Dicke—737(L)
Complex permeabilities of metals at UHF, M. H. Johnson, G. T. Rado, and M. Maloof—472(A)
Computor for mechanical system, F. T. Rogers, Jr.—836(A)

Conductivity pulses induced in diamond by alpha-particles, D. E. Wooldridge, A. J. Ahearn, and J. A. Burton—913(L)
Cosmic ray directional counter, Alfredo Baños, Jr. and M. L. Perusquía—276(A)
Delays in firing time of counters, Chalmers W. Sherwin —479(A)
Detecting the neutrino, K. C. Wang—645(L)
Detector for high energy electrons and mesons, I. A. Getting—123(L)
Determinations of *XR* for high energy particles, F. T. Rogers, Jr.—833(A)
Diffraction by cellulose acetate yarns, Emmett Martin —488(A)
Double focusing beta-ray spectrometer, Franklin B. Shull and David M. Dennison—681
Eigenfunctions and eigenvalues in solids, application to Na, Fred C. Von der Lage, and H. A. Bethe—612
Elastic losses in rubber, H. S. Sack and H. L. Raub— 486(A)
Electron attachment and ambipolar diffusion, Manfred A. Biondi and Sanborn C. Brown—481(A)
Escape from earth by multiple-step rockets, Martin Summerfield—279(A)
Evaporation of Ga; thin films, S. K. Haynes—832(A)
Facilities of Kensington Magnetic Laboratory, B. P. Ramsay and F. L. Yost—834(A)
Fast neutrons, detection of in presence of gamma radiation, Paul W. Reinhardt—836(A)
Ferromagnetism at very high frequencies. I—Magnetic iron at 200 mc, M. H. Johnson, G. T. Rado, and M. Maloof—322(L)
Film for neutron monitoring, J. S. Cheka—836(A)
Focusing cosmic-ray telescope, W. T. Harris—135(A), 310
Fringing flux corrections, Norman D. Coggeshall— 482(A)
Gamma- and beta-ray energies by magnetic lens beta-ray spectrometer, Waldo Rall and Roger G. Wilkinson— 321(L)
G.M. counter data, correction, Donald N. Gideon and J. D. Kurbatov—140(A)
Half-life of metastable ions, J. A. Hipple—594
High potential source, Samuel K. Allison, Leticia Del Rosario, Joan Hinton, and Howard Wilcox—139(A)
High rotational speeds, J. W. Beams and J. L. Young, III—835(A)
Integrating $\sin^2 x/x$, S. M. Christian—836(A)
Intense positive ion source for solids, A. E. Shaw— 277(A)
Interferometry of faster-than-sound phenomena, Rudolf Ladenburg—464(A)
Introducing short-lived radioactive samples into cloud chamber, T. Lauritsen, W. A. Fowler, and C. C. Lauritsen—275(A)
Ionization chamber techniques in measurement of C^{14}, W. P. Jesse, L. A. Hannum, H. Forstat, and A. L. Hart—478(A)
Ionization potential of gases, Arthur Waltner—834(A)
Linear amplifier for general use, W. H. Jordan and P. R. Bell—482(A)
Low temperature thermometry, Edward Gerjuoy and A. Theodore Forrester—276(A), 375(L)
Macromolecular configurations in dilute solution, P. M. Doty, W. A. Affens, and B. H. Zimm—485(A)
Measuring half-lives, A. C. Graves and R. L. Walker—1
Micro-wave spectrograph, Richard H. Hughes and E. Bright Wilson, Jr.—562(L)
Molecular weight of liquid polymers, Alfred Weissler, J. W. Fitzgerald, and Irving Resnick—488(A)
Neutron velocity spectrometer, L. J. Rainwater, W. W. Havens, Jr., C. S. Wu, and J. R. Dunning—65
Nomogram for resolving time of counters, L. Jackson LaSlett—144(A)
Non-linear springs, G. W. Crawford and F. T. Rogers, Jr.—833(A)
Nuclear electrostatic generator, E. G. Linder—129(L)
Nuclear energy and rocket propulsion, H. S. Seifert and M. M. Mills—279(A)
Particle diameters and histograms from electron micrographs, E. E. Hanson and J. H. Daniel—487(A)
Particle size by low angle x-ray scattering, A. E. Smith —277(A)
Performance of the 184-inch cyclotron, W. M. Brobeck, E. O. Lawrence, K. R. MacKenzie, E. M. McMillan, R. Serber, D. C. Sewell, K. M. Simpson, and R. L. Thornton—449
Perot-Fabry interferometers as filters, H. M. O'Bryan —134(A)
Photoelectric nephelometer, N. Underwood and A. H. Doermann—834(A)
Photo-galvanometer feedback amplifier, Demetrius G. Jelatis—483(A)
Photographic neutron detection, R. A. Peck, Jr.— 464(A)
Photography of fluid flow patterns, Garrett Birkhoff and Thomas E. Caywood—470(A)
Polyatomic gases in a fast counter, S. S. Friedland— 377(L)
Positive grid characteristics of a triode, George W. Wood—832(A)
Probe for measurement of magnetic fields, E. C. Gregg —482(A)
Propagation of discharges in counters, Ernest Wantuch —646(L)
Radiation thermocouple, Howard Cary and K. P. George—276(A)
Radiofrequency switch, Donald E. Kerr, Sanborn C. Brown, and Walter P. Kern—480(A)
Reduction of data, F. T. Rogers, Jr.—837(A)
Refractive index of films, Fred W. Billmeyer—489(A)
Remark on the variational method, B. Davison—694
Servo-operated recording potentiometer, F. T. Rogers, Jr. and Marguerite M. Rogers—836(A)
Single field mass spectrometer, E. P. Ney and A. K. Mann—835(A)
Small variations in isotopic abundance; detection of, Henry E. Duckworth and Benjamin G. Hogg—212(L)

Methods and instruments (continued)
Sound velocity method for determination of molecular weight of liquid polymers, Alfred Weissler, J. W. Fitzgerald, and Irving Resnick—488(A)
Spherical harmonic method applied to the Milne problem, R. E. Marshak—443
Spectrophotometric study of reflectance, E. J. Eastmond —274(A)
Stable species $_{39}Y^{89}$, $_{40}Zr^{90}$, and $_{56}Ba^{134}$, M. H. Kurbatov and J. D. Kurbatov—466(A)
Static method of simulating accelerations, John J. Gilvarry and S. F. Eyestone—482(A)
Thermal noise and low temperature thermometry, Edward Gerjuoy and A. Theodore Forrester—276(A), 375(L)
Thermodynamic propulsion for wind tunnels, Francis Clauser—465(A)
Threshold detectors for fast neutrons, Bernard T. Feld, R. Scalettar, and L. Szilard—464(A)
Time intervals between related nuclear events, H. L. Schultz—134(A)
Ultrasonic interferometer, I. F. Zartman—479(A)
Variational method for asymptotic neutron densities, R. E. Marshak—688
Votaic effects in waterglass, E. Scott Barr—832(A)
Wave guides for slow waves, L. Brillouin—483(A)
Microwaves (see also **Electromagnetic theory; Electronic tubes**)
Absorption by O_2, J. H. Van Vleck—413
Absorption by uncondensed water vapor, J. H. Van Vleck—425
Absorption coefficients of water and related molecules, Gilbert King, R. M. Hainer, and Paul C. Cross—433
Absorption lines in OCS, T. W. Dakin, W. E. Good, and D. K. Coles—640(L)
Absorption of $N^{14}H_3$ and $N^{15}H_3$, W. E. Good and D. K. Coles—383(L)
Forces exerted on dielectric media, Otto Halpern—277(A)
Hyperfine structure of NH_3, Walter Gordy and Myer Kessler—640(L)
Inversion spectrum of NH_3, M. W. P. Strandberg, R. Kyhl, T. Wentink, Jr., and R. E. Hillger—326(L), 639(L)
Quadrupole moments and spins of Br, Cl, and N, C. H. Townes, A. N. Holden, J. Bardeen, and F. R. Merritt —644 (L), Erratum—829(L)
Quadrupole moments, spectra of NH_3, Richard J. Watts and Dudley Williams—639(L)
Rotational spectra of linear molecules, C. H. Townes, A. N. Holden, and F. R. Merritt—64(L)
Spectra of methyl iodide, Walter Gordy, A. G. Smith, and James W. Simmons—917(L)
Molecular structure and constants (see also **Spectra, molecular; Raman spectra**)
Dissociation energy of CO, H. D. Hagstrum—376(L)
Energy of positronium molecule, Egil A. Hylleraas and Aadne Ore—493
Field strengths and nuclear quadrupole moments, C. H. Townes—909(L)
Force constant and interatomic distance, C. K. Wu and S. C. Chao—118
Metastable state $\alpha^1\pi g$ of N_2, active nitrogen, Roland Meyerott—133(A)
Relation between ω_e and reduced mass, R. L. Purbrick —137(A)

Neutrino (see also **Radioactivity; Scattering of electrons, neutrons, and ions**)
Electron-neutrino angular correlation, Donald R. Hamilton—456(L)
K-capture in Cd, evidence from, Byron T. Wright—839
Maximum β-energies and neutrino mass, O. Kofoed-Hansen—451
Neutrons (see also **Scattering of electrons, neutrons, and ions**)
Absorbing isotopes in Gd and Sm, R. E. Lapp, J. R. Van Horn, and A. J. Dempster—745
Activities in rare earths, Mark G. Inghram and Richard J. Hayden—144(A)
Cross section for twenty-three elements, R. Fields, B. Russell, D. Sachs, and A. Wattenberg—508
Cross-section measurements, L. J. Rainwater, W. W. Havens, Jr., C. S. Wu, and J. R. Dunning—65
Cross section of Au, In, Ta, W, Pt, Zr, W. W. Havens, Jr., C. S. Wu, L. J. Rainwater, and C. L. Meaker—165
Cross section of I, Os, Co, Tl, Cb, Ge, C. S. Wu, L. J. Rainwater, and W. W. Havens, Jr.—174
Cross sections with a crystal spectrometer, William J. Sturm—757
Delayed neutrons from Pu^{239}, Robert R. Wilson—560 (L)
Diffraction by single crystal, W. H. Zinn—752
Distribution in infinite medium, M. Verde and G. C. Wick—852
Electron waves in field of neutrons, Charles L. Critchfield—258
From $C^{12}+D$, energy spectrum, W. E. Bennett and H. T. Richards—565
Photo-neutrons from U^{238} fission products, S. Bernstein, W. M. Preston, G. Wolfe, and R. E. Slattery—573
Photo-neutron sources; energy, A. Wattenberg—497
Production in cosmic radiation, S. A. Korff and B. Hamermesh—842
Scattering in polycrystalline materials, R. M. Langer and J. F. Daly—464(A)
Scattering of slow neutrons, phase charge, E. Fermi and L. Marshall—666
Spherical harmonic method applied to the Milne problem, R. E. Marshak—443
$_{38}Sr^{86}(n,\gamma)_{38}Sr^{87}$ reaction produced by thermal neutrons, Leo Seren, Herbert N. Friedlander, and Solomon Turkel—454(L)
Theory of slowing down neutrons, S. H. Browne and T. Dantzig—463(A)
Thermal neutron activation cross sections, Leo Seren, Herbert N. Friedlander, and Solomon H. Turkel—463(A)
Threshold detectors for fast neutrons, Bernard T. Feld, R. Scalettar, and L. Szilard—464(A)

Transmission through microcrystalline materials, E. Fermi, W. J. Sturm, and R. G. Sachs—589
Variational method for asymptotic neutron densities, R. E. Marshak—688
Nuclear moments and spin (see also **Hyperfine structure**)
Coupling of nuclear quadrupole moments in polyatomic molecules, J. H. Van Vleck—468(A)
Electric quadrupole spectrum, homonuclear diatomic molecule, H. M. Foley—747
Electron waves in magnetic dipole fields of a neutron, Charles L. Critchfield—258
Of H_1 and H_2, F. Bloch, A. C. Graves, M. Packard, and R. W. Spence—551(L)
Of H_3, H. L. Anderson and A. Novick—372(L); F. Bloch, A. C. Graves, M. Packard, and R. W. Spence—373(L), 551(L)
Magnetic moments, neutron and deuterons, Wayne R. Arnold and Arthur Roberts—878
Magnetic moment of triton, R. G. Sachs—457
Nuclear quadrupole interactions, W. A. Nierenberg, N. F. Ramsey, and S. B. Brody—466(A)
Quadrupole moments, C. H. Townes—909(L)
Quadrupole moments and spins of Br, Cl, and N, C. H. Townes, A. N. Holden, J. Bardeen, and F. R. Merritt—644(L), Erratum—829(L)
Relativistic corrections, G. Breit—400
Of Na by polarization of resonance radiation, Marguerite M. Rogers—833(A)
Spin from the Stark effect, microwave spectra, W. V. Smith—126(L)
Of U^{235}, O. E. Anderson and H. E. White—911(L)
Nuclear structure (see also **Disintegration of nucleus**)
Classical model, J. G. Winans—379(L); B. Davison and W. H. Watson—742(L)
Disintegration energy of Na^{24}, Edgar C. Barker—453(L)
Energy levels in Mn^{56}, A. B. Martin—466(A)
Integral and rational numbers in nuclear domain, Enos E. Witmer—126(L)
Interaction between meson and nucleon, Charles L. Critchfield—908(L)
Levels in Mn^{56}; spacing, A. B. Martin—127(L)
Meson theory of nuclear forces, Leslie L. Foldy—276(A)
Metastable state in Re^{187}, S. De Benedetti and F. K. McGowan—380(L)
Nuclear energy surface, Eugene Feenberg—468(A)
Nuclear radius and mass number, E. Amaldi and B. N. Cacciapuoti—739(L)
Number of elements, Miguel Masriera—458(L)
Reality of exchange forces, H. S. W. Massey and R. A. Buckingham—558(L), Erratum—829(L)

Optical constants and properties
Diffuse reflection from dielectrics, Wm. A. Rense—832(A)
Infra-red vibrations in NaCl, Jordan J. Markham—473(A)
Specular reflection from Hg vapor, J. M. Hansen and H. W. Webb—483(A)
Strain birefringence in visco-elastic materials, Turner Alfrey, Jr.—486(A)

Phosphorescence
Cu-activated ZnS_1, Hubert M. James—137(A)
Mechanism of infra-red-sensitive phosphors, Ferd E. Williams—831(A)
Photo-disintegration
Gamma-p reaction in Be^9, Wm. Ogle, Leon Brown, and Richard Conklin—378(L)
Range-momentum of particles emitted in disintegrations induced by 100-Mev x-rays, G. S. Klaiber, E. A. Luebke, and G. C. Baldwin—649
Photoelectric effect and properties; cells
Emission from a rough surface, Hugh Bradner—269(L)
Energy distributions of photoelectrons from W, L. Apker, E. Taft, and J. Dickey—473(A)
From liquid ammonia solutions of alkali metals, Gordon K. Teal—138(A)
Photo-ionization
Fluctuations of ionization yield, U. Fano—480(A)
Photons
Angular momentum, José A. Balseiro—79
Piezoelectric effect
In barium titanate, Shepard Roberts—890
Piezoelectric vibrations of Rochelle salt plates, N. Chako—485(A)
Polymerization, properties of polymers
Cellulose acetate, ultracentrifuge, S. Singer and H. Mark—487(A)
Dielectric properties of butadiene-containing polymers and copolymers, R. F. Boyer, E. B. Baker, and P. C. Woodland—488(A)
Diffraction by cellulose acetate yarn, Emmett Martin—488(A)
Intrinsic viscosity and molecular weight in polymer solutions, P. Debye—486(A)
Positrons
Electron affinity of positronium, Egil A. Hylleraas—491
Energy of positronium molecule, Egil A. Hylleraas and Aadne Ore—493
Probability
First passage time problem, Markoffian random function, A. J. F. Siegert—485(A)
Two-dimensional Markoffian random function, A. J. F. Siegert—469(A)
Proceedings of the American Physical Society
New Haven, Connecticut Meeting October 26, 1946—133
Minneapolis, Minnesota Meeting November 29–30, 1946—136
Los Angeles, California Meeting January 3–4, 1947—274
New York, New York Meeting January 30–31 and February 1, 1947—460
Salisbury, North Carolina Meeting April 4–5, 1947—831
Rochester, New York Meeting April 12, 1947—744

Radiation
Radiation from accelerated electrons, F. R. Elder, A. M. Gurewitsch, R. V. Langmuir, and H. C. Pollock —829(L)
Radio (see also **Ionosphere**)
Interpretation of radiation from an antenna, Ronold W. P. King—134(A)
Radioactivity (see also **Disintegration of nucleus**)
Alpha-particles emitted in coincidence with fission, G. Farwell, E. Segrè, and C. Wiegand—327
Alpha-particles from 94^{239} and 94^{238}, O. Chamberlain, J. W. Gofman, E. Segrè, and A. C. Wahl—529
Alpha-ray image in emulsions, Herman Yagoda and Nathan Kaplan—910(L)
Of As^{72}, Allan C. G. Mitchell, Ed. T. Jurney, and Margaret Ramsey—825(L)
Of Be^{10}, J. Levinger and E. Meiners—586
Decay rate and chemical compounds, Emilio Segrè—274(A)
Decay scheme of Cs^{134}, Kai Siegbahn and Martin Deutsch—483(A)
Double focusing beta-ray spectrometer, Franklin B. Shull and David M. Dennison—681
Electron-neutrino angular correlation, Donald R. Hamilton—456(L)
Energy limit of K^{40} beta-ray spectrum, W. J. Henderson —323(L)
Energy produced by plutonium, J. W. Stout and W. M. Jones—582
Of Eu and Ho by neutron bombardment, M. G. Inghram and R. J. Hayden—130(L)
Fifty-five hour element 61, M. G. Inghram, David C. Hess, Jr., Richard J. Hayden, and George W. Parker —743(L)
Of fission products, S. Bernstein, W. M. Preston, G. Wolfe, and R. E. Slattery—573
Forty-three day $_{48}Cd^{115}$, Leo Seren, D. Engelkemeir, W. Sturm, H. N. Friedlander, and S. Turkel—409
Of Ga^{72}, coincidence experiments, Allan C. G. Mitchell, Ed. T. Jurney, and Margaret Ramsey—324(L)
Gamma- and beta-ray energies by magnetic lens beta-ray spectrometer, Waldo Rall and Roger G. Wilkinson —321(L)
Gamma-meson reactions induced by 100-Mev x-rays; search for, N. A. Bonner, G. Freidlander, L. P. Pepkowitz, and M. L. Perlman—511
Gamma-ray of N^{13}, L. M. Langer, C. S. Cook, and M. B. Sampson—906(L)
Gamma-rays from W and Mo, W. M. Schwarz and M. L. Pool—122(L)
Gamma-rays from U(235) fission, S. Bernstein, W. M. Preston, G. Wolfe, and R. Slattery—463(A)
Gamma-rays of Po^{210}, S. De Benedetti and E. H. Kerner—122(L)
Half-life of Be^{10}, D. J. Hughes, C. Eggler, and C. M. Huddleston—269(L)
Induced by neutron bombardment of Sm, Mark G. Inghram, Richard J. Hayden, and David C. Hess, Jr. —643(L)
Of isotopes of Re, Os, and Ir, Leon J. Goodman and M. L. Pool—288
Of K^{40}, H. A. Meyer, G. Schwachheim, and M. D. de Souza Santos—908(L)
Of La^{140}, Allan C. G. Mitchell, Lawrence M. Langer, and Leon J. Brown—140(A)
L-converted isomeric transition, M. Goldhaber, C. O. Muehlhause, and S. H. Turkel—467(A), 372(L)
Long-lived radio-iodine, L. E. Glendenin and R. R. Edwards—742
Long-lived I^{129}, Seymour Katcoff—826(L)
In Lu, Yb, and Dy, Mark G. Inghram, Richard J. Hayden, and David C. Hess, Jr.—270(L)
Measuring half-lives, A. C. Graves and R. L. Walker—1
Metastable state in Re^{187}, S. De Benedetti and F. K. McGowan—380(L)
Neutrino, evidence for, Byron T. Wright—839
Neutron induced activities in rare earths, Mark G. Inghram and Richard J. Hayden—144(A)
Ninety-day activity in element 43, E. E. Motta, G. E. Boyd, and A. R. Brosi—210(L)
Ninety-three kev-γ-line of UX_1, H. L. Bradt and P. Scherrer—141(A)
Pu in pitchblende, M. I. Corvalen—132(L)
Of Po, Bi, and Pb, J. J. Howland, D. H. Templeton, and I. Perlman—552(L)
Stable species $_{39}Y^{89}$, $_{40}Zr^{90}$, and $_{56}Ba^{134}$ by nuclear transmutations, M. H. Kurbatov and J. D. Kurbatov —466(A)
Theory of alpha-radioactivity, Melvin A. Preston—865
Thermal neutron activation cross sections, Leo Seren, Herbert N. Friedlander, and Solomon H. Turkel—463(A)
Tolerance concentrations of radioactive substance, Karl Z. Morgan—835(A)
Raman spectra
Low frequency lines in organic crystals, A. Kastler and A. Rousset—455(L)
Range of particles
Range-energy values for protons in air and Al, J. H. Smith—32
Rectifier (see also **Electrical conductivity and resistance**)
Contact potential difference in silicon rectifiers, Walter E. Meyerhof—727
Photo- and thermo-effects in *p*-type Ge rectifiers, Ralph Bray and K. Lark-Horovitz—141(A)
Relativity
Clock paradox, E. L. Hill—143(A)
Notes on Wheeler-Feynman Theory, Carlton W. Berenda—550(L)
Problem of homogeneous incompressible fluid sphere, Brownie Newman and Nathan Rosen—833(A)
Relativistic wave equations, Harish-Chandra—793
Rotational motion, E. L. Hill—318(L), Nathan Rosen—54

Scattering of electrons, neutrons, and ions (see also **Neutrons**)
Angular distributions in resonance reactions, G. Breit and B. T. Darling—141(A)

Collision of neutrons with deuterons, H. S. W. Massey and R. A. Buckingham—558(L), Erratum—829(L)
Collision of neutrons with deuterons and the reality of exchange forces, John H. Williams—908(L)
Elastic scattering of electrons by nuclei, W. W. Buechner, E. A. Burrill, A. Sperduto, R. J. Van de Graaff, and H. Feshbach—142(A)
Fast neutrons by protons and deuterons, M. Ageno, E. Amaldi, D. Bocciarelli, and G. C. Trabacchi—20
Interference phenomena of slow neutrons; phase change, E. Fermi and L. Marshall—666
Multiple scattering of protons in air, E. A. Luebke, G. S. Klaiber, and G. C. Baldwin—657
Neutron cross section for Hg, Mark G. Inghram, David C. Hess, Jr., and Richard J. Hayden—561(L)
Neutron-proton and proton-proton scattering, J. Ashkin and R. E. Marshak—467(A)
Neutron-proton interaction, H. M. Moseley and Nathan Rosen—835(A)
Neutron-proton scattering, Melvin Eisner and Nathan Rosen—833(A)
Neutron scattering in ortho- and parahydrogen, Morton Hamermesh and Julian Schwinger—678
Of neutrons by Dy and Nd, William J. Sturm and George P. Arnold—556(L)
Of neutrons by Mn, N. H. Barbre and M. Goldhaber—141(A)
Of neutrons by protons, angular distribution, J. S. Laughlin and P. Gerald Kruger—736(L)
Of neutrons in deuterium and oxygen, Richard G. Nuckolls, Carl L. Bailey, William E. Bennett, Thor Bergstrahl, Hugh T. Richards, and John H. Williams—140(A)
Of neutrons in infinite medium, M. Verde and G. C. Wick—852
Proton-proton scattering at 8 Mev, Robert R. Wilson and Edward C. Creutz—339
Proton-proton scattering at 10 Mev, Robert R. Wilson—384(L)
Proton-proton scattering at 14.5 Mev, Robert R. Wilson, Edward J. Lofgren, J. Reginald Richardson, Byron T. Wright, and Robert S. Shankland—560(L)
Range-energy values for protons in air and Al, J. H. Smith—32
Range, straggling, of fast protons, Robert R. Wilson—385(L)
Scattering and absorption by atomic nuclei, H. Feshbach, D. C. Peaslee, and V. F. Weisskopf—145; Erratum—564(L)
Slow neutrons by bound protons, methods of calculation, G. Breit—215
Slow neutrons by bound protons, harmonic binding, G. Breit and P. R. Zilsel—232
Statistics of single and plural scattering, S. A. Goudsmit and H. S. Snyder—478(A)
Theory of multiple scattering, H. S. Snyder—478(A)
Theory of refraction and diffraction of neutrons, M. L. Goldberger and Frederick Seitz—294
Of thermal neutrons by Al and Sr, E. Fermi and L. Marshall—915(L)
Of thermal neutrons in polycrystalline materials, R. M. Langer and J. F. Daly—464(A)

Scattering of radiation (see also **Raman spectra**)
From statistically distributed scatterers, Peter G. Bergmann—469(A)
Gamma-radiation, large angle, E. C. Pollard and B. B. Benson—134(A)
In an inhomogeneous medium, C. L. Pekeris—268(L)

Semi-conductors (see also **Electrical conductivity and resistance**)
Surface states and rectification at a metal semi-conductor contact, John Bardeen—717
Transition from classical to quantum statistics in semi-conductors at low temperatures, Vivian A. Johnson and K. Lark-Horovitz—374(L)

Shock waves (see also **Hydrodynamics**)
Glancing reflection of shocks, V. Bargmann—473(A)
Initial motion of a spherical shock, Y. H. Kuo—476(A)
Interaction between boundary layer and shock waves, H. W. Liepmann—465(A)
Interaction of shock-waves, R. W. Wood—471(A)
Interferometry of faster-than-sound phenomena, Rudolf Ladenburg—464(A)
Intersection of shock-waves, H. A. Einstein—473(A)
Normal reflection of waves, R. Finkelstein—42
Propagation in water, R. H. Cole and J. S. Coles—128(L)
Refraction of shocks in gases, A. H. Taub—465(A)
Stability of shock-waves in channel flows, Arthur Kantrowitz—465(A)
Theory of propagation, Stuart R. Brinkley and John G. Kirkwood—606

Solutions
Orientation of atoms in metallic solid solution, Clarence Zener—34

Specific heat
Bounded linear harmonic oscillator, B. Suryan—741(L)
Oscillator concept, theory of solids, E. M. Corson and I. Kaplan—130(L)

Spectra, absorption (see also **Absorption of radiation**)
Bond distances in OCS, T. W. Dakin, W. E. Good, and D. K. Coles—640(L)
Of HDO at 1.3 cm, Gilbert W. King and R. M. Hainer—135(A)
In formaldehyde beyond 10μ, Willard E. Singer—531
Infra-red spectrum of H_2S, Robert H. Noble and Harald H. Nielsen—484(A)
Infra-red spectrum of CH_3F, Kenneth P. Yates and Harald H. Nielsen—349
Intensities of vibrational absorption bands, E. Bright Wilson, Jr. and A. M. Thorndike—479(A)
Of linear molecules near 1-cm wave-length, C. H. Townes, A. N. Holden, and F. R. Merritt—64(L)
Line width in rotation spectrum of water vapor, Arthur Adel—806
Of methyl alcohol and methylamine, W. D. Hershberger and John Turkevich—554(L)
Microwave absorption coefficients of water and related molecules, Gilbert King, R. M. Hainer, and Paul C. Cross—433

Spectra, absorption (continued)
Of microwaves by oxygen, J. H. Van Vleck—413
Of microwaves by uncondensed water vapor, J. H. Van Vleck—425
Microwave of $N^{14}H_3$ and $N^{15}H_3$, W. E. Good and D. K. Coles—383(L)
Nuclear magnetic resonance, N. Bloembergen, R. V. Pound, and E. M. Purcell—466(A)
Rotational spectra of some molecules, nuclear quadrupole moments of Br and Cl, C. H. Townes, A. N. Holden, and F. R. Merritt—479(A)
Rotational structure of InCl bands, J. G. Winans and H. M. Froslie—137(A)

Spectra, atomic
Fine structure of H_α, L. Giulotto—562(L)
Line strengths in FeI, Winston M. Gottschalk—133(A)
Of Th III, R. J. Lang—907(L)

Spectra, general
Nuclear magnetic resonances, low temperature, F. Bitter, N. L. Alpert, H. L. Poss, C. G. Lehr, and S. T. Lin—738(L)
Solar spectra at 55 and 75 km, E. Durand, J. J. Oberly, and R. Tousey—827(L)

Spectra, molecular (see also **Molecular structure and constants**)
Analysis of the vibration-rotation band ω_3 for $C^{12}O_2^{16}$ and $C^{13}O_2^{16}$, Erratum, Alvin H. Nielsen and Y. T. Yao—825(L)
Of NH_3, inversion spectrum, M. W. P. Strandberg, R. Kyhl, T. Wentink, Jr., and R. E. Hillger—639(L)
Of NH_3, quadrupole moment, Richard J. Watts and Dudley Williams—639(L)
Atmospheric bands of O_2, Joseph Kaplan—274(A)
Coupling of nuclear quadrupole moments in polyatomic molecules, J. H. Van Vleck—468(A)
Hyperfine structure of NH_3, Walter Gordy and Myer Kessler—640(L)
Inversion spectrum of NH_3, M. W. P. Strandberg, R. Kyhl, T. Wentink, Jr., and R. E. Hillger—326(L)
Molecular coupling effects, J. G. Valatin—458(L)
Spectra and calculation of thermodynamic quantities, Enos E. Witmer—137(A)
Spectroscopic study of hydrogen peroxide, thermal combination of hydrogen and oxygen, R. B. Holt and O. Oldenberg—479(A)
Ultraviolet bands of N_2, R. B. Setlow, Roland Meyerott, and W. W. Watson—133(A)

Spectroscopy, technique
Automatically recording spectrograph for infra-red, Alvin H. Nielsen—831(A)
Microwave spectrograph, Richard H. Hughes and E. Bright Wilson, Jr.—562(L)

Thermal conductivity
In liquid He, Lothar Meyer and William Band—828(L)
Of natural and synthetic rubbers, H. D. Smith, T. McC. Dauphinee, and D. G. Ivey—487(A)

Thermodynamics
Equilibria of second order, E. O. Hall—916(L)
Spectra and calculation of thermodynamic quantities, Enos E. Witmer—137(A)

X-rays, absorption
K absorption of Ge and As in $GeCl_4$ and $AsCl_3$, S. T. Stephenson—84
K x-ray absorption of Si, Vola P. Barton and George A. Lindsay—406; Erratum, 736(L)
Range-momentum of particles emitted in disintegrations induced by 100-Mev x-rays, G. S. Klaiber, E. A. Luebke, and G. C. Baldwin—649

X-rays, diffraction, scattering, reflection, refraction, and polarization
Stacking disorder in layer structures, W. H. Zachariasen—715

X-rays, emission (see also **X-rays, spectra and spectroscopy, etc.**)
Absolute energy of $K\alpha$-radiation from Ag targets, Paul Kirkpatrick and A. V. Baez—470(A), 521
Analysis of high energy spectra, G. C. Baldwin and G. S. Klaiber—554(L)
Probability of *K* ionization of Ni, Leonard T. Pockman, David L. Webster, and Paul Kirkpatrick—330, 470(A)
From thick targets; 1250 to 2350 kv, W. W. Buechner, R. J. Van de Graaf, E. A. Burrill, and A. Sperduto—470(A)

X-rays, spectra and spectroscopy, wave-length measurements (see also **X-rays, emission**)
Analysis of high energy spectra, G. C. Baldwin and G. S. Klaiber—554(L)

JUL 1 1947

THE PHYSICAL REVIEW

VOLUME 71 Second Series NUMBER 12

JUNE 15, 1947

Published for the

AMERICAN PHYSICAL SOCIETY

by the

AMERICAN INSTITUTE OF PHYSICS

LANCASTER, PA., AND NEW YORK, N. Y.

PHYSICAL REVIEW

A journal of experimental and theoretical physics established by E. L. Nichols in 1893

BOARD OF EDITORS

Editor

JOHN T. TATE

Assistant Editors

J. W. BUCHTA and E. L. HILL

Associate Editors

J. B. FISK
W. PAULI
L. I. SCHIFF
E. J. KONOPINSKI
H. H. NIELSEN
S. C. PULLARD
H. A. BETHE
L. A. RIDENOUR
W. H. ZACHARIASEN

Manuscripts for publication should be submitted to John T. Tate, University of Minnesota, Minneapolis, Minnesota.

Proof and all correspondence concerning papers in the process of publication should be addressed to the Publications Manager, American Institute of Physics, 57 East 55 Street, New York 22, New York.

Subscription Price

United States and Canada $15.00
Elsewhere $16.50

Back Numbers

Complete set: Series 2,[1] Vol. 1, 1913–Vol. 70, 1946—$612.00
Yearly rate: $20.00
Single copies: $2.00 each, prior to July, 1929;
$1.00 each, July, 1929–December, 1941;
$4.00 each, January, 1942–December, 1946.
Current issues: $1.00 each.

Subscriptions and orders for back numbers should be addressed to Prince and Lemon Streets, Lancaster, Pennsylvania, or to the American Institute of Physics, 57 East 55 Street, New York 22, New York.

Changes of address in the case of members of the American Physical Society should be addressed to the Treasurer; in the case of other subscribers to the Business Manager, American Institute of Physics.

[1] For Series 1 inquire of Physics Department, Cornell University, Ithaca, New York.

The Physical Review is published semimonthly at Prince and Lemon Streets, Lancaster, Pennsylvania.
Entered as second-class matter March 6, 1947, at the Post Office at Lancaster, Pennsylvania, under the Act of March 3, 1879.
Accepted for mailing at special rate of postage provided for in paragraph 4, section 538, P. L. & R., authorized January 27, 1933.

THE AMERICAN INSTITUTE OF PHYSICS

INCORPORATED

57 East 55 Street New York 22, N.Y.

MEMBER SOCIETIES:

American Physical Society
KARL K. DARROW, *Secretary*, Columbia University, New York 27, New York.

Optical Society of America
ARTHUR C. HARDY, *Secretary*, Massachusetts Institute of Technology, Cambridge 39, Massachusetts.

Acoustical Society of America
WALLACE WATERFALL, *Secretary*, 330 Fifth Avenue, 64th floor, New York 1, New York.

Society of Rheology
R. B. DOW, *Secretary*, Bureau of Ordnance, Navy Department, Washington 25, D. C.

American Association of Physics Teachers
C. J. OVERBECK, *Secretary*, Northwestern University, Evanston, Illinois.

ASSOCIATED SOCIETIES:

American Society for X-Ray and Electron Diffraction

Electron Microscope Society of America

Physical Society of Pittsburgh

Physics Club of Chicago

Physics Club of Philadelphia

Cleveland Physics Society

ASSOCIATES:

Over seventy-five leading industrial enterprises and other institutions which contribute to the support of the Institute.

JOURNALS:

The Physical Review
Reviews of Modern Physics
JOHN T. TATE, *Editor*—J. W. BUCHTA, E. L. HILL, *Assistant Editors*

Journal of the Optical Society of America
GEORGE R. HARRISON, *Editor*

The Journal of the Acoustical Society of America
FLOYD A. FIRESTONE, *Editor*

American Journal of Physics
DUANE ROLLER, *Editor*—JOSEPH D. ELDER, *Assistant Editor*

The Review of Scientific Instruments
GAYLORD P. HARNWELL, *Editor*

The Journal of Chemical Physics
JOSEPH E. MAYER, *Editor*

Journal of Applied Physics
ELMER HUTCHISSON, *Editor*

OFFICERS

GEORGE R. HARRISON, *Chairman*
Massachusetts Institute of Technology
WALLACE WATERFALL, *Secretary*
The Celotex Corporation
GEORGE B. PEGRAM, *Treasurer*
Columbia University
JOHN T. TATE,
Adviser on Publications
University of Minnesota

GOVERNING BOARD

E. U. CONDON
A. J. DEMPSTER
W. F. FAIR, JR.
FLOYD A. FIRESTONE
HARVEY FLETCHER
R. C. GIBBS
K. S. GIBSON
GEORGE R. HARRISON
PAUL E. KLOPSTEG
GEORGE B. PEGRAM
A. H. PFUND
JOHN T. TATE
WALLACE WATERFALL
M. W. WHITE
A. C. WORTHING

ADMINISTRATIVE STAFF

HENRY A. BARTON, *Director*
MARGARET S. GRIFFIN,
Publications Manager
THEODORE VORBURGER,
Business Manager

THE American Institute of Physics was founded in 1931 as a federation of leading societies in the field of Physics. It combines into one operating agency those functions on behalf of physics which can best be done by the Societies jointly. Its purpose is the advancement and diffusion of physics and its applications to human welfare. To this end it publishes for itself or the Societies the eight journals listed on this page; promotes unity and effectiveness of effort among all who are interested in physics; renders numerous direct services to physicists and to the public; and cooperates with government agencies, national associations, educational institutions, technical industries, and others in such manner as to realize the opportunities and fulfill the responsibilities of physics as an important and constructive human activity.

CONTENTS

[illegible] Survey [illegible] Survey No. 51, Part 1 . . . . . [illegible]

[illegible] Beach Fish in Relation to Currents . . . . . Daniel T. Simpson 1

[illegible] of Seedlings by the Gypsy Moth . . . . . S. A. Graham and R. Hawksworth 25

[illegible] of the Genus *Pinus* Allow . . . . . Clarence Jones 35

[illegible] Distribution of Nutrients in an Inkwell Bottom . . . . . M. Vaga and G. C. Best 49

[illegible] Alpha-Radioactivity . . . . . Mildred A. [illegible] 65

[illegible] of the Region and Its Drainage . . . . . Wayne E. Ackerly and Arthur Bevington 81

[illegible] with Some Tidewater . . . . . W. W. Watson, J. C. Stockbridge, and F. K. Hare 97

[illegible] and Physiological Properties of Rotting Tidewater . . . . . Samuel [illegible] 109

[illegible] Life Expectancy of the Tideland Residents of Seaside Silver Valley and Its Relation to Occupation and Environment . . . . . E. J. Baldwin and D. S. [illegible] 125

[illegible] Quantitative Analytical Method . . . . . W. [illegible] 141

[illegible] in the Ridge? . . . . . [illegible]

[illegible] of the North [illegible] Expedition . . . . . A. G. Vernon, E. C. Barrington, and J. L. Phipps 153

[illegible] on the Natural Relationships of Fish . . . . . L. M. Lucas, G. S. Cook, and M. P. [illegible] 163

[illegible] Intestinal Microflora of Certain Mammals and Nonvegetable Objects . . . . . J. R. Weiss and A. E. [illegible] 177

[illegible] on the Evolution of Tit Bill . . . . . [illegible] 191

[illegible] of Ecology . . . . . H. A. Bullis, Jr., Commissioner, and M. Dean [illegible] 201

[illegible] of Tideland Fish Hatchery and the Quality of Hatchery Brood . . . . . Jane E. [illegible] 215

[illegible], Lowland Moors and Bogs . . . . . Gustaf L. [illegible] 227

[illegible] from Chemical Constituents in Respiratory Metabolism of Low Temperature . . . . . Virgil Jones and E. Lane Rosevear 241

[illegible] Rock, Sediment and Surface Contour . . . . . C. E. Tyrrell 253

[illegible] of Transpiration Rate Based in Resistance . . . . . Philip Wayne and Marion Kaplan 265

[illegible] Harvest and the Weather Side of Life . . . . . C. S. Anderson and W. E. Wayne 281

[illegible] in the Marsh and Water Shrew of Ill . . . . . Warren A. Paterson, C. T. Lash, L. C. Anderson, and Arnold O. Hill 293

[illegible] Fishes Reared in Ditched vs. Open Pastures . . . . . H. E. Westerman, A. L. Anderson, and C. E. Bennett 317

[illegible] of the Southeastern . . . . . Adam Gee 331

[illegible] Phenomena of Atomic Explosion and Detonation . . . . . J. T. Rule, E. B. Stanton, and L. L. Kopf 341

[illegible] of Spawning of Channel Bass in Aransas and Matagorda . . . . . E. Simon and L. Summerlin 355

[illegible] of the Atmosphere at Altitude . . . . . H. Rose, B. Stewart, and E. LaGow 367

[illegible] of Rainfall on Certain Forest Soils of the Ozarks Group . . . . . E. O. Rue 379

[illegible] Rainfall Data . . . . . Wendell Green, A. G. Hays, and Lewis W. Swanson 391

[illegible] Some Northern Hardwoods of Shortleaf Pine Belong . . . . . E. E. Shaw, Jr., E. J. Hess, and P. W. Dawson 403

[illegible] Concerning Supplements about the Atmosphere . . . . . W. E. Berge and E. C. Kemp 415

Index to Volume 71 429

List of Subject Index to Volume 71 441

Table of Contents v

[illegible] PRESS, INC., LANCASTER, PA.